Naval Surface Warfare Center
Carderock Division
West Bethesda, MD 20817-5700

NSWCCD-TR-97/010 November 1997

Survivability, Structures, and Materials Directorate

Technical Report

Development of a SEAL Delivery Vehicle Battery

by

J. L. Gessler, A. Romero, and R. J. Staniewicz (Saft America)

Edited by Charles W. Fleischmann (Advanced Technology & Research Corporation)

Naval Surface Warfare Center
Carderock Division
West Bethesda, MD 20817-5700

NSWCCD-TR-97/010 November 1997

Survivability, Structures, and Materials Directorate

Technical Report

Development of a SEAL Delivery Vehicle Battery

by

J. L. Gessler, A. Romero, and R. J. Staniewicz (Saft America)

edited by

C. W. Fleischmann (Advanced Technology & Research Corporation)

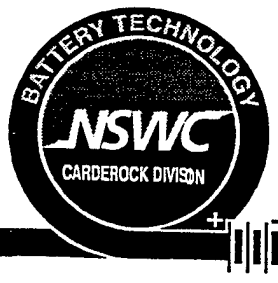

REPORT DOCUMENTATION PAGE

Form Approved
OMB No. 0704-0188

1. AGENCY USE ONLY *(Leave blank)*	2. REPORT DATE	3. REPORT TYPE AND DATES COVERED
	November 1997	

4. TITLE AND SUBTITLE
Development of a SEAL Delivery Vehicle Battery

5. FUNDING NUMBERS

6. AUTHOR(S)
Joseph L. Gessler, Antonio Romero, and Robert J. Staniewicz

7. PERFORMING ORGANIZATION NAME(S) AND ADDRESS(ES)
Naval Surface Warfare Center
Carderock Division
9500 MacArthur Boulevard
West Bethesda, MD 20817-5700

8. PERFORMING ORGANIZATION REPORT NUMBER
NSWCCD-TR-97/010

9. SPONSORING/MONITORING AGENCY NAME(S) AND ADDRESS(ES)
Office of Naval Research
Ballston Tower 1
800 N. Quincy Street
Arlington VA 22217

10. SPONSORING/MONITORING AGENCY REPORT NUMBER

11. SUPPLEMENTARY NOTES

12a. DISTRIBUTION/AVAILABILITY STATEMENT
Approved for public release; distribution is unlimited.

12b. DISTRIBUTION CODE

13. ABSTRACT ***(Maximum 200 words)***

The goal of this program was to demonstrate performance in cells sized for use in the SEAL Delivery Vehicle. Development efforts by Saft, America, Inc. are reported for batteries to power undersea vehicles. Large, prismatic cells were designed, built, and tested in sizes up to 150 Ah, and demonstrated energy densities up to 130 Wh/Kg. The anodes were either metallic lithium or a lithium-intercalating carbon. Cathodes were lithiated metal oxides of cobalt or nickel (Li_xCoO_2 or Li_xNiO_2). The electrolyte was 1.2 M $LiAsF_6$ in mixed solvents ethylene carbonate, propylene carbonate, and dimethyl carbonate in a 1:1:2 ratio. Several different cell designs were explored, some of which included novel features such as case strengthening by pinning together opposing faces and orienting the plates parallel to the narrow case faces. These and other design features were needed to address the effect of stack bulging during cycling. Electronics to control charge and discharge and to ensure safe operation were proposed. Safety of the electrochemistries was evaluated by testing 4/5 A-size cells.

14. SUBJECT TERMS
lithium/metal oxide, lithium rechargeable battery, lithium-ion/metal oxide

lithium-ion battery, Li_xNiO_2, Li_xCoO_2, large prismatic lithium cell

15. NUMBER OF PAGES
163

16. PRICE CODE

17. SECURITY CLASSIFICATION OF REPORT	18. SECURITY CLASSIFICATION OF THIS PAGE	19. SECURITY CLASSIFICATION OF ABSTRACT	20. LIMITATION OF ABSTRACT
UNCLASSIFIED	UNCLASSIFIED	UNCLASSIFIED	SAR

NSN 7540-01-280-5500

Standard Form 298 (Rev. 2-89)
Prescribed by ANSI Std. Z39-18
298-102

Contents

Contents (Continued)

Figures

Figures (Continued)

Figures (Continued)

Tables

Preface

The Office of Naval Research funded the work described in this report under Naval Surface Warfare Center contract number N60921-93-C-0134 which was awarded to Saft, America, Inc. The contracting officer's representative was Dr. Patricia Smith, Electrochemistry Branch (Code 683), Naval Surface Warfare Center, Carderock Division, West Bethesda, Maryland.

The principal investigator, Mr. Antonio Romero, and Dr. Robert J. Staniewicz and Mr. Joseph L. Gessler, thank Saft for the support afforded this work, and particularly staff member Mr. David Alban for the painstaking effort of test cell assembly.
Dr. Charles W. Fleischmann and Ms. Adrien Meskin, Applied Research & Technology Corporation reviewed and edited this report.

Chapter 1

Introduction

The goal of this program was to demonstrate performance in cells sized for use in the SEAL (SEa-Air-Land) Delivery Vehicle (SDV). The object of this procurement was to develop a rechargeable lithium/lithium cobalt dioxide (Li/Li_XCoO_2) cell with a minimum 100 Ah capacity that would serve as a design precursor to the SDV-sized cell. The minimum 100 Ah cell (sub-SDV cell) would embody the essential design features of an engineering baseline SDV cell. A successful development effort would conclude with the testing of sub-SDV cells. The cell was to deliver not less than 100% of its rated capacity every cycle for 50 cycles and at least 100 Wh/lb every cycle under the following cycling regime: charge in 10 hours and discharge in 6 hours.

Background

The US Navy sought the development of the electrochemical couple, Li/Li_xCoO_2, in order to provide a battery with improved performance as the propulsion power source for underwater vehicles. The range of the present vehicles is limited by the energy density provided by the silver oxide/zinc (AgO/Zn) batteries currently being used. The Li/Li_xCoO_2 was expected to provide an energy density that would double the vehicle range.

Under prior Navy funding, 30 Ah cells demonstrated an energy density of 58 - 60 Wh/lb at the six hour discharge rate over 40 cycles.[1] This was independent of temperature over the range of -2°C to +35°C and of charging rates between 2 and 20 hours.

Requirements

The SDV battery had the following specifications:

- Total battery weight (cells only): 776 lbs
- Nominal Battery voltage: 128V
- Operating temperature: -2°C to 35°C
- Cells equally divided among four canisters, connected in series, in two trays per canister (see Figure 1.1)*

* To avoid tooling for deep-drawn cans, welded cans were used, which required thicker sheet steel for ready weldability.

Approach

A prismatic (rectangular parallelepiped) rather than cylindrical geometry allowed for the most efficient packing of the cells. The design is detailed in Chapter 2.

Initially, the cell was designed using a metallic lithium anode in the Li/Li_xCoO_2 electrochemical system. As a result of the problems that were encountered, the contract was modified to design, develop and test cells in which the metallic lithium anode was replaced with a lithium intercalation graphite electrode (LiON®).

Lithium ion cells have three main components consisting of a bonded graphite anode/negative electrode, a bonded transition metal oxide, such as, lithiated nickel oxide (Li_xNiO_2) or lithiated cobalt oxide (Li_xCoO_2), as the cathode/positive* electrode and an organic electrolyte. The lithium ion electrochemistry uses the same type of electrolyte and lithiated metal oxide cathodes as the metallic lithium batteries, but the negative electrode consists of a graphitized carbon structure. As there is no metallic lithium present in the cell, the lithium ion technology is safer and offers greater cycling efficiency. The cell is assembled in a discharged state; it is then formed and charged. During charge, lithium ions deintercalate from the positive electrode and intercalate into the carbon negative electrode. During discharge, the lithium ion moves back into the positive electrode. Reversible cycling between 4.2 V and 3.0 V for these systems may be expressed by the equations:

$$0.5Li + Li_{0.5}\,CoO_2 \leftrightarrow LiCoO_2\,(137mAh/g)$$

$$0.5Li + Li_{0.35}\,NiO_2 \leftrightarrow Li_{0.85}N_iO_2\,(135mAh/g)$$

* The use of "positive" and "negative" in this report refer to the polarity of the electrodes on discharge. It is understood that the polarity is reversed on charge.

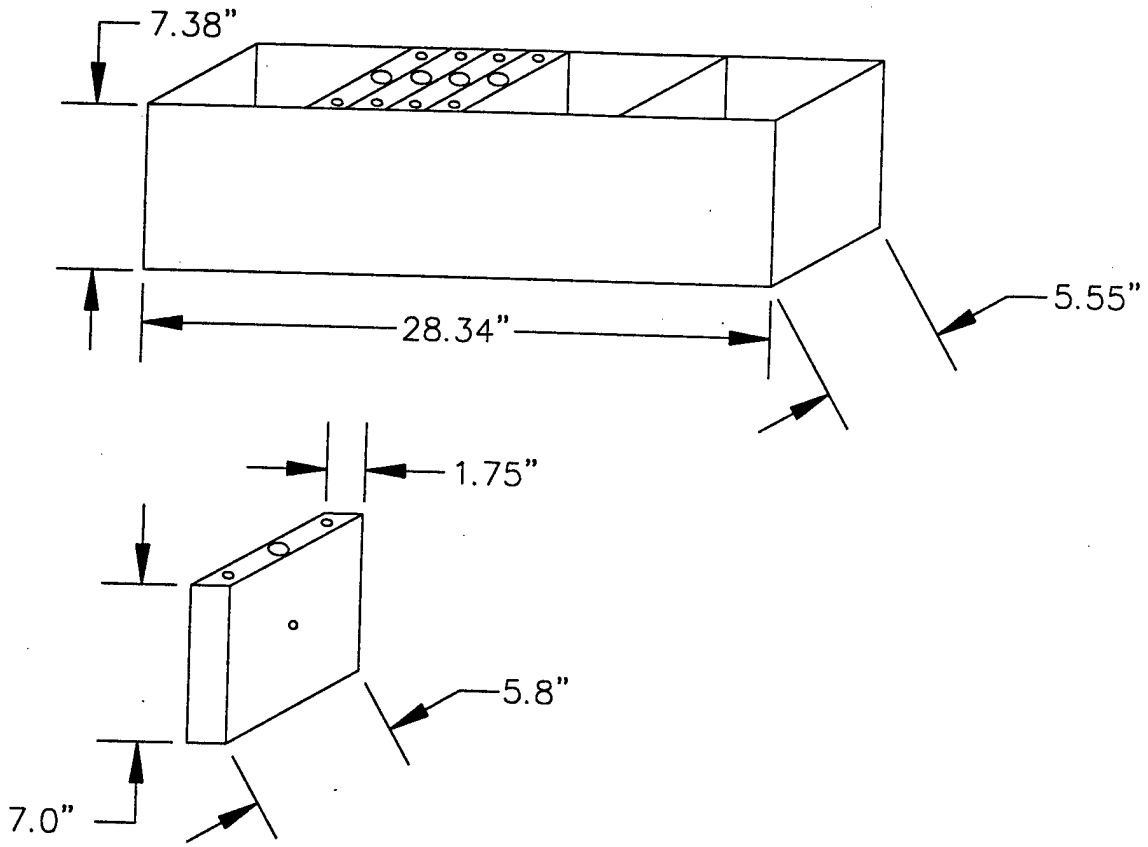

Figure 1.1 SEAL Delivery Vehicle Battery Layout

Chapter 2

The Metallic Lithium Anode Design

This chapter describes several mechanical designs and details the chemical composition of the components. Lessons learned from evaluations of the designs are discussed.

Cell Design

Saft proposed a prismatic cell design for the following reasons:

- An oversize cylindrical design is impractical to manufacture because the length of the electrodes makes winding tracking difficult.
- Dendrites (soft shorts) are avoided by reducing the current densities on the electrodes by increasing the surface area. A safer cell results.
- Inter-electrode separator insulation of the electrode edge is improved.

Furthermore, the energy densities per unit volume and per unit weight were maximized, by reducing hardware size and weight.

Table 2.1 compares the performance of the proposed Li/Li_xCoO_2 battery with the present AgO/Zn battery. Table 2.2 describes the proposed riveted prismatic design.

The successful cycling of a lithium rechargeable cell depends greatly on its mechanical stability. The cell envelope must be designed to control or maintain a particular compression between the electrode plates. This is important to avoid the build up of stripped or cycled lithium, which could penetrate through the separator, causing dendrites or soft shorts, when pressures reach certain limits. Further, it is imperative to avoid a loose pack that will cause plate defoliation, excessive cell impedance, and poor lithium cycling efficiency, which would lead to rapid cell failure.

Proposed Design

The proposed case design incorporated a number of innovative ideas:

- The large planar faces were riveted together to avoid significant dimensional changes.

- The insulated rivets also served to index the planar electrodes.
- The positive electrode was completely enclosed by a polyethylene separator that was heat-sealed at the outer edges and the indexing hole. This secured the electrode position and avoided shifting during shock and vibration.
- The cover and bottom (i.e., the large planar faces) had reinforcing ribs, which limited mechanical deflection.
- The inclusion of a spring plate parallel to the plates allowed for the mechanical growth of the electrodes.
- The use of two pairs of glass-to-metal seal eyelets (one pair for [+] and one pair for [-] terminals), and a BS&B vent disk. The glass material was Corning TA-23. The feed-through current lead was a molybdenum post.
- The fill-port was projection-welded onto the case wall although, alternatively, it could be located on the cover.
- The overall rectangular shape was selected based on analyzing the headspace needed for the tabs and a deliberate intent was made to minimize the number of plates and consequent dimensional growth during charging.
- The use of a "sardine can" design allowed exact electrode stacking and positioning with the rivet in place.
- The use of an electrically neutral or floating potential case, whose interior was coated with a fluorocarbon resin such as Tefzel to avoid any lithium deposition.

One of the unique mechanical properties of a cylindrical cell design is the hoop stress, a force that maintains constant dimensional spacing between electrodes throughout the cycle life of the cell. The mandrel hole in the center of spiral wound electrodes also serves an important function of absorbing the dimensional growth of the electrodes. Therefore, a design of a prismatic cell should incorporate design features that would act similar to the influence of hoop stress and the mandrel hole within a cylindrical cell. These design features for the prismatic cell included the reinforcing ribs on the cell cover and bottom; the rivet which tied the two large surface areas together; and the spring plate, which will partially collapse and allow plate growth during charging similar to hoop stress and the mandrel space in a cylindrical cell. The rivet would be projection welded on the bottom of the case and then mechanically formed over the top cover and tungsten-inert-gas (TIG) welded, effectively controlling dimensional changes between the large planar faces. The rivet would also serve to index the electrodes through their die cut central hole while the positive plate is completely sealed within a separate envelope preventing electrode shifting and shorting during shock and vibration.

The Navy's preference that all hardware should consist of off-the-shelf parts could not be met while still attaining the 100 Wh/lb. Expansion of the electrodes on cycling will bulge an ordinary prismatic steel case. The 5" x 7" planar faces would be subjected to deformation without incorporation of the rivet and reinforced ribs. Successful development of a rechargeable prismatic cell required that a unique and novel design be applied against the challenges of maintaining constant stack pressure. The case design shown in the drawings can be realized by folding and welding stainless steel sheet to the exact dimensions. The sheet can be embossed to form the ribs. In summary, the mechanical design aspects shown in Figures 2.1 through 2.6 are equal in importance to the electrochemical design challenges for this program.

Amended Design

When vendors were requested to quote on fabricating the can and top cover, they stated that a compound die would be required because of the ribs. This would cost approximately $60,000. An attempt was made to fabricate the cover with tooling, which was available at Saft. It could put in two ribs at a time. When the rib was formed across the grain, the 304 stainless steel (s.s.) plate buckled and cracked (Figure 2.7). Because of the cost of the compound die, the battery was redesigned without the ribs as detailed in Figure 2.8 through 2.17. In order to allow more space for active material, the "sardine can" design and the spring plate were not used. The case was made by folding and welding stainless steel to the dimension as shown in Figure 2.10. Rivets tied the two large planar surfaces of the can together as described in Chapter 4.

A test fixture was designed to investigate the placement of the rivet(s), which would minimize the effect of stack bulging during cycling. The fixture was designed to hold three positive and four negative plates in a parallel configuration. The fixture base was a one-quarter inch 304 s.s. plate with a 0.093 inch well milled out for the plates to sit in (Figure 2.18). The wall thickness of the cavity was, therefore, 0.157 inches. The positive and negative electrodes were welded to the appropriate terminals on the face of the steel plate. There was a fill port for electrolyte filling (Figure 2.19) on the flat side of the base plate. A polytetrafluoroethylene valve was fitted to the fill port. The assembled cell was evacuated and then filled with the electrolyte under pressure. Next, a polyethylene gasket and a metal shim stock (Figure 2.20) were used to cover the cell. The shim stock varied in thickness and allowed the study of the effect of the flexibility of the battery "can." In one fixture (#5), the shim stock was replaced with the flat side of another fixture base, in order to represent a very thick cover. To simulate the rivet that was used to hold the center of the cell at a fixed thickness, an arm and screw assembly was developed (Figure 2.21). The arm was attached to the frame, which was used to screw the fixture closed and fitted over the assembly on the shim side. The center screw was tightened down on the center of the stack. The effect of the pressure of the screw on the stack was studied in comparing Fixtures 2 and 3 with Fixture 4 (Table 2.3).

The cell consisted of three plates of $LiCoO_2$-based positive electrodes and four metallic lithium electrodes. The positive plates (Figure 2.22) were made from a mix that had the following composition:

	Weight Percent
$LiCoO_2$	89.5
Ketjenblack EC-600	5.0
Graphite	2.0
Polytetrafluoroethylene	3.5

The mix was pasted on one side of aluminum expanded metal, type 4A18-077 from Delker Corporation, which was calendered prior to pasting to a thickness of 0.006 inches from the original 0.010 inches. The cathodes were calendered to a final thickness of 0.016 inches. The plates were cut to the final dimensions. One positive assembly consisted of a single side of a pasted plate, folded with the active material facing out. A small area of the active material was brushed off to expose the aluminum expanded metal for welding. Then, a 0.001-inch thick aluminum tab was sandwiched between the two halves and welded.

For the negative electrode, it was originally proposed to use a lithium aluminum alloy (15% aluminum by weight), but the minimum thickness that was available was 0.006 inch, which was too thick. The negative electrode, (Figure 2.23), alternately was made by pressing 0.003-inches thick lithium onto both sides of a 0.003-inch thick copper mesh. A 0.001-inch thick nickel tab was welded directly through the lithium. The plates were 5.63 inches by 6.50 inches and the overall laminated thickness was 0.0085 inches.

Two layers of separator, one of porous polypropylene (Celgard 2400) and the other of porous polyethylene (Celgard K-869), were used. The polypropylene offers a degree of rigidity to the cell stack and a layer that is difficult for dendritic lithium to penetrate. The polyethylene is a softer material but melts at a low temperature (100 - 110°C), offering a cell shutdown mechanism that enhanced safety. The positive plates were placed in pouches made from two sets of separators as shown in Figure 2.24. In Fixture #1, the pouch was sealed on all four sides. In later fixtures, the pouch was unsealed on at least one side. The electrolyte used throughout these studies consisted of a solvent mixture of ethylene carbonate, propylene carbonate, and dimethyl carbonate in a 1/1/2 ratio by volume, with 1.2 *M* $LiAsF_6$ as the dissolved salt.

Test Cell Builds and Test Results

The fixtures (Figure 2.25) were assembled using the hardware described above and filled with electrolyte. The cells were charged and discharged at a C/17 rate for the first two cycles between 4.2 volts and 3.0 volts. To avoid dendrites and to allow for full absorption of the electrolyte, a low rate of charge and discharge was required during these formation cycles. From the third cycle on, the cells were charged at C/11 rate to either 4.3 volts or 7.25 Ah and discharged at C/5 rate to 3.0 volts. The theoretical capacity was 7.5 Ah.

Cell Navy T1

Cell Navy T1 was the first fixture made. The cell was made with a 0.025-inch shim as the top plate. The cathode was sealed into a separator pouch, which was sealed on all four sides. This cell did not cycle past the first cycle. The cell failed because of shorting. When the cell was

disassembled it was found that the cathode was poorly wetted with electrolyte. Because the porous polypropylene and polyethylene separators have pin-hole type pores, the separators do not wick electrolyte very well. The areas that were wetted had a much higher current density than was expected. The areas that did cycle had lithium plating conditions favorable for dendrite formation. This showed that the electrolyte had wicked poorly in the separators and did not make it through the separator under the filling conditions. The easiest fix proposed for this problem was to leave at least one side of the pouch unsealed in order to allow the electrolyte free access to the positive plate.

Cell Navy T2

Cell Navy T2 and T3 were made on the same day. The same shim stock (0.025-inch thick material) was used for the top of both fixtures. Table 2.3 shows stack height (h) measurements. All data shown in this table are Δh measurements in inches relative to the (fixed) corners, points 1 and 2 in Table 2.3. Before tightening the center screw on the arm, the center (point 3 in Table 2.3) was 0.066 inches higher than the corners. The screws were tightened so that the Δh at the center (point 3 in Table 2.3) was 0.000 inches. After filling the cell with electrolyte, the cell bulged about half way between the center and edge (points 4 and 5 in Table 2.3). After forming the cell (the first two cycles), gas pressure in the cell was released and the same points were measured again. Though points 4 and 5 were higher than the corners, they were not as bulged as when the cell was uncycled. The same points grew by a factor of 2.74 after 67 cycles (compare the last four columns of Table 2.3). The cell cycling data are shown in Figures 2.26 and 2.27. After having an initial capacity of 7.1 Ah (Figure 2.26), the capacity dropped off to an average of 5.5 Ah after the fifth cycle. The average voltage for both the charge and discharge half cycles did not vary much from their initial values (Figure 2.27). This cell cycled 46 times before shorting.

Cell Navy T3

This fixture was made to the same specifications as Cell Navy T2. The deflections (Ah) were measured as described above. Again, without the center screw, the center point of the fixture was deflected 0.057 inches above the corners. When the center screw, which simulated a central rivet, was screwed down so the central point had 0.000-inch deflection, points 5 and 6 in Table 2.3 each had a significant Ah. On filling the cell with electrolyte, points 5 and 6 in Table 2.3 bulged to 0.040 inches and 0.054 inches, respectively. When the pressure was released after cycle two, the bulge decreased to 0.021 inches for both points. After 80 cycles these two points bulged over 0.07 inches (Table 2.3). Again, the growth of the stack during cycling is indicative of the design problems inherent in a prismatic cell. When the cell was disassembled and the gas was released, the stack thickness was the same thickness as the sum of the electrode thicknesses. This showed that the growth of the lithium electrode thickness with cycling was in large part responsible for the observed stack deflections.

Cell Navy T3 was cycled at both room temperature and at -2°C. The overall discharge capacity versus cycle number is shown in Figure 2.28. At cycle 25, the cell was removed from ambient temperature and placed in a -2°C chamber for three cycles. Voltage-time profiles for the discharge of cycles 25 and 26 are shown in Figures 2.29 and 2.30, respectively. The voltage

drop at the end of the discharge in Figure 2.30 is not as sharp as that in Figure 2.29. The cell capacity and average voltage (E_{AV}) were also lower at the lower temperature. Over the three cycles at -2°C, the capacity decreased from 7.61 Ah at room temperature to 6.23 Ah for cycle 28. After cycle 28, the cell was returned to room temperature. The observed rapid capacity decline was a result of the loss of electrolyte. Because the different materials thermally expand and contract at different rates, the electrolyte leaked out of the seal between the shim stock and base through the polyethylene gasket. When the cell was refilled with electrolyte at cycle 30, the capacity of the cell returned to the levels it had before being exposed to -2°C. The lack of electrolyte is also shown by the increase in the difference between the charge E_{AV} and the discharge E_{AV}, as shown in Figure 2.31, suggesting a large impedance since all charges and discharges were at the same rate.

Cell Navy T4

Cell Navy T4 was constructed similarly to Cell Navy T2 and Cell Navy T3, with the exception that the shim stock top used to cap this cell was 0.030-inches thick. As indicated in Table 2.3, the deflection of the central point, unsupported, was significantly lower than those for Cells Navy T2 and Navy T3. As a test, the central screw was tightened down to compress the central points with a 0.020-inches inward deflection. Points 5 and 6 (Table 2.3) showed the same degree of bulging as in the previous two cells, both after filling and after pressure release after cycle 2. The cell shorted soon after cycle 2 and was then disassembled. It was found that the dendrites were such that they grew through the separator layers and shorted out the cell. The dendrites were so well embedded in the separator that pieces of lithium came off of the copper mesh still stuck to the separator. The center of the stack also bore the mark of the central screw. The screw pushed into the stack with such pressure that the cathode material was imbedded into the separators. The dendrites formed a halo around the center push mark with a region of unwetted cathode between. While little can be concluded from the shim thickness results, it is clear that a central rivet needs to be able to hold the stack together without compressing it too much.

Results

The lesson learned from the above studies was that the design of the final battery hardware must account for the deflections of the cell stacks. No matter how the cell is constructed, there will be some bulging of the electrodes. The key is to be able to contain the growth of the electrodes within a fixed volume as happens in a cylindrical cell design. Table 2.4 shows some calculations made on the pressures exerted in the cell that cause the bulging of the sides of the cell container. Based on the results of Cells Navy T2 and Navy T3 in Table 2.3, the electrodes exert 250 pounds per square inch, gage (psig) of pressure on the cell walls. In order to minimize the deflection in the container sides, 0.080 inch thick 304 stainless steel would be needed. Because of the weight penalty and the difficulty of forming a case with that thickness, it was decided to stay with the 0.035-inch thickness and three rivets. The key is to balance the need for dimensional integrity with the need to keep the weight of the cell down.

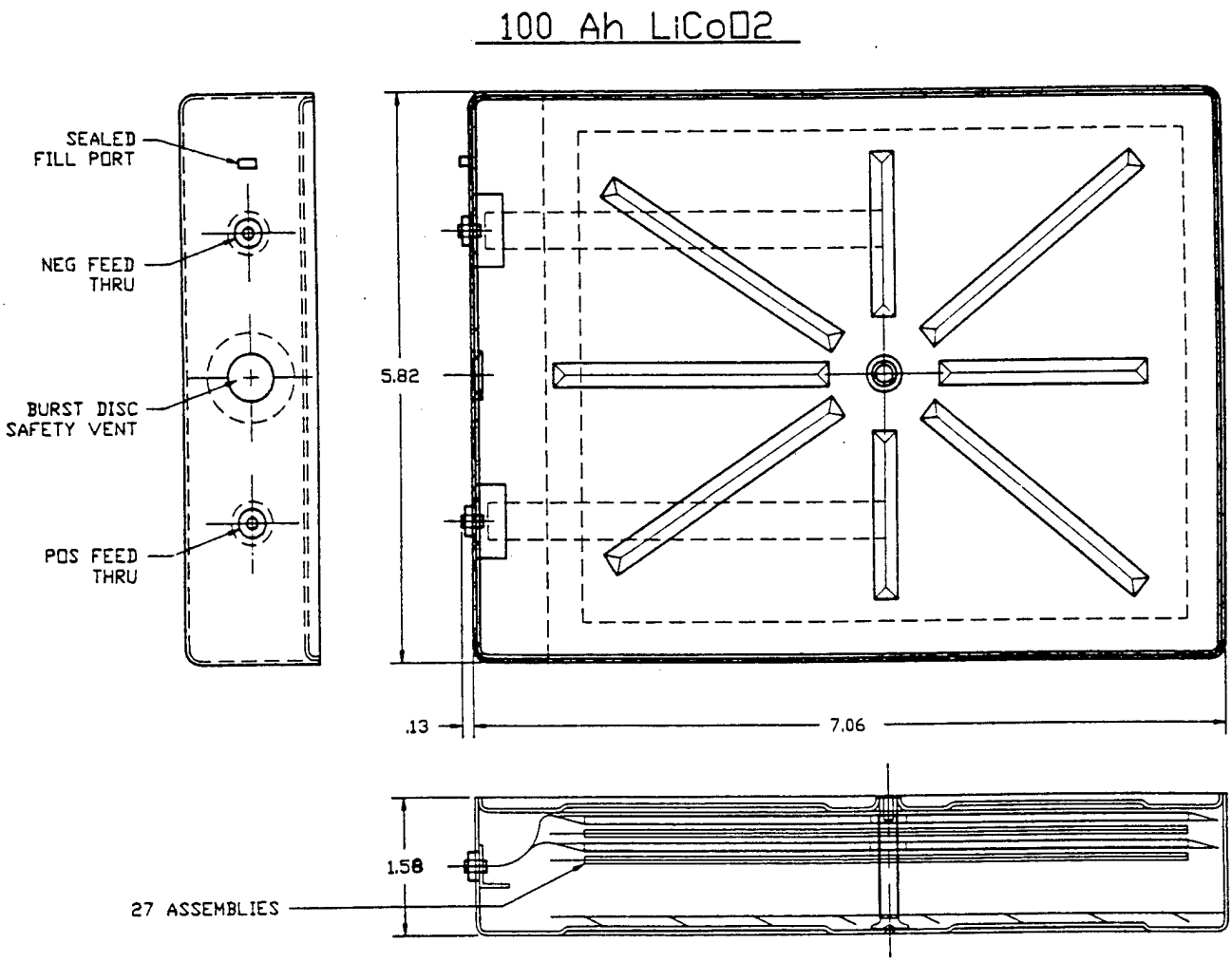

Figure 2.1 Proposed 100 Ah Li/$LiCoO_2$Cell

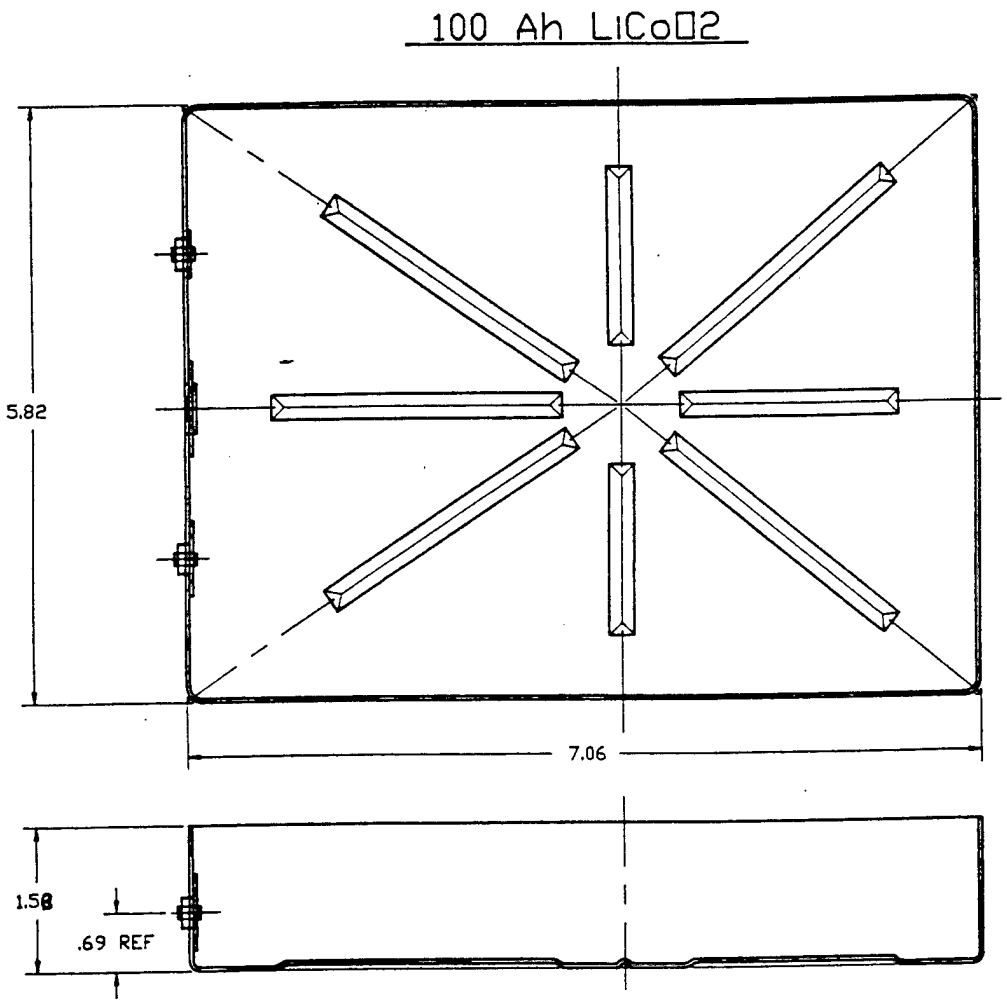

Figure 2.2 Can

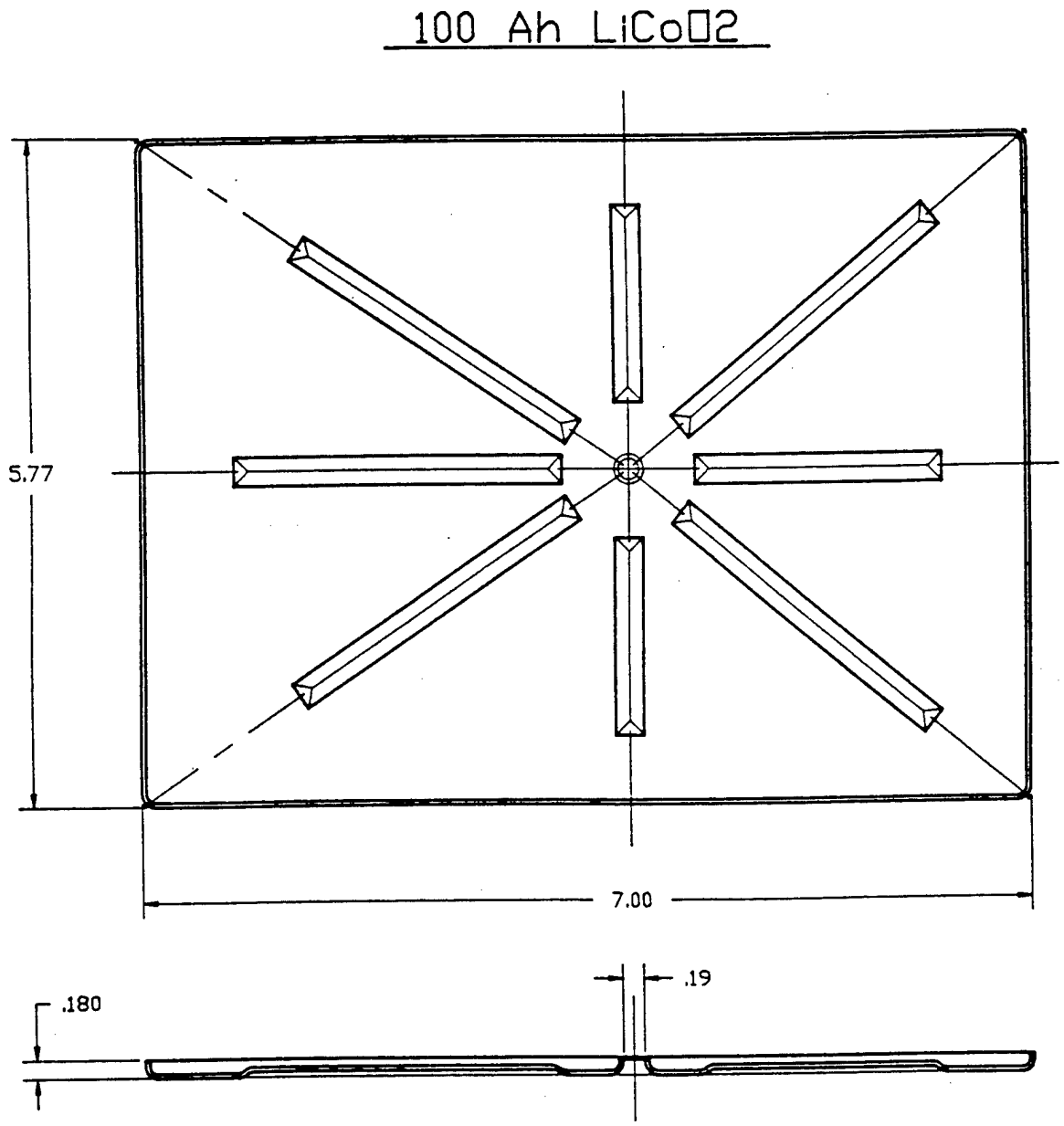

Figure 2.3 Top Cover

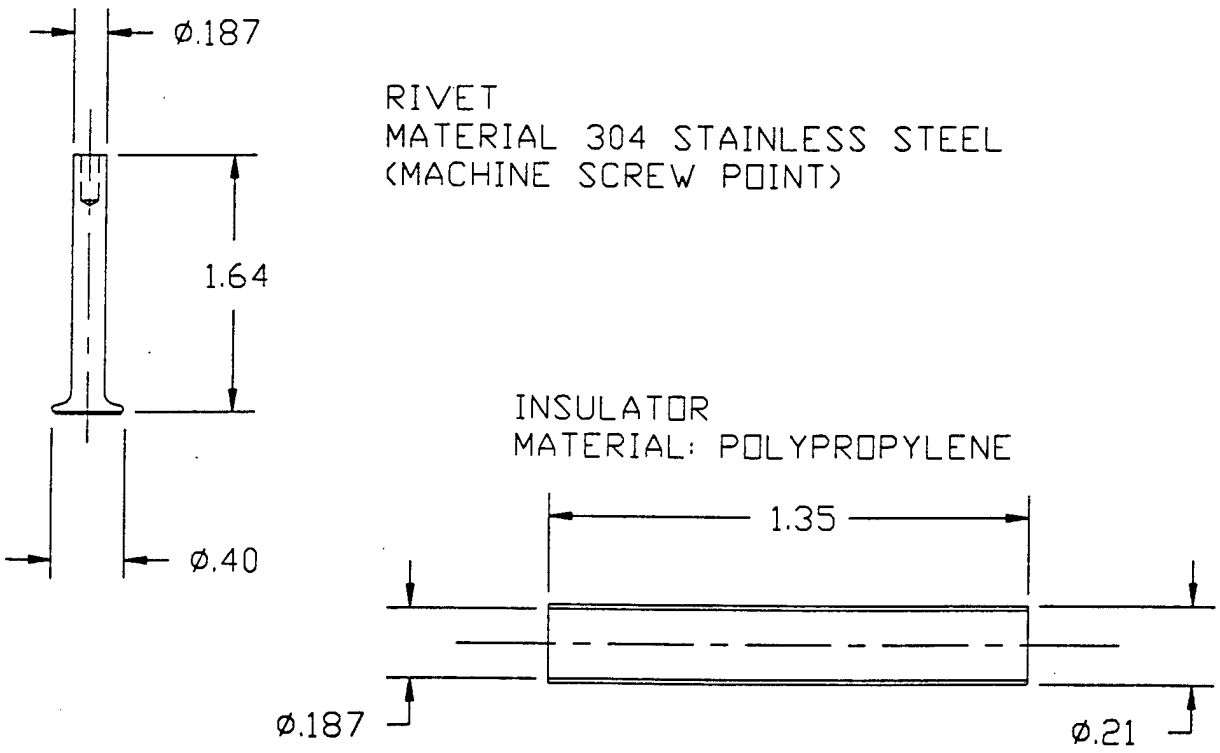

Figure 2.4 Rivet and Rivet Insulator

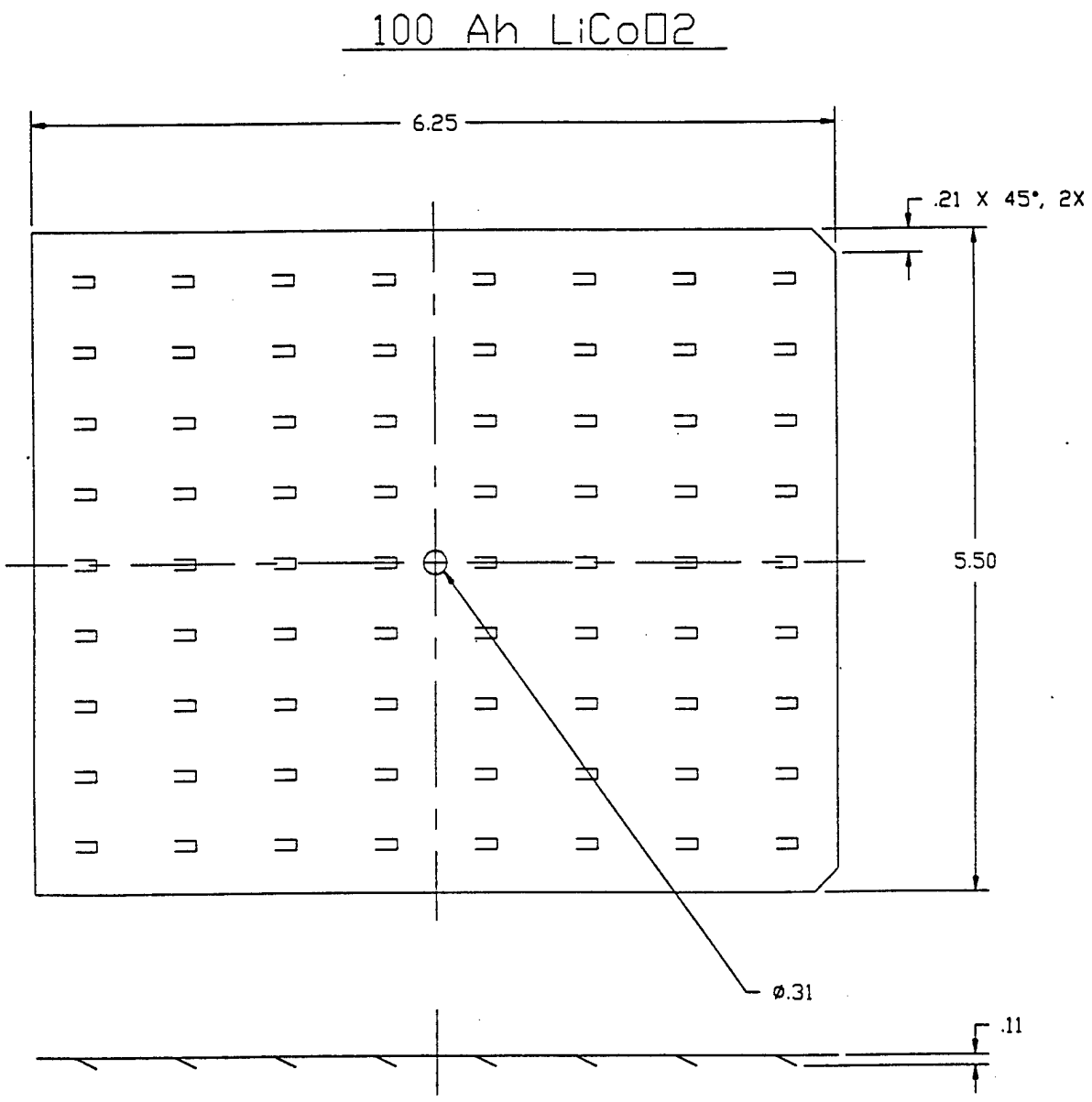

Figure 2.5 Spring Plate

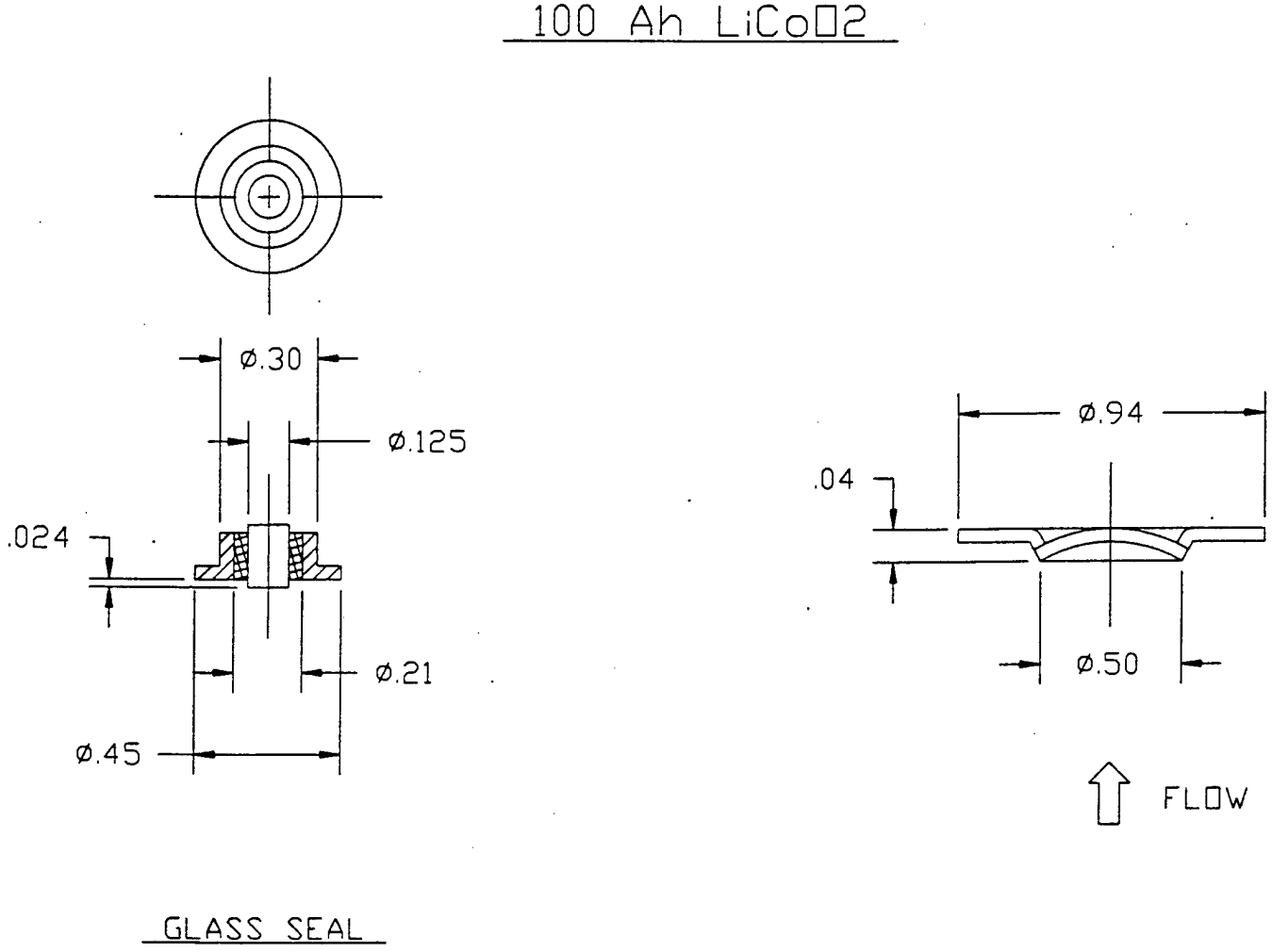

Figure 2.6 Glass-to-Metal Seal and Vent

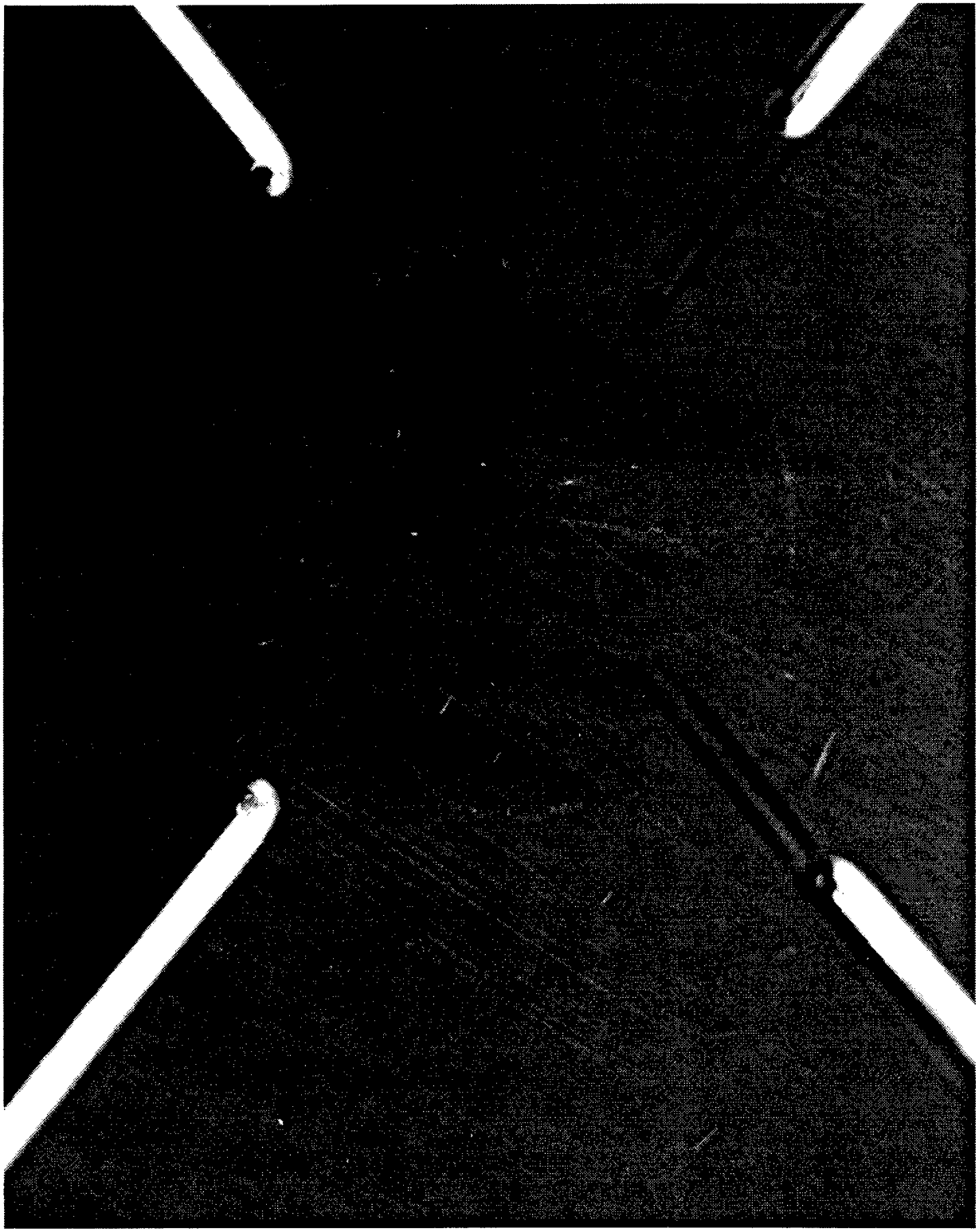

Figure 2.7 Photograph of Ribbed Cover with Crack

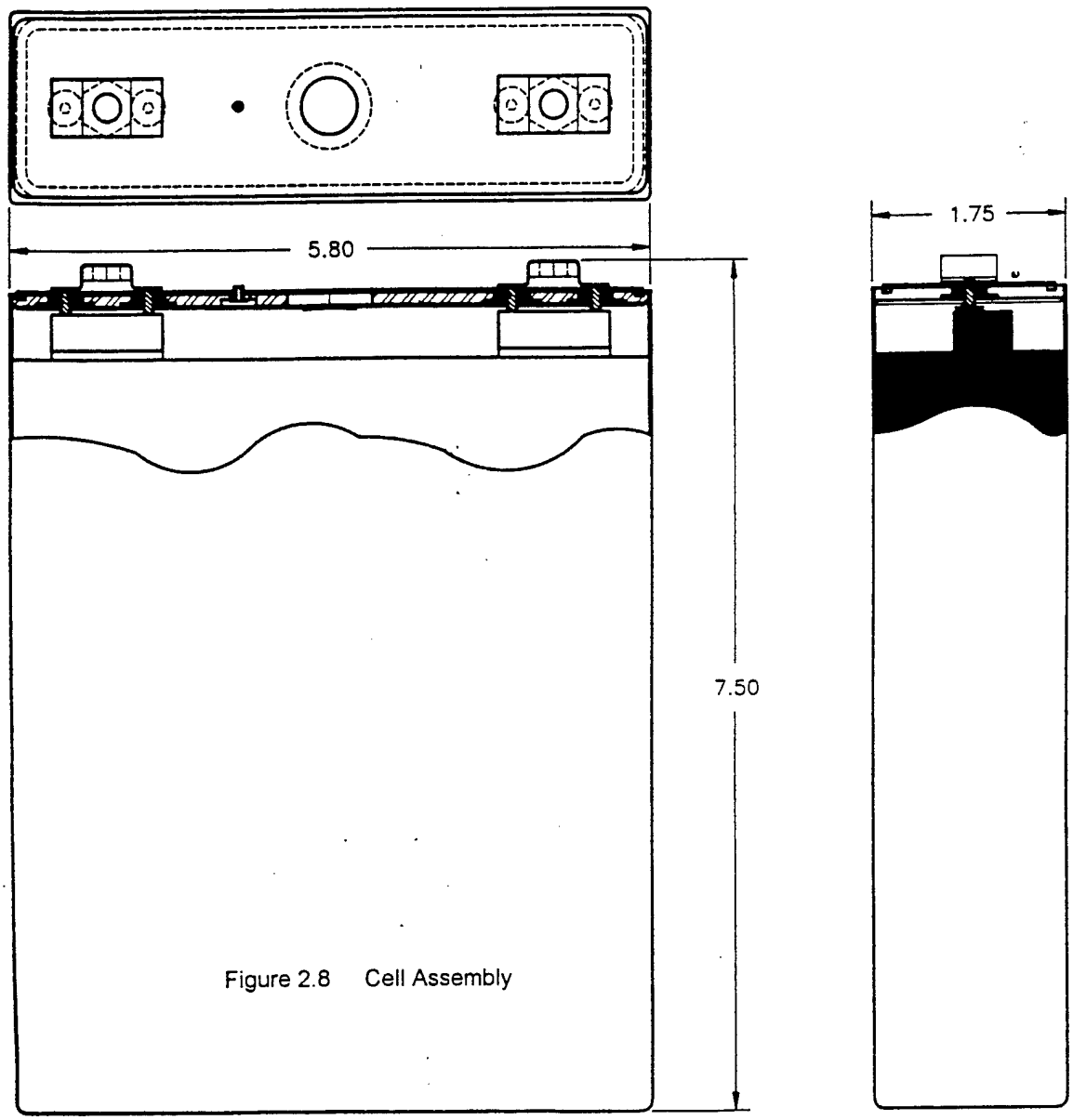

Figure 2.8 Cell Assembly

Figure 2.8 Cell Assembly

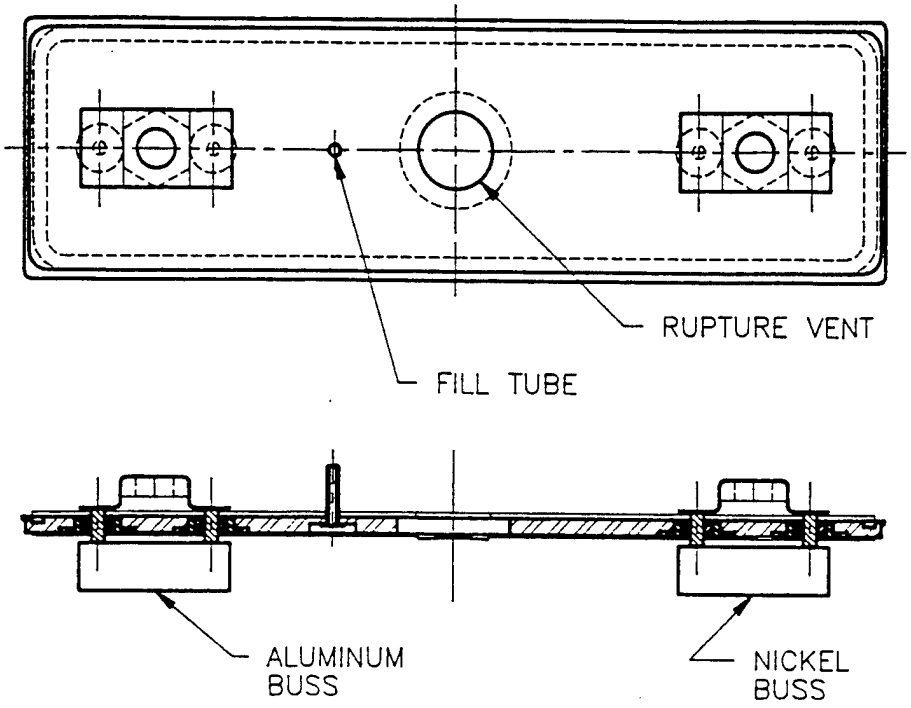

Figure 2.9 Cover Assembly

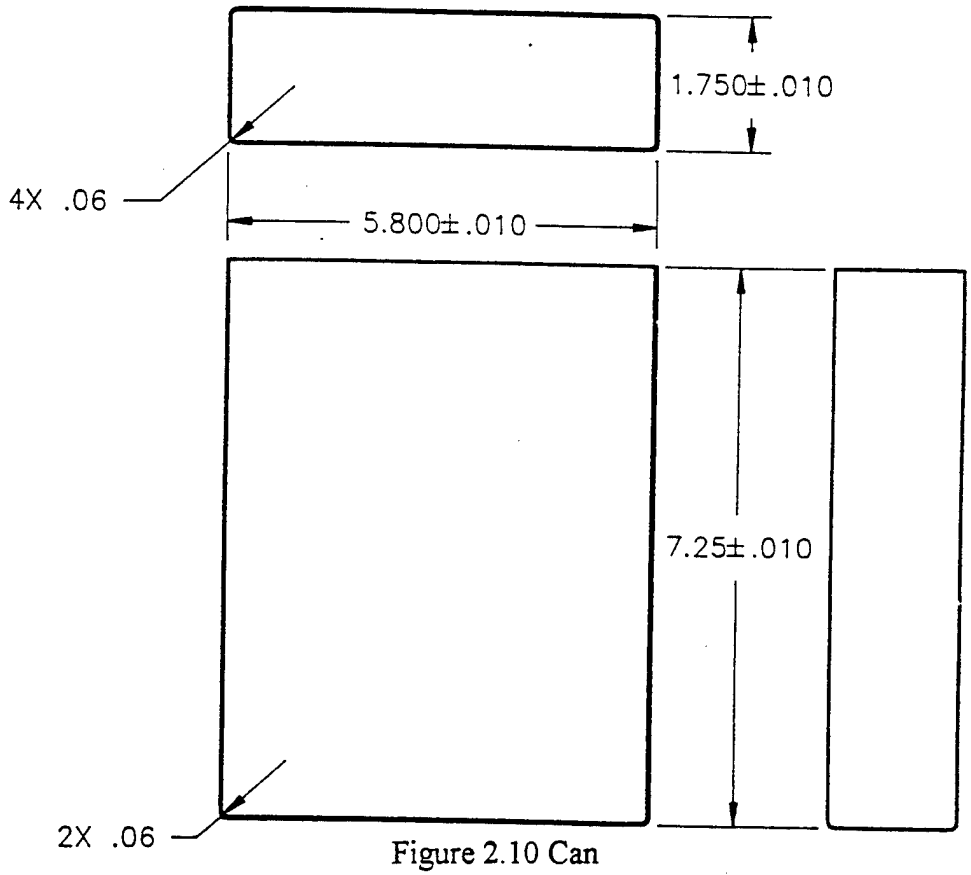

Figure 2.10 Can

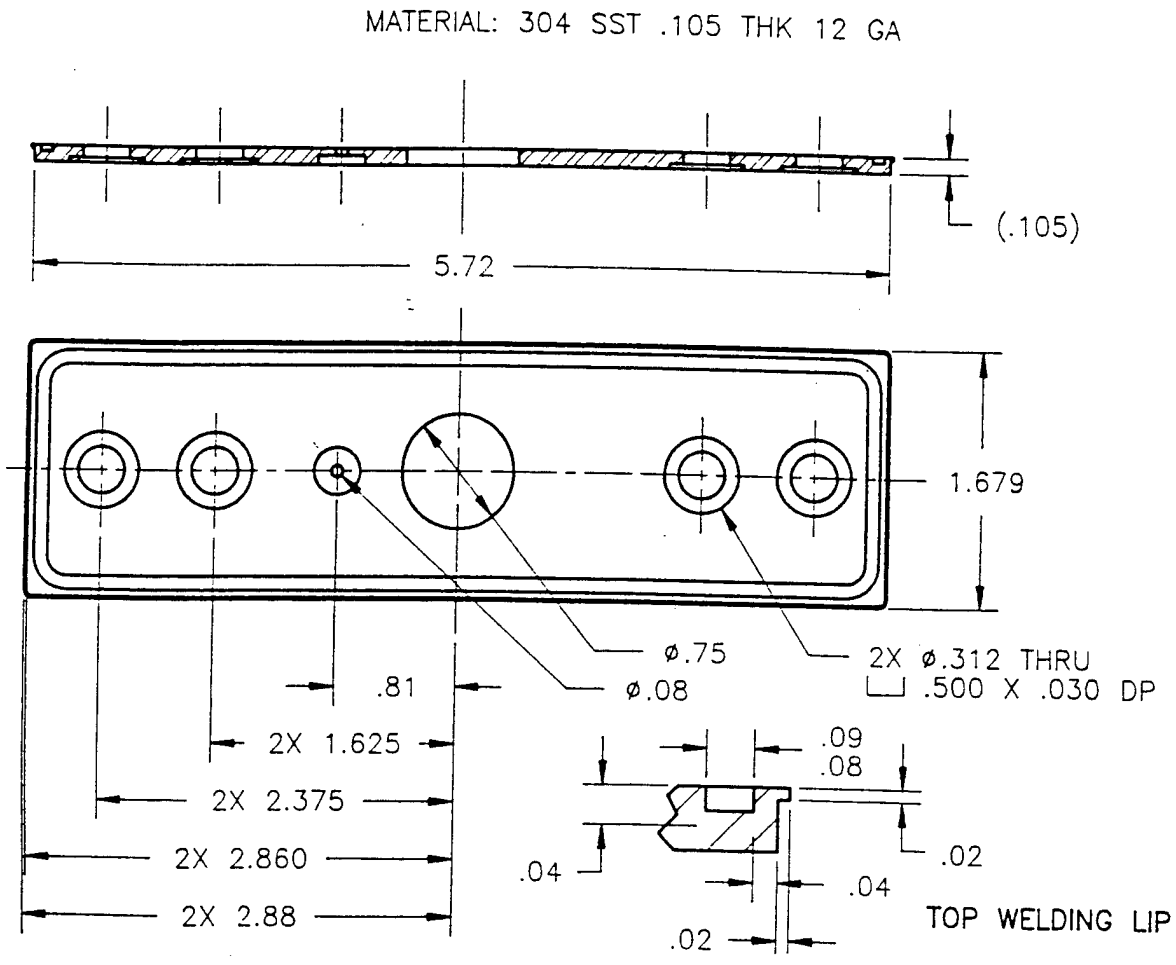

Figure 2.11 Top

MATERIAL: NICKEL & BRASS NUT BRAZED ASSY
NICKEL: .010–.012" THICK
NUT: 1/4–28

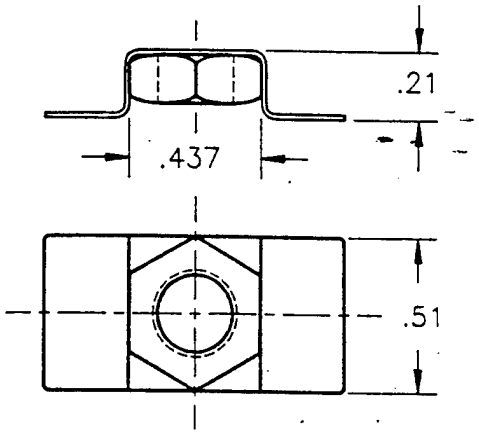

Figure 2.12 External Terminal Bracket

POSITIVE – ALUMINUM: .010–.012" THICK
NEGATIVE – NICKEL: .010–.012" THICK

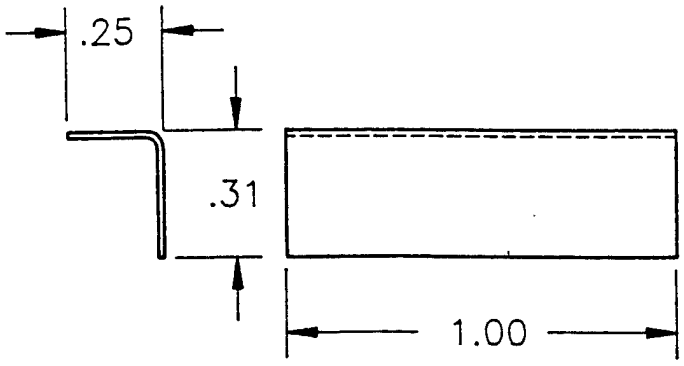

Figure 2.13 Internal Terminal Bracket

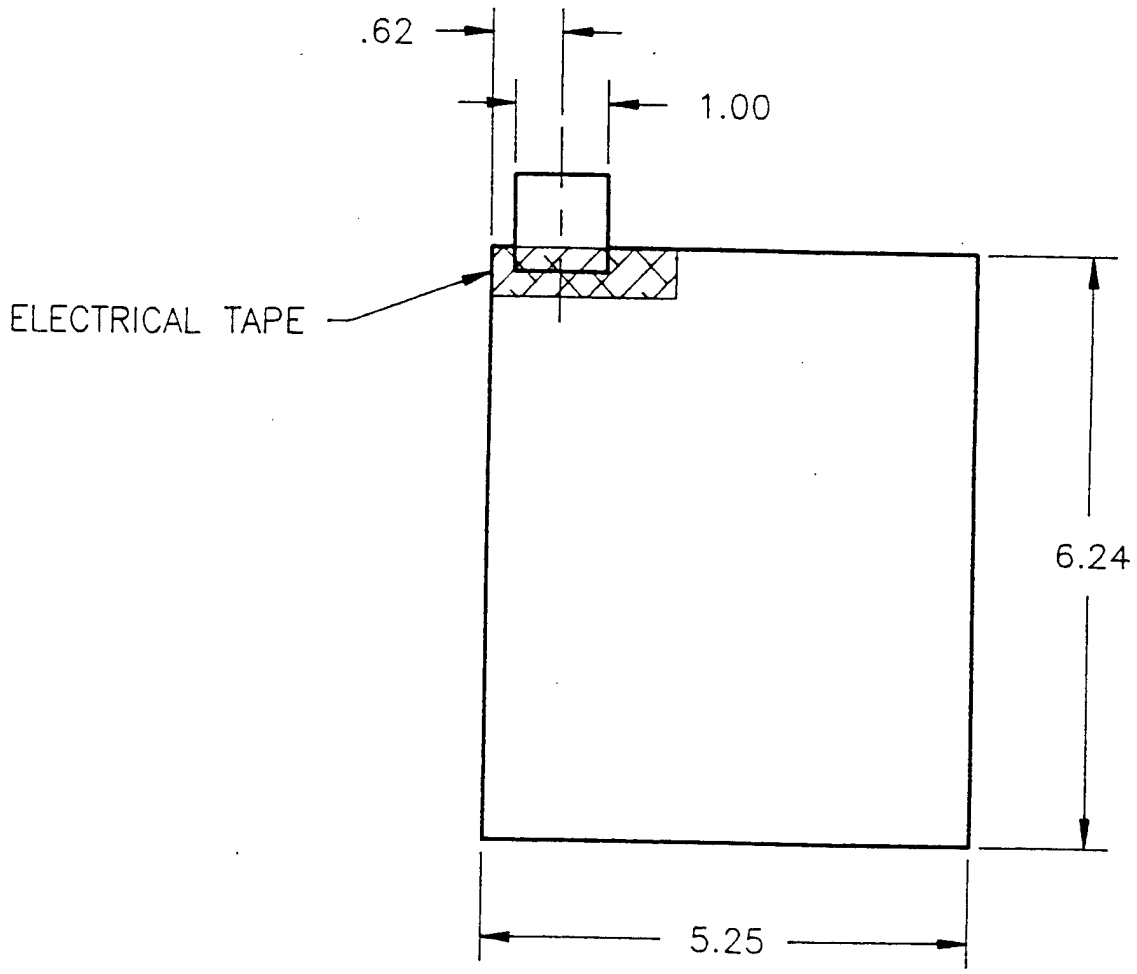

Figure 2.14 Tabbed Positive Plate

1. TABBED CATHODE ASSY.
2. K–869 & 2400 SEPARATOR (K–869 FIRST) FOLDED OVER CATHODE.
3. SEPARATOR EDGES – HEAT SEALED.
4. SEPARATOR CENTER HOLE – HEAT SEALED.*
5. ASSY TRIMMED TO SIZE.

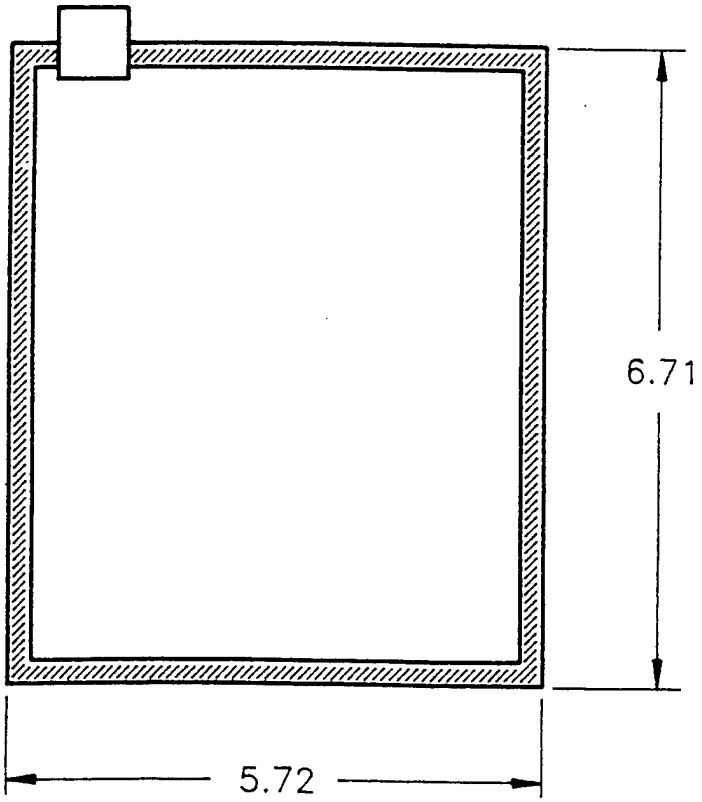

Figure 2.15 Positive/Separator Assembly

* When center hole design variation is used.

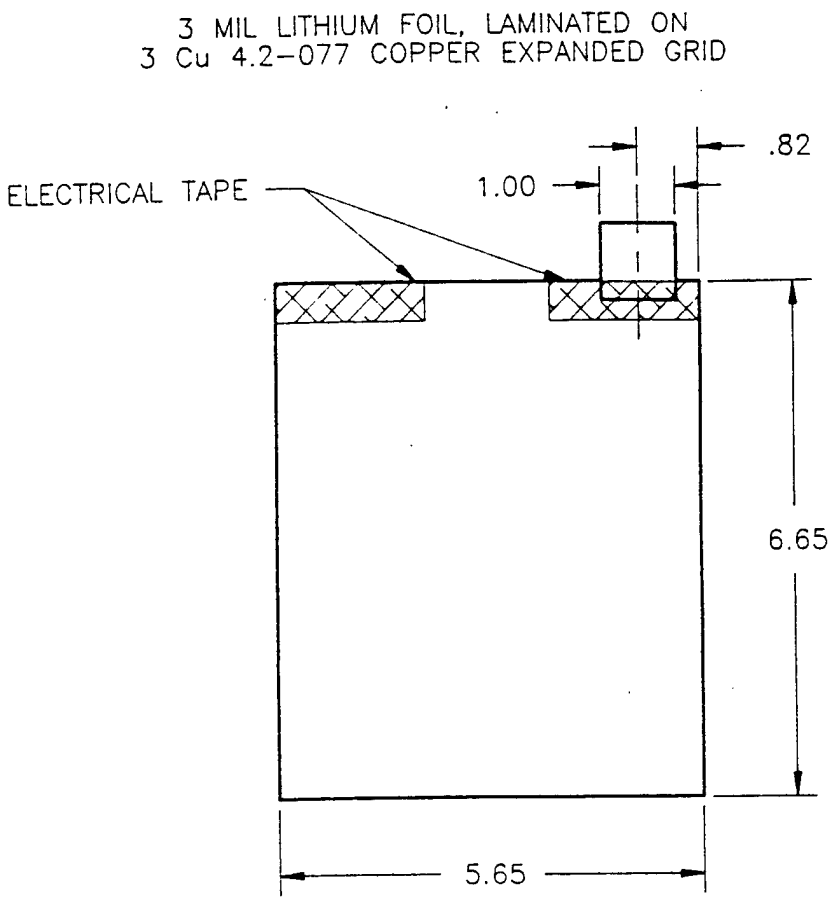

Figure 2.16 Tabbed Negative Plate

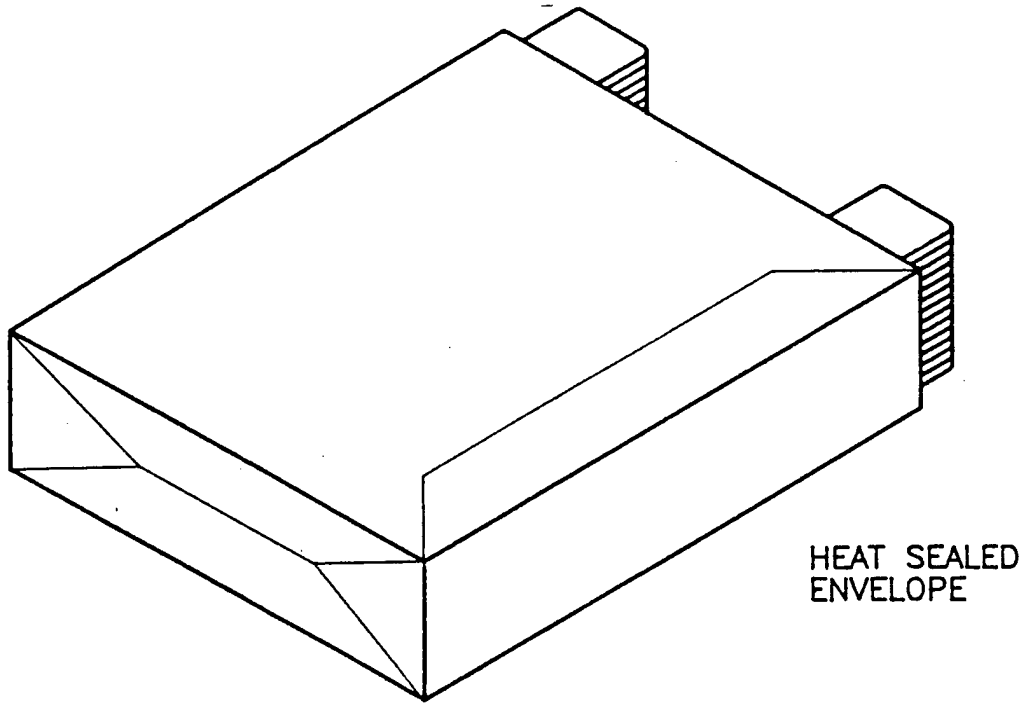

Figure 2.17 Electrode Stack

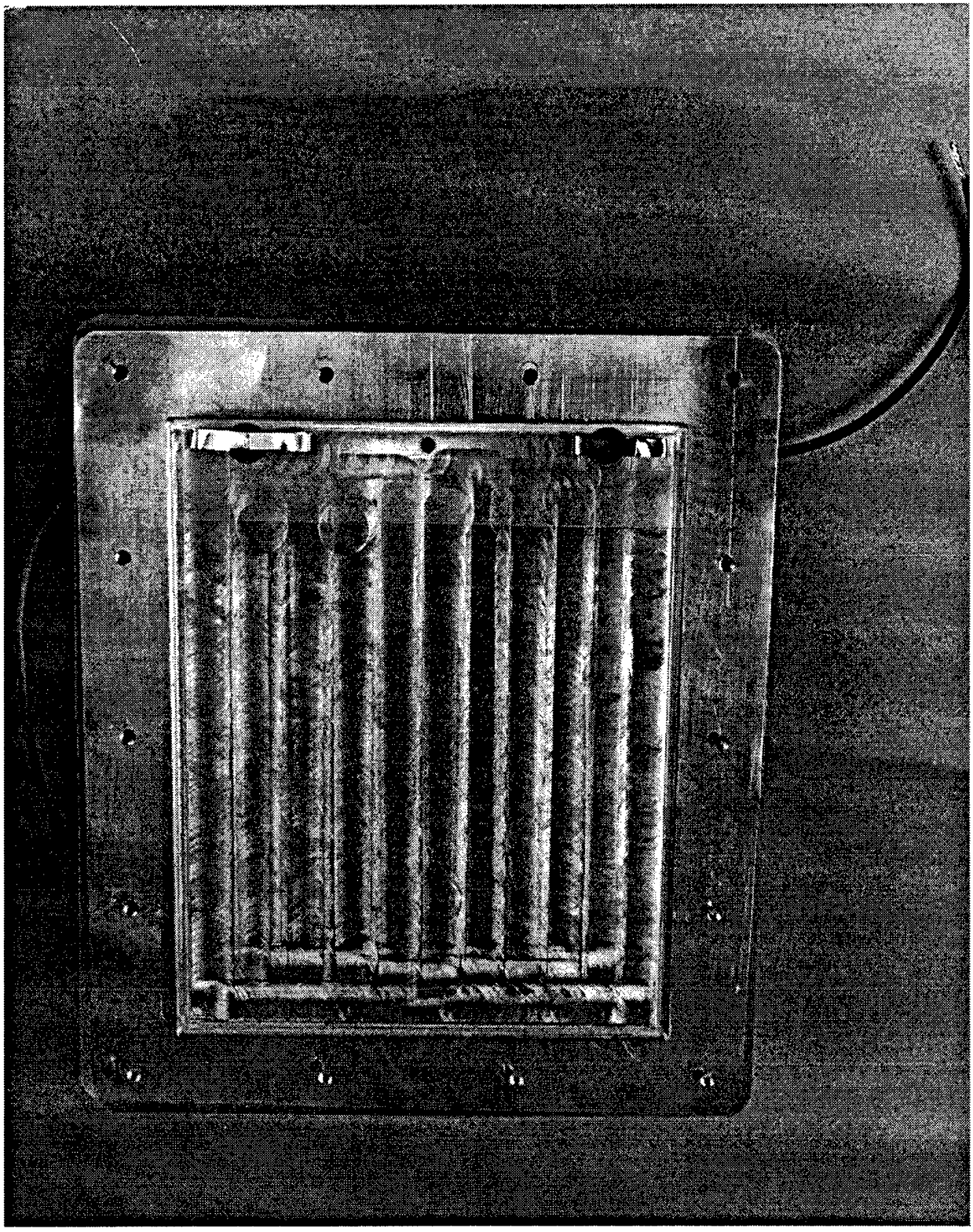

Figure 2.18 Test Fixture Base

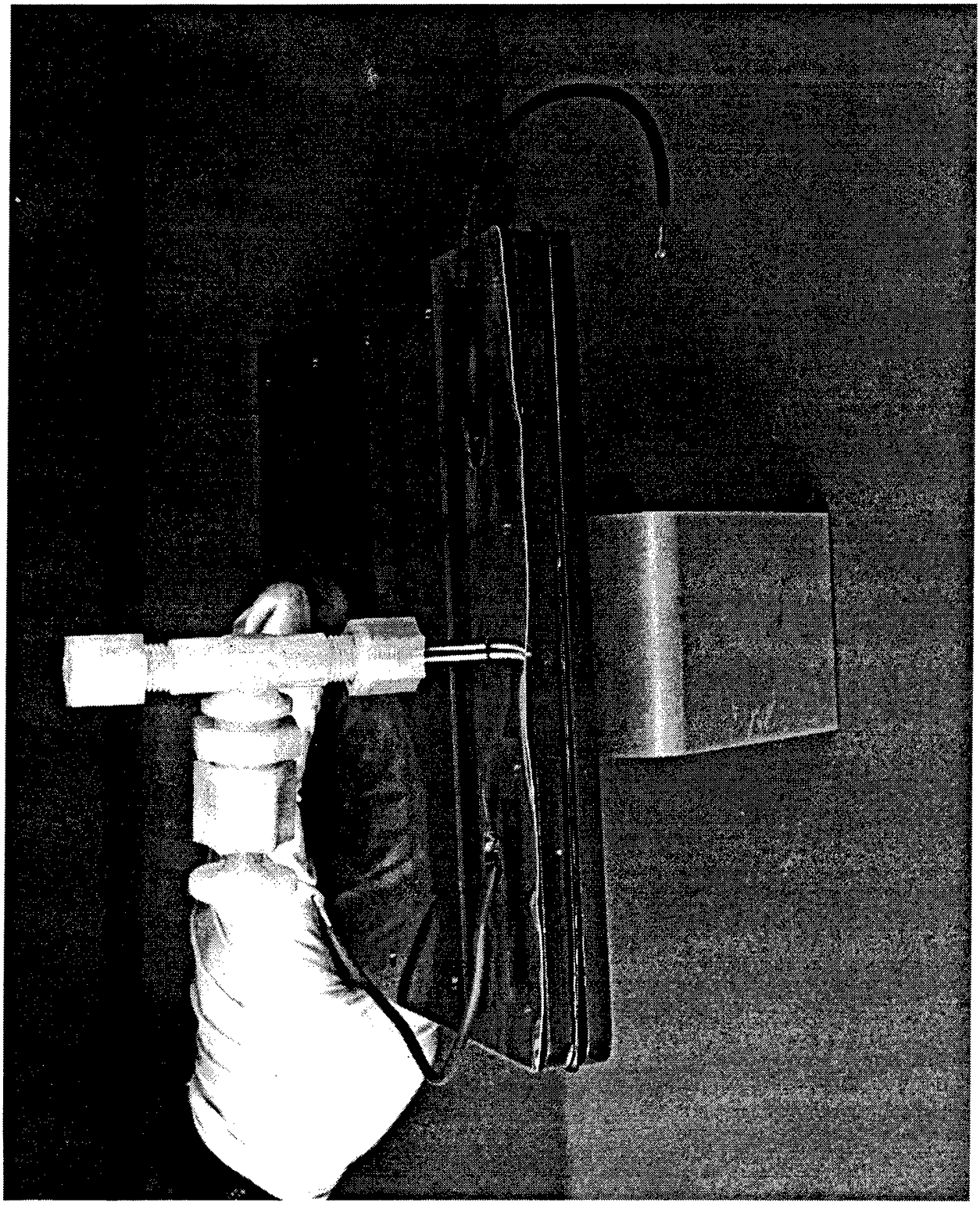

Figure 2.19 Fill Port for Electrolyte Filling

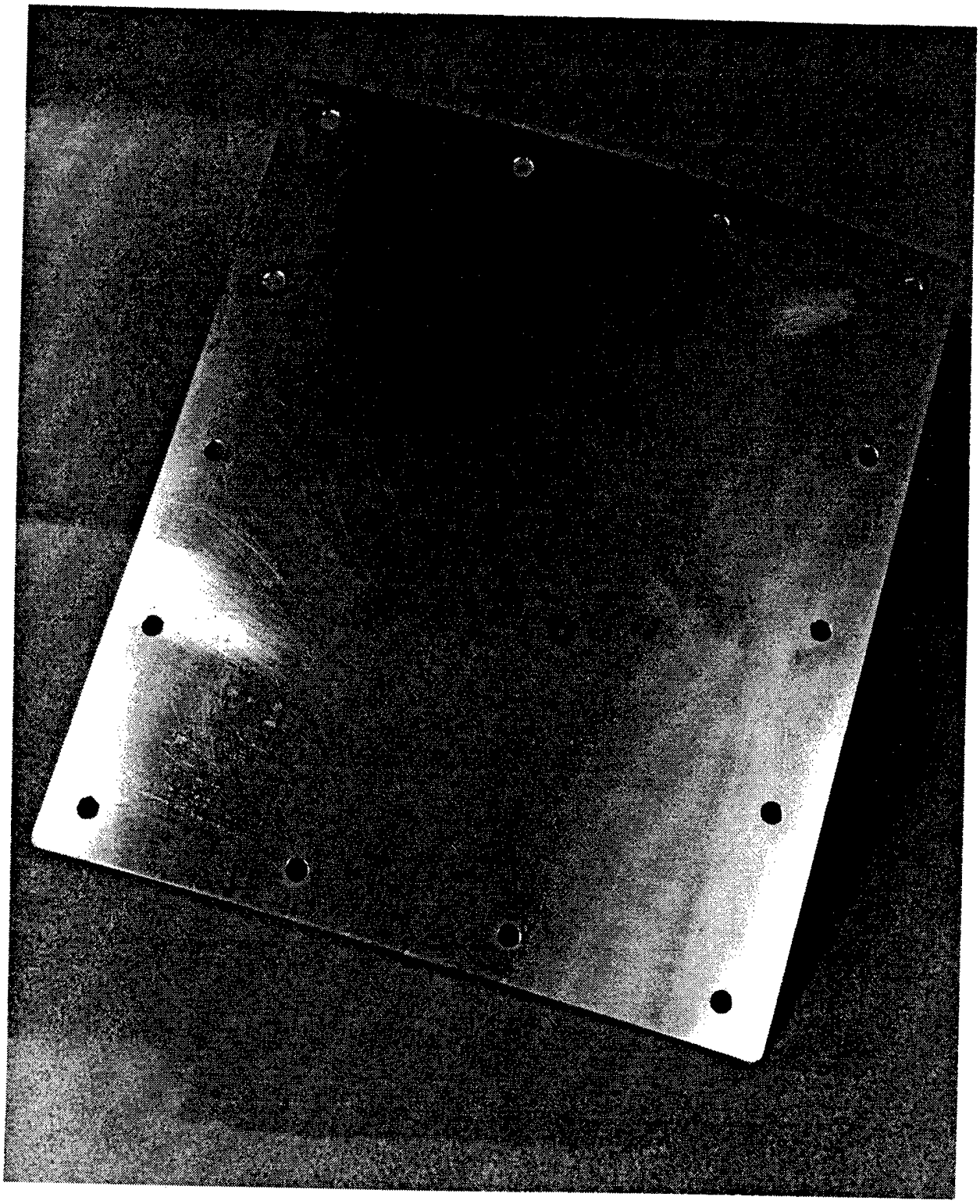

Figure 2.20 Metal Shim Stock

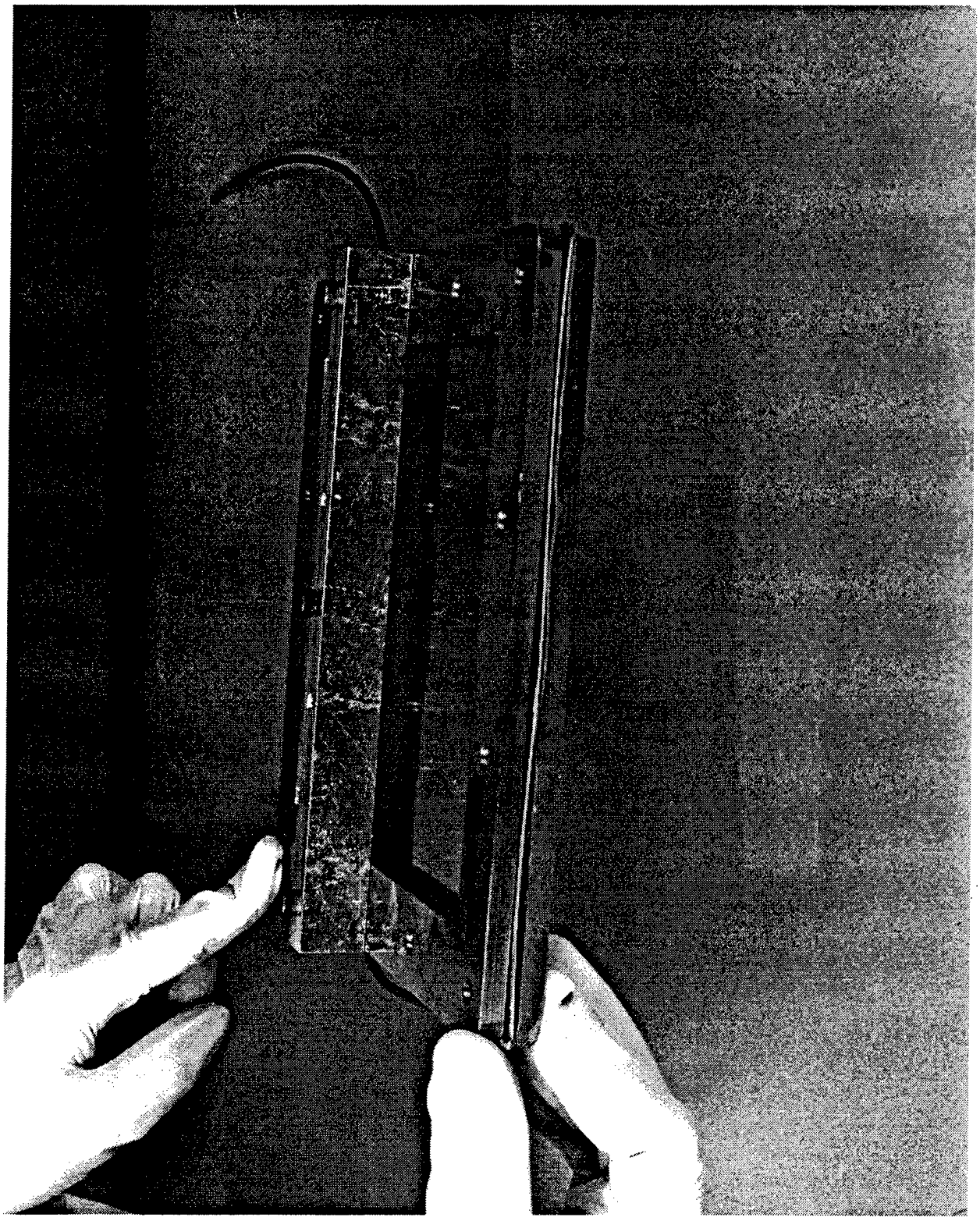

Figure 2.21 Center Support

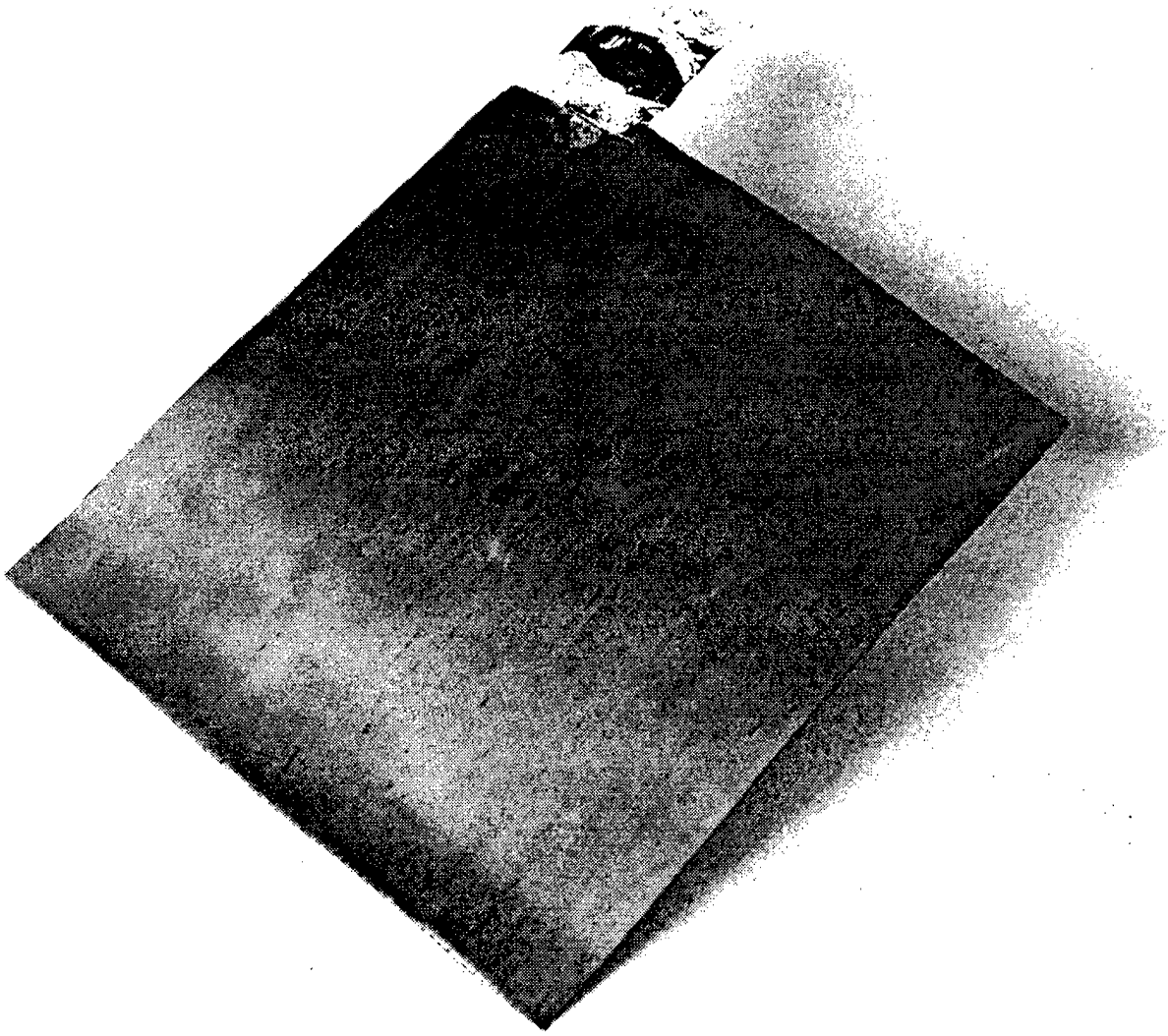

Figure 2.22 Tabbed Positive Assembly

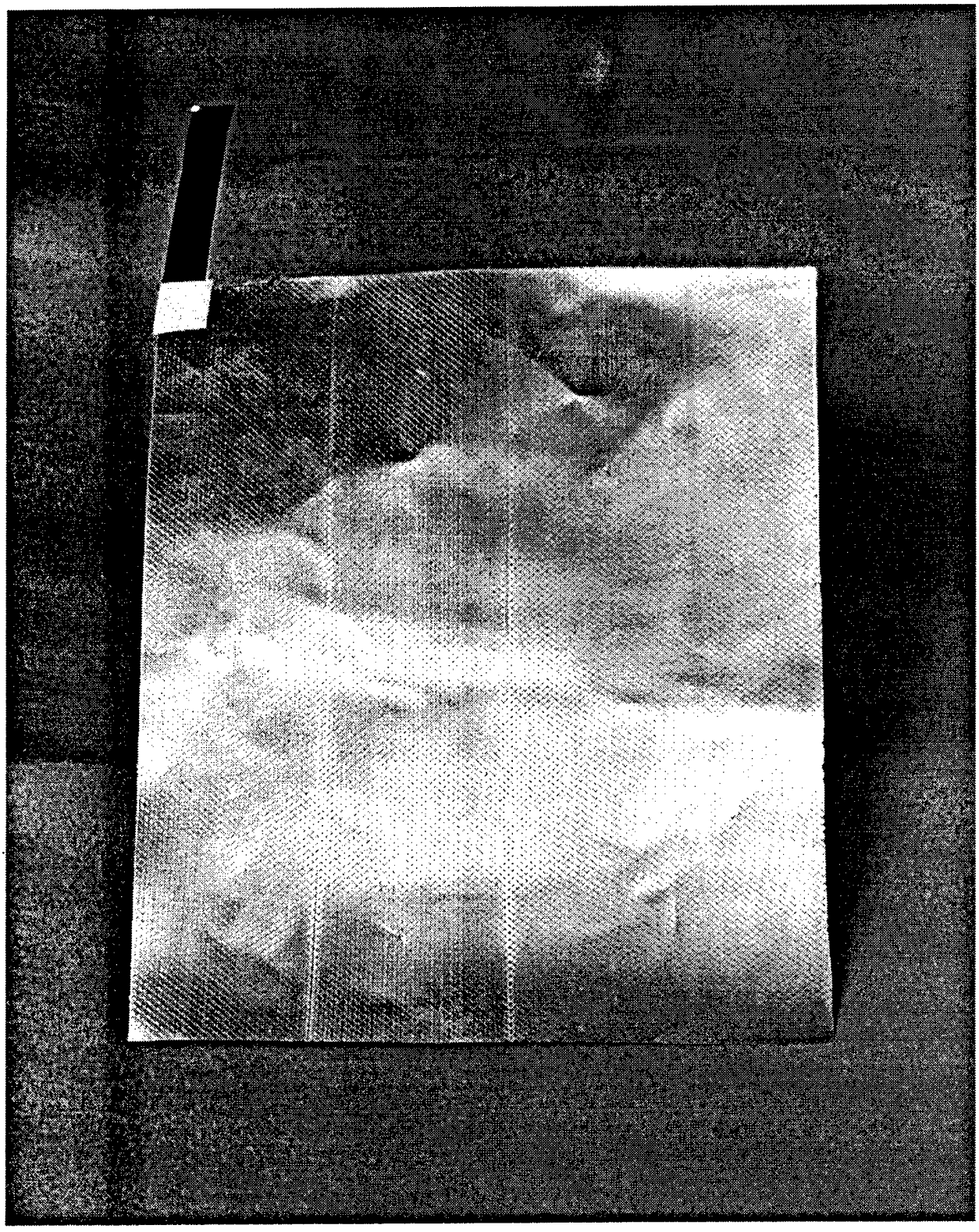

Figure 2.23 Tabbed Negative Assembly

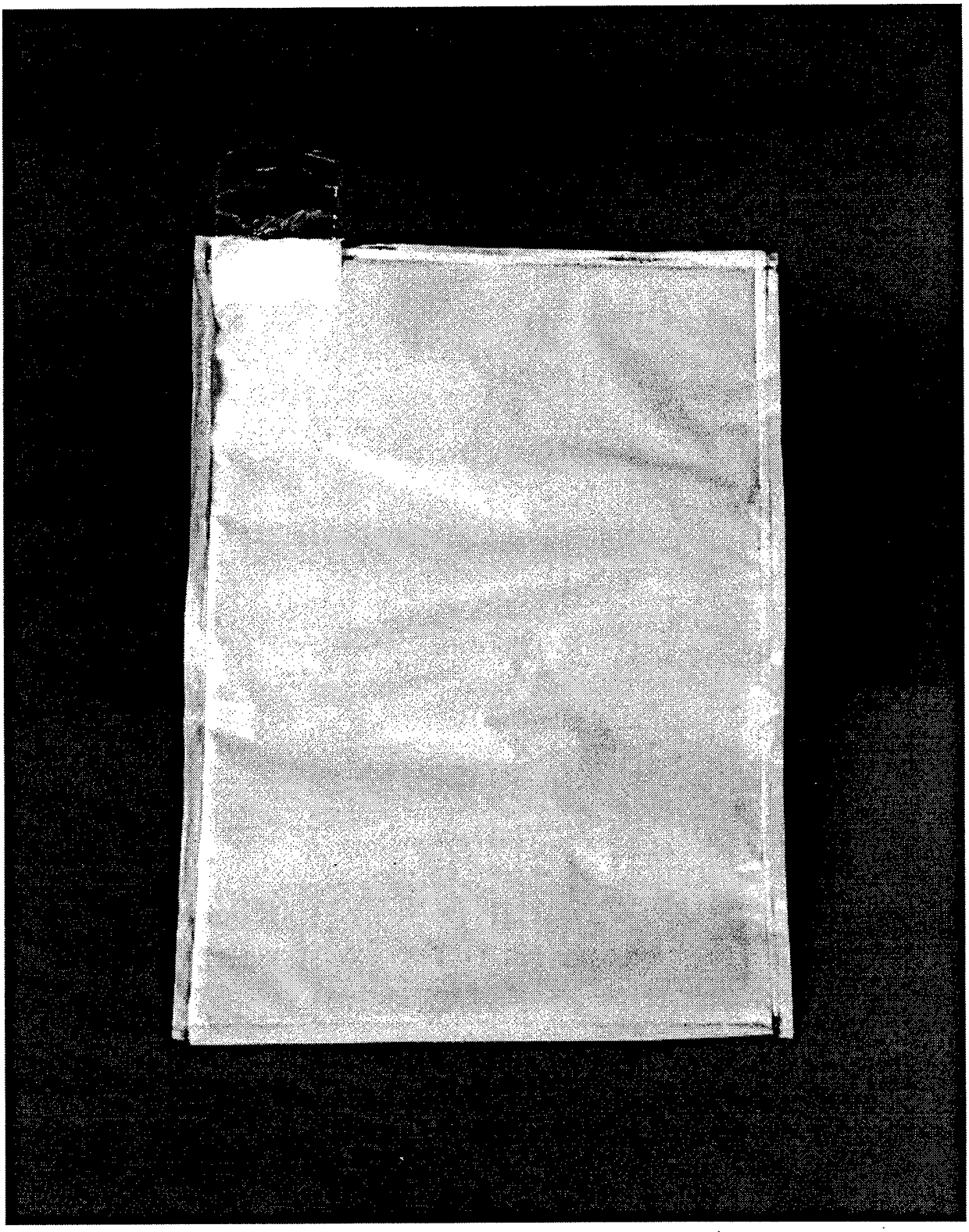

Figure 2.24 Separator/Tabbed Positive Assembly

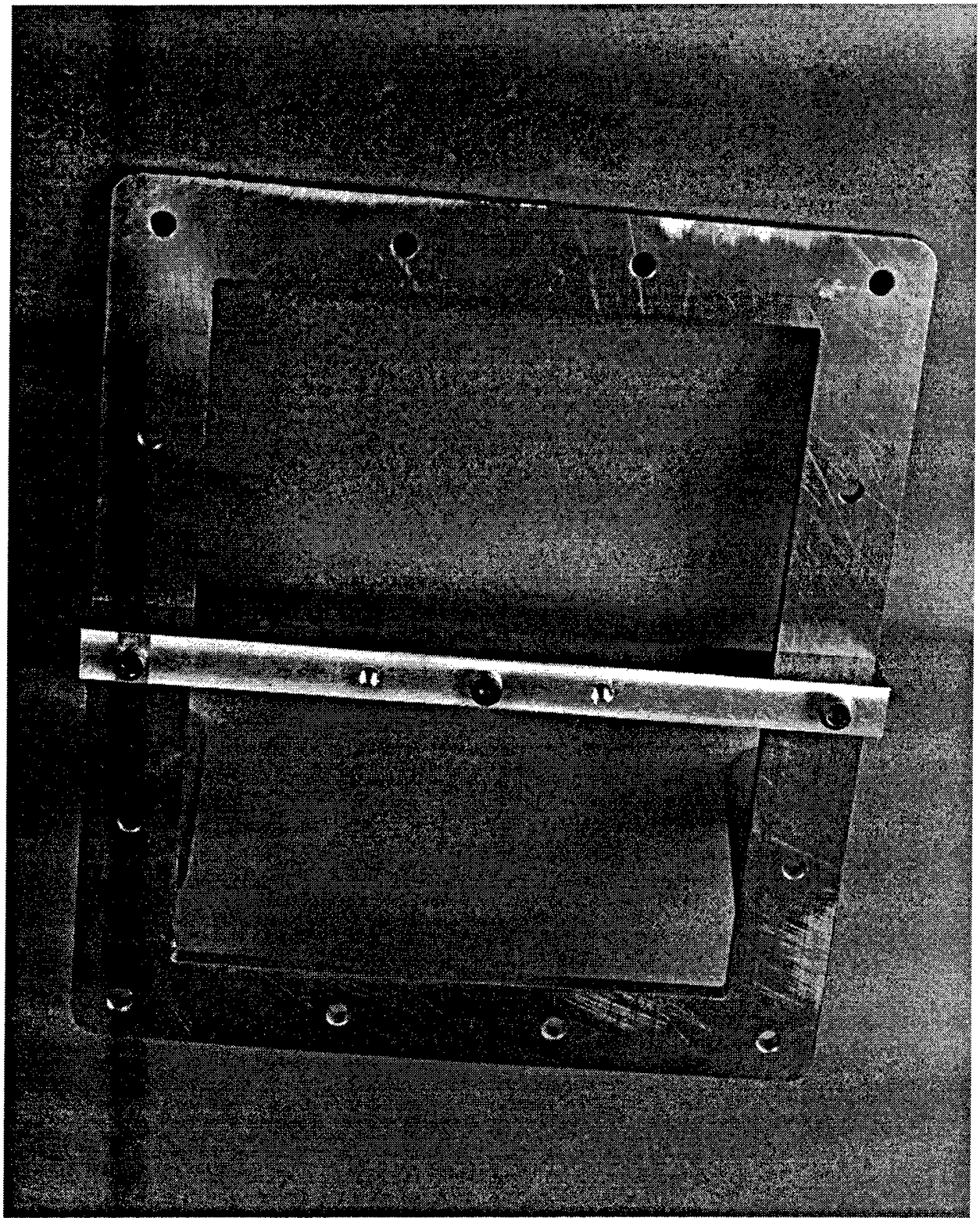

Figure 2.25 Holder Frame

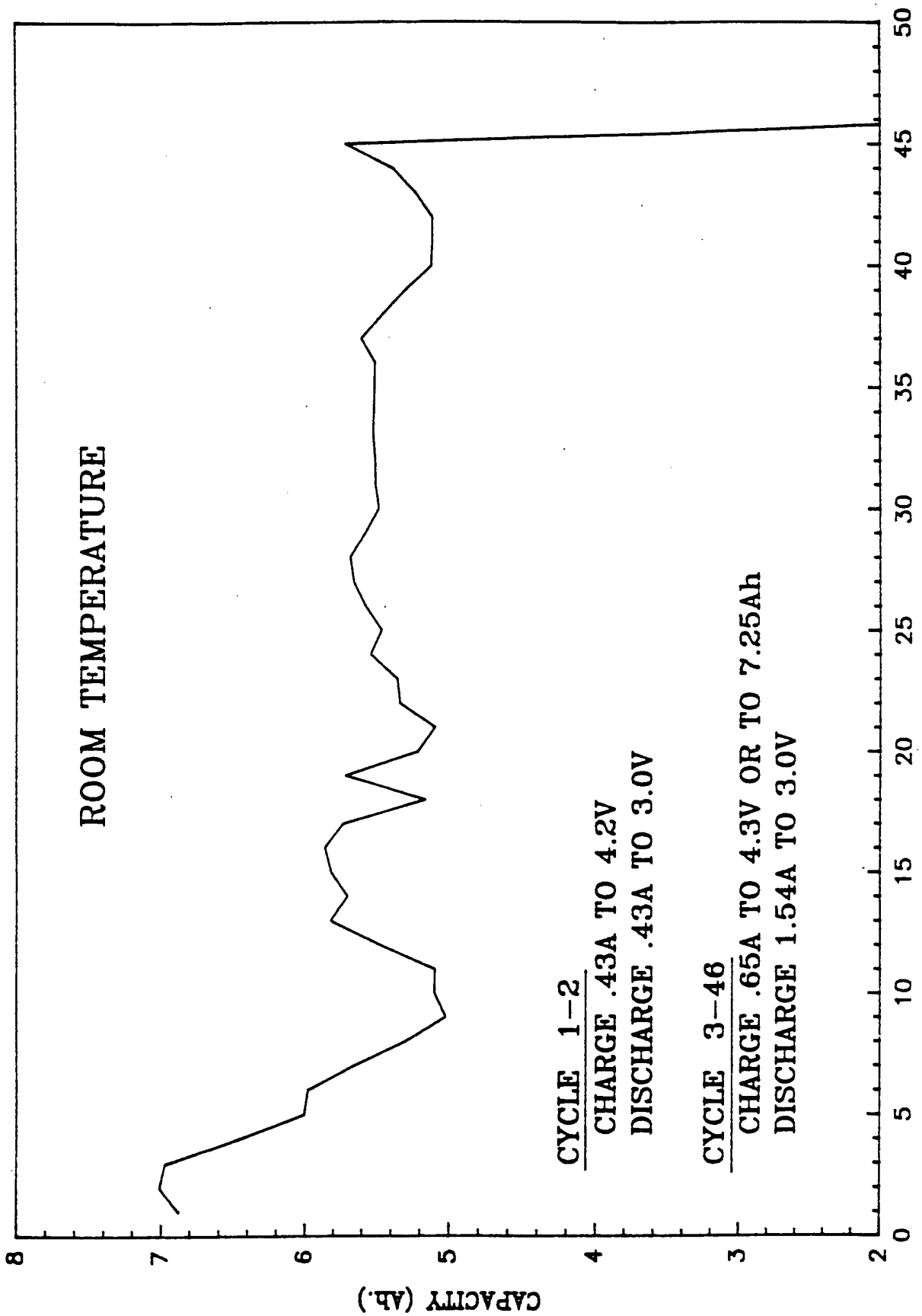

Figure 2.26 Capacity (Ah) versus Cycle Number for Cell Navy T2 Test

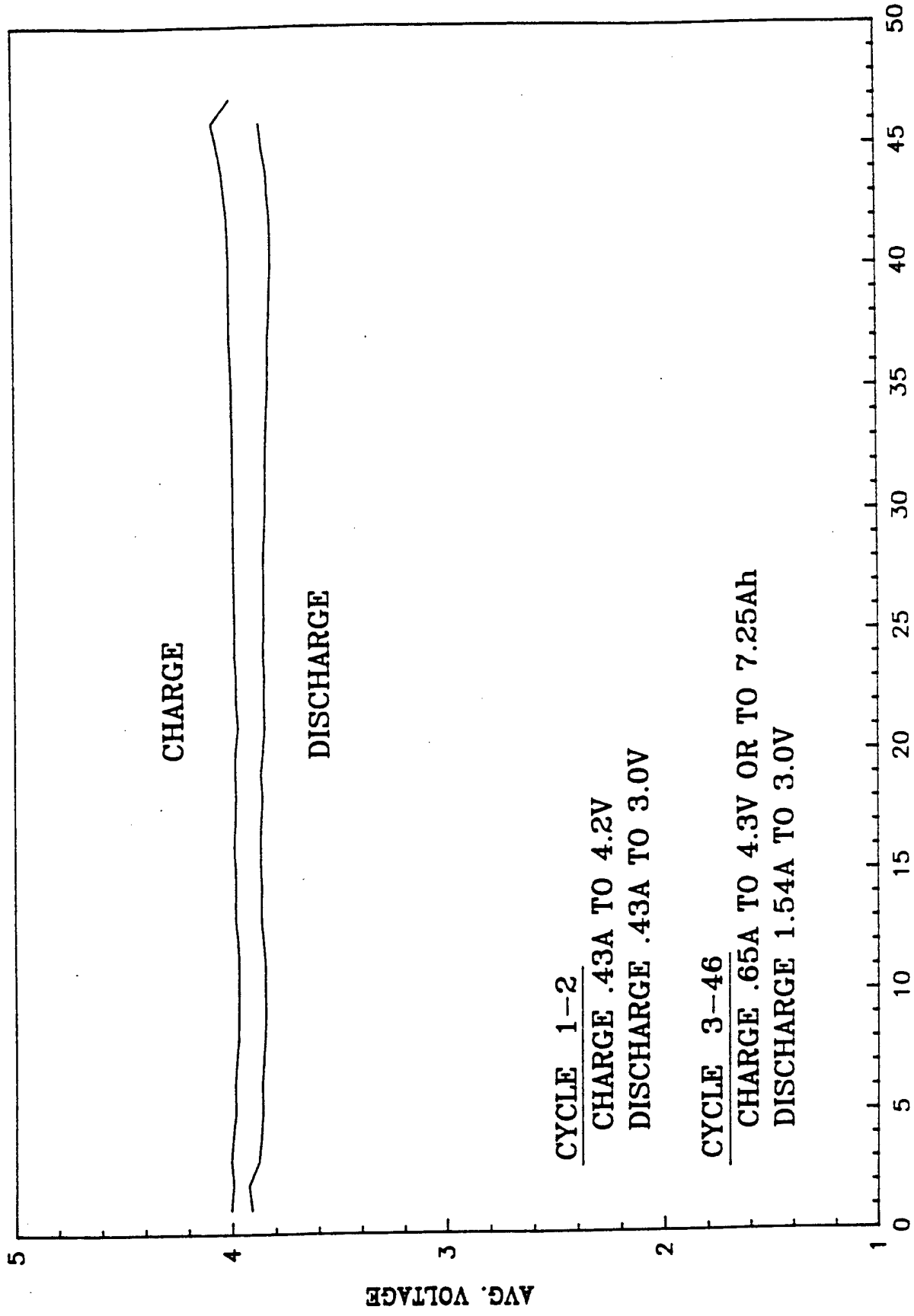

Figure 2.27 Average Voltage versus Cycle Number for Cell Navy T2 Test

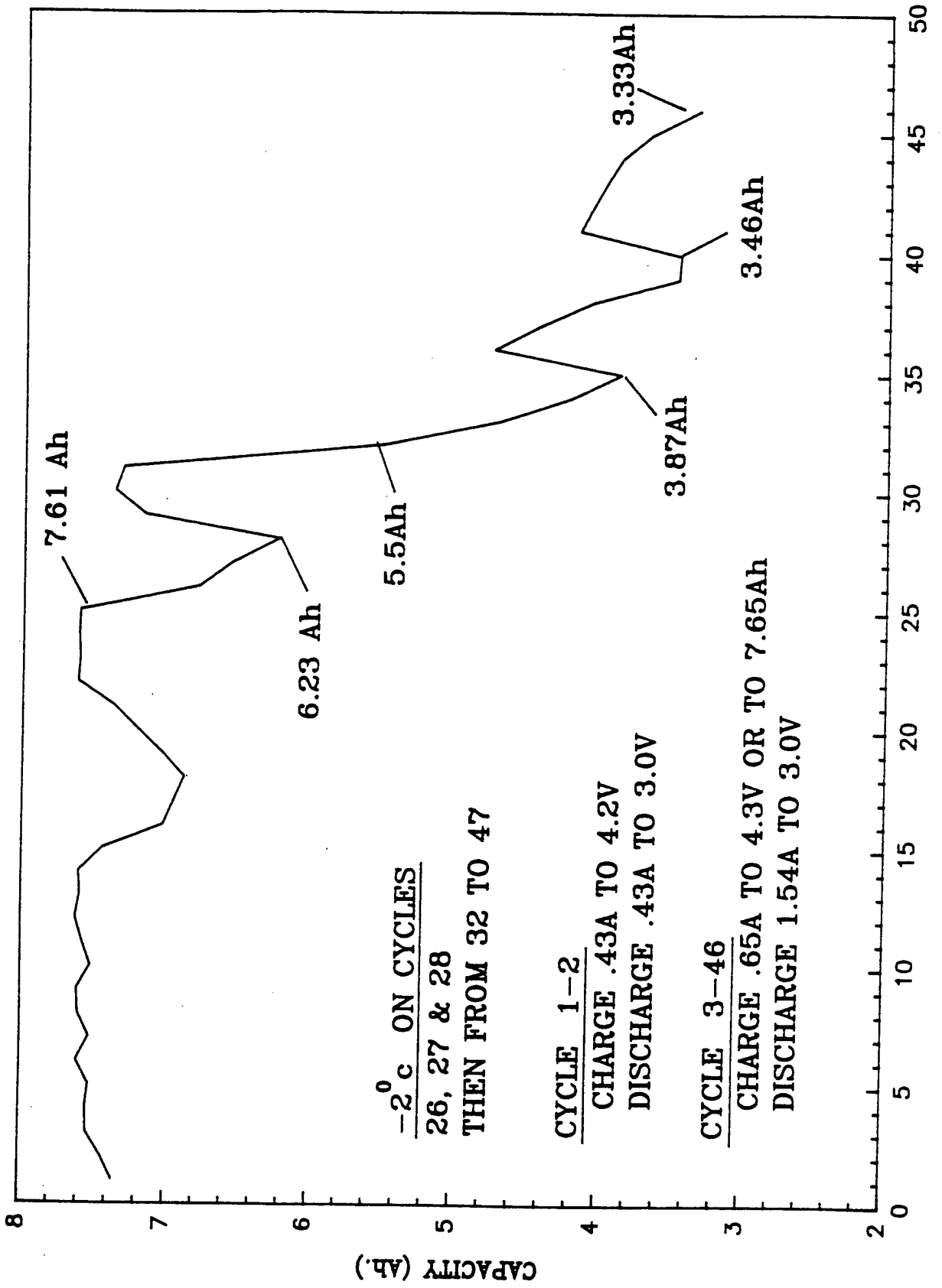

Figure 2.28 Capacity (Ah) versus Cycle Number for Cell Navy T3 Test

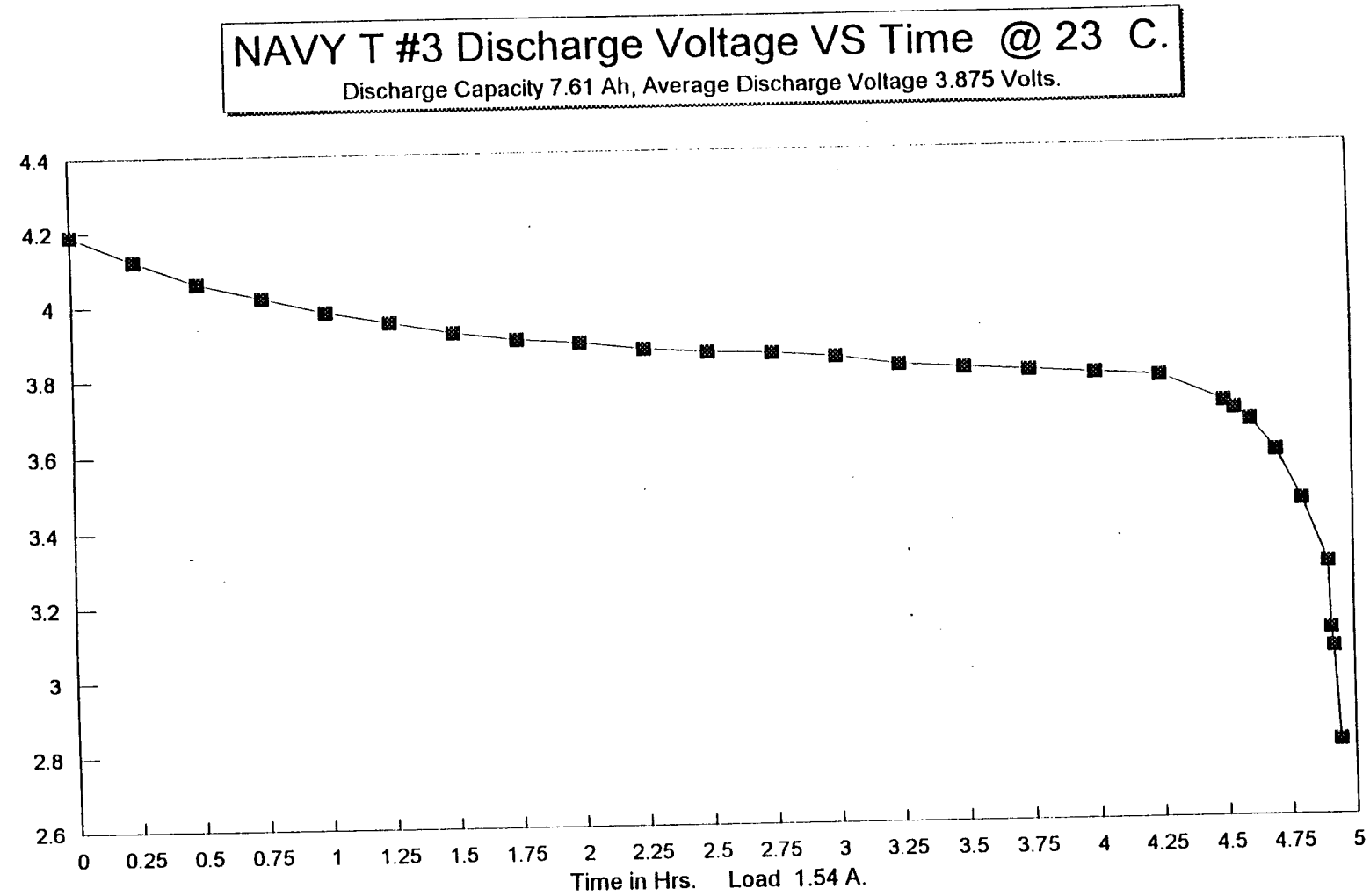

Figure 2.29 Voltage versus Time in Test for Discharge of Cycle Number 25 for Cell Navy T3

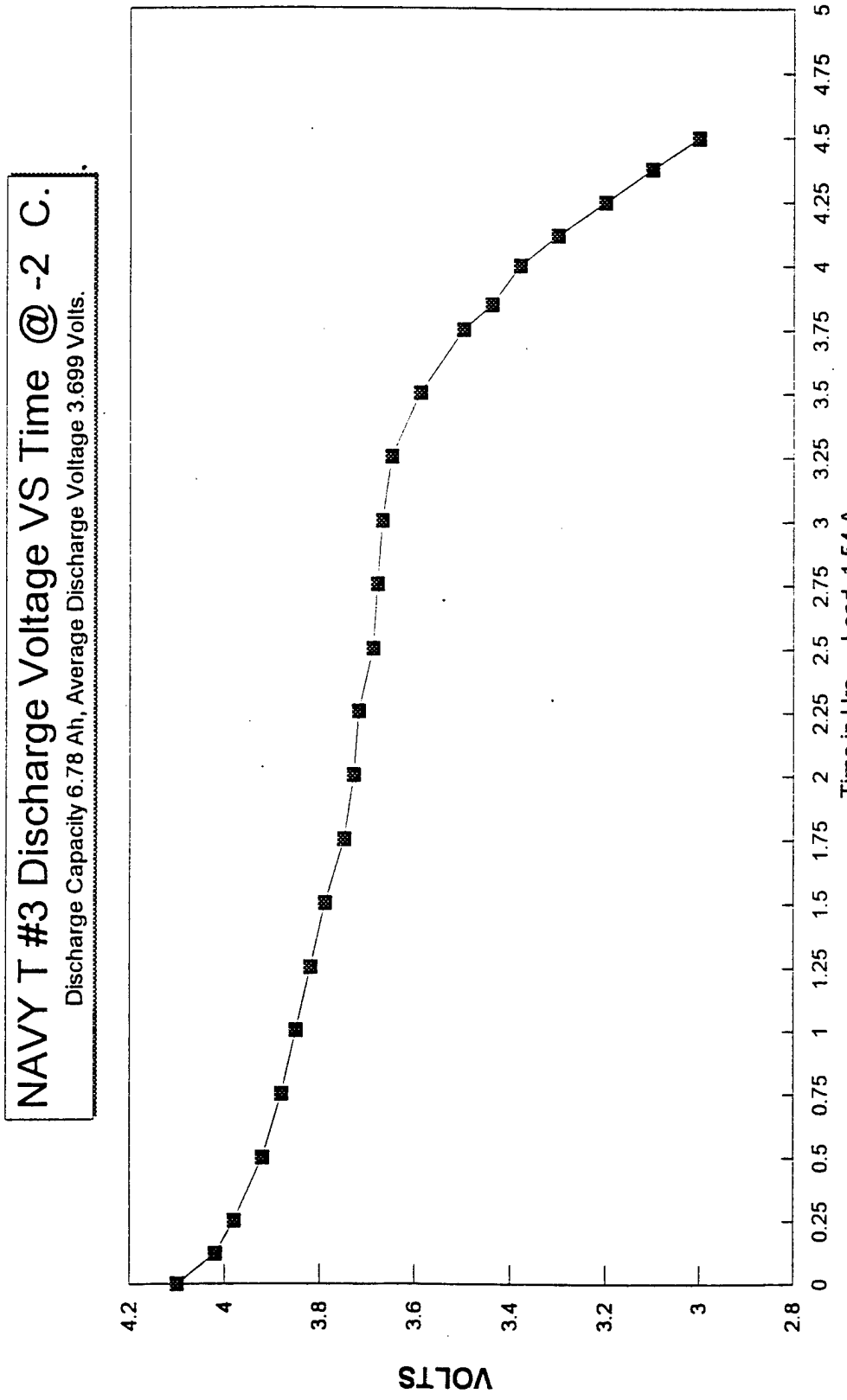

Figure 2.30 Voltage versus Time in Test for Discharge of Cycle Number 26 for Cell Navy T3

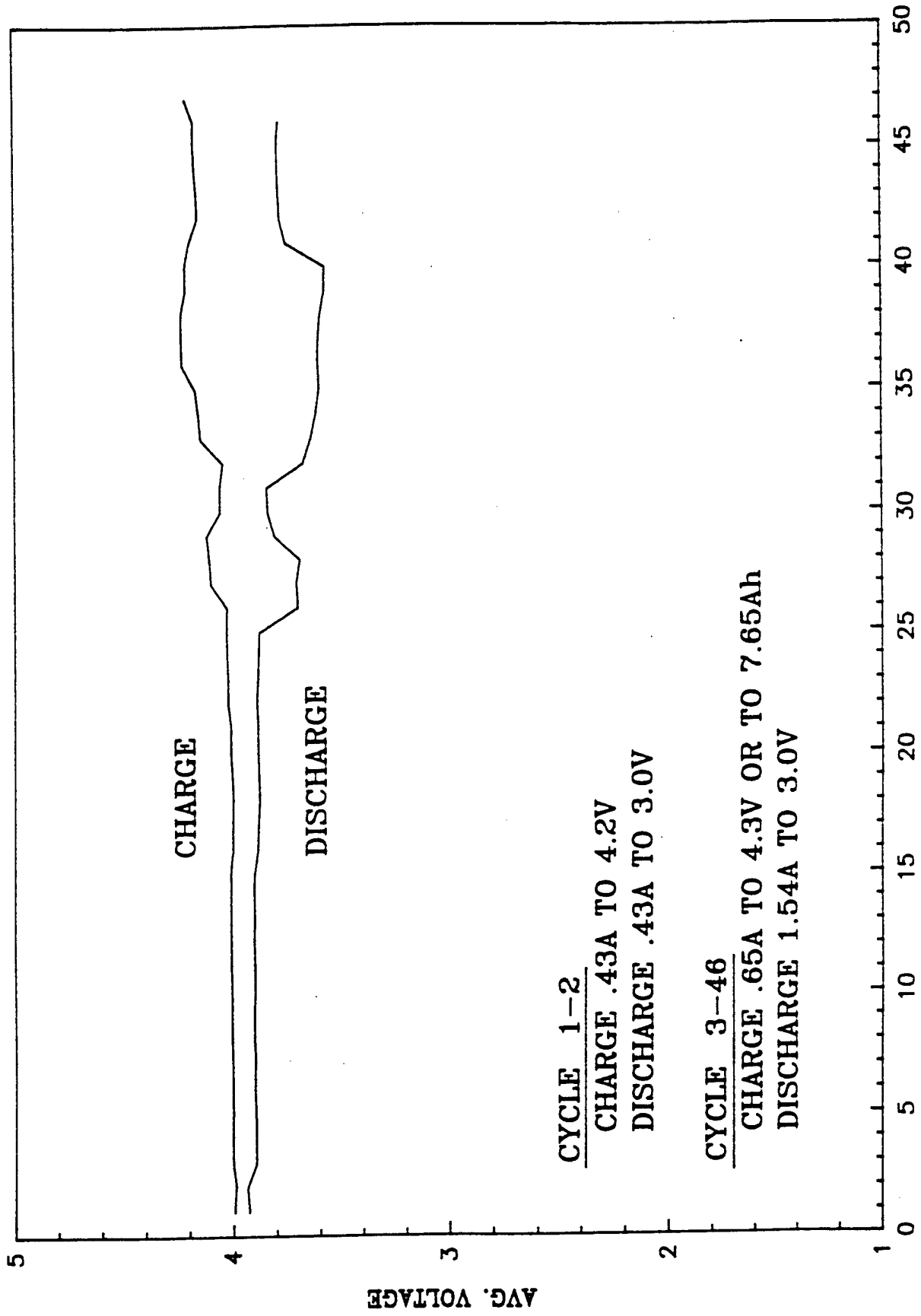

Figure 2.31 Average Voltage versus Cycle Number for Cell Navy T3 Test

Table 2.1 Comparison of Performance of Proposed Li/Li_xCoO_2 with Present Ag/Zn Battery

Chemistry:	$LiCoO_2/Li$
Output:	128 VDC/100 amp
Capacity:	600 amp hours (Ah)
Temperature:	-2C to +35C
Cycle regime:	charge 10 hr, discharge 6 hr
Cycles:	50 minimum
Weight:	776 lbs 352 Kg
Dimensions:	7.88 in x 27.50 in x 59.00 in 20 cm x 70 cm x 150 cm
Volume:	210 liters (L)

System Comparison	Ag/Zn	$LiCoO_2$
Cell weight (lb)	9.46	5.94
Cell volume (L)	1.9	1.2
Cell load voltage (V)	1.5	3.9
Cell capacity (Ah)	320	150
Cell energy (Wh)	480	585
Gravimetric energy density Wh/lb)	50	100
(Wh/Kg)	112	222
Battery capacity (Ah)	320	600
Battery Use Range (hr) (at 60 amp load)	5.3	10
Battery cycle life	20-30	50-60
Battery cells arrangement	80 in series	128, 4 in parallel (module) 32 modules in series

Table 2.2 Proposed Navy SDV 140 Ah Cell Design

$LiCoO_2$/Li Prismatic "Riveted"

Dimensions	1.75 in. x 5.80 in. 7.25 in.* 44.4 mm x 147.3 mm x 184.1 mm	
Volume	1.2 liter	
Weight	6.6 lb	3000 gms.
Replaces	Ag/Zn	
Electrode dimensions:		5.25 in. x 6.12 in. 133.3 mm x 155.4 mm

Total of 57 Negatives and 56 Positives

Negatives:	lithium on copper grid
Positives:	$LiCoO_2$ on aluminum grid
Separator:	Celgard (polypropylene) one Celgard (polyethylene) two
Electrolyte:	1.2M $LiAsF_6$ PC/EC/DMC (1:1:2)
Hardware:	302 SS. Three rivets through.

Expected Performances under C/11 Charge and C/7 Discharge

Voltage (V)	3.8
Ampere Hours	142
Energy	540 Wh
Volumetric energy density	450 Wh/L
Gravimetric energy density	82 Wh/lb 180 Wh/Kg

* Includes wall thickness, approximately 0.04 inches.

Table 2.3 Flat Plate Deflection Study

TEST FIXTURE - SINGLE RIVET

		Dry stack		After electrolyte fill		After 2 cycles (pressure release)		#2 After 67 cycles #3 After 80 cycles	
		Center		Middle points		Middle points		Middle points	
Sample #	Shim stock Mat'l thick.	Without Rivet	With Rivet						
NAVY T2	(.025")	0.066	.000	0.035	0.034	0.025	0.026	0.0685	0.066
NAVY T3	(.025")	0.057	.000	0.040	0.054	0.025	0.022	0.076	0.078
NAVY T4	(.030")	0.03	- .020	0.031	0.036	0.021	0.021		

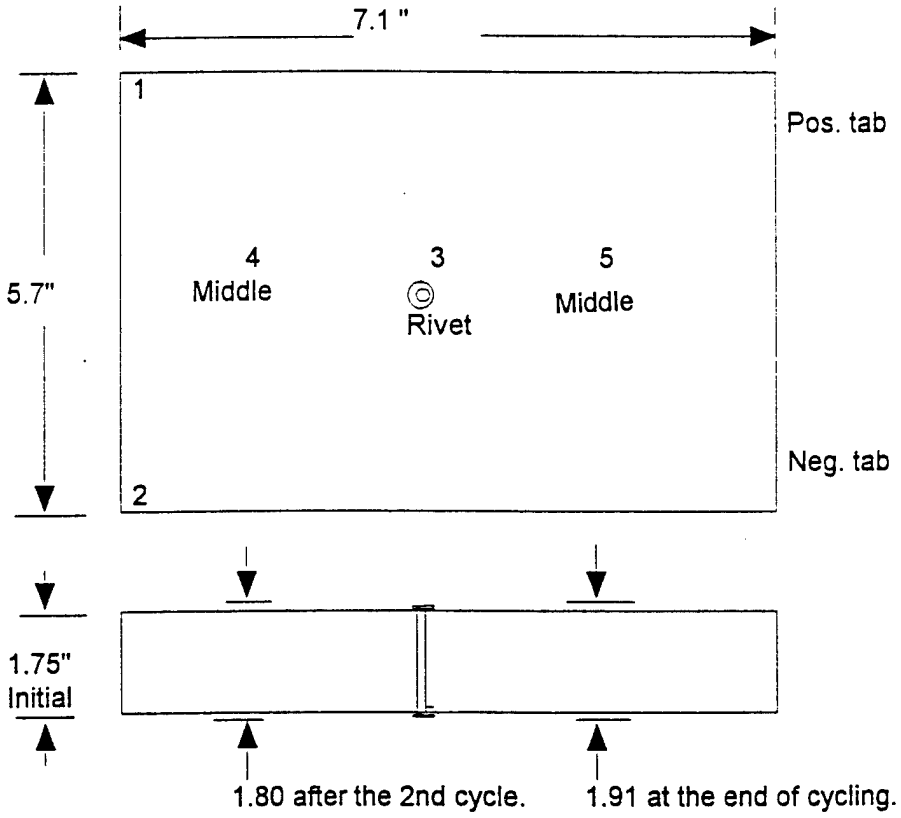

Plate material thickness 0.025 inches.
With a single rivet or support the estimated overall cell stack hight would be increased by 0.050 inches after the two formation cycles.
It could be increased by 0.160 inches through the cycling life of the battery.

Table 2.4 Deflection of a Flat Plate for a Given Area and Pressure

Mat'l. 304 SS Module of Elasticity $E=30 \times 10^6$

Plate Surface 5.8 x 7.2 42.050 Sq.in. Pressure 100 PSI.

Can thick.	in inches			**0.035**	0.060	0.080		0.040	0.060	0.080
Deflection				d1	d2	d3		d4	d5	d6
				Fixed edges				Supported edges		
Sides ratio	l1	L2								
1.0	6.485	6.485	0.04889	0.045	0.006	0.004	0.07634	0.291	0.054	0.036
1.1	6.183	6.801	0.04764	0.046	0.006	0.004	0.07655	0.290	0.054	0.036
1.2	5.920	7.104	0.04878	0.045	0.006	0.004	0.07804	0.285	0.053	0.036
1.25	5.800	7.250	0.05002	0.044	0.006	0.004	0.07920	0.281	0.052	0.035
Center rivet	**3.600**	**5.800**	0.13641	**0.016**	0.002	0.001	0.19001	0.117	0.022	0.015

Fixed edges.

Formula $d=.0284 \times W/E \times t^3 \times (L/l3+(1.056 \times l2/L4)$

Machinery's Handbook
22th edition Page 326

t = .035	.0284 x 100/30/42.8 =	0.00221
t = .06	.0284 x 100/30/343 =	0.00028
t = .08	.0284 x 100/30/512 =	0.00018

t = material thickness
l = small side
L = large side

Supported edges.

Formula $d= 0.1422 \times W/E \times t^3 \times (L/l3+2.21/L2)$

t = .04	.1422 x 300/30/64 =	0.02222
t = .06	.1422 x 300/30/343 =	0.00415
t = .08	.1422 x 300/30/512 =	0.00278

Chapter 3

Development of the 100 Ah Li/Li_xCoO_2 Cell

A series of tests evaluated different design elements considered for the ultimate 100 Ah cell. Most of these tests were conducted using fixtures for the cell cases. A common element was the electrolyte composition which was the 1.2 *M* $LiAsF_6$ in EC/PC/DMC (1:1:2), mentioned previously. Design features which were varied for testing included the number of rivets for deflection control, the effect on electrolyte distribution due to holes (for rivets) in the plates, the number of separators, electrode spacing, and the electrolyte filling technique. The variation in cathode performance as a function of production lot of $LiCoO_2$ was also evaluated.

Cell Navy T5

It was determined that in order to control the swelling of the plates, the final cell would need at least one rivet to tie the two large planar faces of the can together. This cell was put together using another fixture base as the cell top. This is like using a 0.157-inch shim (See Chapter 2). The cell was filled with 27 cc of electrolyte using a back pressure of 60 psig of carbon dioxide (CO_2).

The cell was put on test for two formation cycles at 23°C. At the fifth cycle, the charge capacity was 7.75 Ah and the discharge capacity was 7.43 Ah. The cycling data for the cell (Figure 3.1) show that the discharge capacity remained relatively constant over 36 cycles even though the cell leaked some electrolyte at the sixth cycle. After the sixth cycle there was a high voltage during charging because of the high impedance caused by the electrolyte starvation. Because of the leakage problem, the fixtures were modified to include an O-ring seal in place of the polyethylene gasket.

Cell Navy T6

In order to determine if the O-ring seal design would prevent electrolyte leakage, some tests were run (Table 3.1) using both 0.025-inch shim top plate with three rivets and 0.050-inch shim top plate with one rivet at various pressures (10, 20, 30 psig). The plate was supported at one and three points and the amount of deflection was measured. Since there was not much difference in deflection between the two plates, this cell had three rivets and a 0.025-inch shim top plate. It was filled with 28 cc of electrolyte with a back pressure of 10 psig for 8 hours in order to force the electrolyte to fill the plates. Before charging, the pressure was then reduced to 7 psig to maintain some pressure to force the electrolyte into the plates, and the cell was cycled twice at ambient temperature. The cell was vented before being cycled at -2°C.

After the fortieth cycle (Figure 3.2), the fixture was opened. Some electrolyte had leaked at the bottom of the cell, but there was good absorption of the electrolyte by the cathode under the separator bag. Where the separator bag had wrinkles, there was still a fresh lithium surface indicating that there had been no reaction. The deflection between the rivets and the edges of the cell was 0.066 to 0.067 inches. This indicated that the thickness of the anode had increased from 0.004 to 0.020 inches The fading at cycle 25 was typical for cells cycled at the low temperature. The growth of the anode disturbed the insulation.

Cell Navy T7

This cell had two rivets and a 0.025-inch thick shim end plate to see if two rivets would be sufficient. The cell was cycled at 23°C. At the second cycle the charge capacity was 7.562 Ah and the discharge capacity was 6.448 Ah. The cell shorted at the third cycle. When the cell was opened, there were black spots on the positive plate through the separator indicating the possibility of dendritic growth, which could have been caused by high spots on the cathode. The tape over the positive tab was melted indicating that the tape was not attached properly.

Cell Navy T8

This cell lost vacuum during filling. Because of insufficient electrolyte, the cell would not charge. When the cell was opened, there was a buildup of material on the glass-to-metal-seal. One observation was that the charge imbalance in the first two cycles was larger than previously observed. There was 8 to 12 percent more capacity in the charge relative to the discharge half cycle. Previously, 2 to 4 percent more charge capacity than discharge capacity was observed in the first few cycles. This imbalance started with the use of a new lot of $LiCoO_2$ from FMC. Even after forming the cells, there was 4 percent more charge capacity than discharge capacity. If the cause of this cycling inefficiency was short circuits caused by dendritic lithium (so called "soft shorts"), then the addition of an extra layer of polypropylene separator should help. For that reason, Cell Navy T9 was made with the extra separator.

Cells Navy T9 and T10

Cells were built with the plates cut to the dimensions and configuration anticipated for the final 100 Ah cell (See Figures 3.3 and 3.4). A cell was built that was nominally 7.7 Ah cell (labeled as Cell Navy T9) and a nominal 35.8 Ah cell (labeled as Cell Navy T10). Both positive and negative plates were die cut to give reproducible dimensions. The positive plate was based on our standard paste on expanded aluminum grid and the negative was a 0.004 inch lithium metal foil on one side of an expanded copper grid current collector. Figures 3.3 and 3.4 show the plate design for the negative and positive plates. The figures show the position of the rivet holes. Both Cells Navy T9 and Navy T10 were constructed without rivets. Therefore, these holes were not cut. These cells were put on test for two formation cycles at 23°C followed by cycling at -2°C.

Cell Navy T9

This cell was constructed from three positive plates (5.25" x 6.12" x 0.0165") and four negative plates (5.63" x 6.5" x 0.0045"). The positive plates were inserted into a sack constructed from three layers of separator on each side. The layout for the sack is shown in Figure 3.5. The outer layer of each wall of the sack was Celgard 2400 polypropylene separator and the two inner layers were of Celgard K-869 polyethylene separator. Two sets of these three layer assemblies were heat sealed together around three sides, as shown in Figure 3.5, so that the Celgard K-869 is next to the positive plates and the Celgard 2400 separator is next to the negative.

The first two cycles for formation were at 23°C under constant current conditions. The cells were charged at C/17 rate (0.43 A) to a 4.2 V upper voltage limit and discharged at C/17 (0.43 A) to a 3.0 V lower voltage limit. After the second cycle, the cell yielded a charge capacity of 7.063 Ah (0.133 Ah/g vs. 0.140 Ah/g theoretical based on $LiCoO_2$ in the cell) and a discharge capacity of 7.013 Ah (0.132 Ah/g based on $LiCoO_2$ in the cell). The cell was cycled for two more cycles at 23 °C with a charge rate of 0.63 A (C/11.5) to 4.3 V and a discharge rate of 1.54 A (C/5) to 3.0 V. After two cycles under these conditions, the observed charge capacity was 7.500 Ah (0.141 Ah/g based on $LiCoO_2$ in the cell) and a discharge capacity of 7.453 Ah (0.140 Ah/g based on $LiCoO_2$ in the cell). At this point, the cell was placed in a chamber at -2°C.

The cell was cycled using the same currents for both charge and discharge as in the last two cycles at 23°C. However, the charge half cycle was limited to either a 4.35 V endpoint or 7.5 Ah, whichever came first. The higher upper voltage limit at -2 °C was chosen to compensate for over-voltages caused by the lowered reactivity of the cell at lower temperatures. The discharge limits were unchanged (see above). The capacity (Ah) versus cycle number data of this cell are presented in Figure 3.6. The cell cycled well up to the fifth cycle at -2°C. At this cycle, the cell showed an over-voltage when the charge half cycle was initiated. The voltage jumped up and then returned to a normal charge profile. There was a difference in the overvoltage starting with the thirteenth cycle. This over-voltage increased as the test progressed. The charge step was cut off by the 7.5 Ah cycling limit up to cycle 12, after which the cell reached the 4.35 V upper voltage limit well before the cell reached the capacity cycling limit. As indicated in Figure 3.7, the capacity for cycle 13 was 7.325 Ah.

The swelling of the stack was quite noticeable. At cycle 23, the deflection in the unsupported regions of the stack were observed to be on the order of 0.04 inches. As a hypothesis, it was assumed that the swelling of the stack had caused the cell to become electrolyte starved. The cell was stopped at cycle 23 and 20 cc.of electrolyte were added (the cell was initially filled with 27 cc.of electrolyte). The addition of the extra electrolyte helped the cell recover capacity along with the disappearance of the over-voltage when the cell started in its charge half cycle. The cell quickly lost capacity and was allowed to cycle in this low capacity condition for a total of 80 cycles.

The cell was disassembled and the electrode plates were measured. The results of the thickness measurements are presented in Table 3.2. The data show that the overall stack growth

was 0.074 inches. This number was in good agreement with the 0.068- to 0.073-inch growth measurements made before disassembly. The majority of the increase in stack height was the result of the increase in thickness of the anode. The anode also had little electrolyte. All of the remaining electrolyte in the cell was found in the separators and cathodes (positive plates). Thus it seems that the cell developed a high impedance due to electrolyte starvation at the anode. The anode was covered with a mossy lithium layer which must have been the result of charging a lithium electrode at low temperatures. Only the lithium directly against the separator was in contact with any electrolyte. There were several places where a wrinkle in the separator caused a dry spot on both the cathode and anode adjacent to the wrinkle.

Cell Navy T10

Cell Navy T10 was a nominally 32 Ah cell built similar to cell Navy T9. The electrode assemblies were as described in Figures 3.3 through 3.5 using 14 positive and 15 negative plates. The cell was assembled using the external support arm shown in Figure 2.21. The cells were formed by charging at C/17 rate (2.03 A) to a 4.2 V upper voltage limit and discharging at C/17 (2.03 A) to a 3.0 V lower voltage limit. The second charge capacity was 33.199 Ah (0.129 Ah/g $LiCoO_2$) and the second discharge capacity was 32.141 (0.125 Ah/g $LiCoO_2$). The cell was then cycled at -2°C (Figure 3.8) The cell was charged at C/10 rate (3.02 A) to either a 4.35 V upper voltage limit or a 32 Ah capacity limit. The cells were discharged at C/6 rate (4.99 A) to a 3.0 V lower voltage limit. After cycle 17, the cell reached the 4.3 V cutoff before it reached the 32 Ah endpoint. The data show that after cycle 22 the cell quickly deteriorated in terms of performance. The hysteresis in average charge and discharge voltages increased, indicating an increase in cell impedance, and the capacity declined. By cycle 30, the discharge capacity was only 23.45 Ah.

The cell was placed at room temperature (23°C) at cycle 31 to see if it would recover. A comparison of voltage-time profiles for cycles 30 and 31 are given in Figure 3.9. As shown, the capacity of the cell continued to decline. In the first 20 cycles at 23°C, the capacity dropped to 10 Ah, and the cell ended its test at 9 Ah at cycle 60. Clearly, the deterioration that started at cycle 22, at -2°C, continued at 23°C.

In general, we can ascribe the observed performance of both Navy T9 and Navy T10 to low temperature cycling. In order to determine if the performance of the two cells was affected solely by the temperature, or limited by the cell chemistry, or other factors, three 4/5A cylindrical cells were built using Lot #104 of the FMC $LiCoO_2$ which was the same lot of material used in Cells Navy T9 and T10. These cells had the typical capacity decline after 17 or 18 cycles (Figure 3.10). A third cell, C473, was discharged at -2°C, starting with the fourteenth cycle, the capacity decreased, but the slope of the discharge curve was similar to Cells C468 and C469 which continued to be discharged at 23°C.

In the cylindrical design, the hardware does not allow the negative plates to increase in thickness once the radial equilibrium between the electrode expansion and the can is reached. This is not the case with a prismatic enclosure where any flat surface will have the tendency to conform to a more stable circular profile as the internal electrode expansion forces progress.

Therefore, the performance of the Cells Navy T9 and Navy T10 was affected more by the expansion of the negative electrodes at the low temperature than by the electrochemistry.

Better methods for filling the cells with electrolyte were investigated. The filling of cylindrical cells is simplified by the ability of these cells to withstand higher pressures. Thus electrolyte can be forced into the separator and cathode pores. Prismatic cells cannot withstand such pressures, so alternative filling methods are needed. In order to fill the cell with electrolyte under pressure, the expansion of the cell was controlled by clamping it in a fixture composed of heavy plates bolted against the large faces of the can. (Further discussed in Chapter 4.) The cell was evacuated and flushed several times under pressure with a mixture of the solvents that are used for the electrolyte and carbon dioxide in order to remove the oxygen. The cell was filled with electrolyte under pressure. After the formation cycles, the pressure was released and the cell was removed from the clamping fixture.

Cells Navy T11, Navy T12, and Navy T13

These were the first cells built with plates that had holes for the rivets (Figures 3.3 through 3.5). Cells Navy T11 and Navy T12 were damaged during assembly. These cells had 0.025-inch thick shim end plates. Cell Navy T13 was filled with 20 cc of electrolyte at 10 psig of pressure. The cell was cycled for 33 cycles (Figure 3.11), after which the cell was opened. The glass-to-metal seal for the positive terminal was cracked and showed some corrosion. This could have led to electrical shunting across the seal. No gas or liquid was expelled. The positive plates were flexible and evenly discharged. One positive plate had one small black dot. The opposite negative plate was evenly discharged. The edges around the holes for the rivets showed fresh lithium which indicated that there was good spacing between the positives and the negatives. The thickness of the negative plates at the center of the plates (between rivets) was 0.020-to 0.022-inches and 0.012-inches for the end plates.

The following observations can be made: (1) having holes in the center of the plates improves the distribution of the electrolyte in the center, and (2) the anode will increase in thickness wherever space is available.

Cell Navy T14

Cell Navy T14 was built to test out the hardware for the final cell construction. This cell consisted of ten separator/positive plate sandwiches with holes punched for accepting rivets and 11 negative plates similarly perforated for rivets. The remaining volume in the cell can was taken up by polyethylene blocks of the appropriate dimension. The cell was built and closed like the final cell would be except for the presence of the polyethylene blocks. The cell was filled with electrolyte at 8 psig and this pressure was released after the first discharge because it was thought that it was not necessary to wait for two cycles.

The capacity fade behavior of the cell is shown in Figure 3.12. The capacity faded between cycles 25 and 30, which is typical of cells made with $LiCoO_2$. However, the cell recovered after cycle 30 and steadily increased. At cycle 46 the cell had a capacity of 22.6 Ah. The performance was probably caused by temperature fluctuation in the freezer. At the time that the capacity decreased, the average charge and discharge voltage decreased. The temperature of the chamber may have fluctuated by 10 to 12°C.

Cathode Material Performance - Lot Variation

Cell capacity can decline from one cell to another due to the loss of compression between electrodes or to a deleterious change in raw materials. One of the unique mechanical properties of a cylindrical cell design is the hoop stress which is a force that maintains constant dimensional spacing between electrodes throughout the cycle life of the cell.

In order to determine the effect of changing lots of materials, 4/5A cylindrical cells were made from different lots of $LiCoO_2$ from FMC. Table 3.3 shows that the percent capacity decline of these cylindrical cells from the fourth to the fortieth cycle was much less with Lot #353 (6.4%) and Lot #104 (4.5%) than with Lot #106 (24.3%). The difference in capacity may be due to the difference in the specific surface area (m^2/gm) of the different lots. Using the average cell discharge voltage as an indication of the capacity decline, Figure 3.13 shows that cells built with Lot #104 have less capacity loss than cells built with Lot #106. This is whether the cell is the cylindrical (C469 and C485) or the prismatic (Navy T13 and Navy T14) design.

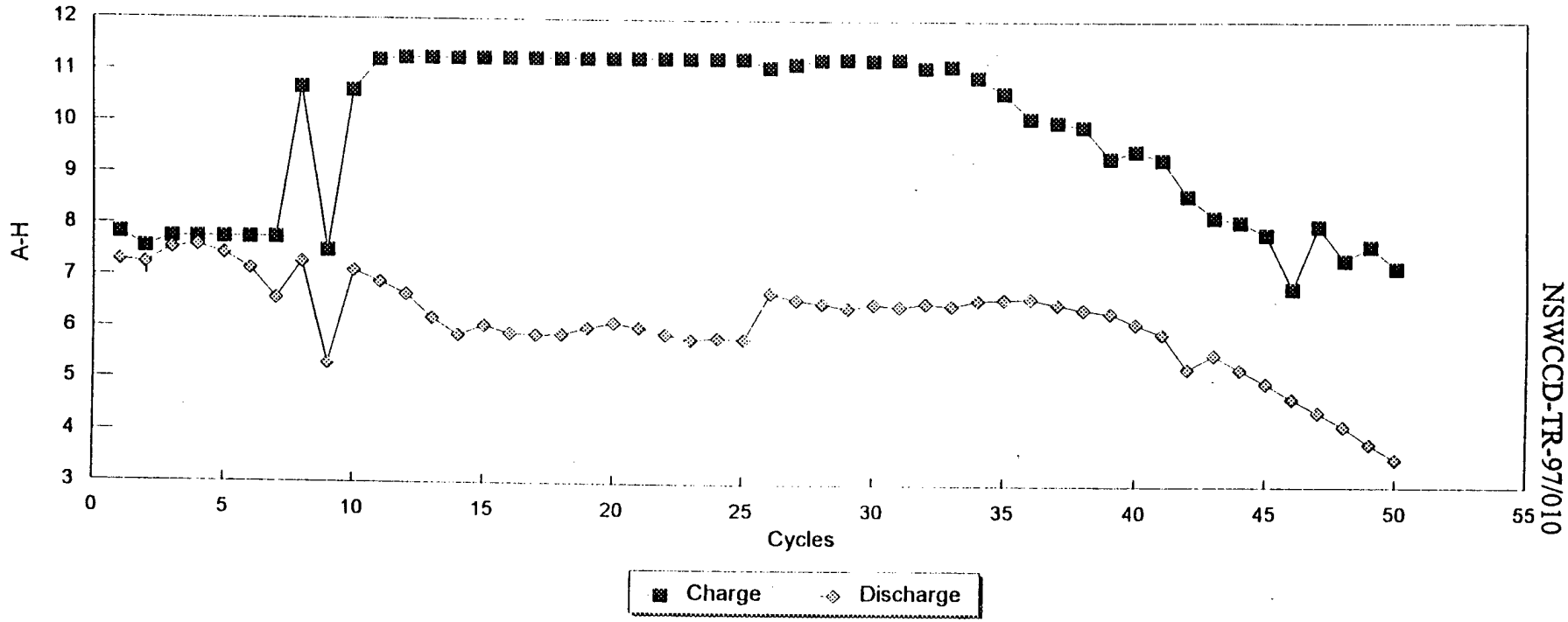

Cycles 1 and 2 charged at .43 A. to 4.2 V.
Cyles 1 and 2 discharged at .43 A. to 3.0 V.

Full test at +23 C.

Cycles 3 through 7 charged at .65 A.to 7.75 Ah.
From cycle 8th charged at .75 A.to 4.3 V. and .25 A. trickle.
From cycle 3 discharged at 1.54 A. to 3.0 V.
Fixture leaked after cycle # 6.

Figure 3.1 Capacity (Ah) versus Cycle Number for Cell Navy T5

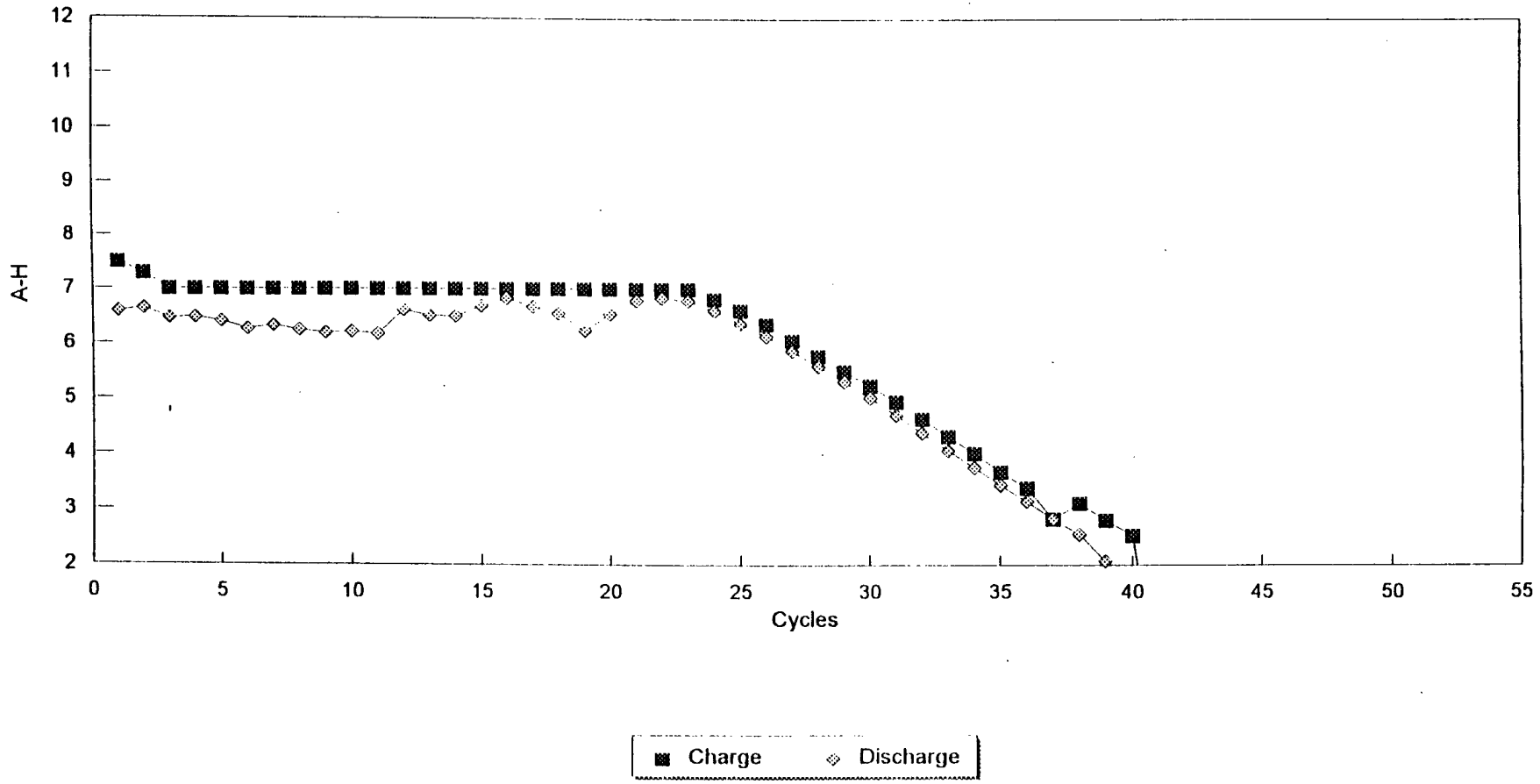

Cyles 1 and 2 discharged at .43 A. to 3.0 V. at +23 C.
From cycle 3 discharged at 1.54 A. to 3.0 V. at -2 C.

Cycles 1 and 2 charged at .43 A. to 4.2 V. at +23 C.
From cycle 3 charged at .65 A. to 7.00 Ah, and 4.40 V. at -2 C.
Plate deflection .067 "
O -ring sealed fixture.

Figure 3.2 Capacity (Ah) versus Cycle Number for Cell Navy T6

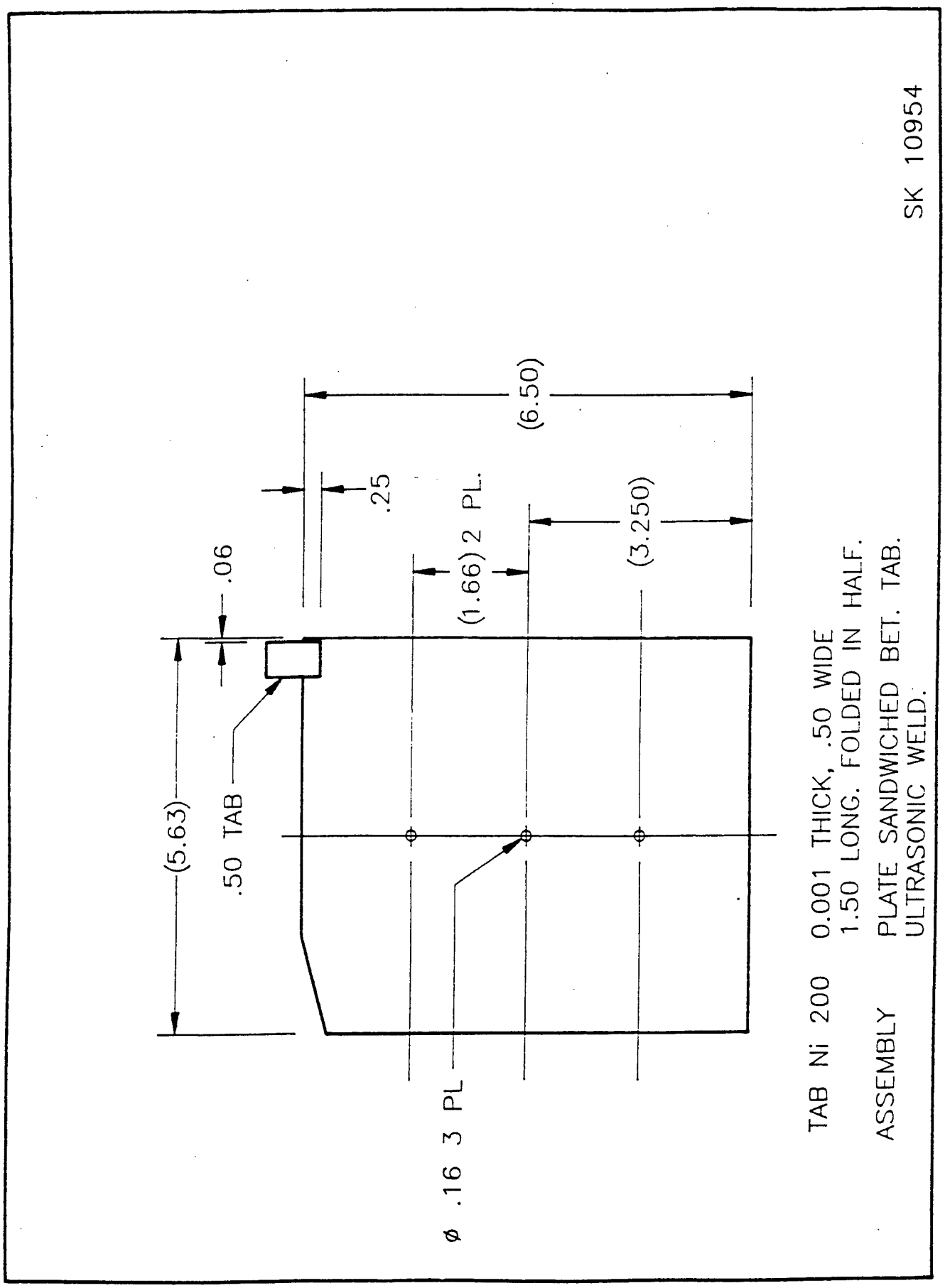

Figure 3.3 Tabbed Negative Plate

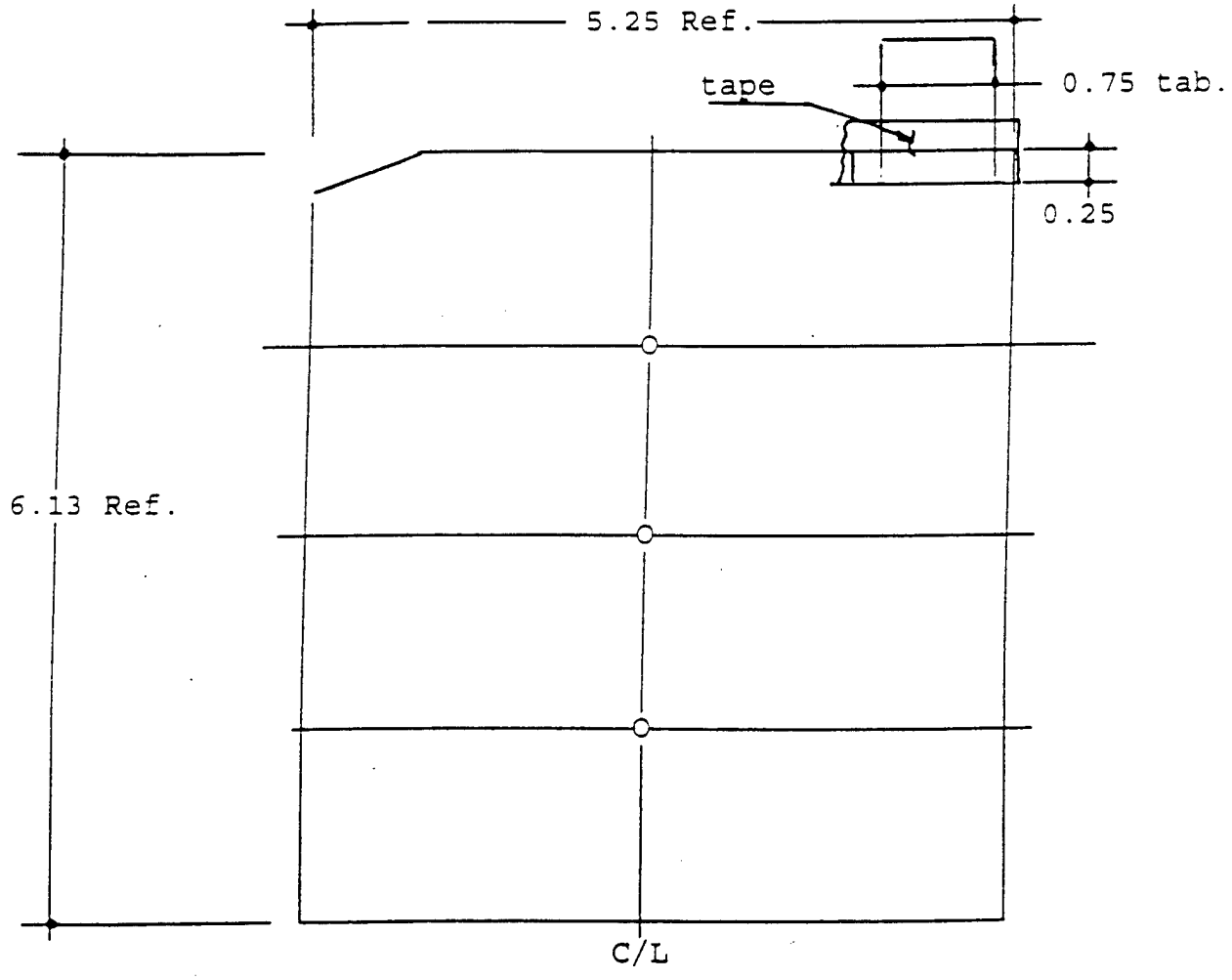

Tab - 0.001 thick Aluminum foil
0.750 wide
Ultrasonic welded to grid.
Tab folded and grid sandwich between the two haves of the tab.

Tape - 0.50 wide ,to cover exposed grid and tab. Both sides.

Figure 3.4 Tabbed Positive Plate

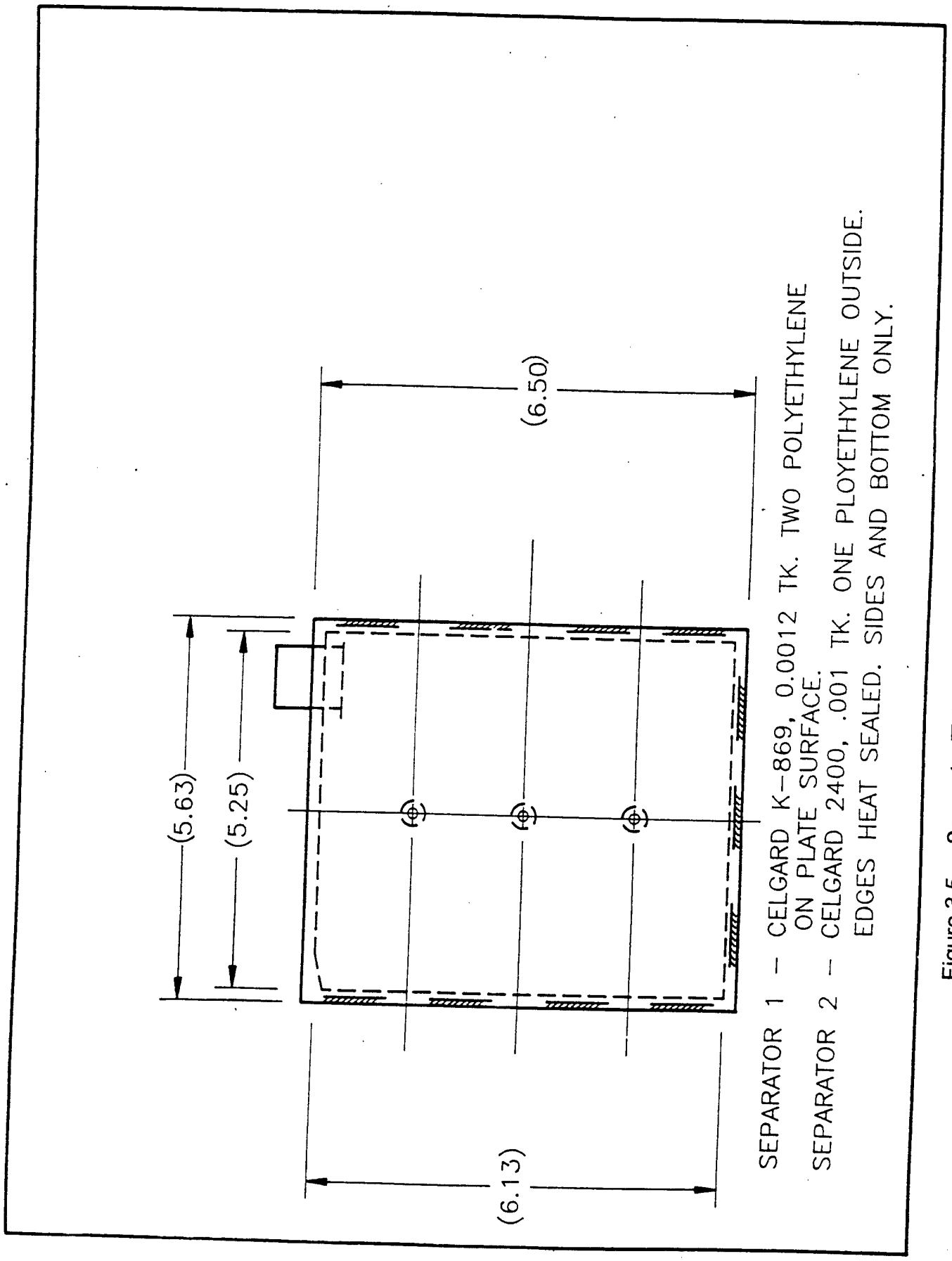

Figure 3.5 Separator/Tabbed Positive Assembly

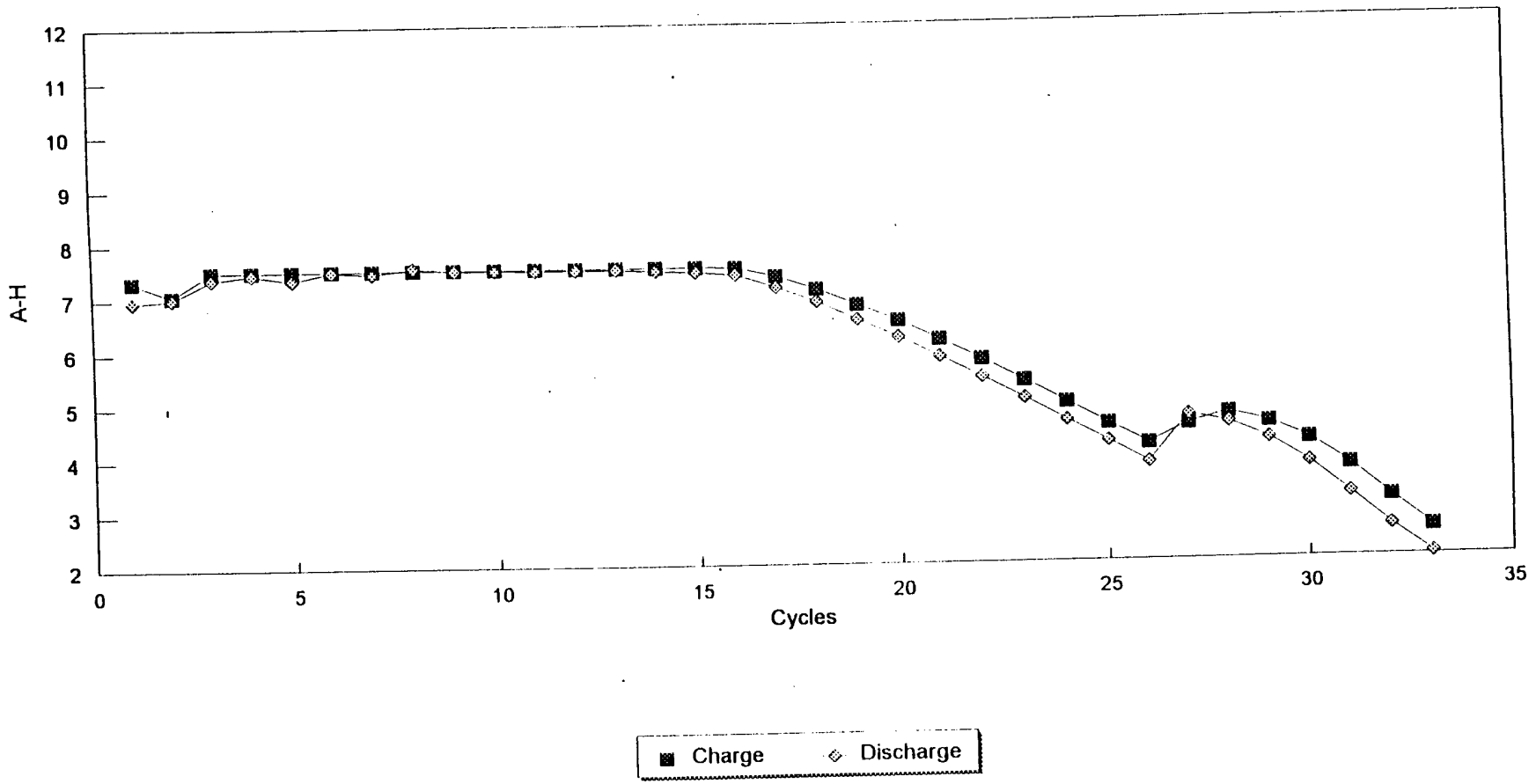

Cycles 1 and 2 charged at .43 A. to 4.2 V. at +23 C.
Cycle 1 and 2 discharged at .43 A. to 3.0 V. at +23 C.

From cycle 3 charged at .65 A. to 7.5 Ah., and to 4.35 V. at -2 C.
From cycle 3 discharged at 1.54 A. to 3.0 V. at -2 C.
At cycle 23 the plate deflection .040". At 80 cycles .073"
At cycle 23, 20 cc. of electrolyte was added.

Figure 3.6 Capacity (Ah) Versus Cycle Number for Cell Navy T9 at -2°C

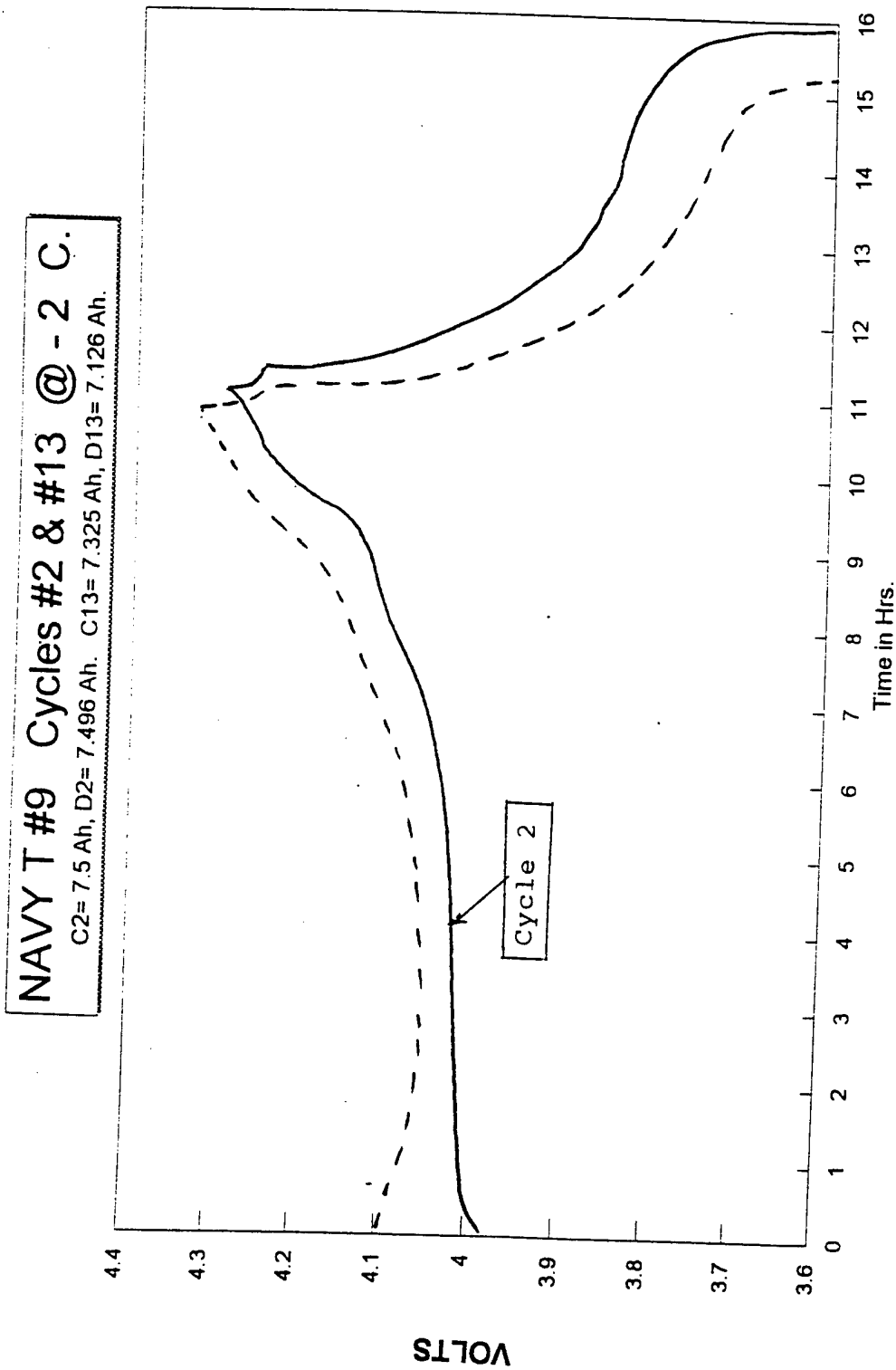

Figure 3.7 Voltage versus Time in Test for Cell Navy T9 at -2°C

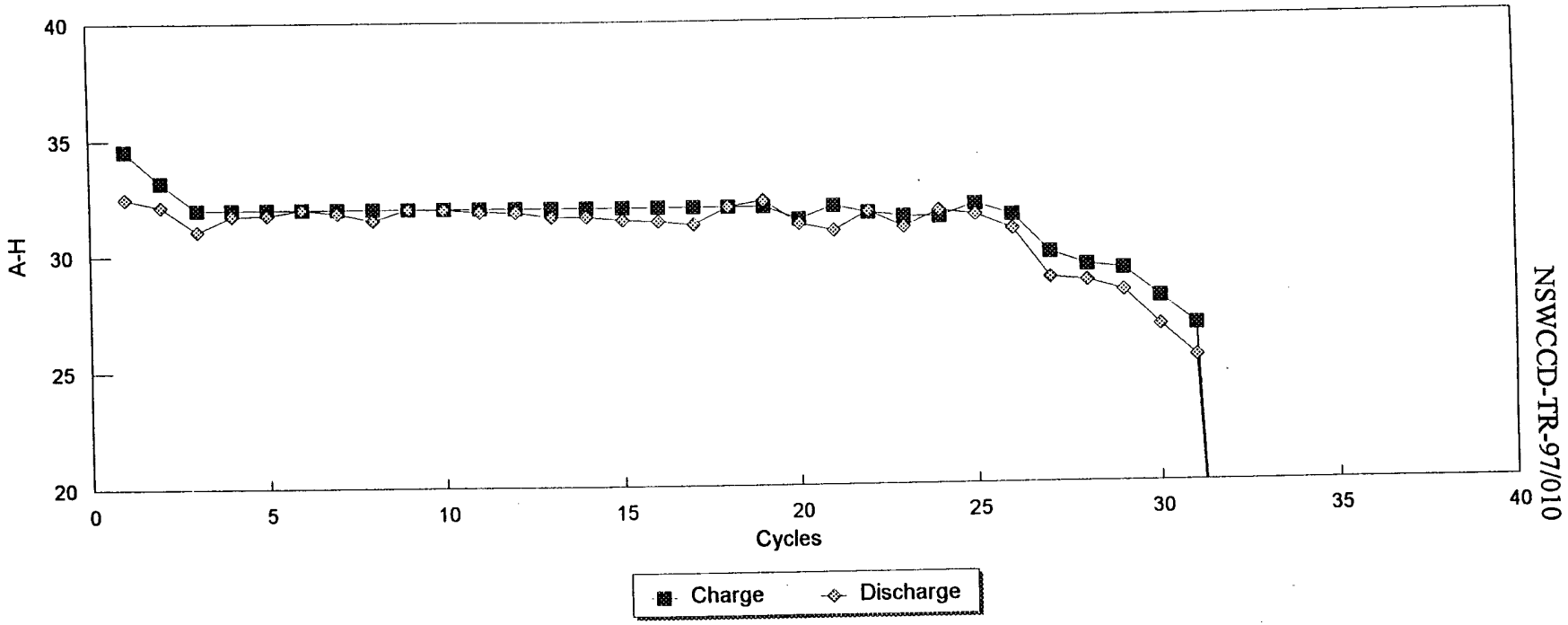

Cyles 1 and 2 discharged at 2.03 A. to 3.0 V. at +23 C.
From cycle 3 discharged at 5.00 A. to 3.0 V. at - 2 C.

Cycles 1 and 2 charged at 2 .03 A. to 4.2 V. at +23 C.
From cycle 3 charged at 3.02 A.to 32.00 Ah. and 4.3 at - 2 C.
At cycle 23 added 20cc. of electrolyte.
Double cavity fixture.

Figure 3.8 Capacity (Ah) Versus Cycle Number for Cell Navy T10 at -2°C

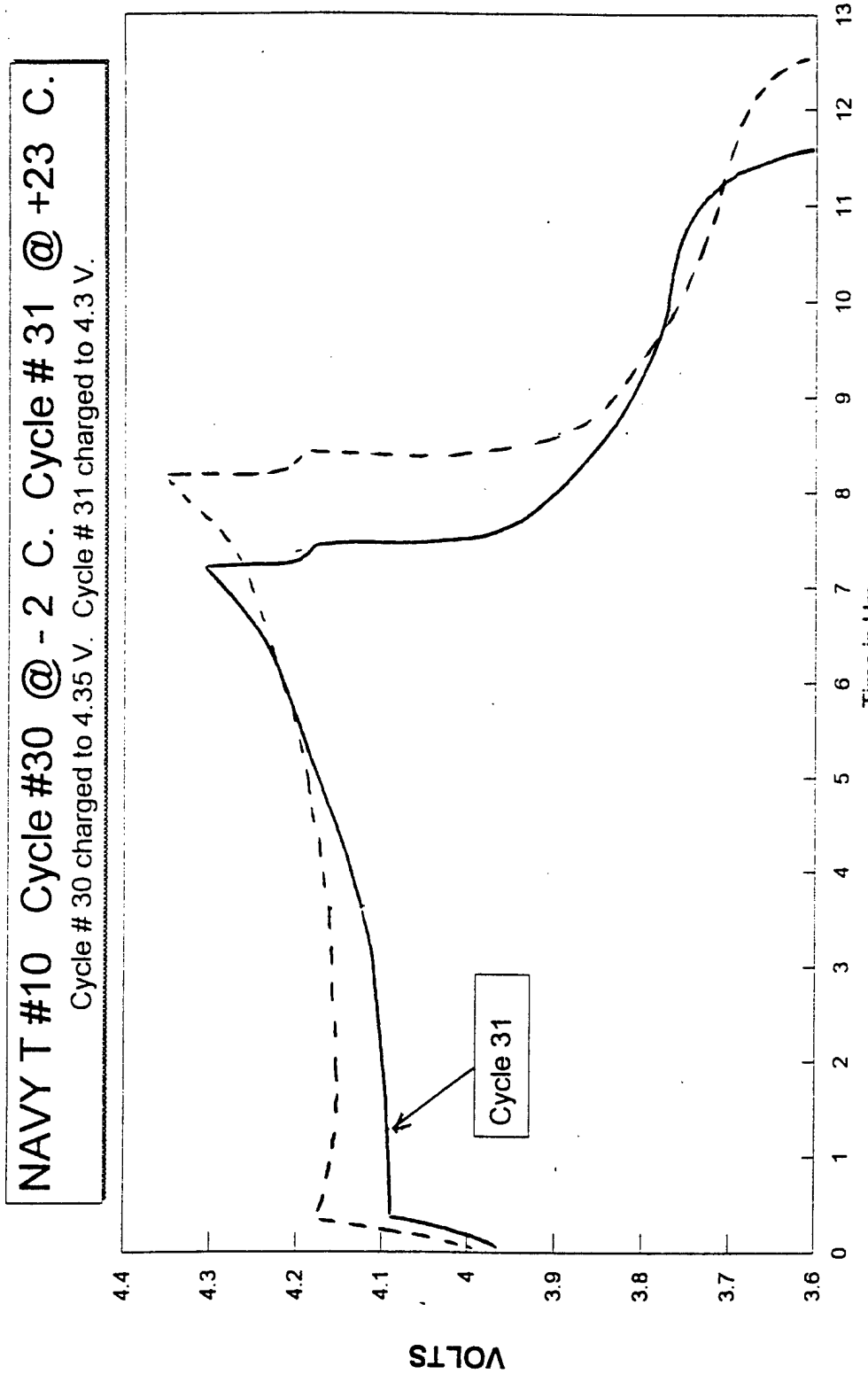

Figure 3.9 Voltage versus Time in Test for Cell Navy T10 at -2°C

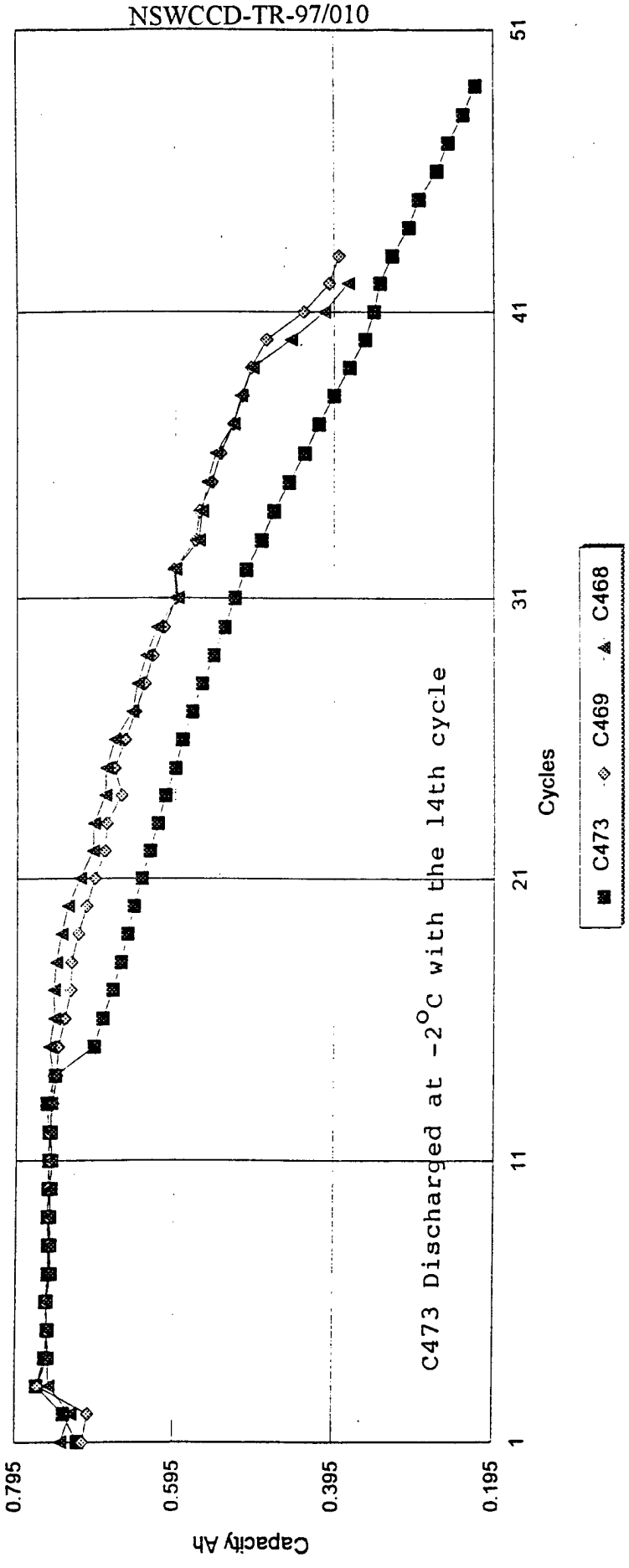

Figure 3.10 Capacity (Ah) Decline Versus Temperature for Cylindrical Cells

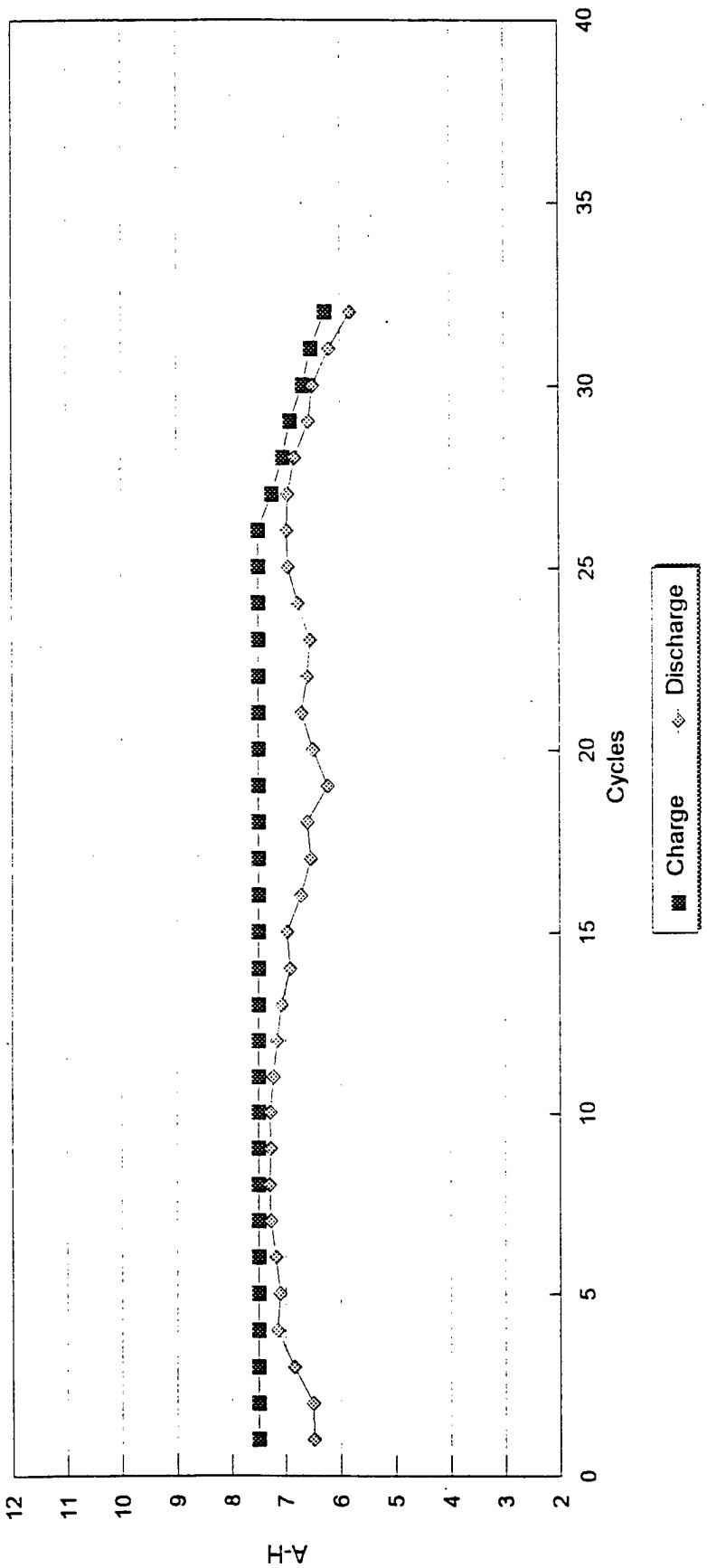

Charged at 0.75 A to 4.30 V., or to 7.50 Ah.
Discharged at 1.25 A to 3.00 V.

Figure 3.11 Capacity (Ah) Versus Cycle Number for Cell Navy T13

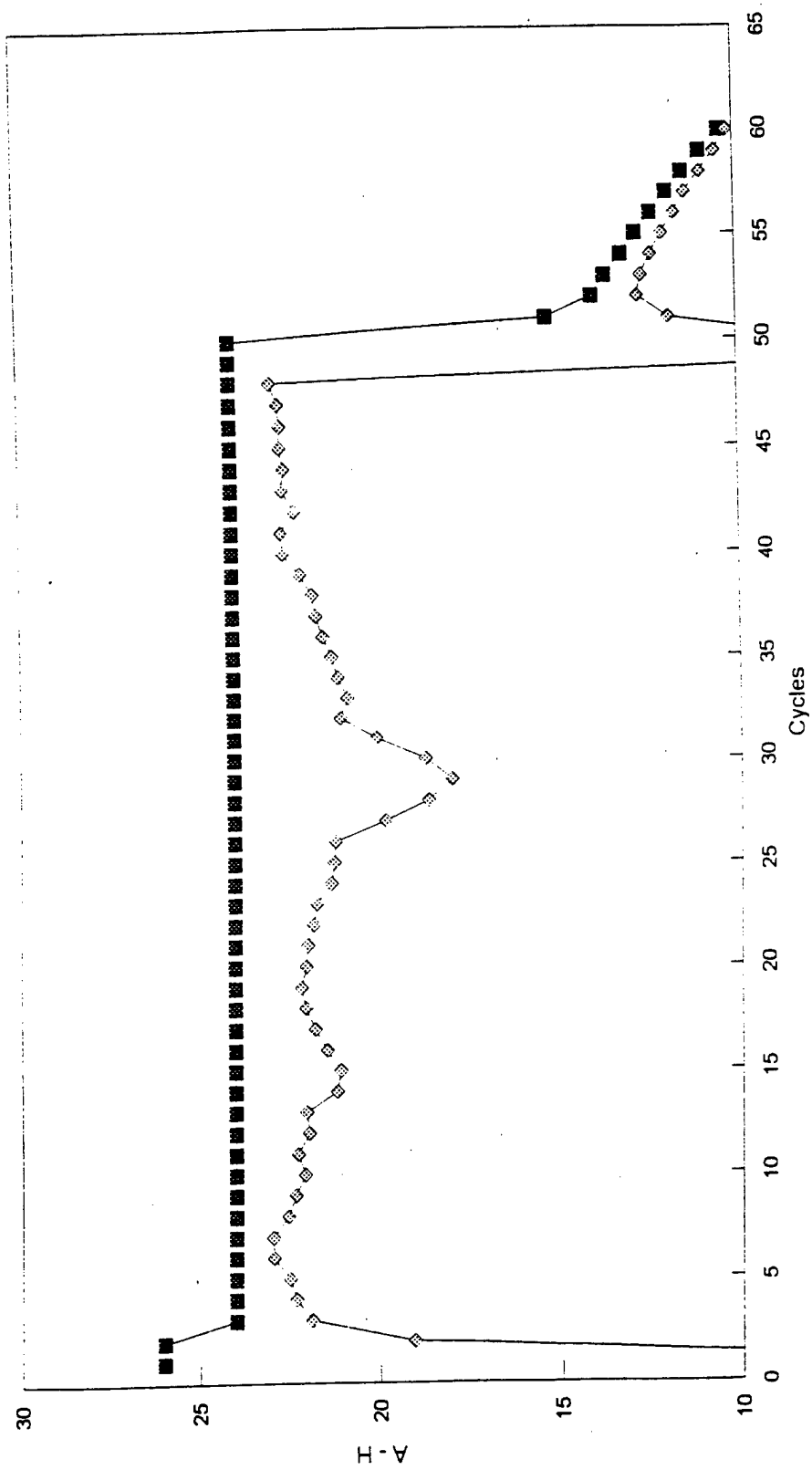

Cycles 1 and 2 discharged at 1.45 A to 3.0 V.
From cycle 3 discharged at 4.15 A. to 3.0 V.
At cycle 49, equipment malfuntion, cell discharged to 1.6 V.
Cell constructed with two 5/8" thick plastic end plates. Not rivet used.
Max. cell deflection at 60 cycles .180 ".

Figure 3.12 Capacity (Ah) Versus Cycle Number for Cell Navy T14

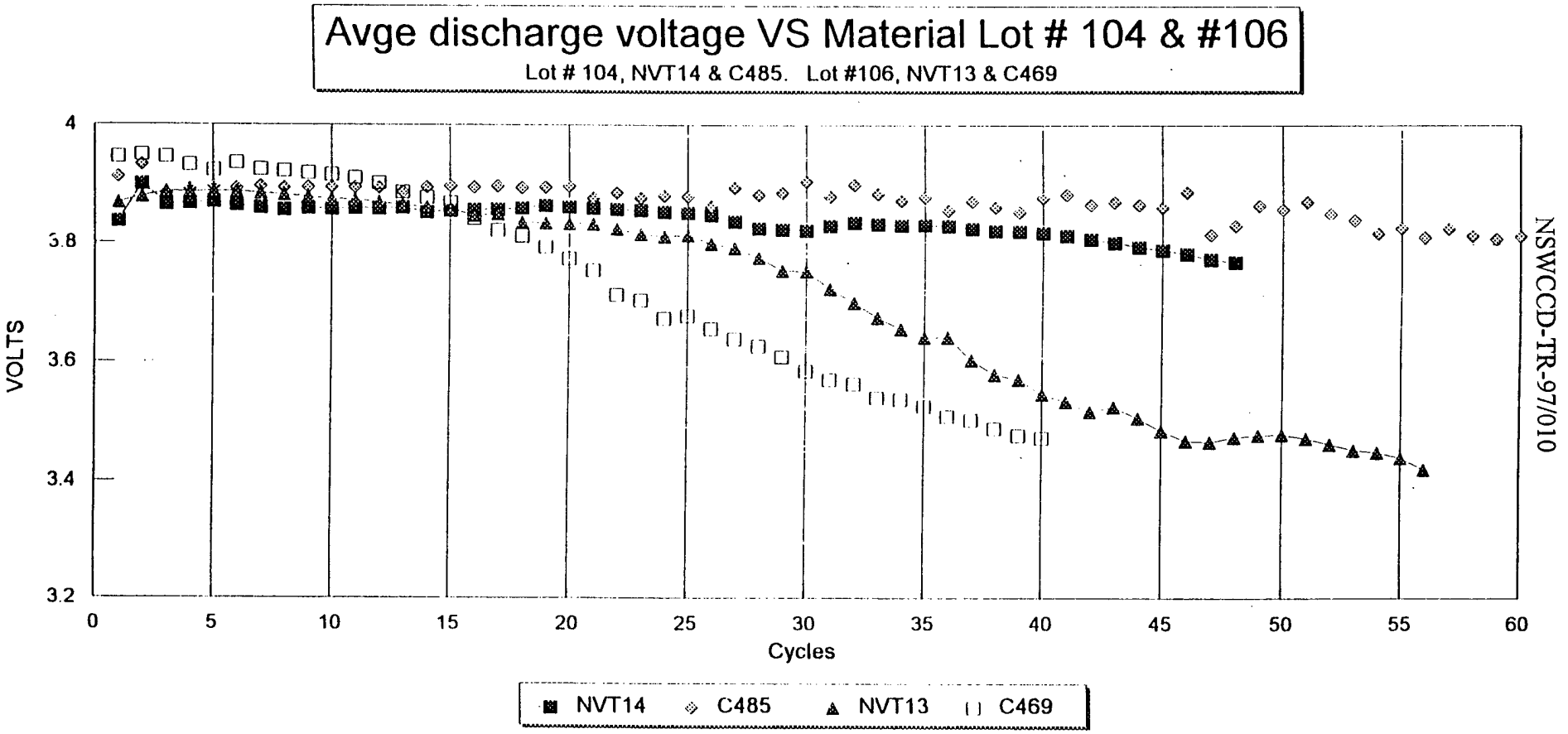

Figure 3.13 Average Discharge Voltage Versus Lot of $LiCoO_2$

Table 3.1 Deflection of the Top Plate as a Function of Thickness and Pressure

Plate material: 0.025" 302 S.S. PLATE

Plate dimensions: 5.75 x 7.10 40.83 sq. in.

	SINGLE PLATE		DOUBLE PLATE	
	Thickness	0.025	Thickness	0.05
	POINTS OF SUPPORT		POINTS OF SUPPORT	
Pressure PSI	ONE	THREE	ONE	THREE
1	0	0	0	0
2	0.03	0.011		
4	0.036	0.018	0.023	0.019
6	0.044	0.024	0.024	0.021
8	0.049	0.03	0.031	0.026
10	0.054	0.034	0.035	0.029
12	0.057	0.038	0.038	0.033
14	0.062	0.042	0.041	0.036
16	0.066	0.044	0.044	0.0385
18	0.068	0.048	0.047	0.042
20	0.071	0.05	0.05	0.043

TABLE 3.2 Plate Swelling Data for Cell Navy T9 Prismatic Cell After Failure

Electrode and Position	**Initial Thickness (Inches)**	**Final Thickness (Inches)**	**Δ Thickness (Inches)**
Sandwiched Cathode	0.0220	0.0250	0.0030
Sandwiched Cathode	0.0220	0.0265	0.0045
Sandwiched Cathode	0.0220	0.0260	0.0040
Endplate Anode	0.0035	0.0135	0.0100
Endplate Anode	0.0035	0.0140	0.0105
Sandwiched Anode	0.0035	0.0230	0.0195
Sandwiched Anode	0.0035	0.0260	0.0225
TOTAL			0.0740

CM1141
ALRM 07/14/94
Rev. 08/05/94

Table 3.3 Material Evaluation for Cylindrical and Prismatic Cells

BATCH MATERIALS Product# Saft P.O #	LOT #	m2/gm	QTY Kg.	Recived	BAG #	Used on cells	Material Utilization Ah/gm C1	Ah/gm D4	Capacity Ah D4	Ah D40	Ah D60	% Capacity decline D4 to D40	Avge. Discharg Voltage at D40	Cells 4/5A Built as
CAS # 12190-79-3 641-12-001	353		10	01/15/93		C365-C370	0.15	0.149	0.846	0.792	0.688	6.4		2 Cu wires STD
PO# 48563	353					C372-C376	0.146	0.149	0.846	0.792	0.72	6.4		NAVY STD
CAS # 12190-79-3 501-01-001 PO# 50169	106	0.20	10	04/12/94	2	C468-C473	0.149	0.1457	0.758	0.479	0.224	36.8		NAVY STD
CAS # 12190-79-3 501-01-001	106	0.20	10	04/27/94	3	C492-C498	0.14	0.139	0.875	0.816	0.448	6.7	3.855	NAVY STD
PO# 50232	106				3	C511-C522	0.145	0.142	0.954	0.709	0.448	25.7	3.826	Separator D101.
	106				3	C508-C510	0.143	0.139	0.716	0.6202	0.558 Last cycle # 47	13.4	3.704	D101,Exmet02,Kynar
	106				3	NAVY T #16	0.144	0.136	6.85	1.4		79.6	3.487	Prismatic 3 plates 7 AH
	106				3	NAVY T #17	0.138	0.14	6.99	5.51		21.2	3.566	Prismatic 3 plates 7 AH
CAS # 12190-79-3 501-01-001	104	0.30	20	04/27/94	4	C480-C485	0.14	0.1347	0.708	0.702	0.7	0.8	3.878	NAVY STD
	104				4	C486-C491	0.147	0.139	0.84	0.84	0.688	0.0	3.925	D 101,Separator
	104				4	CK090-CK095	0.139	0.141	0.895	0.782	Shorted at the 42th cycle.	12.6		D101,Exmet02,Kynar
	104				4	NAVY T #14	0.147	0.129	22.5	22.5	10.9	0.0	3.818	Prismatic 10 plates 24 Ah
	104				4	NAVY T # 15	0.147	0.13	140.3	137.7	115.4	1.9	3.713	Prismatic 56 plates 140 Ah

C1 & C2 Charged at 0.35 Discharged at 0.35 mA/cm2 to 3.0 V.
From C3 Charged at 0.52 Discharged at 1.2 mA/cm2 to 3.0 V.

Chapter 4

Construction of the Final Design

A photograph of the Navy SDV 140 Ah test cell is shown in Figure 4.1 and is described in Table 2.2. The electrodes and separators were assembled on the End Plate and Rivet Assembly Fixtures (Figure 4.2). They were then inserted into the can after the cell tabs were attached to the feedthroughs on the cover. While in a fixture, the cover was TIG welded to the case. A 0.062-inch diameter rod was inserted into the rivet holes in the case and TIG welded to the can (as shown in Figure 4.3) while confined inside the electrolyte fill and formation fixture (Figure 4.4). In order to remove oxygen from the cell, the cell was evacuated and filled several times with a mixture of CO_2 and vapor of the solvent (PC/EC/DMC) used in the electrolyte. The cell was then evacuated and filled with a pre-measured amount of electrolyte at 8 psig (the pressure was released after the first discharge). After the cell formation cycle, the fill tube was crimped (by pinching), resistance welded, and trimmed. The filled cell was kept for a minimum of 72 hours at 23°C prior to electrical testing.

The cell was designed with a low-pressure vent system for the release of gaseous products resulting from thermally and/or electrically abusive conditions if the internal pressure became too high. The vent was set up to open at 125 to 150 psig.

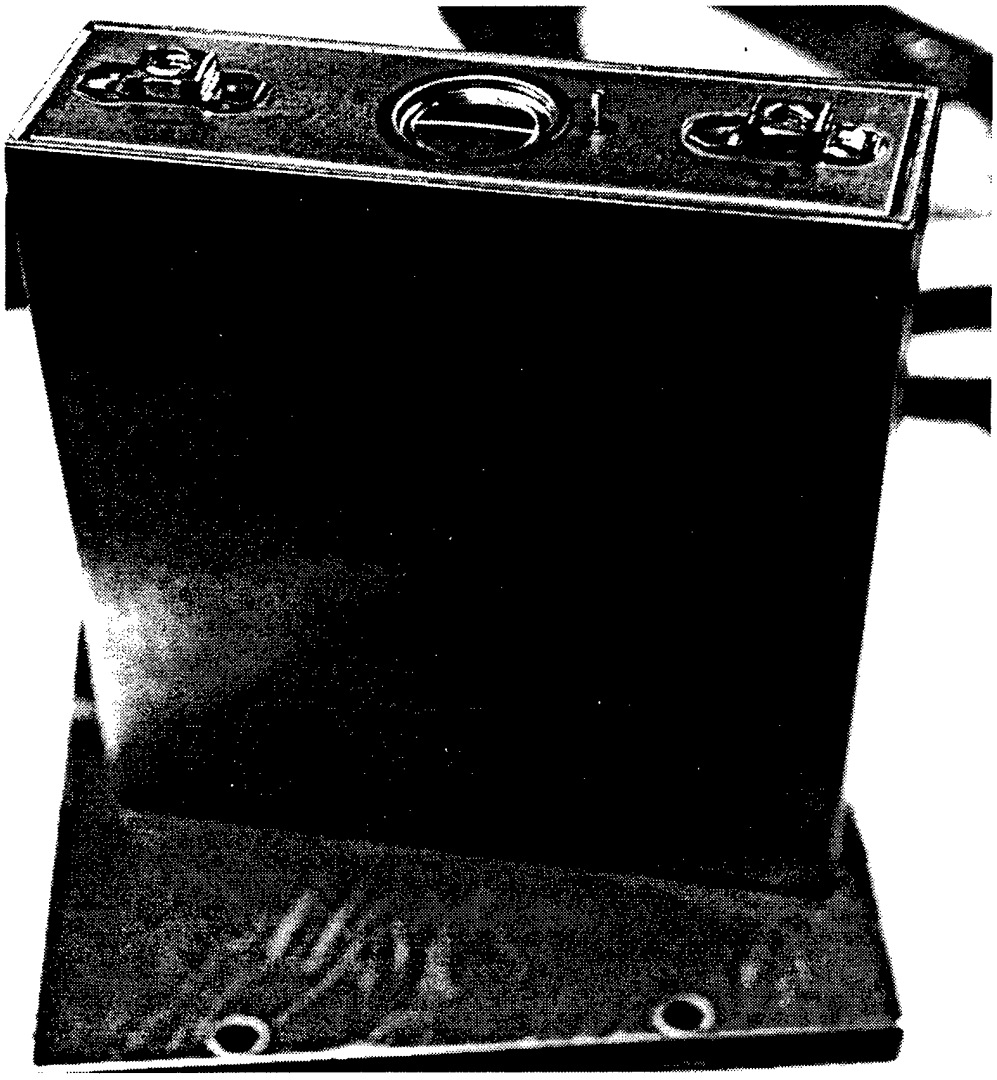

Figure 4.1 Photograph of Navy SDV 140 Ah Test Cell

NOTE:

1. REMOVE ALL BURRS AND SHARP EDGES.
2. RIVETS TO BE PERPENDICULAR TO PLATE WITHIN 1~2°.
3. TOLERANCES 3 DECIMALS ± .005
4. TOLERANCES 2 DECIMALS ± .015

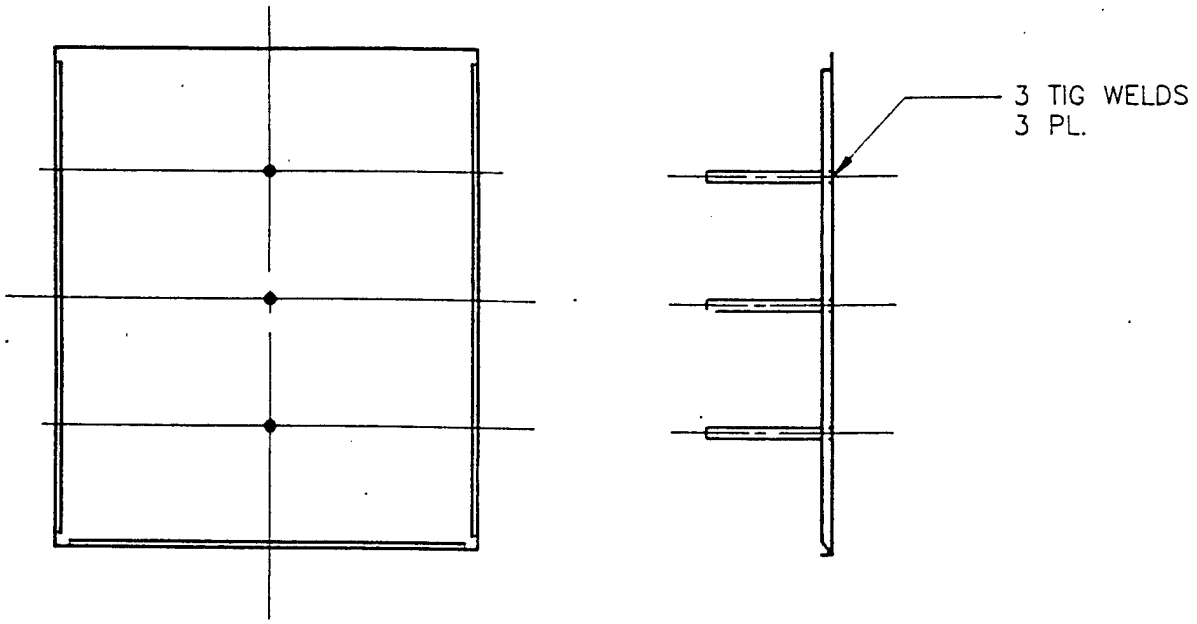

Figure 4.2 End Plate and Rivets Assembly

NOTE:

1. ALL WELD JOINTS MUST BE HERMETIC SEAL.

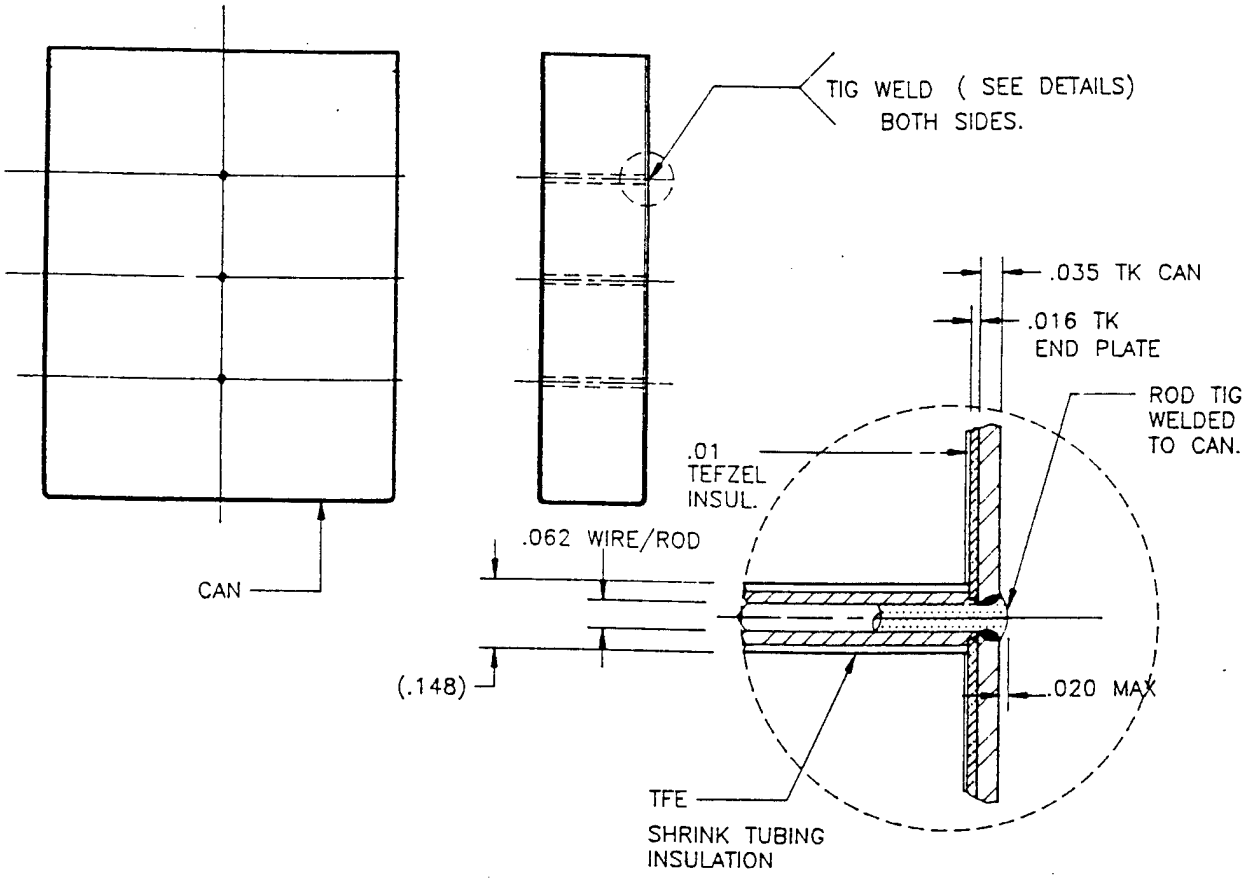

Figure 4.3 Can/Rivet Tie Rod Assembly

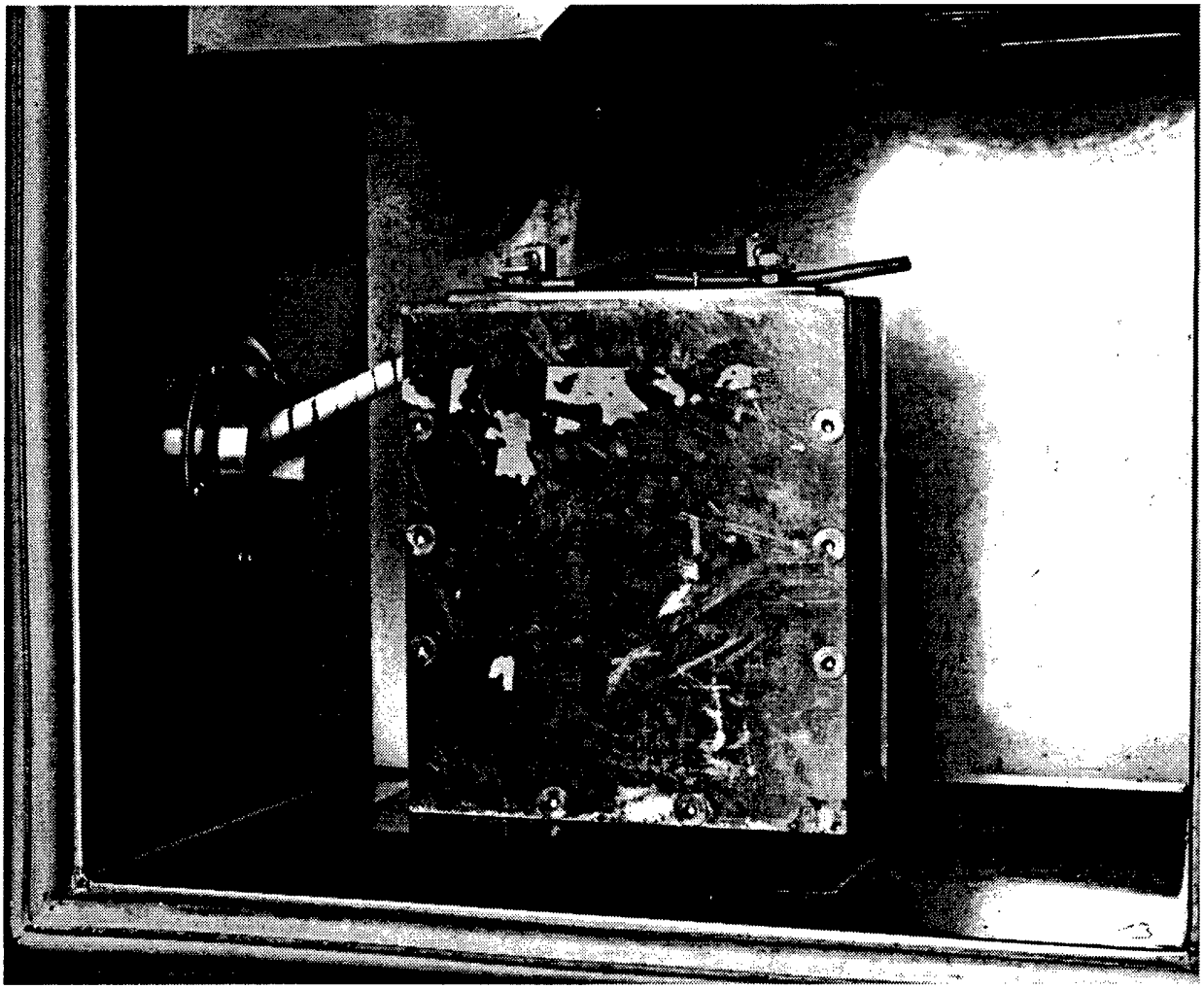

Figure 4.4 Photograph of Cell on Test Inside of the Electrolyte Fill and Formation Fixture

Chapter 5

Performance of the Final Design

This chapter describes the test results on the final design for cells using metallic lithium anodes. The test results demonstrated that a considerable force is developed perpendicular to the plates as a result of plate swelling during cycling and that the restraining rivets were underdesigned for that force. Table 5.1 is a summary of the test results on Cells Navy T15, Navy T18, and Navy T19.

Cell Navy T15

Figure 5.1 shows the capacity of Cell Navy T15 as a function of the number of cycles. Figure 5.2 shows the charge and discharge voltage. The cell was charged to 150 Ah. Some soft shorting occurred during the first 11 cycles. From cycle 12 to 40 it delivered a capacity that averaged 141 Ah with a high of 145 Ah at cycle 17. From cycle 41 to 51 the capacity declined from 139 Ah to 130.5 Ah. At cycle 17 the test equipment failed (lost power supply). When the cell was examined, it was observed that two of the three rivets had broken, which allowed some of the electrolyte to leak. Eight grams of electrolyte were added, the leaking rivets were plugged with silicone rubber, and the cell was put in the retaining fixture (Figure 4.4). Previously, the retaining fixture had been used only during the filling with electrolyte and performing the formation cycles. This was the first time the cell was left in the fixture.

The location of the cell rivet was symmetric to the electrodes and not to the cell can. For this reason, the can planar surfaces deflected more at the cell top end. Some time during cycles 52 and 53, the cell was on rest for about 12 hours (computer power out). At cycle 53, the capacity was 119 Ah, indicating that the cell had some self-discharge as it recovered to 121.5 Ah at cycle 56. The capacities at the last two cycles were 112 and 109 Ah. At this point, the test was terminated because of the degree of stress on the holding fixture. At cycle 53, the top edge of the 0.5-inch thick aluminum plate had deflected 0.125 inches.

Cells Navy T16 and Navy T17

Cell Navy T15 was made using Lot #104 of the $LiCoO_2$. Cells Navy T16 and Navy T17 were built using Lot #106, because the supply of Lot #104 was exhausted in order to evaluate the decline in capacity that occurred with Lot #106 of the $LiCoO_2$ (Table 3.3). Figure 5.3 through 5.5 show that there was a rapid decline in capacity of Cells Navy T16 and Navy T17 after the twentieth cycle. Cell Navy T15 did not show a similar decline until after the thirty-fifth cycle.

Cells Navy T18 and Navy T19

Figures 5.6 and 5.7 show the capacity of Cells Navy T18 and Navy T19 as a function of the number of cycles. These were low temperature tests. During the course of the 18 cycles, both cells were physically deformed. The larger planar faces had bulged approximately one-quarter inch per face, or a total of one-half inch. The mechanical design of the cell was predicated on controlling metallic lithium expansion by the use of three rivets extending between the two large planar faces. In contrast with Cell Navy T15, no retaining fixture was used.

By comparison to Cell Navy T15, which was cycled at ambient temperature, the deformation of these two cells was considerably more severe. Two factors probably contributed to the bulging problem: (1) a relatively high rate of charge and (2) cold temperature cycling. Bulging implies uncontrolled growth of an electrode. Every time the lithium cycled, the volume of the negative electrode increased. This volume expansion created the physical condition that could distort the electrode pack, insulation, and the separator. By examining the remains of the hardware, it was concluded that the initial short in Cell Navy T18 started in one bottom corner. In actual use, these cells would have been removed from service and not allowed to continue to deform due to continued cycling.

The overall conclusion is that the physical expansion of the lithium during cycling occurred unimpeded by the can planar face and the rivets. This allowed continuous lithium expansion, giving rise to a distorted stack, which probably shorted.

While the cells were being tested, the following occurred:

- The freezer failed approximately 25 hours before the MACCOR cycler shut down (no current or voltage readings) on these two channels.
- After the freezer failure, cells cycled at ambient for two full discharges and one full charge. Note that the last charge occurred at ambient with an absolute limit of 4.38 V, which was used for the 0°C charge to compensate for the increased impedance.
- Computer records indicated cell Navy T18 had a decreasing voltage during the last rest period.
- Cell Navy T18 started the charge for cycle 19 and then computer records showed that this channel could not control voltage. The thermocouple in the freezer showed that the temperature was about 100°C and that, within ten minutes, the temperature returned to ambient.
- Cell Navy T19 almost simultaneously was disconnected from the cycler leads. The data show that this cell was in a rest period. The last point for this cell was 1.18V possibly indicating that the cell was shorted.

- The hypothesis is that the short for cell Navy T19 was produced by a fire from cell Navy T18, which fused the two current leads.

- For the next 9.5 hours, the temperature fluctuated between 50 to 60°C and ambient.

- The final event occurred after 9.5 hours when the thermocouple opened, probably indicating a second fire arising from cell Navy T19.

- Cell Navy T19 was expanded on all four sides. It approached a sphere in shape. All rivets were torn free. One corner had opened and the vent had opened. The top was opened on cell Navy T18 attached at only one narrow side. The cell element (electrode pack) was ejected into the oven.

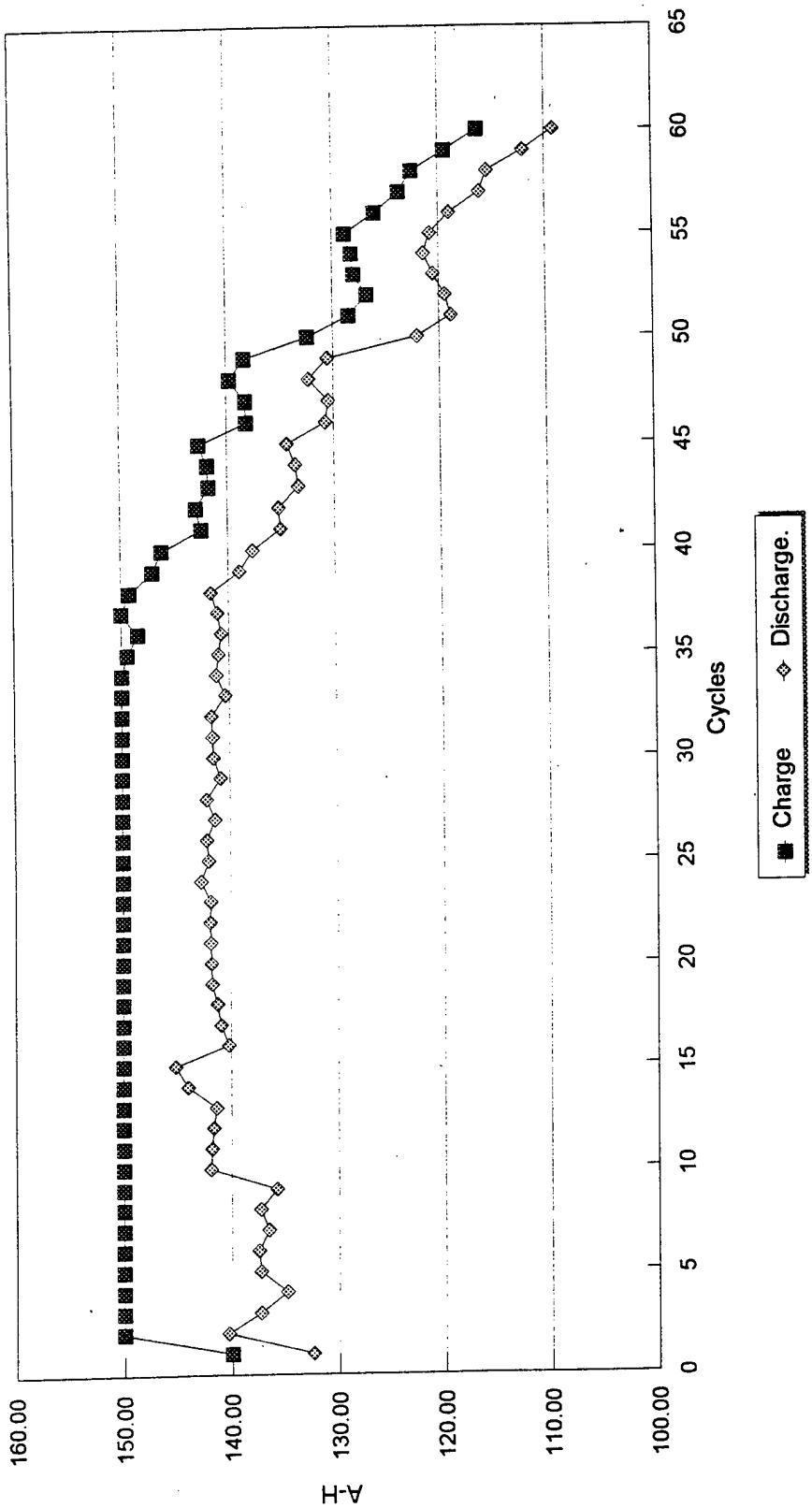

Charged at 12.1 A. to 4.30 Volts, or to 150 Ah.
Discharged at 19.97 A. to 3.00 Volts.

Figure 5.1 Capacity (Ah) Versus Cycle Number for Cell Navy T15

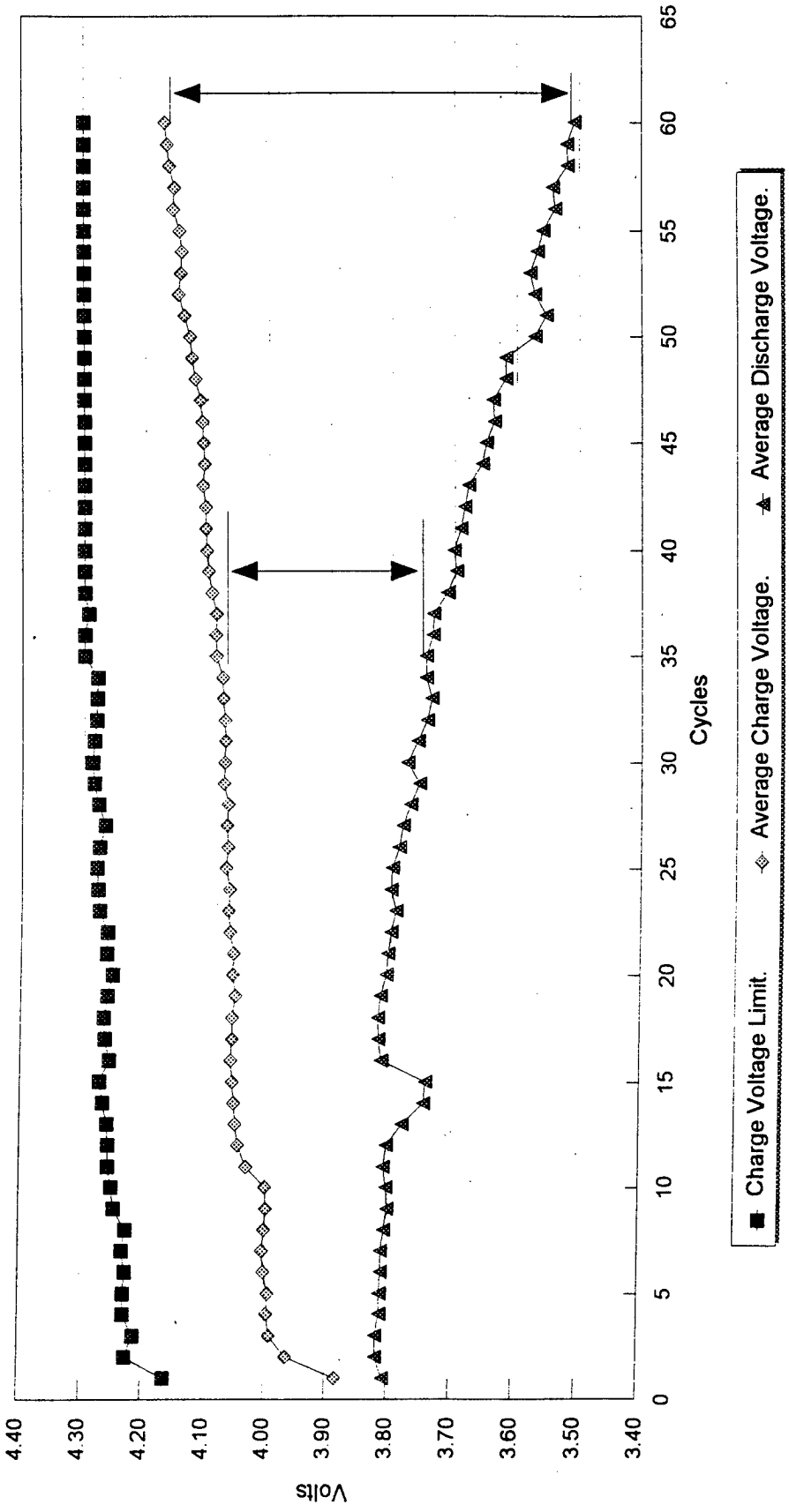

Charged at 12.1 A. to 4.30 Volts, or to 150 Ah.
Discharged at 19.97 A. to 3.00 Volts.

Figure 5.2 Charge and Discharge Voltage Versus Cycle Number for Cell Navy T15

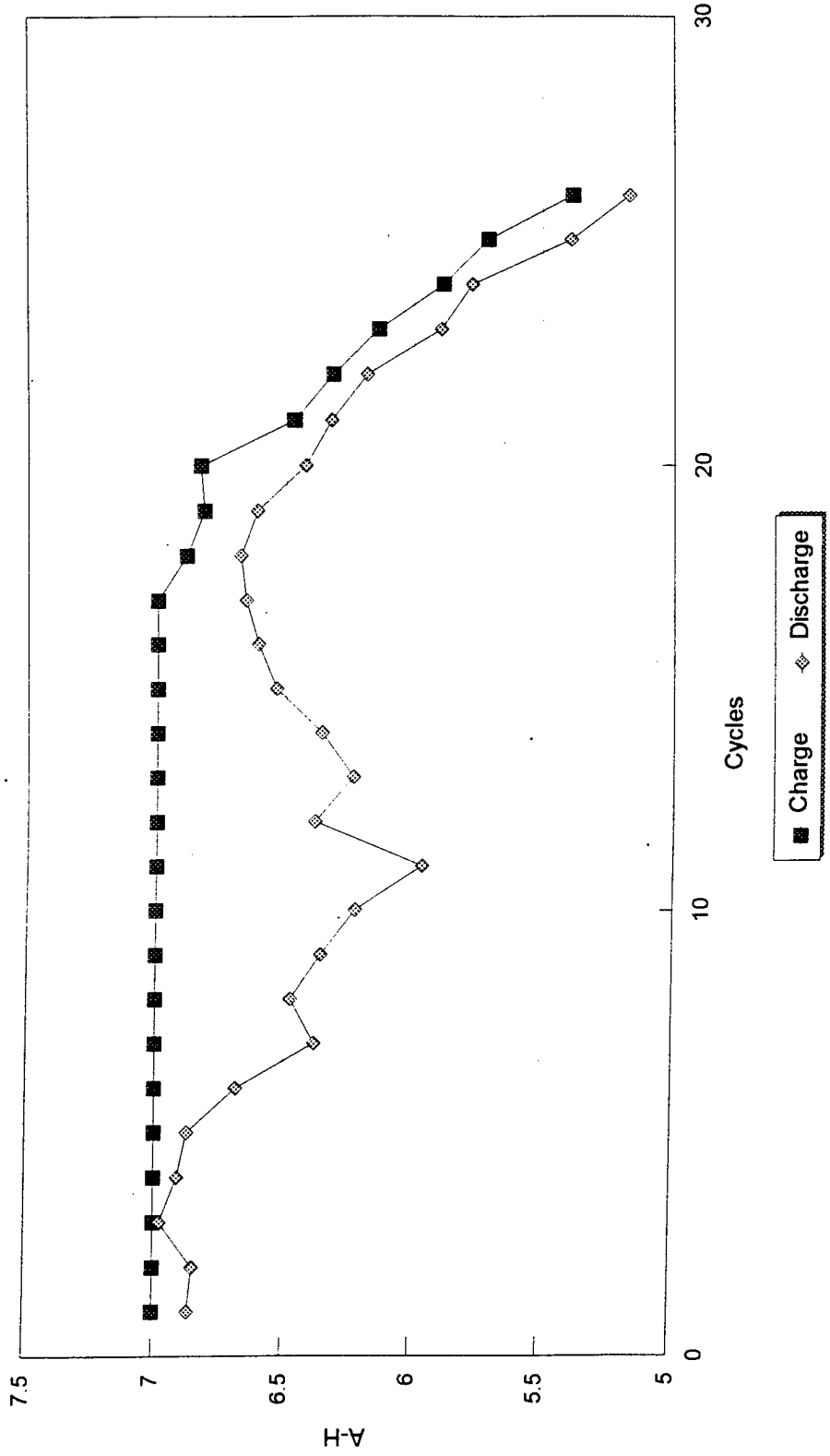

Charged at 0.65 A. to 4.30 Volts or to 7.00 Ah.
Discharged at 1.25 A. to 3.00 Volts.

Figure 5.3 Capacity (Ah) Versus Cycle Number for Cell Navy T16

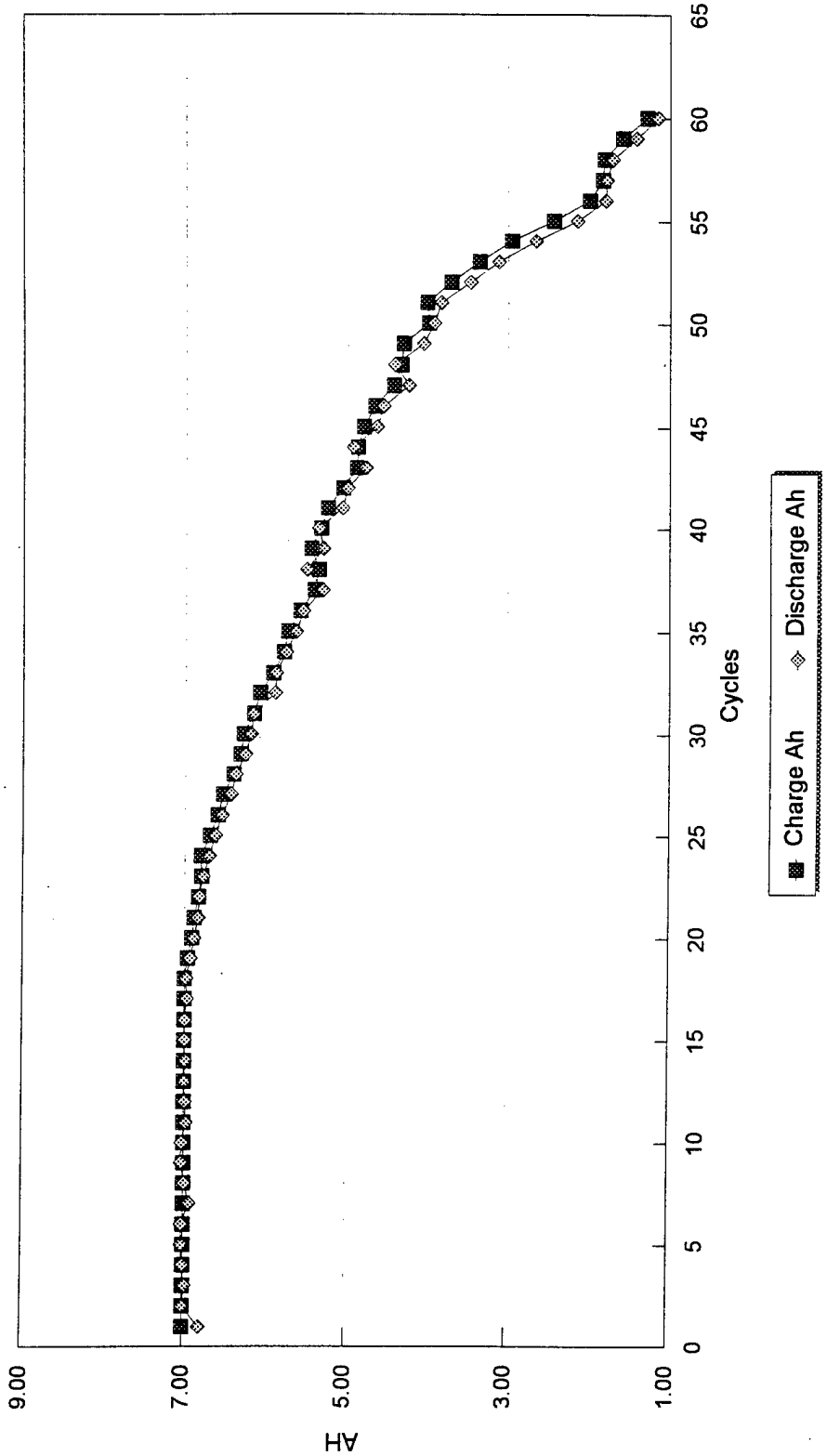

Charged at 0.65 A. to 4.30 V. or to 7.00 A.
Discharged at 1.25 A. to 3.00 V.

Figure 5.4 Capacity (Ah) Versus Cycle Number for Cell Navy T17

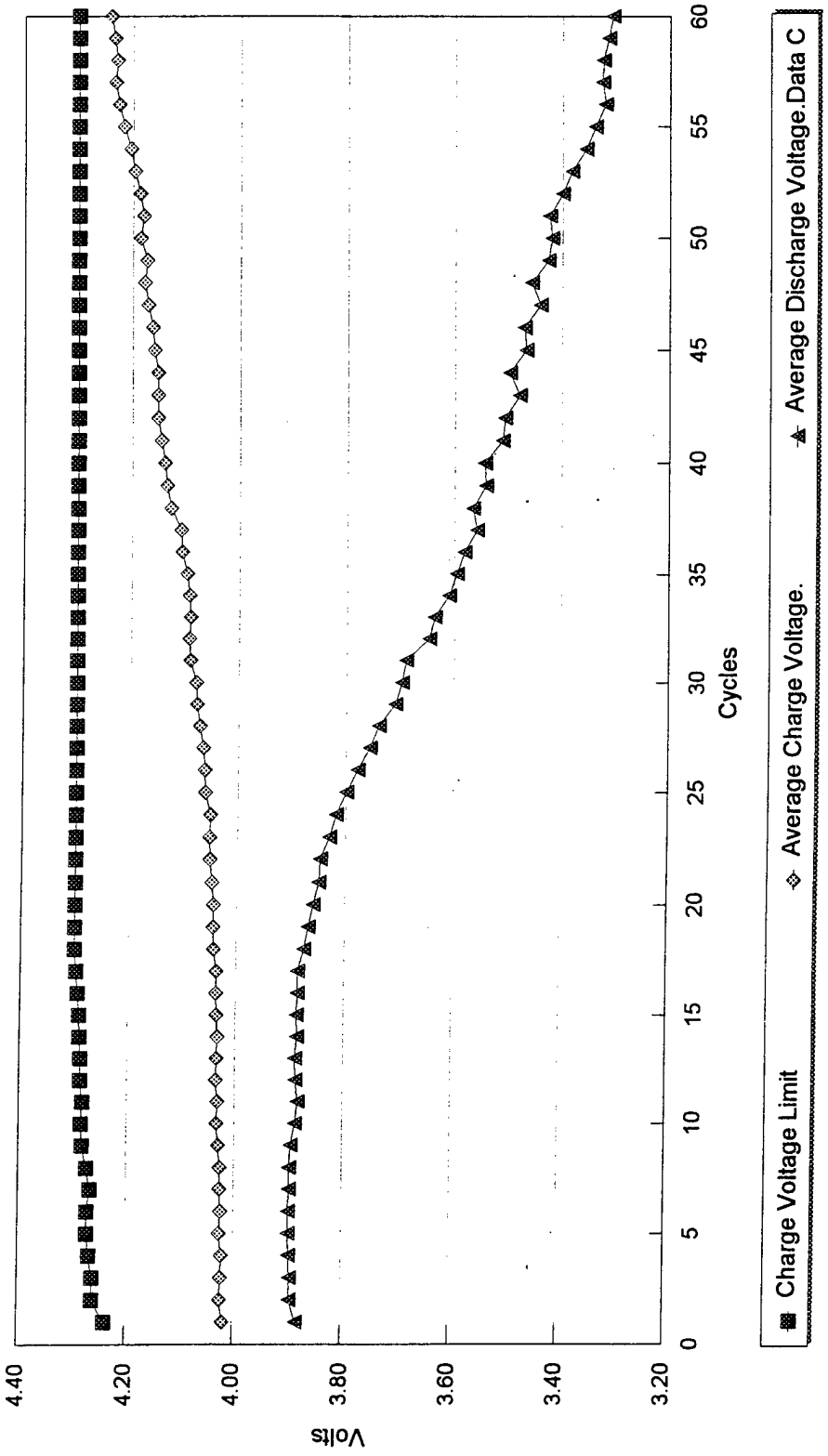

Charged at 0.65 A. to 4.30 V. or to 7.00 A.
Discharged at 1.25 A. to 3.00 V.

Figure 5.5 Charge and Discharge Voltage Versus Cycle Number for Navy T17

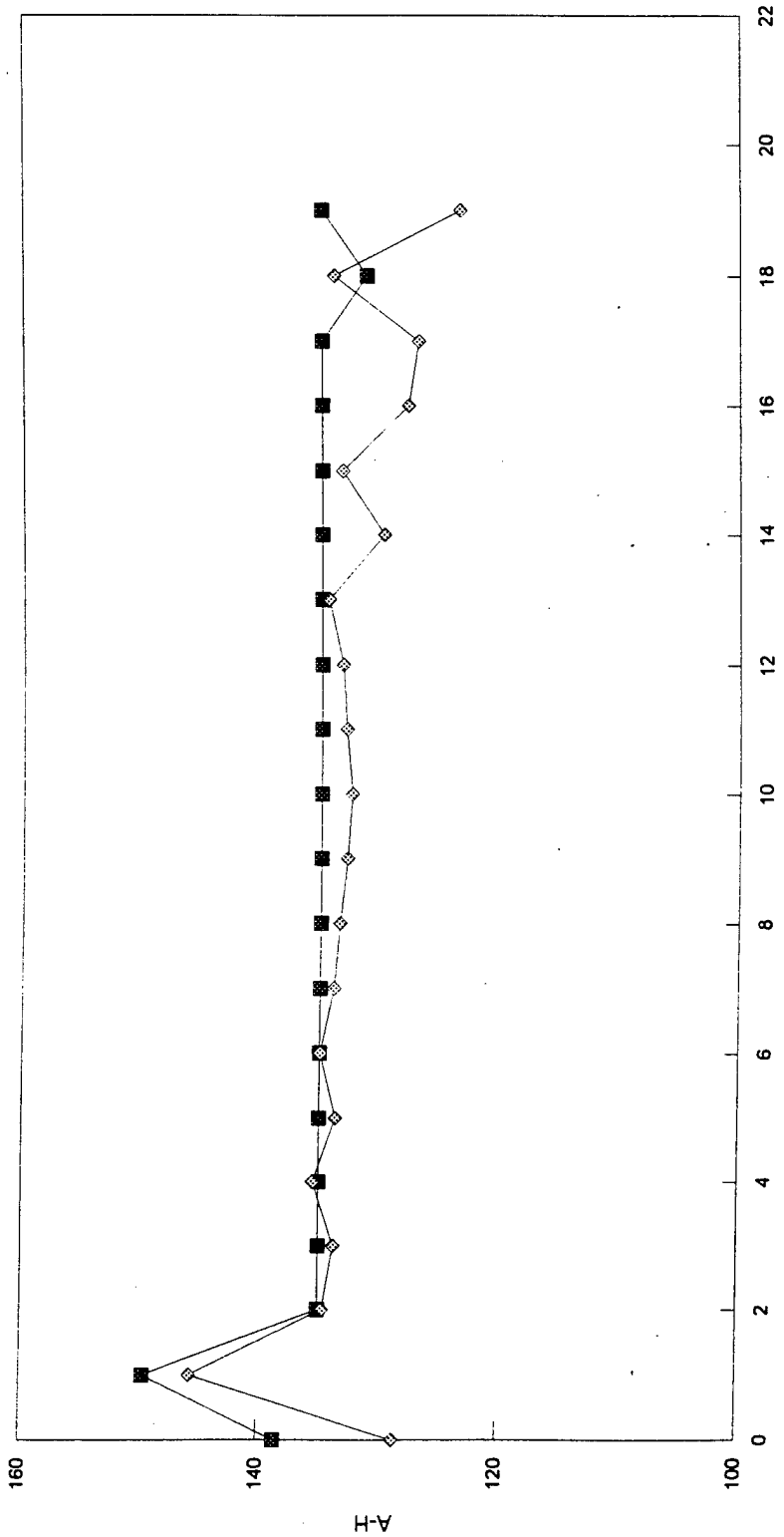

Cycle 0 charged to 4.2 V. @ +20 C. Discharged to 3.0 V. @ + 20 C.
Cycle 1 charged to 4.3 V. @ +20 C. Discharged to 3.0 V. @ +20 C.

From cycle 2 charged to 135 Ah, @ 0 to - 2 C. Discharged to 3.10 V. @ 0 to -2 C.

Figure 5.6 Capacity (Ah) Versus Cycle Number for Cell Navy T18

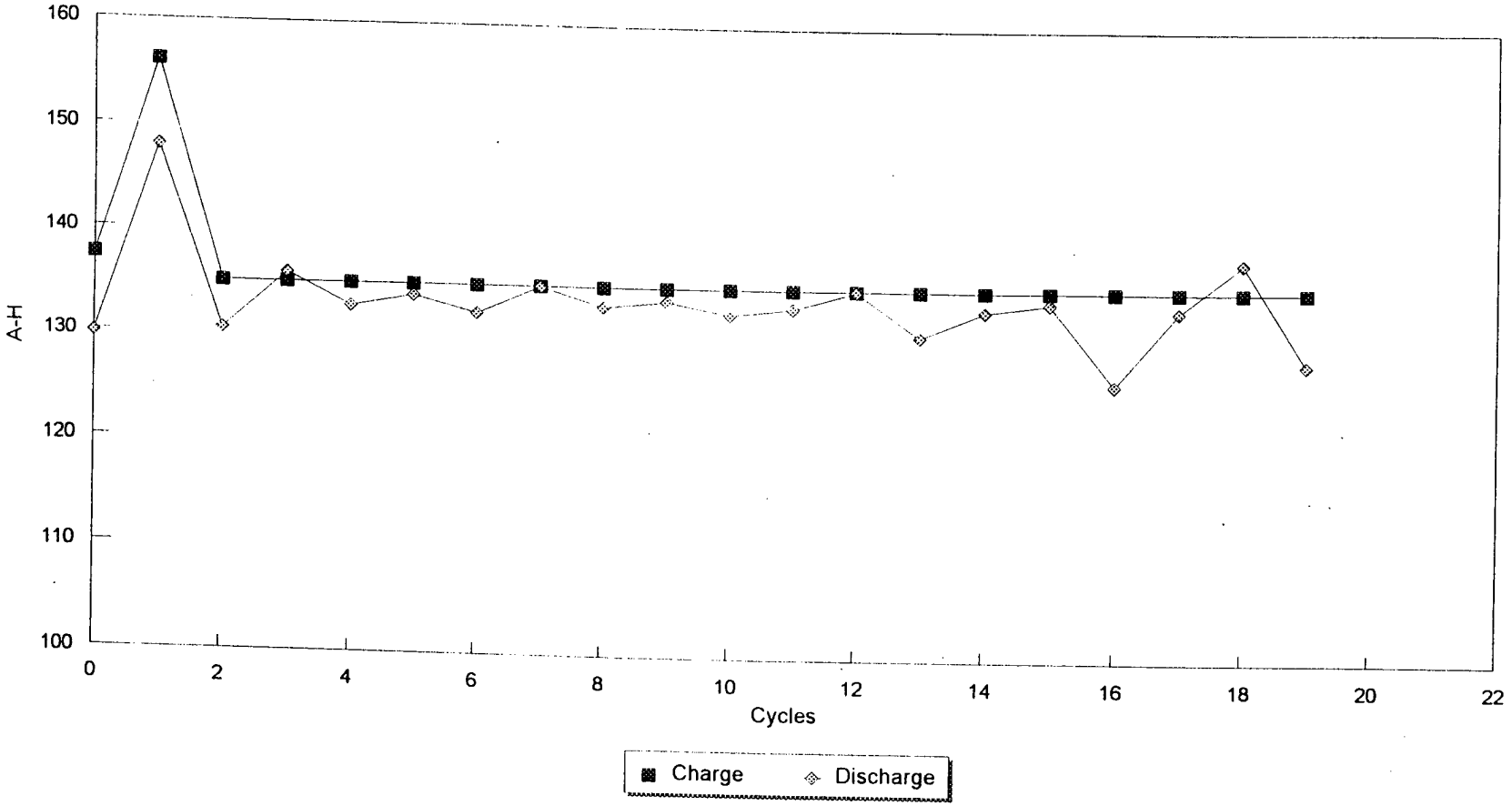

Cycle 0 charged to 4.2 V. @ +20 C. Discharged to 3.0 V. @ + 20 C.
Cycle 1 charged to 4.3 V. @ +20 C. Discharged to 3.0 V. @ +20 C.

From cycle 2 charged to 135 Ah, @ 0 to - 2 C. Discharged to 3.10 V. @ 0 to -2 C.

Figure 5.7 Capacity (Ah) Versus Cycle Number for Cell Navy T19

Table 5.1 Summary of the Test Results on Cells Navy T15, Navy T18 and Navy T19

	LiCoO2 / Li	PRISMATIC "RIVETED"	
CELL	NAVYT15	NAVYT18	NAVYT19
Pos. plate density	2.7	2.57	2.44
Porosity %	32	35	39
No. of pos. plates	56	56	60
LiCoO2 gms.	1065	1022	1006
Li gms.	68	80	82
Electrolyte gms.	532	600	552
Theorical Ah	149.2	143.1	140.8
Pos. surface cm2.	23216	23216	24874
Stack clearance in.	0.11	0.11	0.04
Cell weight gms.	3011	3033	2970
Test results at + 23 C.			
AH	142	145.7	148
ADV	3.8	3.73	3.83
Wh/L	447.3	451.1	470.8
Wh/K	179.1	179.4	191.2
Test results at - 2 C.			
AH		129.8	130.6
ADV		3.42	3.61
Wh/L		368.5	391.7
Wh/K		146.5	159.1
Total no. of cycles	62	20	20

Chapter 6

Limited Safety Testing

The safety tests under abusive electrical conditions were performed on small 4/5A sized cylindrical cells which were (0.62 inches in diameter, overall length of 1.75 inches) (Table 6.1). The electrodes, separators and electrolyte were the same as that used in the large Navy prismatic cell. The capacities of these small cells were from 0.75 Ah to 0.80 Ah. The separator was one ply of polypropylene 2400 on the negative electrode (lithium) and one ply of polyethylene K-869 on the positive. This design is referred to as the Navy STD.

Cells C468 and C469 were cycled for 60 cycles at room temperature. Their last capacities were 0.22 Ah and 0.23 Ah. Cell C473 was cycled for 15 cycles at room temperature and then for 35 cycles at -2°C. Its last capacity was 0.197 Ah.

A block diagram of the short circuit set-up is given in Figure 6.1. The cells were charged individually and connected in a fixture and placed in an oven at 60°C. The cells were wired through a mercury relay rated at 60 amperes and through a current measuring shunt. There was less than 20 milliohms resistance between the shunt, cables and contacts. The relay was energized remotely and the cell skin temperature, cell voltage and short circuit current were monitored as a function of time *via* the computer. Table 6.2 and Figure 6.2 show the results of the tests.

After 20 minutes, the skin temperatures of cells C468 and C469 were both 60°C. The cells were examined. The heat shrink sleeve on the outside of cells C468 and C469 showed some further shrinking, but there was no evidence of venting. When the cells were opened there was indications that the polyethylene separator had melted and bonded to the positive plate. This was a clear demonstration that the polyethylene had acted as a "shut down" separator.

The can of cell C 473 vented with heat annealing marks around the open vents at the bottom of the can. It is assumed that the cycling of cell C473 at the low temperature had reduced the conductivity of the electrolyte. This induced a greater growth in the thickness of the negative plate because of the roughness of the plated metallic lithium. When similar cells, which had been cycled at low temperature were disassembled, they showed a lithium build up through the separator. Because the anode thickness was 2 to 3 times greater than an uncycled cell, the positive plate was compressed through its expanded metal current collector leading to a direct short circuit. When a cell has a direct short, the "shut down" mechanism does not work because the clogged separator is not able to stop the ionic conduction when it reaches its melting temperature. The deposit build up maintains the electrical path, allowing the cell to reach the run-off temperature. A similar unsafe condition is present when cells are cycled by 10 to 20% more than the number of cycles for which they were designed, regardless of the cycling temperature.

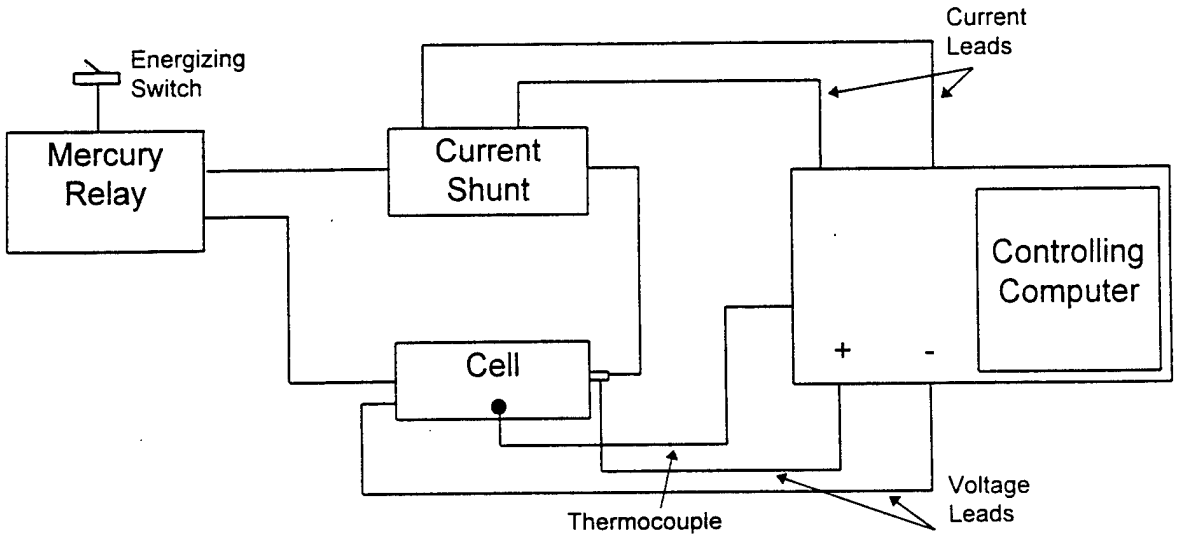

Figure 6.1 Block Diagram of Short Circuit Test Apparatus

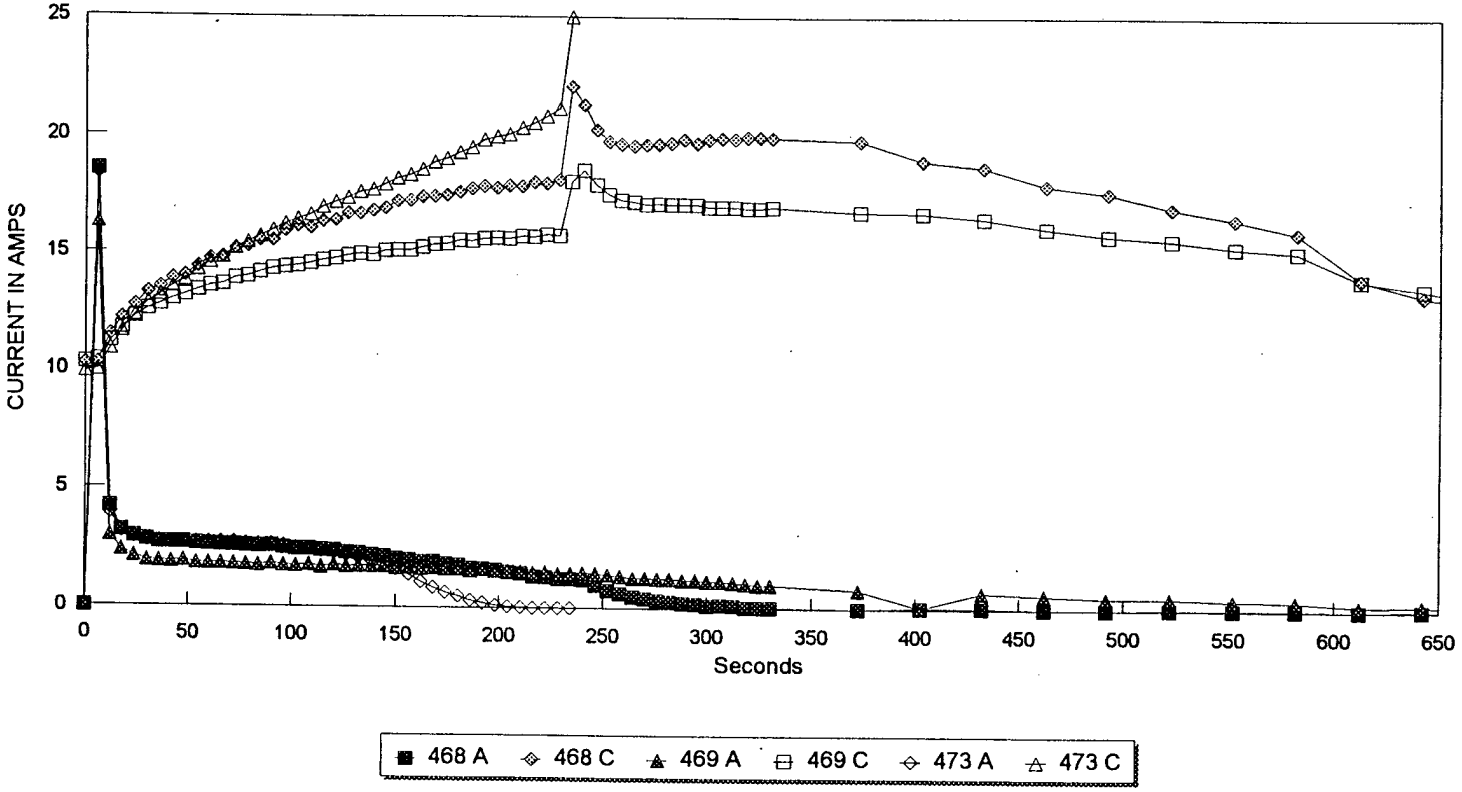

157 C

132 C

111 C

60 C

A. Current
C. Temperature

468 Cycled @ +23 C. 60 cycles. Last capacity .22 Ah. Passed.
469 Cycled @ +23 C. 60 cycles. Last capacity .23 Ah. Passed.
473 Cycled @ - 2 C. 50 cycles. Last capacity .197 Ah. Failed.

Figure 6.2 Short Circuit Safety Tests

Table 6.1. Characteristics of the Tested Cells

Cell No.	C1(Ah/Kg	D4(Ah/Kg)	D4 (Ah)	Li ratio	Cycles	Temp°C
C468	145	141	.753	2.9	60	23
C469	143	147	.754	3.1	60	23
C473	153	140	.758	3.1	50	23 & -2

Table 6.2. Results of Safety Tests

Cell No.	OCV	Peak Amps	At 2 minutes on test Current & Temp	At 4 minutes on test Current & Temp.
C468	3.989	18.5	2.3 A & 98°C	1.2 A & 132°C
C469	3.974	16.3	1.8 A & 88°C	1.4 A & 108°C
C473	3.999	18.3	2.3 A & 103°C	0 A & 150°C

Chapter 7

Redesign of the Battery with Lithium Ion Electrochemistry

After reviewing the results obtained on Cell Navy T15, Cell Navy T18, and Cell Navy T19, it was realized that the design needed to be further adjusted to address the cell bulging problem. This chapter reviews the options considered and presents the test results on several new designs.

Reconsideration of Metallic Anode

Compared to the first 150 Ah cell (Cell Navy T15) cycled at ambient temperature, the deformation of Cells Navy T18 and Navy T19 was considerably more severe. Two factors probably contributed to the bulging problem: (1) a relatively high rate of charge and (2) cycling at cold temperature. The mechanical strength of the case was not sufficient to overcome the forces generated by the expansion of the lithium electrode during cycling. Bulging implies an uncontrolled growth of an electrode. This means that every time the cell was charged, the volume of the lithium electrode increased. This volume increase created the physical conditions, which distorted the electrode pack, the insulation and the separator. The overall conclusion is that during cycling, the physical expansion of the lithium electrode occurred unimpeded by the can planar faces or by the rivets. This allowed the lithium electrode to expand continuously, which gave rise to a distorted stack, which probably shorted.

To control the physical expansion, a redesign of the planar faces (increased wall thickness) and the actual rivets would be necessary. Another possibility is that a reinforced metallic sarcophagus might control expansion of the planar faces, which contain the cells. These design changes would decrease the energy density for the metallic lithium cell to an estimated 120 Wh/kg, and there would be safety concerns as these cells cycle to the end of life. Cell Navy T15 delivered 140 Ah with a positive utilization of 133 Ah/kg. If the thickness of the end plates were increased from .024 inches to 0.190 inches, the number of positive plates in the cell would be reduced from 56 to 48. This would reduce the cell capacity to 121 Ah. (The average capacity per positive plate was 2.53 Ah.) These design changes would not solve the fundamental problem: lithium in rechargeable cells over 100 Ah would always have the potential for a fault mode. A more confident change in direction would be to replace the metallic lithium anode with a lithium intercalation graphite electrode (LiON®). Table 7.1 shows a comparison of the performance at the battery level between a metallic lithium reinforced cell and LiON®. The weight and volume penalty that would occur to reinforce the metallic lithium system results in an energy density similar to LiON®, which offers better cycle life and improved safety.

Figure 7.1 compares the weight disposition of a metallic lithium/lithiated cobalt oxide cell with a lithium ion/lithiated nickel oxide cell. In the lithium ion electrochemistry, the current collectors are lighter because the solid metal foil is thinner than the expanded metal. The foil was not used in the metallic lithium design because it would require lithium on both sides of the foil. This would result in an electrode that was much thicker than when using expanded metal, which required lithium on only one side. Only one separator that is 0.001 inches thick is used instead of three that have a total thickness of 0.003 inches. As a result, less electrolyte is required. However, the carbon in the anode is heavier than metallic lithium. To compensate for the increase in weight, the weight of the active material and the hardware were reduced. Table 7.2 compares the two electrochemistries in our proposed cell design. Both systems are designed to fit into the Li/$LiCoO_2$ metallic hardware.

Reconsideration of the Cathode

Both $LiNiO_2$ and $LiCoO_2$ may be used as the cathode in the LiON® system. Table 7.3 compares the design characteristics of $LiNiO_2$ and $LiCoO_2$. $LiCoO_2$ has more of a tendency to form dendrites at the higher charging rate. Because $LiCoO_2$ has a lower utilization, it requires more active material to match the negative electrode. This increases the thickness of the positive electrode and decreases the number of plates per stack. Because of the greater number of plates and the higher density, the stack made with $LiCoO_2$ is heavier.

Cell Construction

The lithium ion cell has three main components: a bonded graphite anode/negative electrode, a bonded transition metal oxide, (such as $LiNiO_2$), as the cathode/positive electrode, and an organic electrolyte. The lithium ion electrochemistry uses the same type of electrolyte and lithiated metal oxide cathodes as metallic lithium batteries, but the negative electrode consists of a graphitized carbon structure. As there is no metallic lithium present in the cell, the lithium ion technology is safer and offers greater cycling efficiency and speed. The electrodes are typically spirally wound and inserted into the container. The cell is then filled with electrolyte and sealed. It is assembled in a discharged state; it is then formed and charged. During charge, lithium ions deintercalate from the positive electrode and intercalate (charge) into the carbon negative electrode. During discharge the lithium ion moves back to the positive electrodes. Before the first charge, the cell's potential is essentially zero, arising from combining the two half-cell reactions as follows:

$E_{negative}$ = solvent reduction on carbon vs Li $\approx$ 3.3 volts

$E_{positive}$ = $LiNiO_2$ vs Li $\approx$ 3.3 volts

$E_{cell} = E_{positive} - E_{negative} \approx 0.0$ volts

Negative Electrode

During charge, the negative electrode is lowered in potential, allowing reduction of propylene and/or ethylene carbonate, forming lithium carbonate on the carbon surface and some dissolved ethylene and/or propylene gas. The lithium carbonate (reaction product) layer forms a solid electrolyte interface (SEI), through which lithium ions communicate either to the solution or carbon structure. The SEI layer forms an ionically conducting, mechanically robust and electrically insulating film on the carbon surface. The irreversible reaction between the lithium atoms and the alkyl carbonate solvent(s) will then stop once the film thickness is great enough to prevent electron tunneling. As the potential becomes more negative, Li intercalates into the crystalline, layered graphite structure according to the reaction:

$$Li + C_6 \rightarrow LiC_6$$

forming a compound of composition of one lithium per hexagonal C_6.

Positive Electrode

The Li ion source is the $LiNiO_2$, which is undergoing oxidation and de-intercalation, according to the reaction.

$$LiNiO_2 \rightarrow xLi^+ + Li_{1-x}NiO_2 + xe^-$$

The overall electrochemical process is not 100% efficient for the first charge and discharge cycle because Li ions are irreversibly and unavoidably consumed forming the intrinsic SEI layer. After a few cycles, the material can be cycled reversibly according to the following reaction:

$$Li_{0.35}NiO_2 + 0.5\ Li^+ + 0.5e^- = Li_{0_{85}}NiO_2(135\ Ah/kg)$$

The remaining 0.15 Li is consumed in the formation of the SEI layer.

Electrode Processes Development

Coating Methods

When this development began, SAFT had broad experience in the preparation of electrodes on expanded metal grids. Electrodes on grids are more flexible and easier to manipulate than those on foils, but foil technology permits the use of thin films (0.006" - 0.010" thick) as opposed to plates of 0.013" thickness, which is the practical minimum for grid-based electrodes. However, the switch from grid to foil technology required the development of a new coating technique to provide for reliable and reproducible deposition of very thin films. One such method is reverse roll coating. It employs a coater in which a slurry of electrode active materials and binder are applied to the foil (web in coating technology terms) *via* an applicator roller that rotates in the opposite direction to the direction of the travel of the web. A reverse roll coater system is shown schematically in Figure 7.2. The doctor roller acts as a metering device

to control the thickness of the slurry on the applicator roller based on its rotation as well as on the gap between the two rollers. The thickness of the coating is determined by the interplay of the web speed, rotation rate of the applicator and doctor roller, and on the gap between the applicator and doctor roller. An additional parameter to consider is the viscosity of the coating slurry. High viscosity slurries will not flow through the gap and thus give a thinner coating. The reverse roll coater method of coating requires a slurry viscosity in the range of 1000 to 5000 centipoise (cp).

In the initial phase of development, the effect of the speed of the rollers, the web speed, and the gap setting were studied to determine what were the main contributing factors to the final coating thickness. The data clearly showed that the coating thickness increased with increased applicator roller speed. Experiments, which increased the doctor roller speed by a factor of 2, caused only a very small decrease in the film thickness. The doctor roller had a much smaller effect on the film thickness than did the applicator speed.

An important aspect of the process was the effect that the drying method had on the resulting film. While there was no effect on film thickness, there was a major effect on adhesion. Ovens can be heated by either radiant heat (like an electric kitchen oven) or by forced hot air (a convection oven). Each of these ovens had its own advantage. Radiant heat, which previously was used to make the pasted electrodes, is a more directed heat with the heat being absorbed by the object being dried. The convection method, because it heats the whole oven, has the advantage of sweeping out any vapors that may accumulate. The oven was divided into four heat zones of 60°C, 100°C, 110°C and 130°C. The coated electrode entered the oven at the 60°C zone and exited at the 130°C zone.

To make the electrodes for the lithium ion cell, the oven was converted to a convection type. In this heating method, forced air was directed over electric heaters and the hot air was then allowed to pass over the coated foil substrate. Using this drying method, the hot air allowed the N - methylene -2- pyrrolidone (NMP) liquid component of the slurry to vaporize near the surface and then be swept away above the film. Convection caused a non-equilibrium condition with respect to the amount of solvent in the film and solvent vapor above the film. This method of heating does not close the top film surface since the solvent vapors are constantly escaping from the mass of the coating. Electrodes made using this method of drying showed vast improvement in adhesion and performance.

Positive Electrode

Plate Manufacture. The weight percentage of active material ($LiNiO_2$) was 86%, with 4% Shawinigan black, 4% graphite and 6% poly (vinylidene fluoride) (PVDF) binder, making up the balance of the solids in the slurry. In the beginning, the target was a loading of 60 mg/cm^2 and a porosity of 25% of active material when coated onto the foil collector. The final target was 40 mg/cm^2 and a porosity of 25 to 30%.

Saft manufactured a uniform, dense, and low impedance positive $LiNiO_2$ cathode by the following process. $LiNiO_2$, graphite, and acetylene black were mixed for 10 minutes and then loaded into a Ross mixer where the PVDF (Kymar 2751) was added and mixed for 5 minutes.

The NMP, which makes up 47% by weight of the final mixture, was added to the solids and mixed for a total of approximately 1 3/4 hours. The mix was checked for viscosity and density. Typical values would be 1500 cp for the viscosity and 1.5 g/cm^3 for the density. The mix was then coated onto a 0.0007" aluminum foil and dried in a convection oven. An aluminum foil current collector was selected because of its low weight, excellent electronic conductivity and electrochemical stability at the system's high oxidizing potential. The second side was then coated and dried in a similar manner. After coating, the rolls were allowed to set for at least 10 hours in the dryroom prior to cutting.

Cathode Plate Assembly. The following steps were employed to convert the cathode strips into electrodes. After being cut into 4.5-inch wide strips, the weights and thickness were determined. From this information, the thickness required for the proper porosity was calculated and the material was calendered in several passes by a roller unit to that thickness. Positive material was scraped away to expose a sufficient area of the foil so that aluminum tabs could be ultrasonically welded to the plates. The tabs and the surrounding areas of the welding were protected with electrical tape. It had previously been determined that the tape had no deleterious effects on the cell. After the weight and thickness were recorded, the cathode assembly was vacuum dried for a minimum of two hours.

Negative Electrodes

Plate Manufacture. The weight percentage of active material was 86% graphite, 3% PLV/accelerator and 11% PVDF binder. PLV is a binder manufactured by Pelmor Laboratories. Initially, the target was a loading of 28 mg/cm^2 and a porosity of 30% of active material when coated onto the foil current collector. This loading was later reduced to 22 mg/cm^2 and a porosity of 40%. It was found that the adhesion was not as good on the thicker plates and that material flaked off during the cutting into electrodes. Because the binder is a rubber-like material, the plates want to return to their original thickness. Since about two weeks elapsed between the time that the electrodes were made and the time that they were assembled into batteries, there was more increase in thickness with the lower porosity. In order to reach the proper porosity, the plates were calendered to reduce the plate thickness. The copper foil current collector, which is 0.0004" thick, provides excellent structural support, high conductivity, and is stable over the normal operating voltage range.

Saft was able to manufacture a uniform, dense and low impedance negative electrode by the following process. The graphite and PVDF (Kynar-741), which is a binder for the mixture, were loaded into a Ross mixer and mixed for 5 minutes. The NMP, which makes up 62% by weight of the final mixture, was added to the solids along with the PLV/accelerator, which binds the mixture to the foil, and mixed for a total of 1 1/2 hours. The mix was checked for viscosity and density. Typical values would be 1500 cp for the viscosity and 1.1 g/cm^3 for the density. The mix then was coated onto one side of 0.0004" copper foil and dried in a convection oven. The second side was coated and dried in a similar manner. The coated rolls were allowed to set for at least 10 hours in the dryroom prior to cutting.

Plate Assembly. The following steps were employed to convert the anode strips into electrodes. After being cut into 4.5-inch wide strips, the weight and thickness were determined.

From this information, the thickness required for the proper porosity was calculated and the material was calendered in several passes by a roller unit to that thickness and cut into parts with a steel rule die. Negative material was scraped to expose sufficient area of the foil so that a nickel tab could be ultrasonically welded to it. The tab and the surrounding area of the welding were protected with electrical tape.

Battery Designs

Full Plate Design

Figure 7.3 shows the dimensions of the trimmed positive plate that would be required for the full plate design. The tab area would not be coated. Because the electrode coating process produced plates that were only 4.5 inches wide, it was proposed that 4.5-inch wide electrodes be used, and the rest of the space in the battery filled with plastic. This idea was discarded because it would decrease the specific energy of the battery (Table 7.4). Instead, it was proposed to add a strip of electrode material to bring the cathode width to the 5.25 inches dictated by the design (Figure 7.4). The two sections of the plate were joined by a double tab, which was sonically welded to the foil, as shown in Figure 7.4 for the positive and Figure 7.5 for the negative. Each positive and negative electrode was contained in a heat-sealed bag (Figure 7.6 and 7.7, respectively). Active material flaked off at the edge during sonic welding of the tab. Due to the electrical insulation required on the tab, there was a difference in thickness between that area and the rest of the plate. Some of the negative plate area at the top of the plate was removed to allow for the positive tab thickness. This was not possible at the bottom. Because of these and several other problems, no cells or batteries were built.

Twin Pack Design

To resolve some of the fabrication problems, the Twin Pack Design was proposed (Table 7.5). In this design, the positives and negatives were prepared as half plates. The positive plate (Figure 7.8) had a thickness of 0.0085 inches, a porosity of 35% and a loading of 0.0456 gs/cm^2 (0.362 g/in^2). The positive plate was fitted into a separator pouch as shown in Figure 7.9. The separator was first folded in half, then heat-sealed in two places along the long side. The positive plate was inserted into the pouch and the center holes and the sides were sealed as shown in Figure 7.9. The negative plate (Figure 7.10) had a thickness of 0.009 inches, a porosity of 46% and a loading of 0.022 g/cm^2 (0.24 g/in^2).

The cell was assembled by placing the nickel end plate, (Figure 7.11), which contained the four rivets (Figure 7.12), and the center rivet (Figure 7.13), on the fixture (Figure 7.14), then two negative electrodes (right and left side), and the positive electrodes with the separator, etc. The rivets were made from flanged copper tubing with slits to allow the electrolyte to flow to the center of the stack. The outside diameter of the rivets was the same dimension as the holes in the negative electrode so that the rivets would be in electrical contact with the negative electrode. The flanges of the rivets were spot welded to the end plate. After the last set of plates was positioned, another end plate was added and the stack was compressed at 50 kilograms of pressure overnight. When the proper height (1.66 inches) was obtained, the rivets in the end

plate were flared over in order to keep the stack under pressure (Figure 7.15). The copper rivets and the nickel end plates were the negative current collector. The two end plates were electrically connected, by spot-welding a nickel strip to each. The positive tabs were welded together into groups of 6 to 10 and a thicker aluminum tab was welded to the bundle. The stack was then inserted into the can. When the hole in the can and the center rivet were properly aligned, pop rivets were inserted into each end of the center rivet (Figure 7.16) to fix the stack geometry. Because of thickness variation in the plates, and tolerance build up, it was not possible to maintain an even pressure on the stack. There was a difference in thickness between the two sides. During charging, during cycling (Figure 7.17), the low-pressure side expanded more, causing the tabs to break. When one side lost contact, the negative contacted the bottom of the can.

Before the cell was disassembled, it weighed 3.052 kilograms, and it had an OCV of 3.452 volts. The top was cut at three sides at 0.09 inches below the TIG weld and the top was folded back to open the cell (Figure 7.18). The connection from the plate busses to the feed-through was very good on both terminals. The area where the TIG. weld joint had been reworked showed melting of the top insulator which was very close to a positive plate. The top of both stacks was covered with a white salt deposit (Figure 7.19). There were gray deposits concentrated in the two areas under the negative terminal. When these deposits were tested under water, they showed high reactivity (an indication of plated lithium). About 25 mL of excess electrolyte was drained. This liquid was black and probably contained residue from the negative plate edges. The cell top cavity was filled with mineral oil and let to stand for two days. When the bussed tabs were removed, most of the positive tabs were disconnected and had a white salt between them. The tabs were cleaned and reconnected using alligator clips. A resistive load of 0.25 ohms was applied to each single twin stack and to the paralleled twin stacks. The results were as follows:

	Open Circuit Voltage (Volts)	Load Voltage (Volts)	Current (Amperes)
Both Twin Stacks	3.415	3.20	10.4
Stack Closest to Negative Terminal	3.427	3.10	9.9
Stack Closest to Positive Terminal	3.427	3.14	10.08

This indicated that the electrical isolation was still good. The negative stack had more unused plates because it had lost electrical contact, due to the disconnected tabs.

The stainless steel can rivet (Figure 7.14) was removed. The large planar side of the can was cut along the can's longer side. When the bottom side of the can was cut, some smoke was produced. The planar side of the can was bent back. The flanged copper rivets (Figure 7.12) on the negative terminal side of the battery were broken. This side was probably looser in the can and did not have the support of the can center rivet.

The electrode pack was removed from the can. There were gray deposits on the side and bottom surfaces of the negative terminal side of the battery. The negative plates were not isolated from the can. In nickel/cadmium and other batteries with aqueous electrolyte, the tabs of the electrodes are clamped and bolted together, welded or fused. In the Twin Pack design, the electrode tabs were joined mechanically. It appears that the lithium ion electrochemical system requires a welded joint between the tabs and the bus terminal to avoid corrosion (oxidation) on the surface of the aluminum tabs. This corrosion caused an increase in the impedance of the cells, which could be the reason for the early and rapid decline of the capacity of the cell even at a moderate load. The gray deposits on the side and the bottom of the stack located on the negative terminal side of the battery could be the results of the weak electrical connection of its positive tabs.

Five to eight electrodes at the end of each stack were extruded into and through the holes in the end plates. This is an indication of the pressure that was produced by the cycling plates. Figure 7.20 indicates that the positive plate had expanded from 0.009 inches (at assembly) to 0.012 inches, an increase of 25%. The negative plate (Figure 7.21) had expanded from 0.010 inches (at assembly) to 0.013 inches, an increase of 25%. This observation reaffirms the importance of maintaining the structural rigidity of the cell. The expansion of the negative plate during charging is not reversed during the discharge cycle unless force is applied. (Saft has now incorporated internal spring plates in its 4.5 Ah prismatic cells.)

Slitted Plate Design

Because of the above problem, the Slitted Plate Design using the $LiNiO_2$ as the cathode was proposed (Table 7.6). The plates were cut on a slitter instead of being cut with steel rule dies. The cell consisted of three electrode packs. They were assembled parallel to the small face of the prismatic cell. This mode of assembly had the following advantages: it avoided the electrode stack pressure on large planar surfaces, because the stack pressure was against the cell end plates; it required less head space for bussing; it eliminated the peeling of the edge of the electrodes caused by cutting with steel rule dies; it eliminated tab welding by using the foil substrate as the tab; it minimized the handling required for tabbing and heat sealing the separator pouches; and it provided a simple mode stacking for easier mechanization. Furthermore, the energy efficiency increased, compared to the Twin Pick Design:

From	To
120 Ah	128 Ah
139 Wh/kg	148 Wh/kg
63 Wh/lb	67 Wh/lb

Cell Navy T24A. The contract required the building of cells with $LiCoO_2$ and $LiNiO_2$ as the cathode. Table 7.7 shows the proposed design using $LiCoO_2$ as the cathode. The electrode plates were cut on the slitter to the proper width and then cut to length to fit the side of the can. The positive plate (Figure 7.22) was 1.55 inches wide. The separator, which was tri-layered polypropylene/polyethylene/polypropylene, was 1.687 inches wide. The positive plate was wrapped with the separator and partially heat-sealed around the edge (Figure 7.23). The negative plate (Figure 7.22) was 1.66 inches wide and was folded in half. The bagged positive plate was placed in the half-folded anode (Figure 7.24). One end of both electrodes was cleaned of active

material and this end was trimmed to form the tab. Because of variation in loading and thickness, it was necessary to group the electrodes by weight and thickness. The negative and positive electrodes were paired in order to maintain a relatively even ratio of active material weight per stack.

The stacking began with a bagged positive in a folded negative, followed by a bagged positive, etc., to form a stack of 312 bagged positive plates (Figure 7.24). The finished stack was kept in the fixture while it was under a 20 kg load overnight before being strapped with adhesive tape. One side of the fixture was partially open to allow for the welding of the tabs. The aluminum (positive) tabs were spot welded together into groups of ten. The copper (negative) tabs were spot welded together into groups of six. Because the negative plates were folded, there was half the amount of these tabs. The pre-welded aluminum tabs were folded against the side of the stack and a 0.010-inch thick aluminum tab was serial/parallel welded to the folded tabs. The copper tabs were also folded and a 0.003-inch thick nickel tab was series/parallel welded to the folded tabs.

The bussed stack was removed from the fixture and inserted into the can. Removing such a large number of plates from the fixture caused some plates at the middle of the stack to shift, making this operation very difficult. For this cell, the plates were cut to a length that permitted more clearance at the bussing area. However, the plates shifted and the loss of electrical isolation persisted. Finally, the completed cell lost its isolation while the cover was being TIG welded to the can. The aluminum bussing at the upper corner absorbed enough heat to cause the separator to melt at the very near edges of the positive and negative plates.

Cell Navy T231. It was recognized that in order to prevent the shifting of the plates in the stack, the number of plates should be minimized and the tabs should be welded after the stack is in the can. The electrodes were made as long as the case height permitted. This minimized the total number of plates in the cell that permitted the electrode tabs to be welded together or bussed after the electrodes were placed in the can.

Two internal dividers were added to the can for two reasons:

1. Since they would not permit the deflection of the can on its large side, there would be better control of the stack pressure during temperature cycling
2. A fixture (Figure 4.4) would not be required in order to fill the cell with electrolyte at a higher pressure.

The existing hardware was modified by making small slots at 1/3 and 2/3 the width of the inside of the can and inserting two small plates of the same thickness as the can that fit loosely into the can. The bottom corners of the divider were rounded so that they would be easier to insert into the can. The dividers were TIG welded to the can through the slots (Figures 7.25 and 7.26). Because of the loose fit and rounded corners, the dividers did not isolate the electrolyte between compartments.

The electrodes were fabricated like those for Cell Navy T24A except that they were one inch longer. The negative and positive electrodes were paired in order to maintain a relatively

even ratio of actual material weight per stack. Each stack was built to fit a cell cavity after the 20-kg compression. The stack was tested electrically for shorts, wrapped with the separator, strapped with adhesive tape and inserted into the can. When the three stacks were in the can, their tabs were folded over the stack. Two 0.010-inch thick aluminum tabs were welded to the aluminum foil tabs and two 0.003-inch thick nickel tabs were welded to the copper foil tabs. The two tabs were located side by side without touching, over the folded tabs and series/parallel welded by placing each welding electrode on each of the two tabs (Figure 7.27). This time the tabs were not pre-welded by groups. Cleaning the active material from the tabs made them very weak, brittle and difficult to weld. For this reason, many plates were replaced or reworked during the building of the stacks. This produced stacks with different weights and stack pressures.

As a result of past experience, it was recommended that when the active material is removed from the electrode foil, that a thicker tab (0.001 to 0.005 inches thick) be sonically welded to the cleaned foil to be used as the tab for the current collector. This procedure would require that both sides of the plate be taped in order to provide short circuit protection. Since this would increase the overall thickness of the plates, this design was not selected for this cell. Several attempts were made to manufacture plates by a process of intermittent coating, so that the plates would have areas without active material. Since one side is coated at a time, often there was misregistration on the second side. There were not enough plates to build a single stack. Two of the stacks used in this cell were reworked from the previous cell. They were reworked because they had lost their electrical isolation while the cover was being welded to the can. After bussing, a 0.5-inch wide glass tape was wrapped around the upper positive end of the stack in order to protect all of that mass of aluminum from the heat of the TIG welding. While welding the cover to the case, the assembly was allowed to cool after each 1.5 inches of welding.

In order to fill the cell with electrolyte, 650 grams of ternary electrolyte, EC/PC/DMC with 1.2*M* $LiPF_6$, were prepared and the electrolyte container was pressurized with CO_2 at 30 psig. The cell was evacuated for ten minutes and refilled with electrolyte vapors and CO_2. This was repeated three times. The fourth time, the electrolyte tank was inverted and the cell was filled with electrolyte. The fill port was fitted with a miniature shut-off valve. This permitted the release of the internal cell pressure after the cell formation. The cell weight was 2448 grams dry and 3060 grams after filling.

The cell was set to charge at 9.53 amperes (C/10) to 4.2 volts and to discharge at 15 amperes (C/6) to 3 volts.* Because of the cell's rapid decline in capacity, the rates were lowered after the fifth cycle. The cell was partially charged and discharged and stored at different temperatures during the formation cycling. The first charge was 75.37 Ah and the first discharge was 41.7 Ah. The second charge was 89.44 Ah and the second discharge was 85.0 Ah. This is a discharge/charge (D/C) ratio of 0.95. From the cycling data (Figure 7.28), the cell discharged at 85.0 Ah, which was very close to the theoretical 87.96 Ah. The fact that the charge and discharge capacities remain very similar throughout the 200 cycles indicated that the cell had good electrical isolation. The sharp capacity decline during the first 20 cycles indicated that a cell stack or single plate had become disconnected. After the 90th cycle, it was assumed that

* These rates were calculated from the cell's theoretical capacity and its total positive electrode area of 35,094 cm^2.

only one of the three stacks was working, because at that cycle the capacity was about one third of the total capacity. This assumption was confirmed by postmortem analysis.

After cycling, the cell was stored for three months in the discharged state. The cell was vented by removing the shut-off valve from its filling port. No gas or liquid was released. There was no change in the 1.75 inch dimension, which indicated that there was no swelling (Figure 7.29) on the large planar surfaces in contrast to what occurred on the Twin Plate and prior designs. The OCV was 1.1 volts.

The cell was opened by cutting three sides of the top/can TIG welded joint and by folding back the top (Figure 7.30). No salt residues or signs of shorting were observed on the top of the electrode stacks. When the top of the cell was lifted back, (Figure 7.31) more than half of the tabs that formed the positive electrodes bussing came loose. When pressure was applied over the tabs, the voltage per stack from the positive terminal side to the negative read 2.5, 2.66, and 2.8 volts. When the bus tabs were reset over the stacks, the voltage reached 3.0 volts. A 20-ohm resistor was connected to the three stack's terminals without any drop in voltage. After 16 hours, the cell voltage was 1.4 volts. A closer examination of the positive electrode showed that only the foil that was in direct contact with the bussing tab had a weld nugget. The rest were only tacked and became disconnected during the first few cycles. There was a much better weld between the nickel bussing tabs and the copper foil tabs of the negative electrodes. This confirms the difficulty of using a cleaned portion of an electrode foil as the current collector tab. When the active material is scraped from the aluminum foil, the resulting surface is not suitable for resistance welding. In order to be able to weld a group of aluminum tabs, their surfaces cannot have been exposed or affected by the active cathode material. Without an intermittent coating process for making the electrode, using the metal foil substrate for the tab is impractical for thin foil technology.

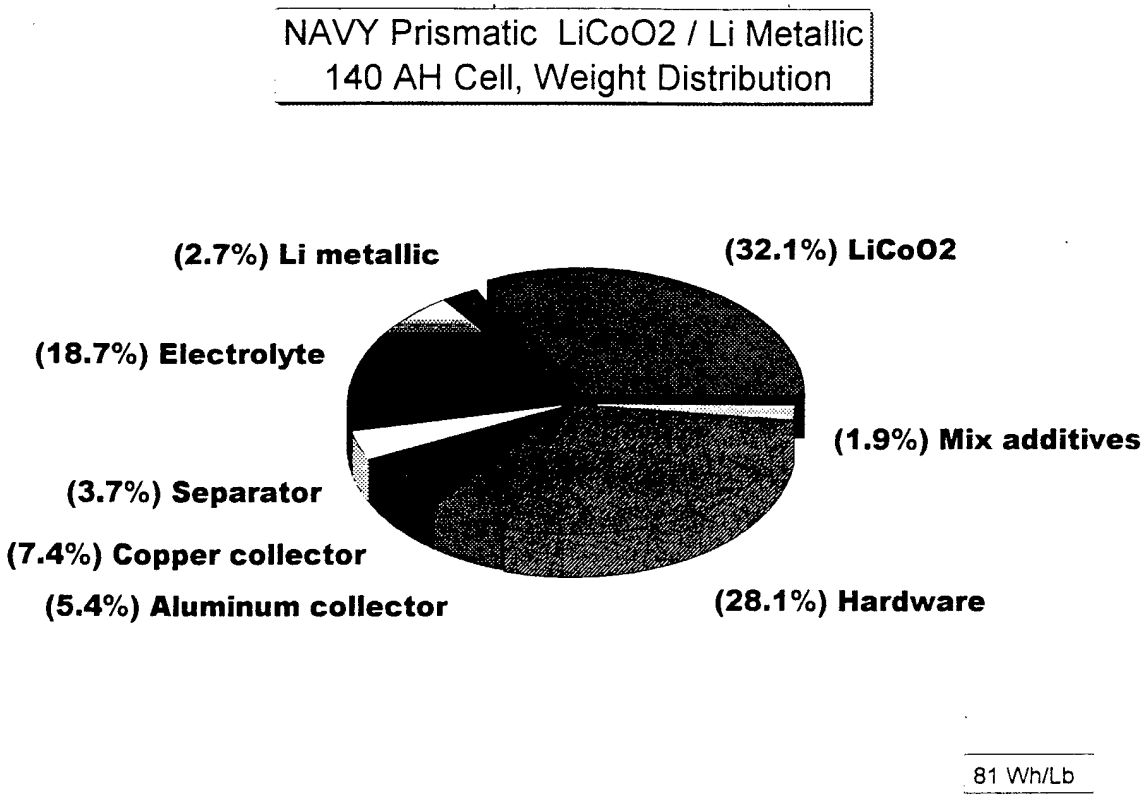

Figure 7.1 Comparison of the Weight Distribution Between $LiCoO_2$/Li Metallic and $LiNiO_2$/Carbon Cells

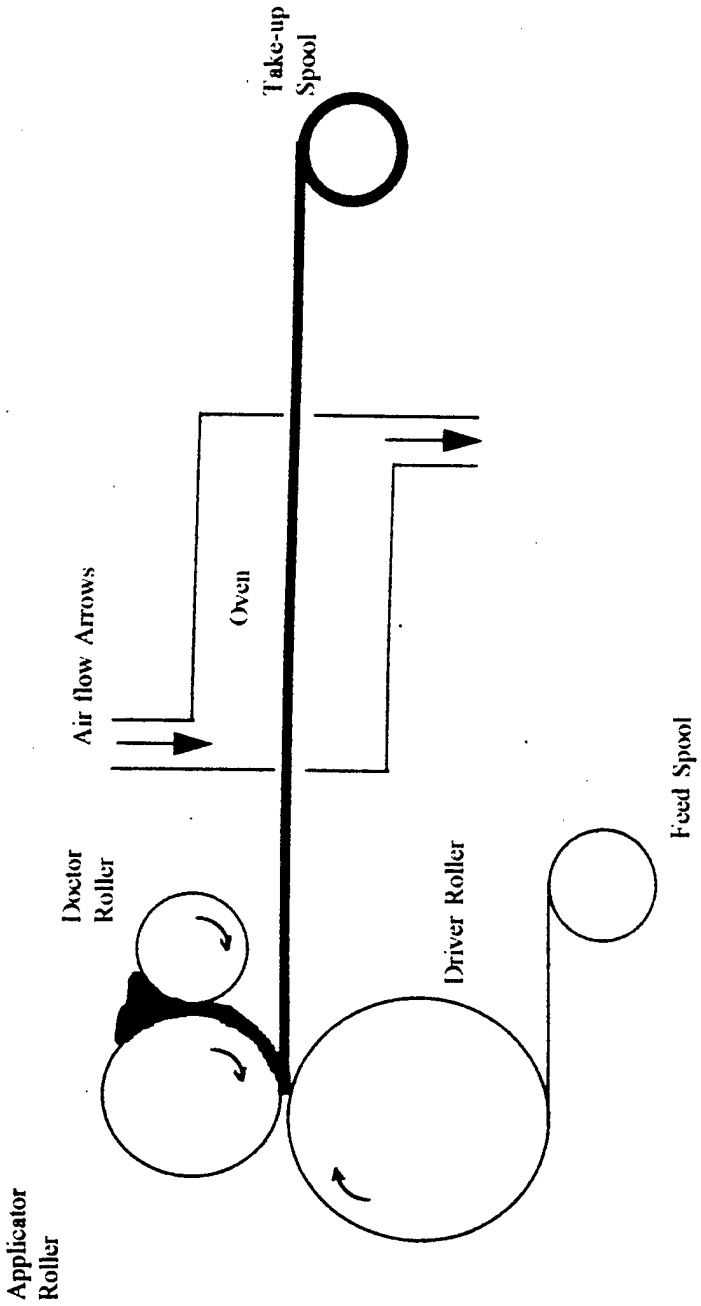

Figure 7.2 Electrode Coating System

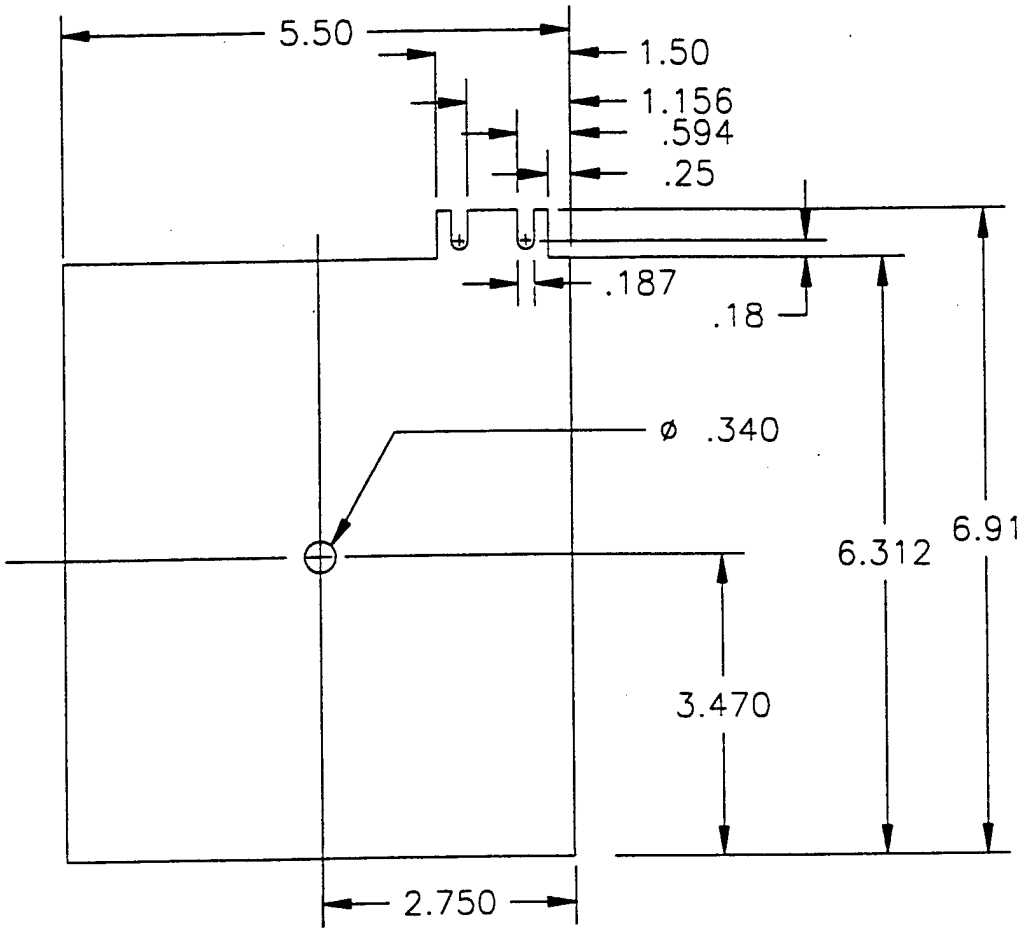

Figure 7.3 Trimmed Positive Plate for Full Plate Design

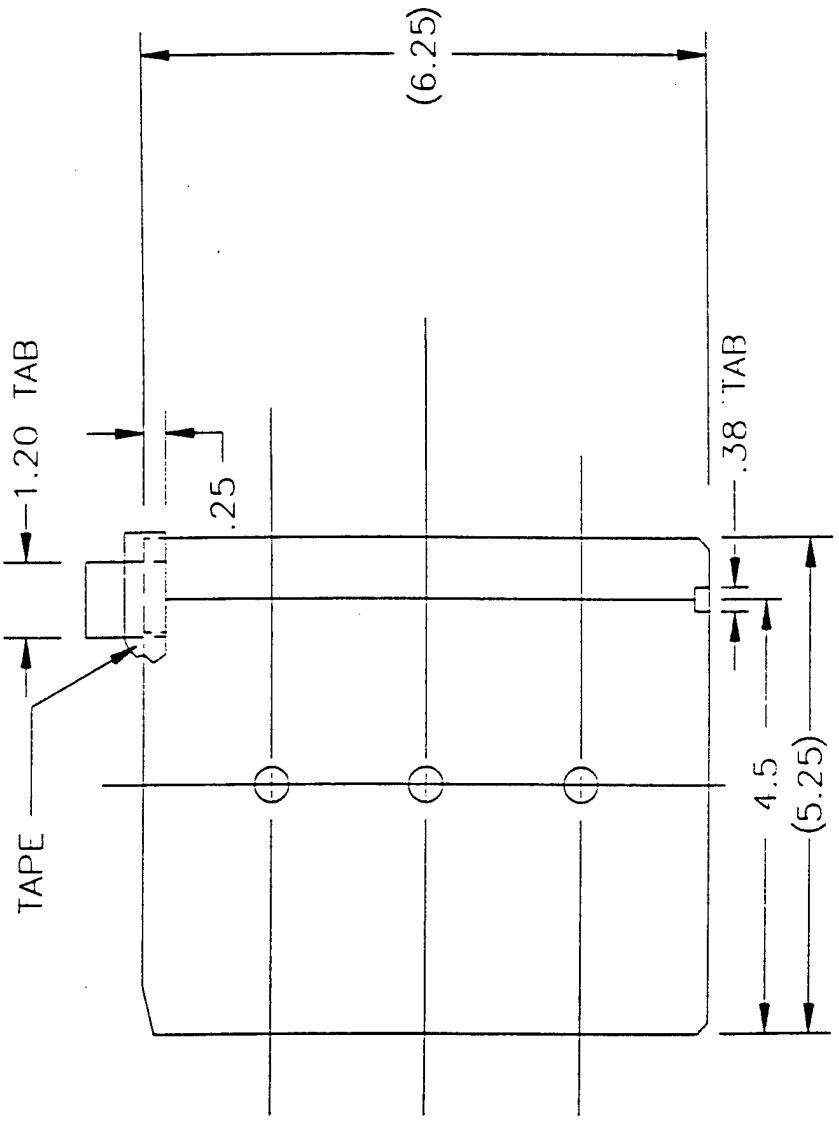

TAB 0.001 THK. ALUMINUM FOIL, 1.20 WIDE ULTRASONIC WELDED TO GRID

TAPE 0.50 WIDE, COVER BOTH SIDES.

Figure 7.4 Tabbed and Insulated Positive Plate for Full Plate Design

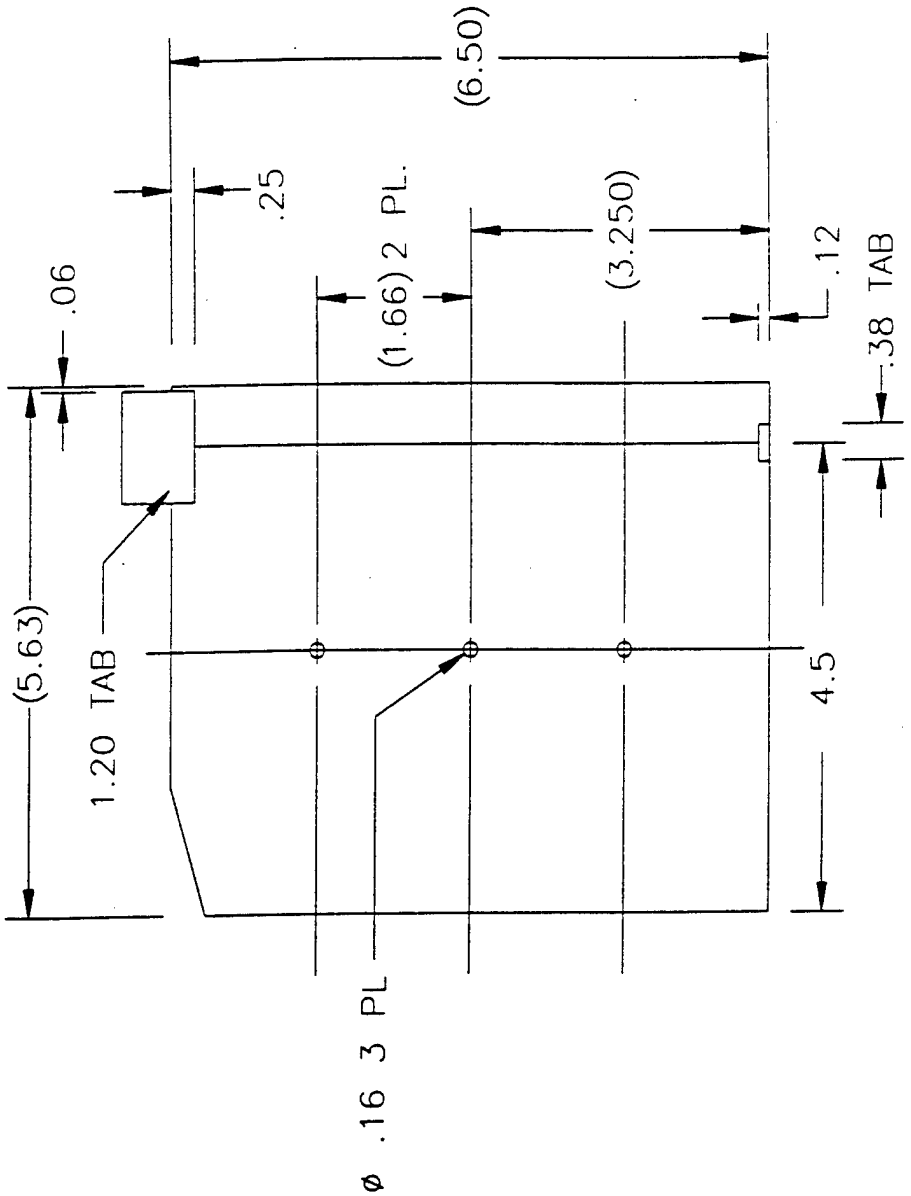

Figure 7.5 Tabbed and Insulated Negative Plate for Full Plate Design

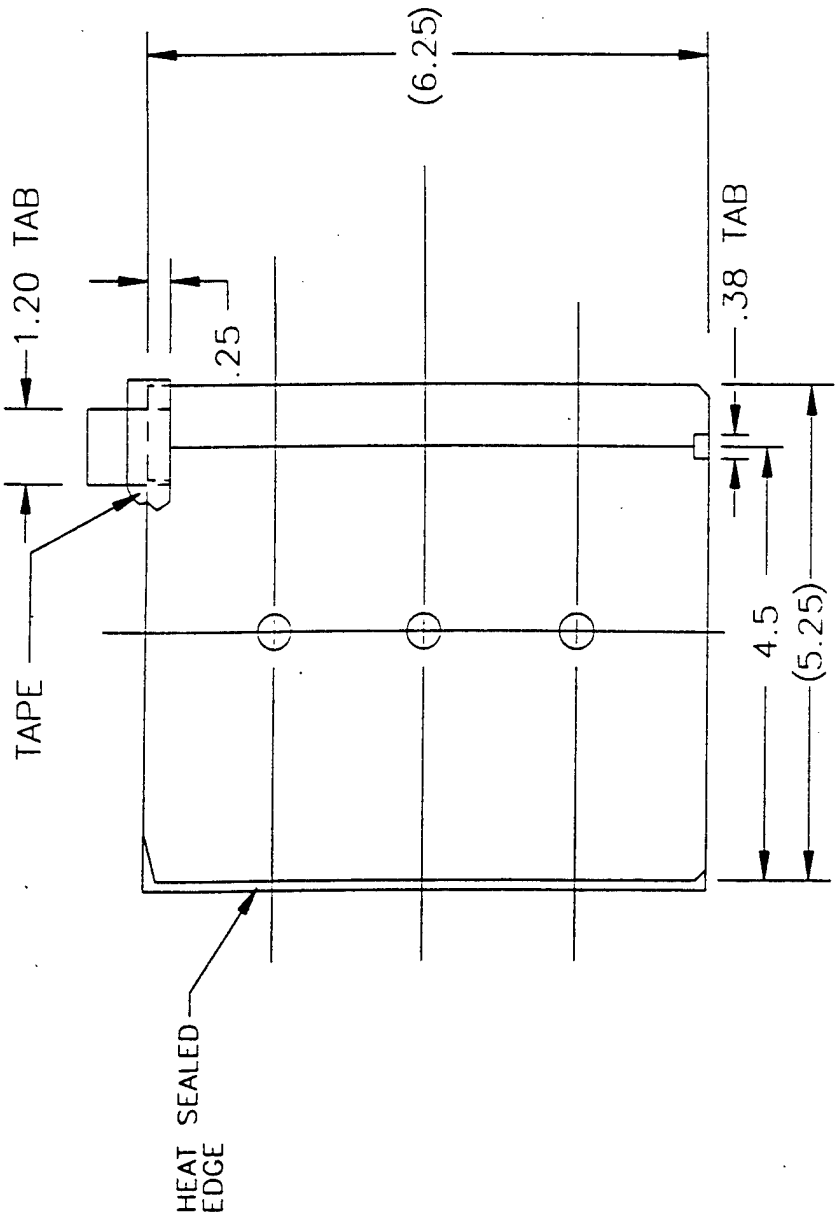

SEPARATOR CELGARD K-869(POLYPROPYLENE)
CUT WIDTH TO 6.50" AND LENGTH TO 11.4".
FOLD SEPARATOR OVER THE EDGE OF THE PLATE.
WITH A SOLDERING TIP, BURN 1/8"ø SPOTS CONCENTRIC WITH PLATE HOLES.
TRIM WITH A HOT KNIFE THE EXCESS AT THE OTHER EDGE OF THE PLATE.

Figure 7.6 Positive Plate with Separator

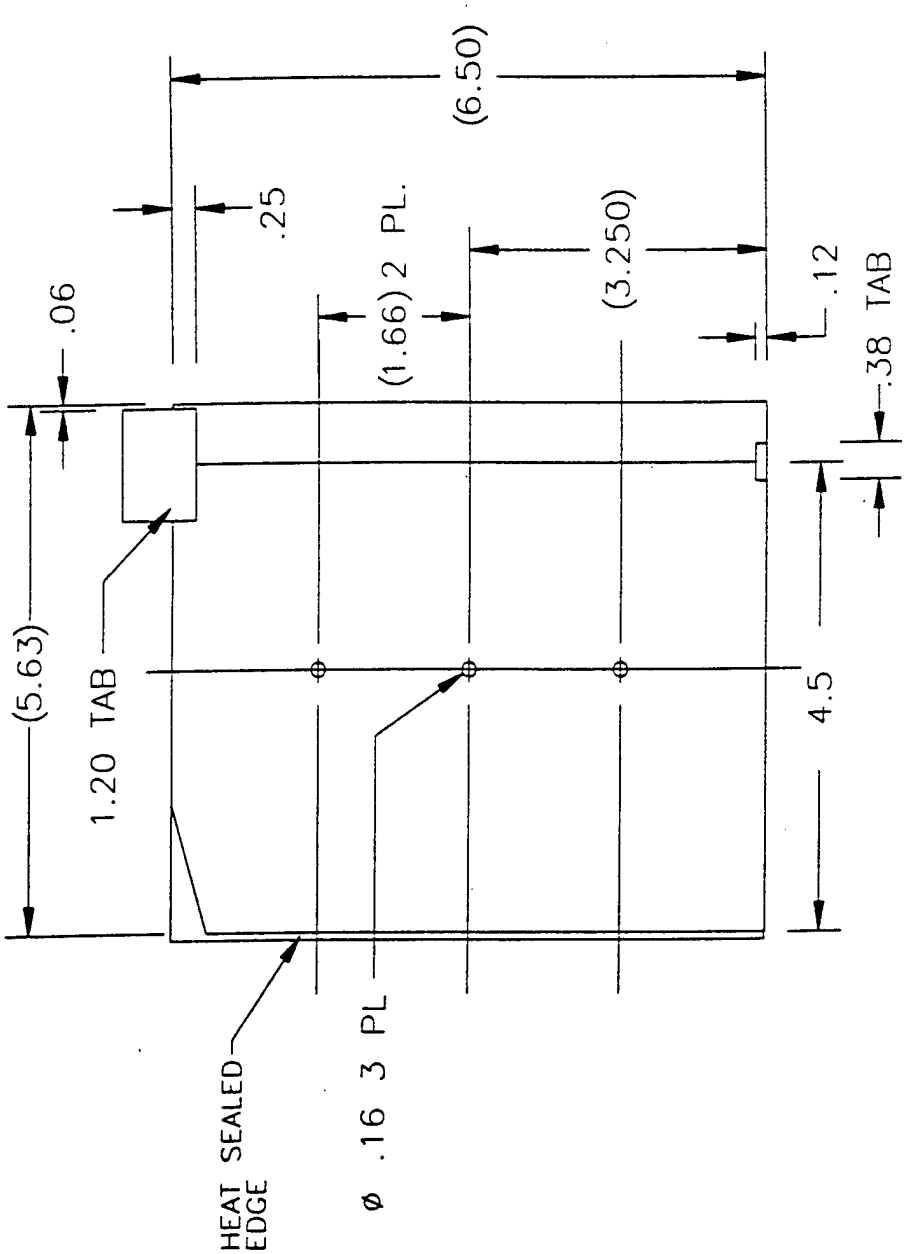

SEPARATOR CELGARD 2400(POLYPROPYLENE)
CUT WIDTH TO 6.50" AND LENGTH TO 11.4".
FOLD SEPARATOR OVER THE EDGE OF THE PLATE.
WITH A SOLDERING TIP, BURN 1/8"ø SPOTS CONCENTRIC WITH PLATE HOLES.
TRIM WITH A HOT KNIFE THE EXCESS AT THE OTHER EDGE OF THE PLATE.

Figure 7.7 Negative Plate with Separator

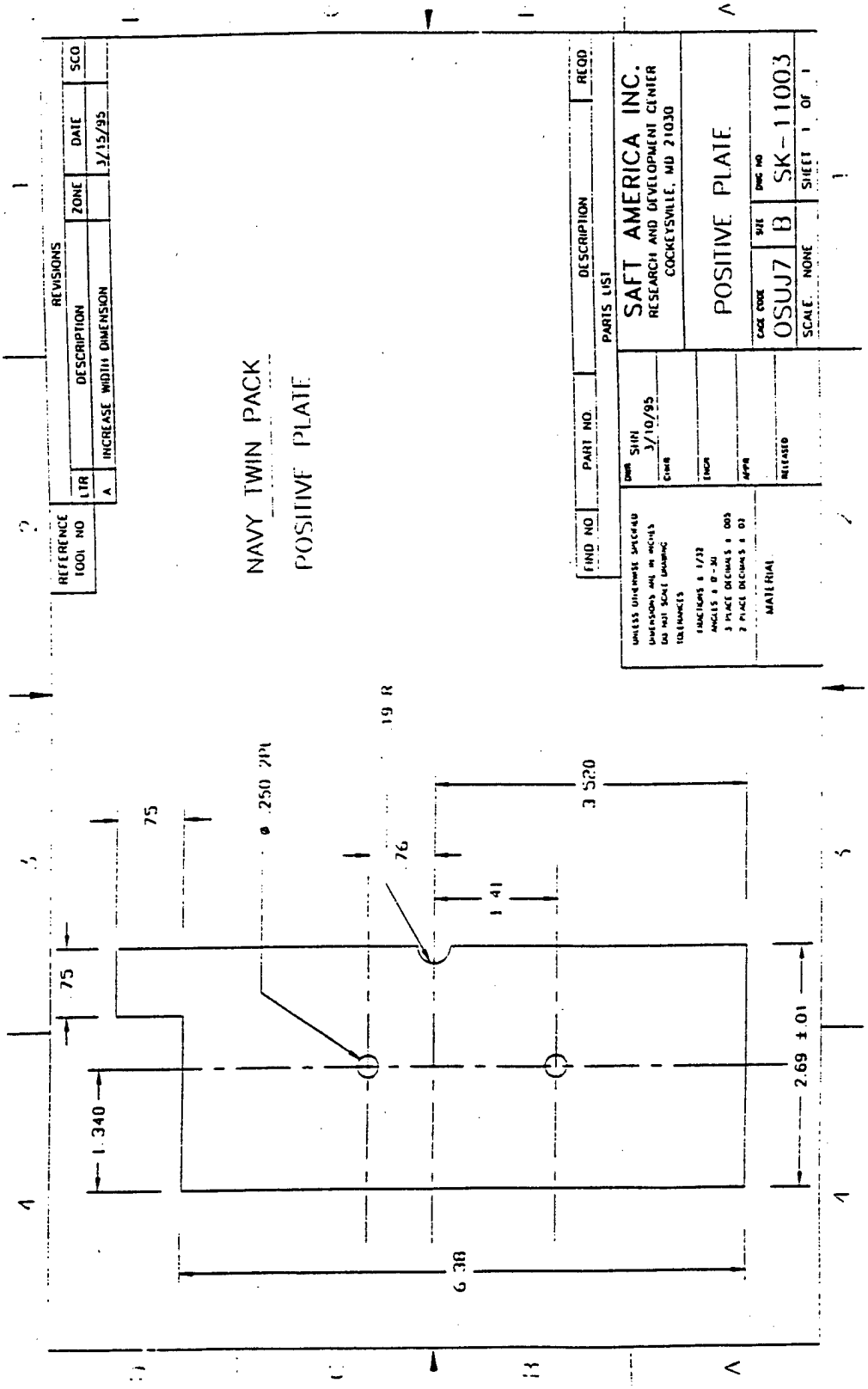

Figure 7.8 Positive Plate for Twin Pack Design

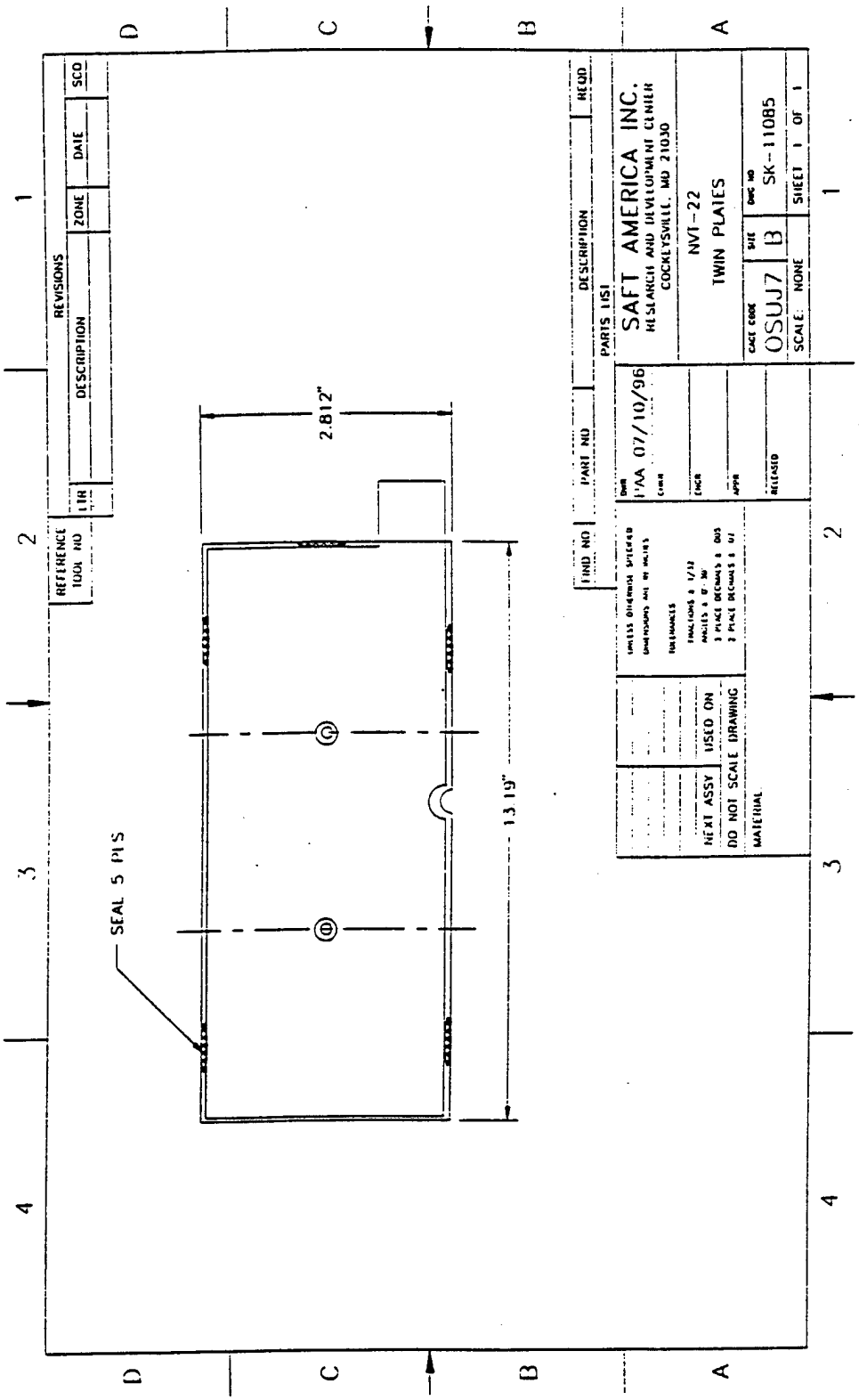

Figure 7.9 Positive Plate with Separator

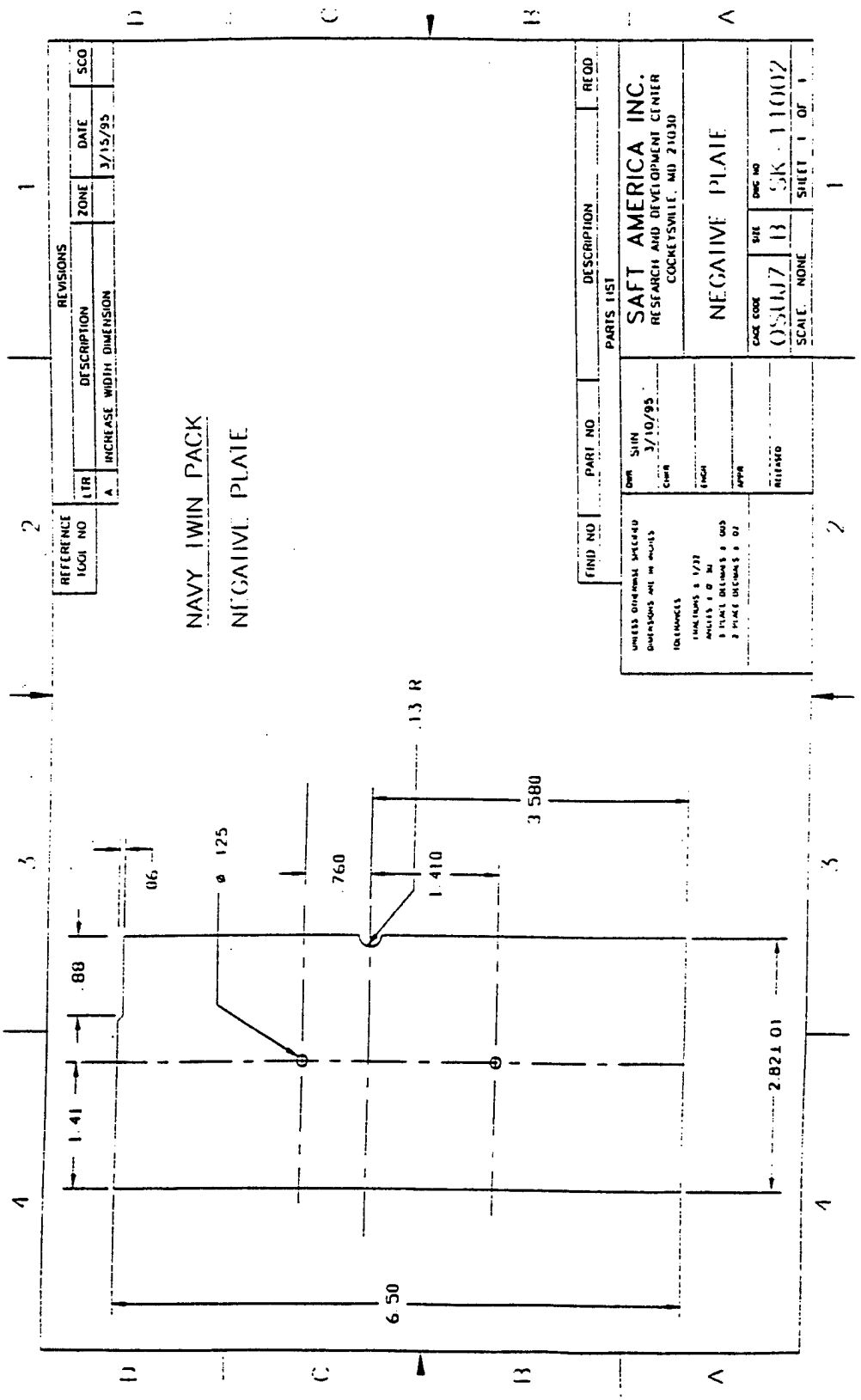

Figure 7.10 Negative Plate for Twin Pack Design

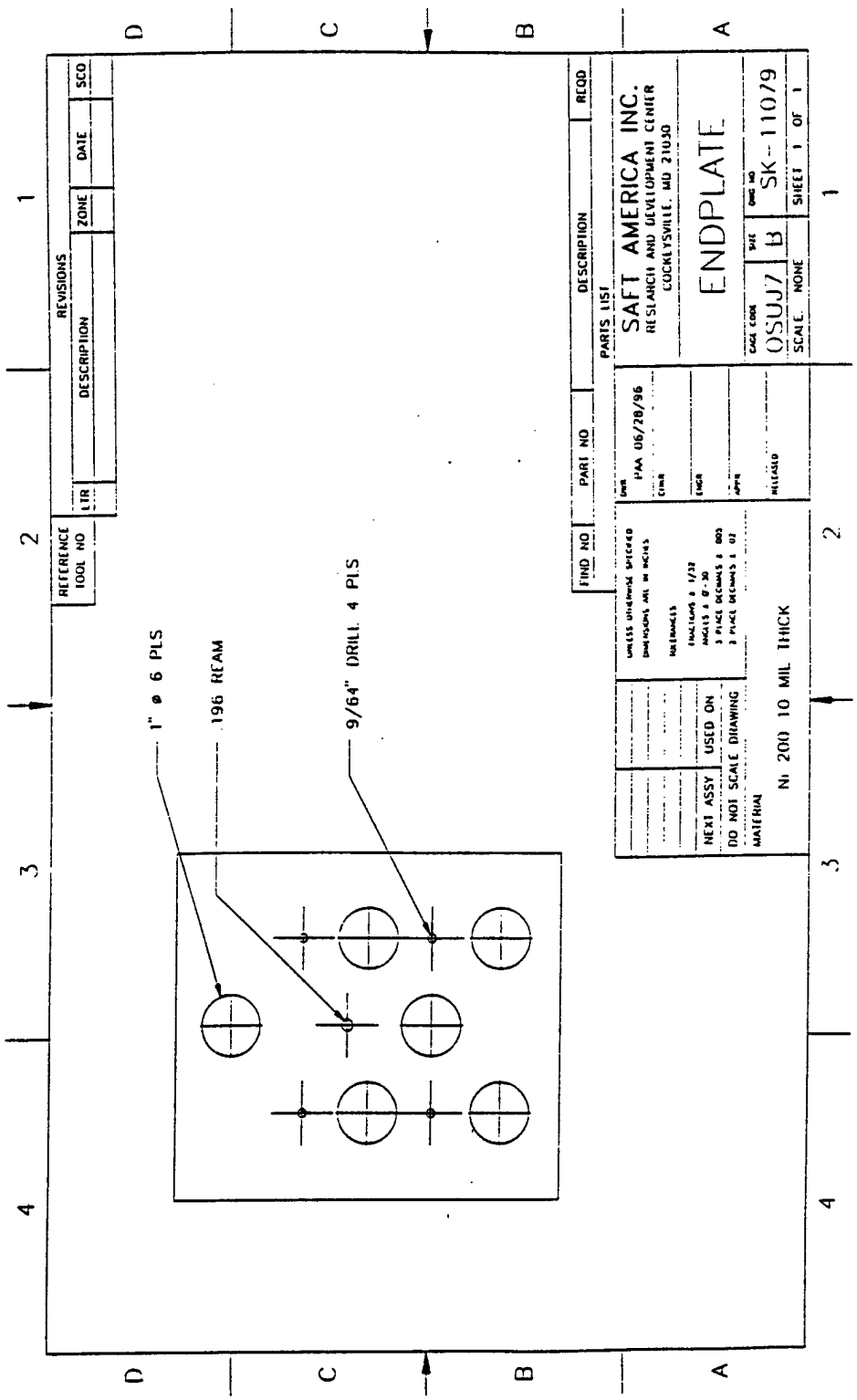

Figure 7.11 End Plate for Twin Pack Design

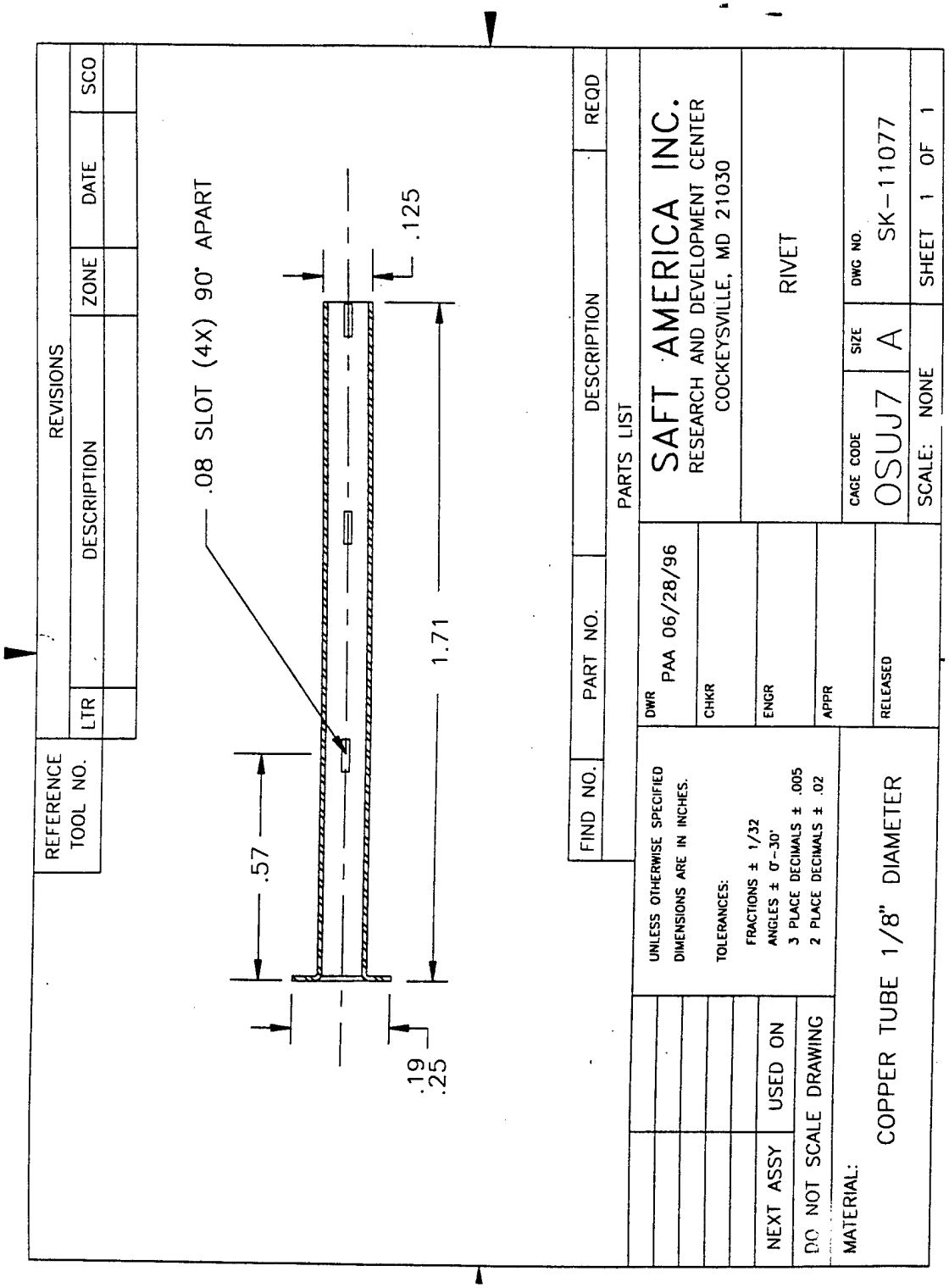

Figure 7.12 Copper Rivet

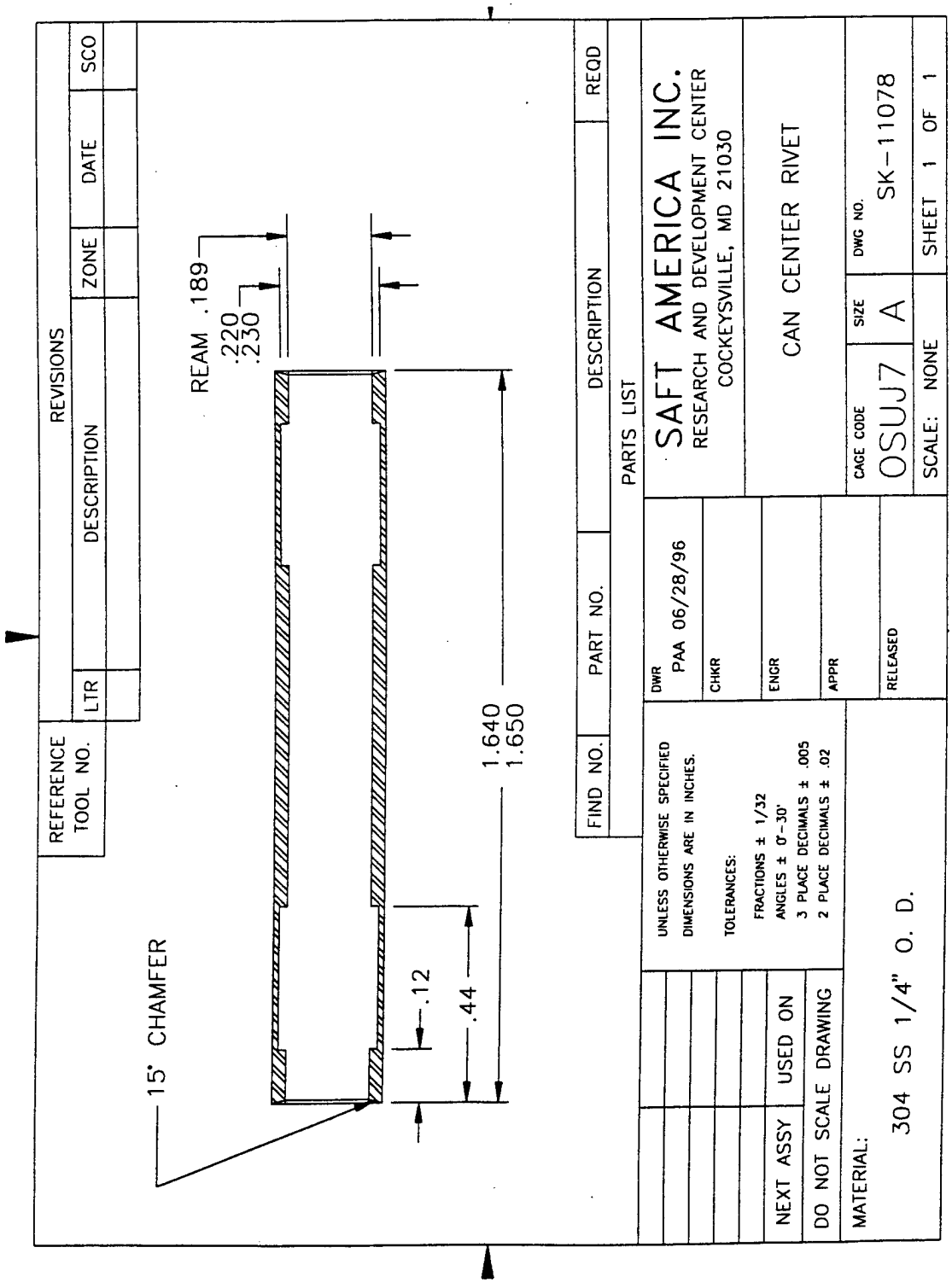

Figure 7.13 Can Center Rivet

TWIN PACK

Figure 7.14 Fixture for Assembling the Twin Pack Design

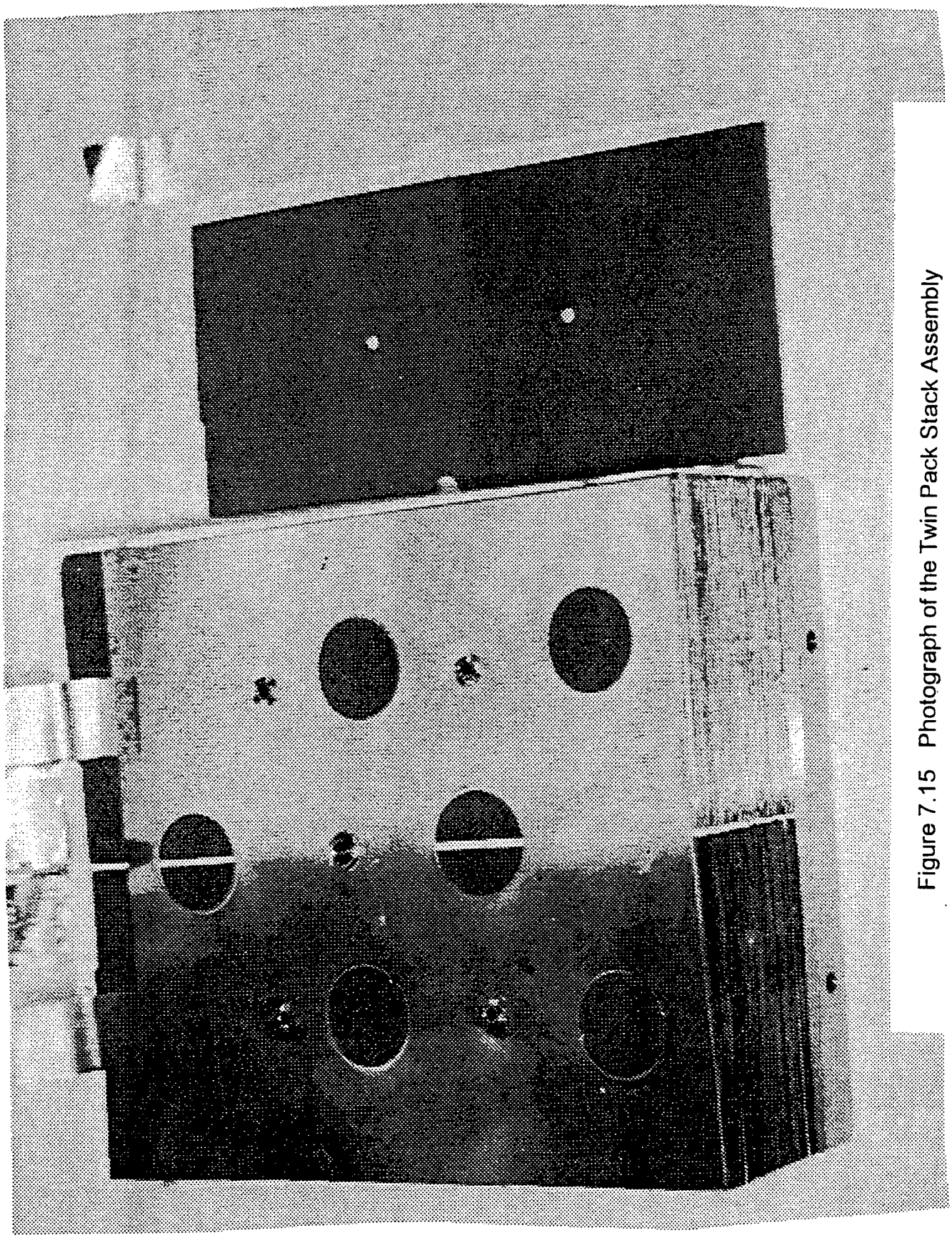

Figure 7.15 Photograph of the Twin Pack Stack Assembly

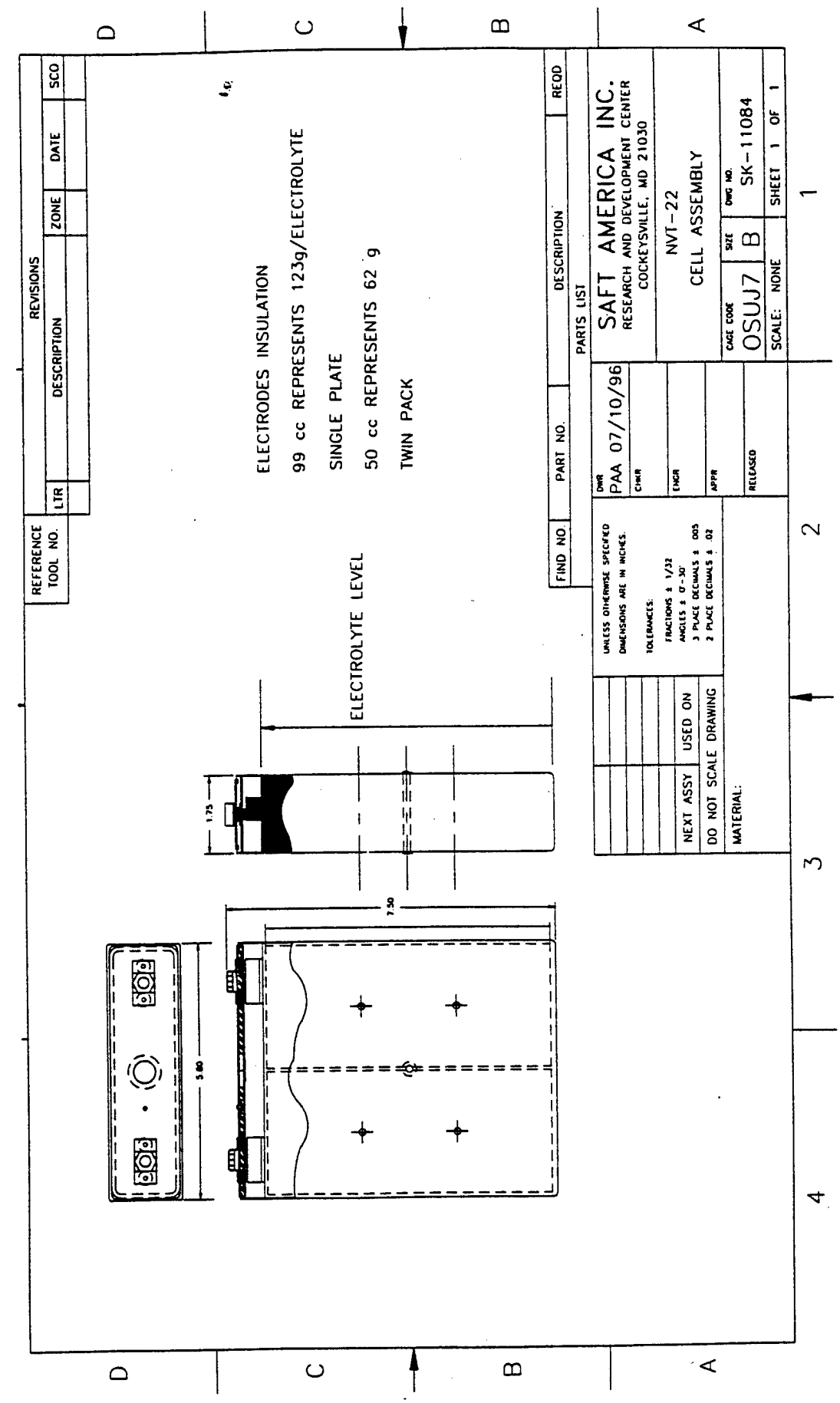

Figure 7.16 Cell Assembly for the Twin Pack Design

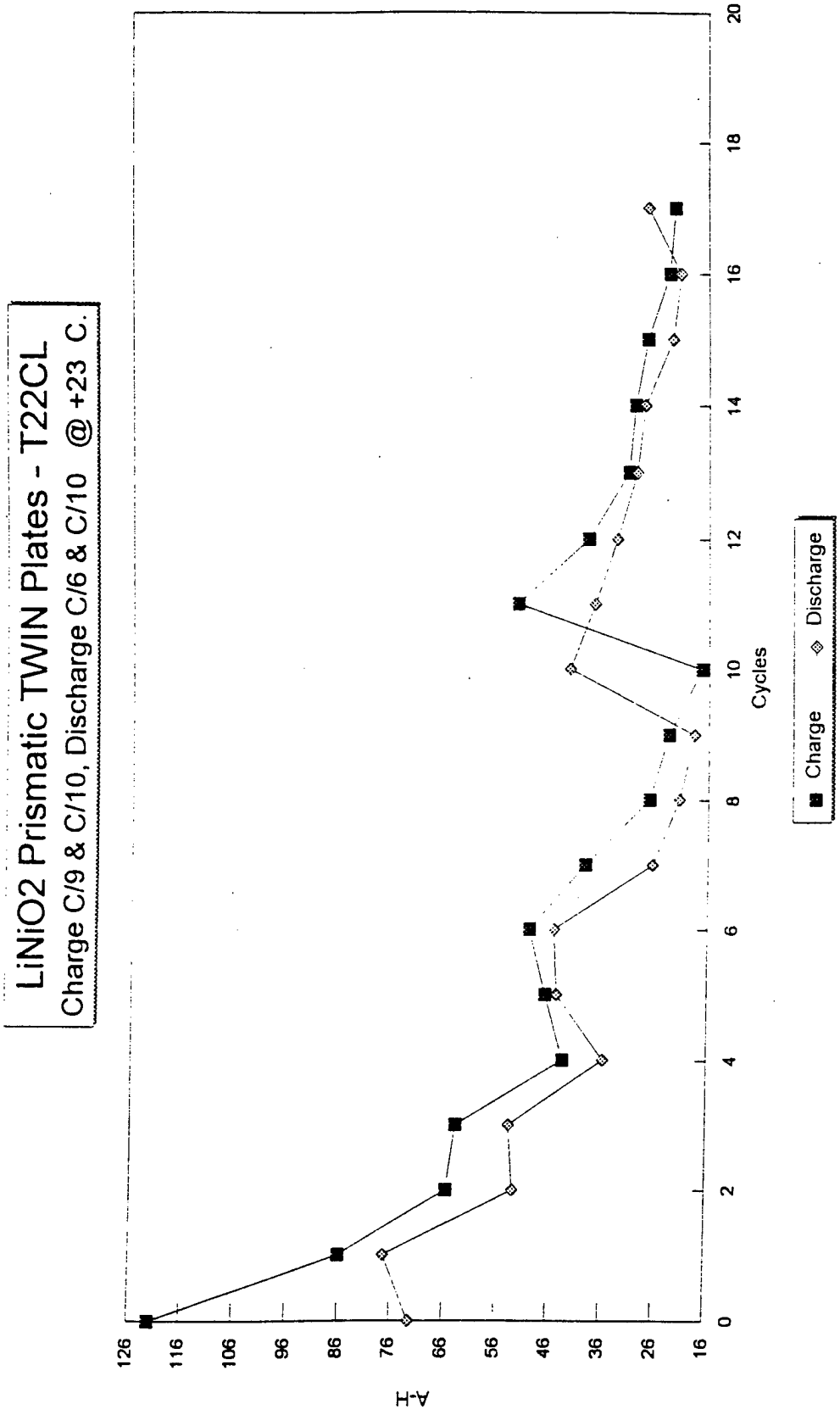

Figure 7.17 Capacity (Ah) Versus Cycle Number for Cell Navy T22CL

Figure 7.18 Photograph of Opened Twin Pack Cell

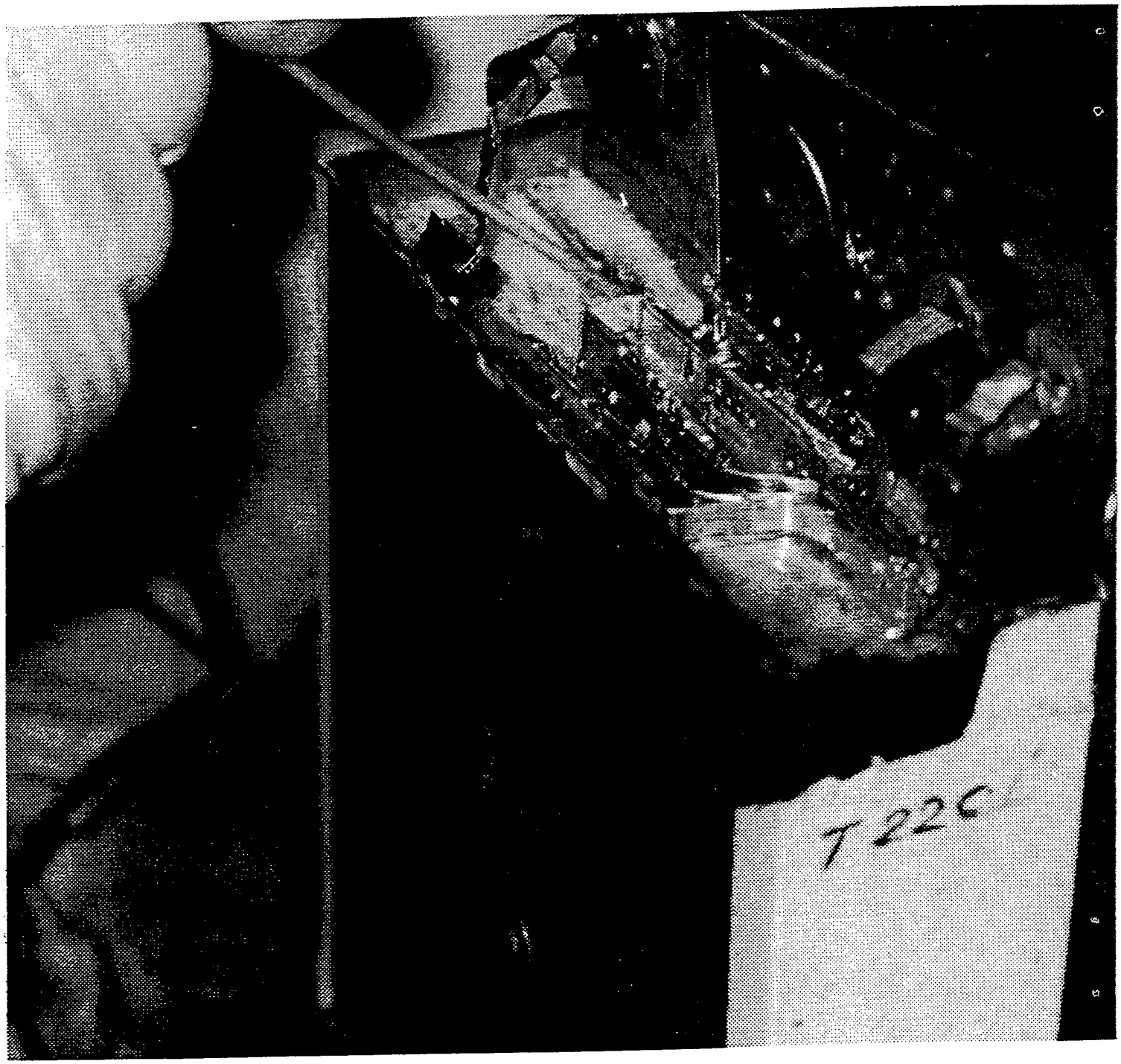

Figure 7.19 Photograph of Opened Twin Pack Cell

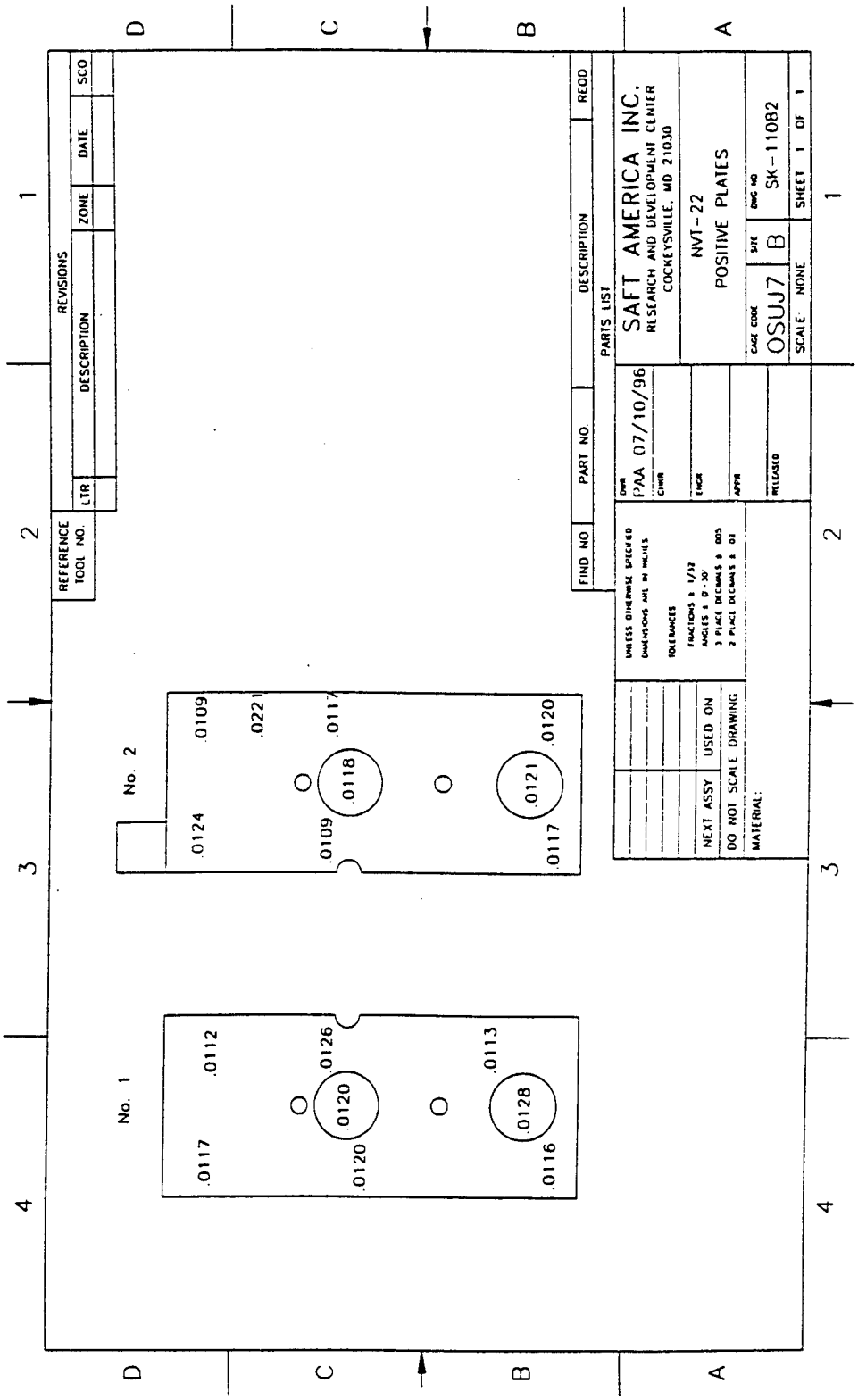

Figure 7.20 Thickness Measurements of Positive Plate After Cycling

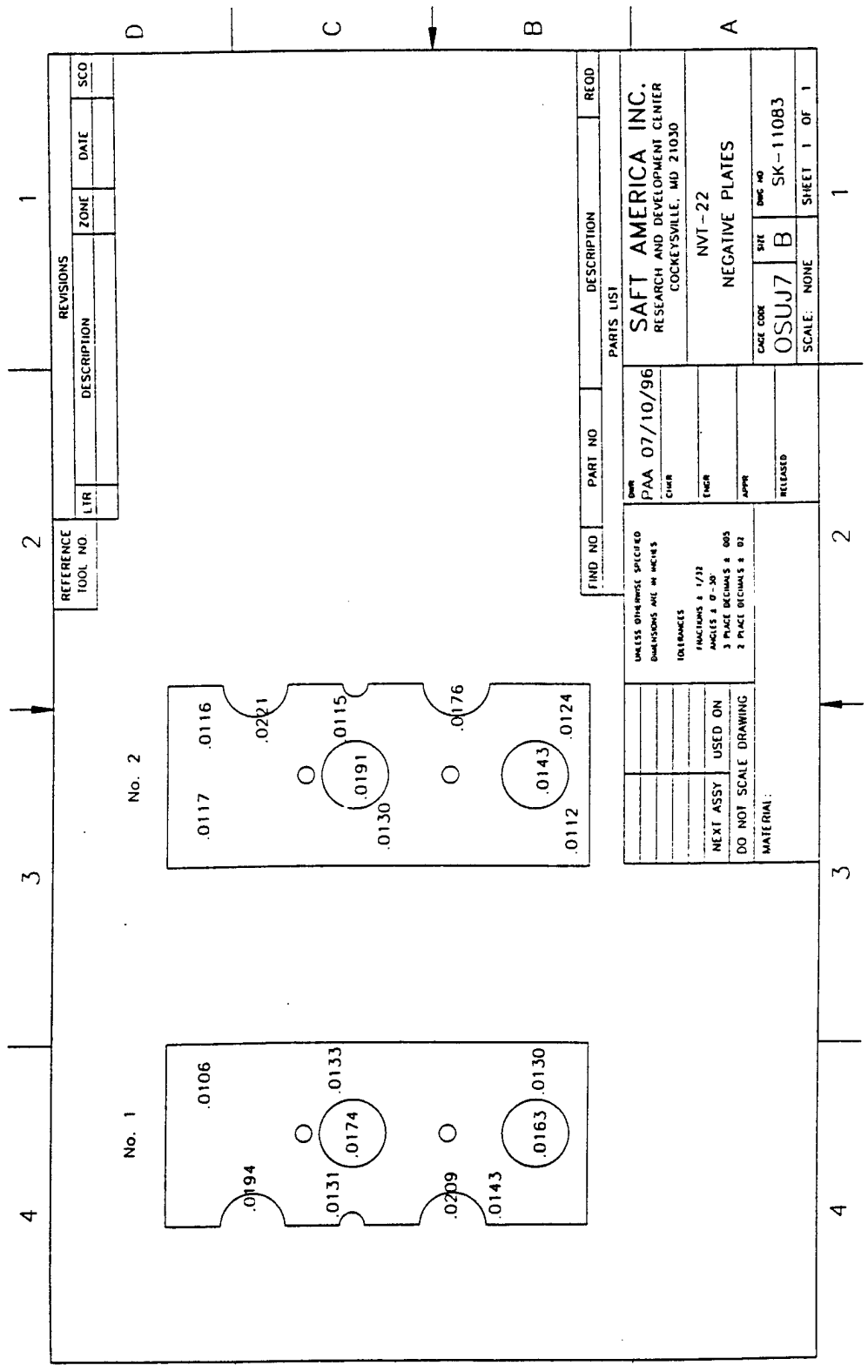

Figure 7.21 Thickness Measurements of Negative Plate After Cycling

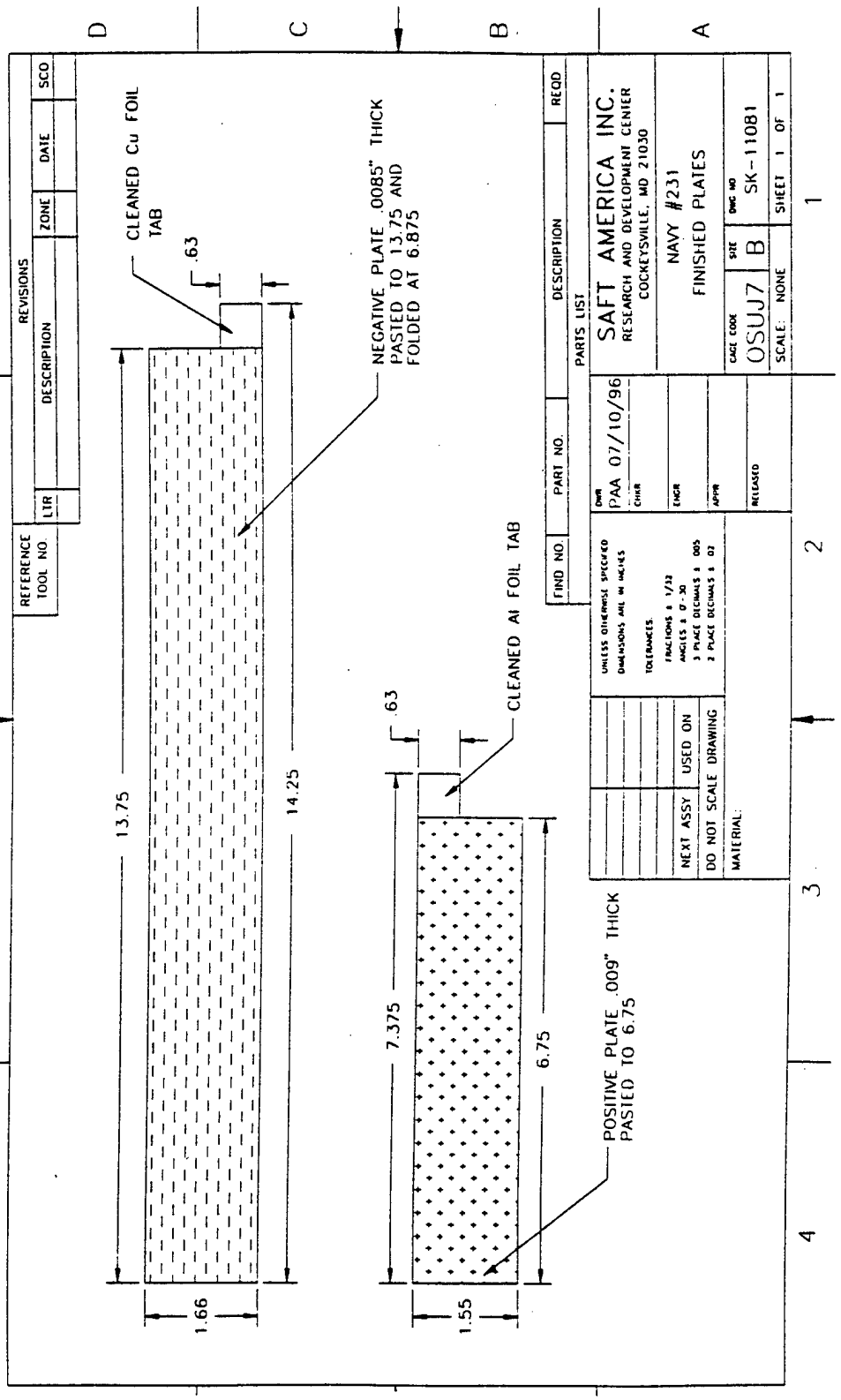

Figure 7.22 Finished Positive and Negative Plates for the Slitted Plate Design

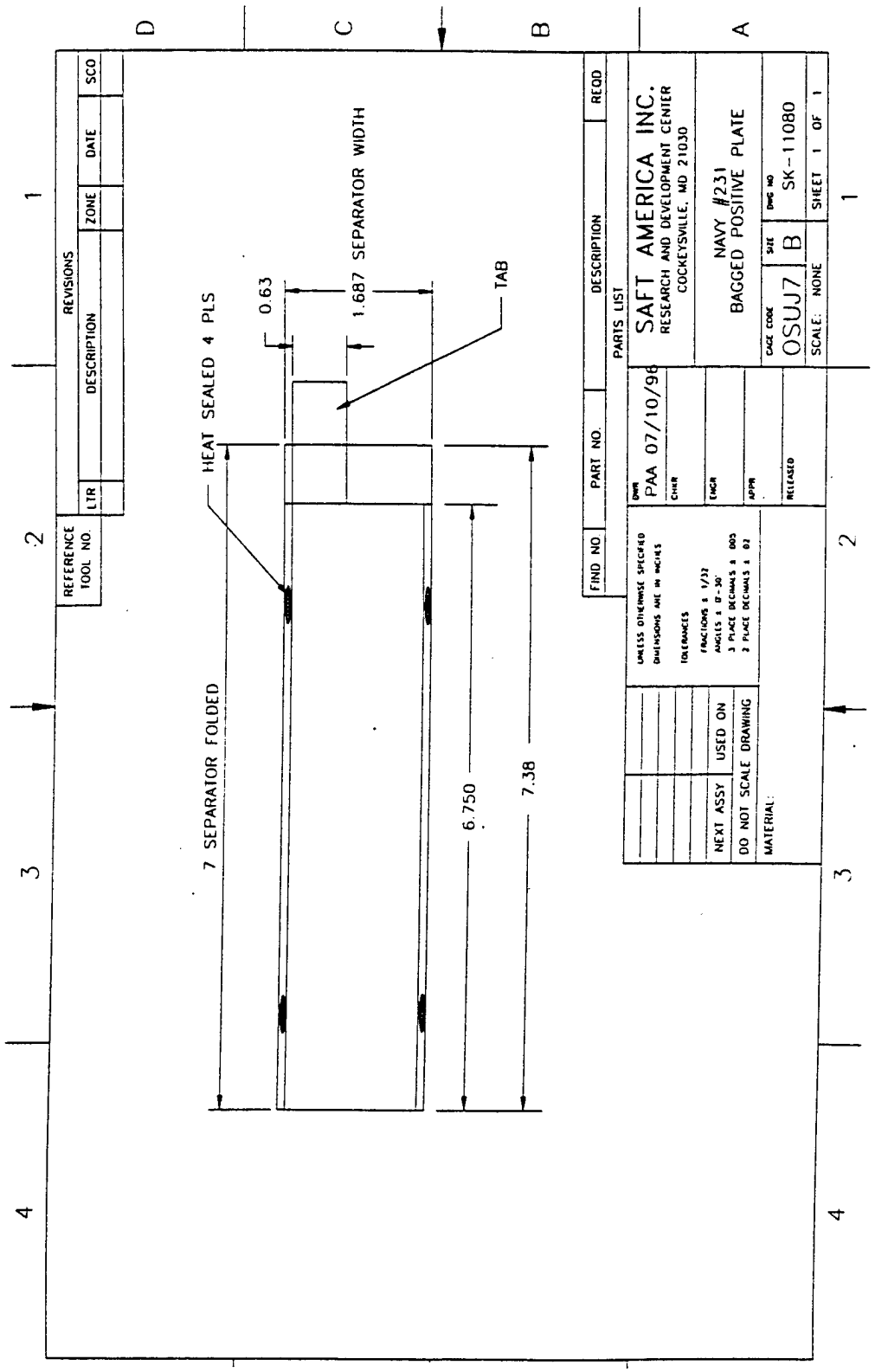

Figure 7.23 Positive Plate with Separator

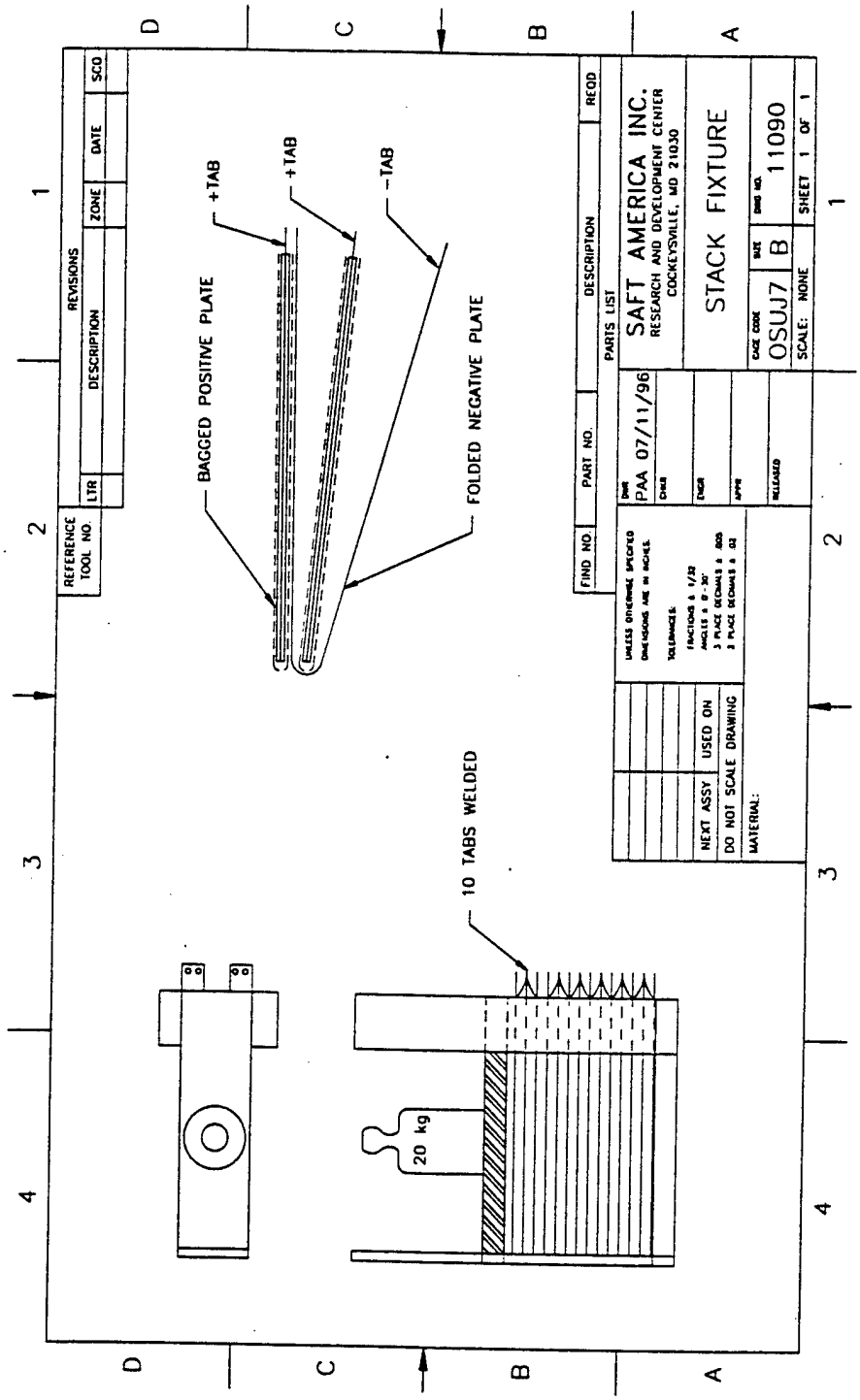

Figure 7.24 Stacking fixture for the Slitted Plate Design

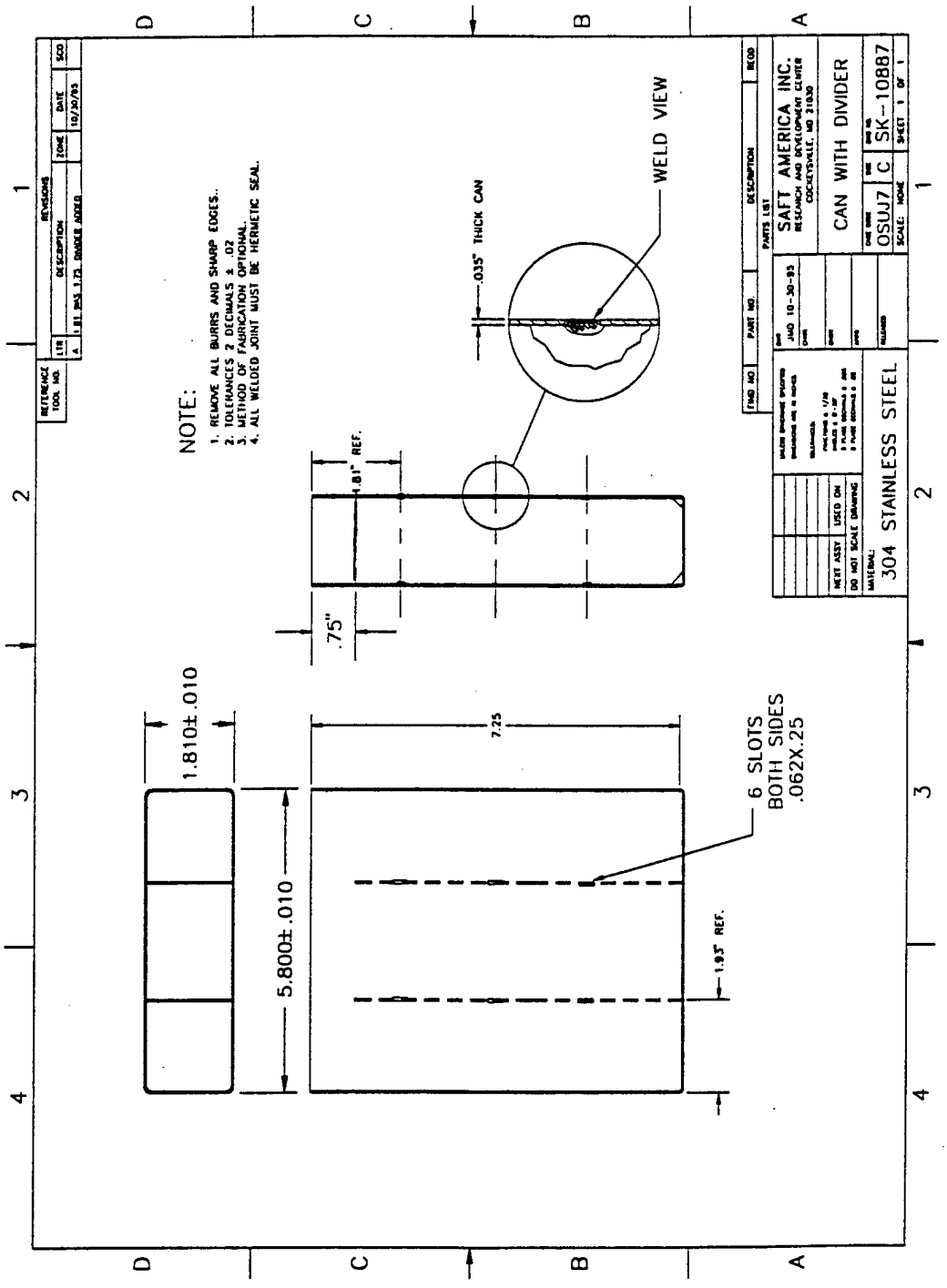

Figure 7.25 Can with Dividers

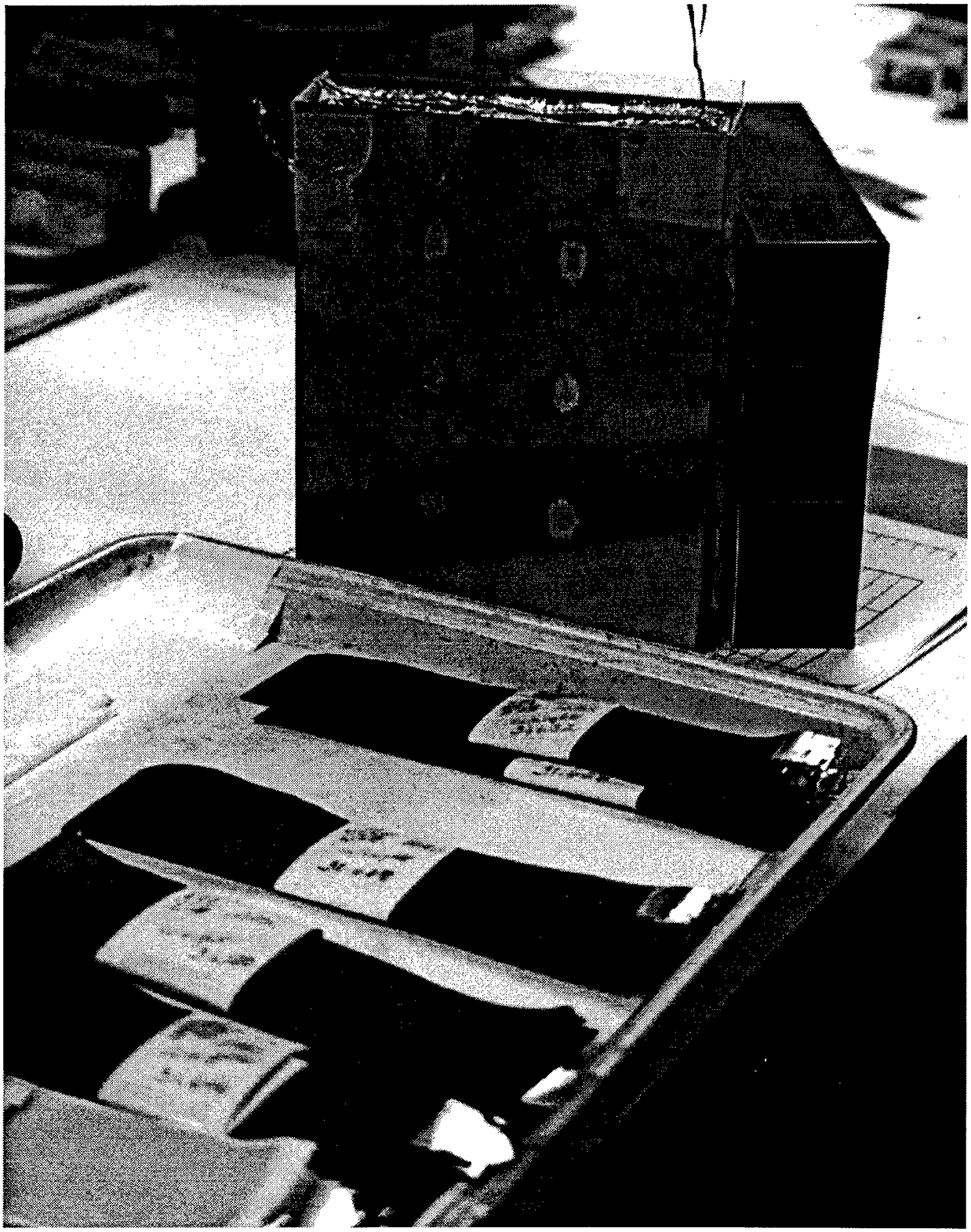

Figure 7-26 Photograph of the Slitted Plate Cell

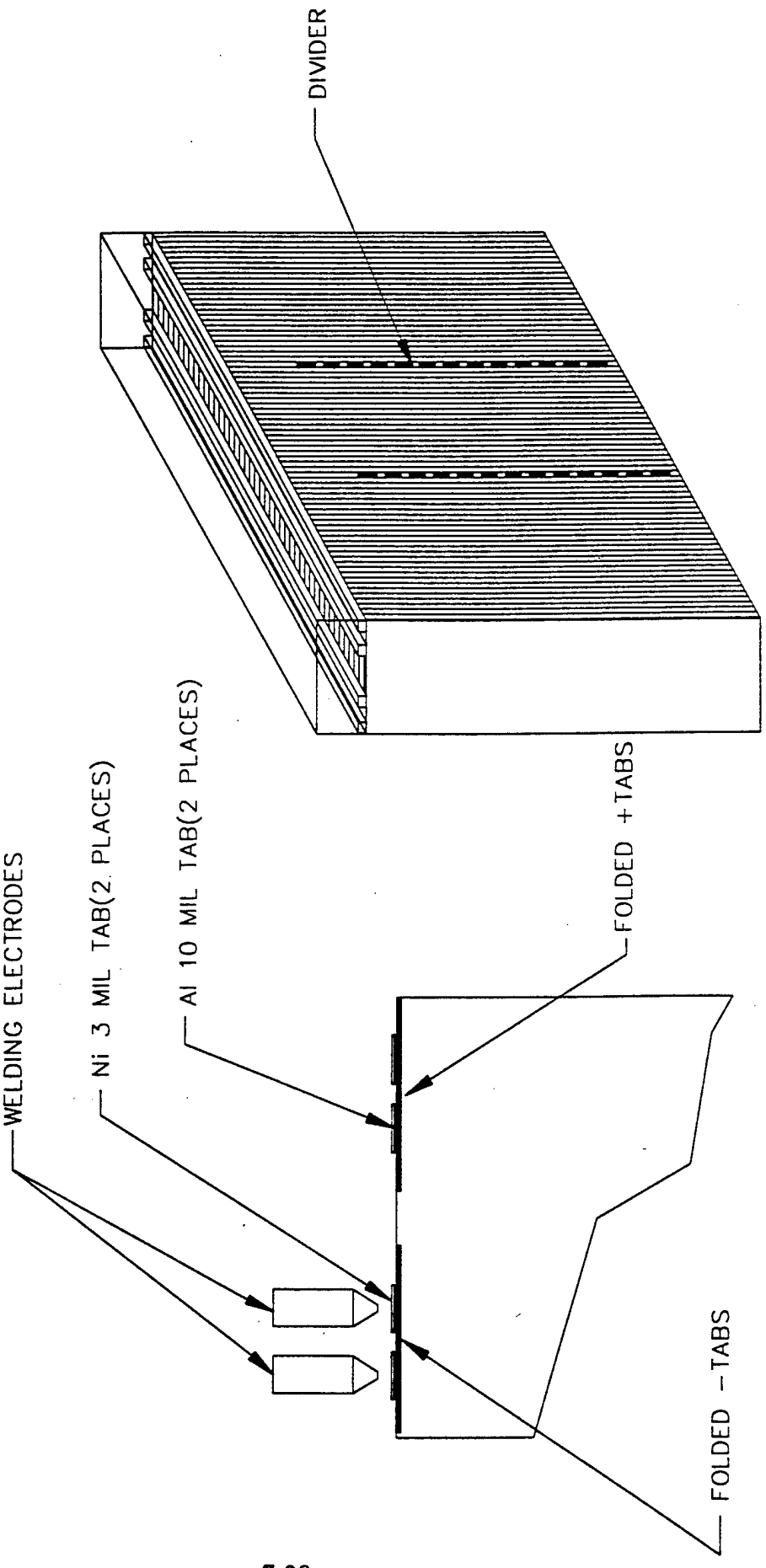

Figure 7.27 Electrode Bussing for Cell Navy T231

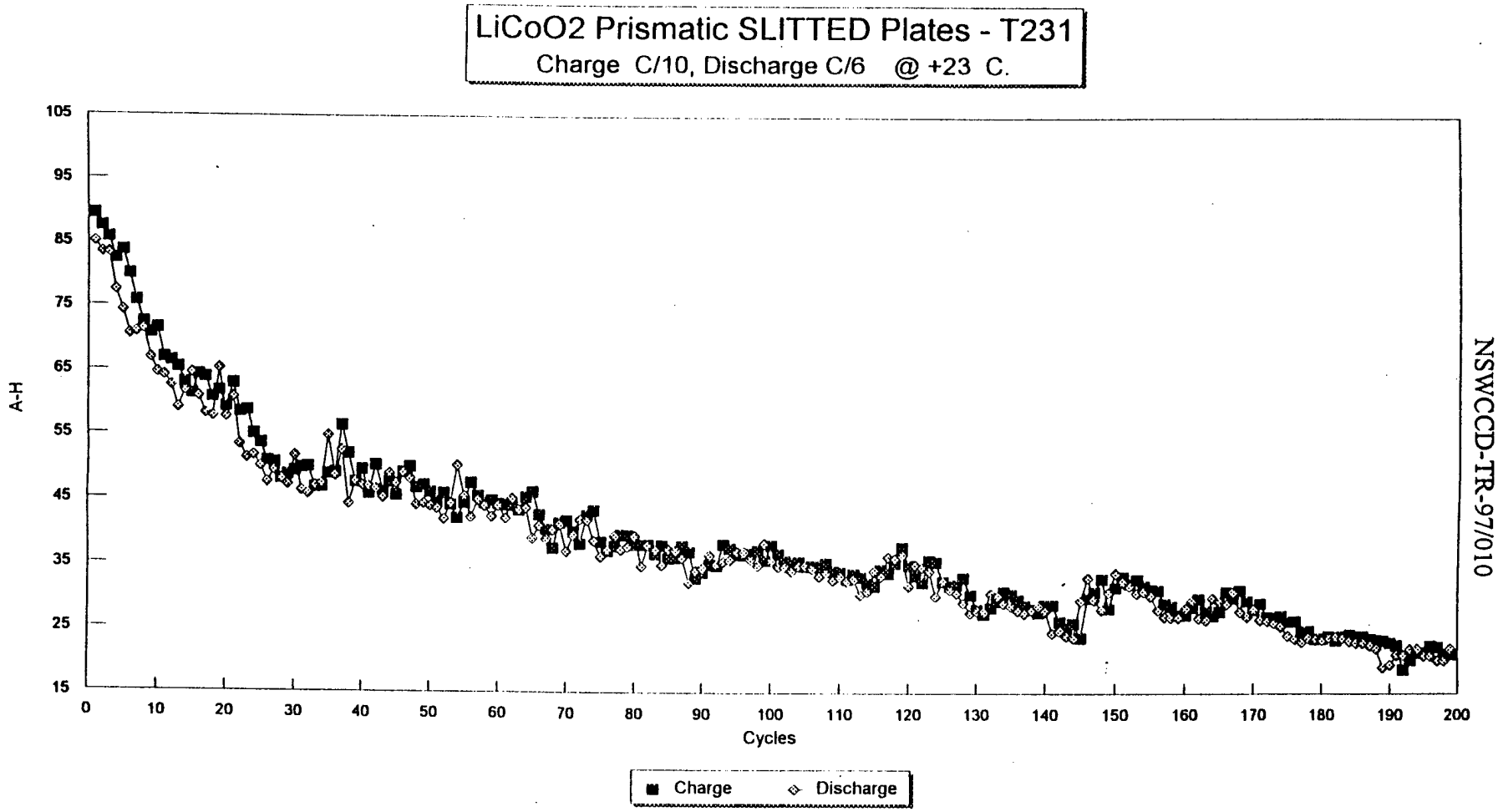

Cycle 1 through 5, charged @ 9.53 A., to 4.2 V. Discharged @ 15 A., to 3.0 V.

From cycle 6 through 42, charged @ 9.53 A., to 4.2 V. Discharged @ 13.5 A., to 3.0 V.

From cycle 43 charged @ 8.5 A., to 4.2 V. Discharged @ 11.89 A., to 3.0 V.

Figure 7.28 Capacity (Ah) Versus Cycle Number for Cell Navy T231

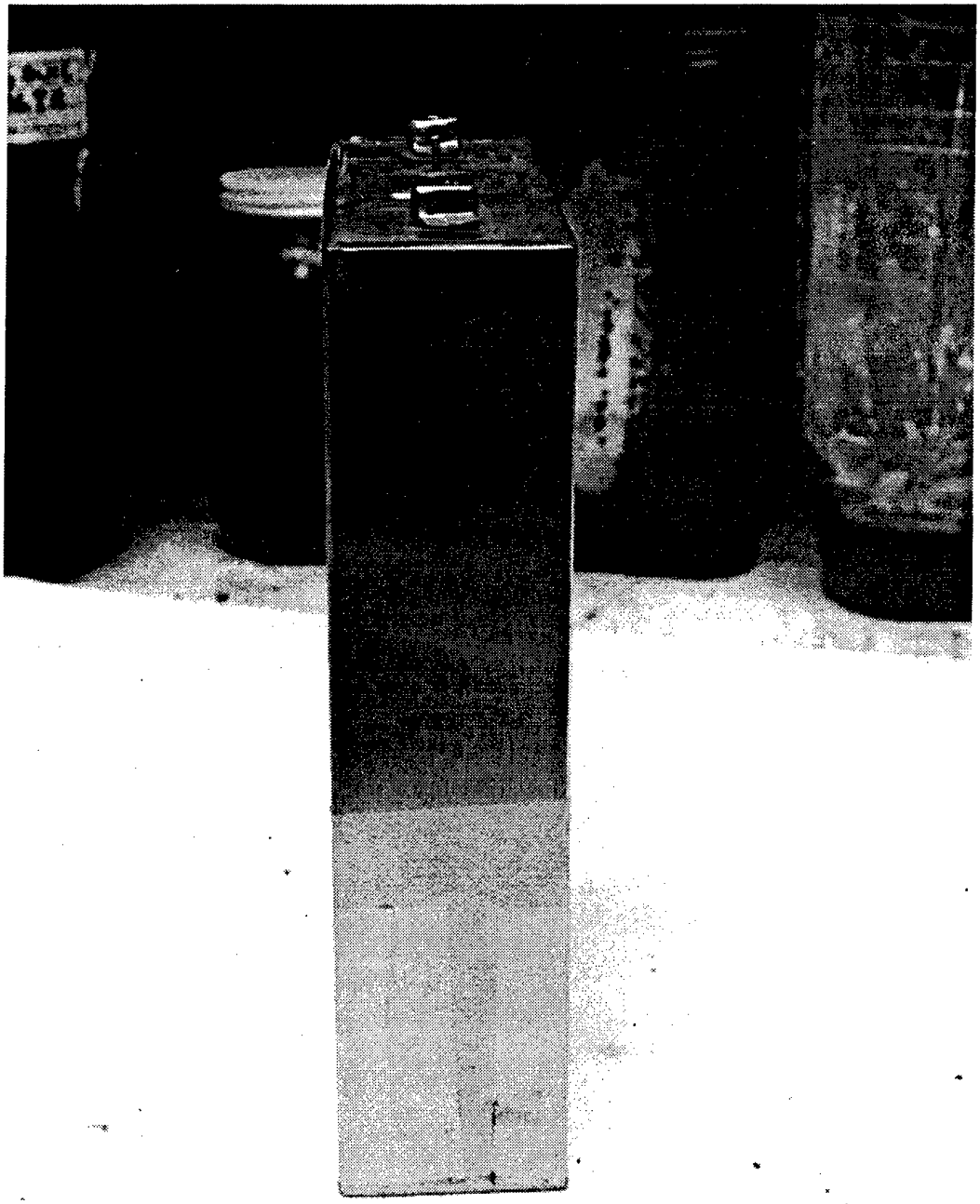

Figure 7.29 Photograph of Cell Navy T231 After Cycling

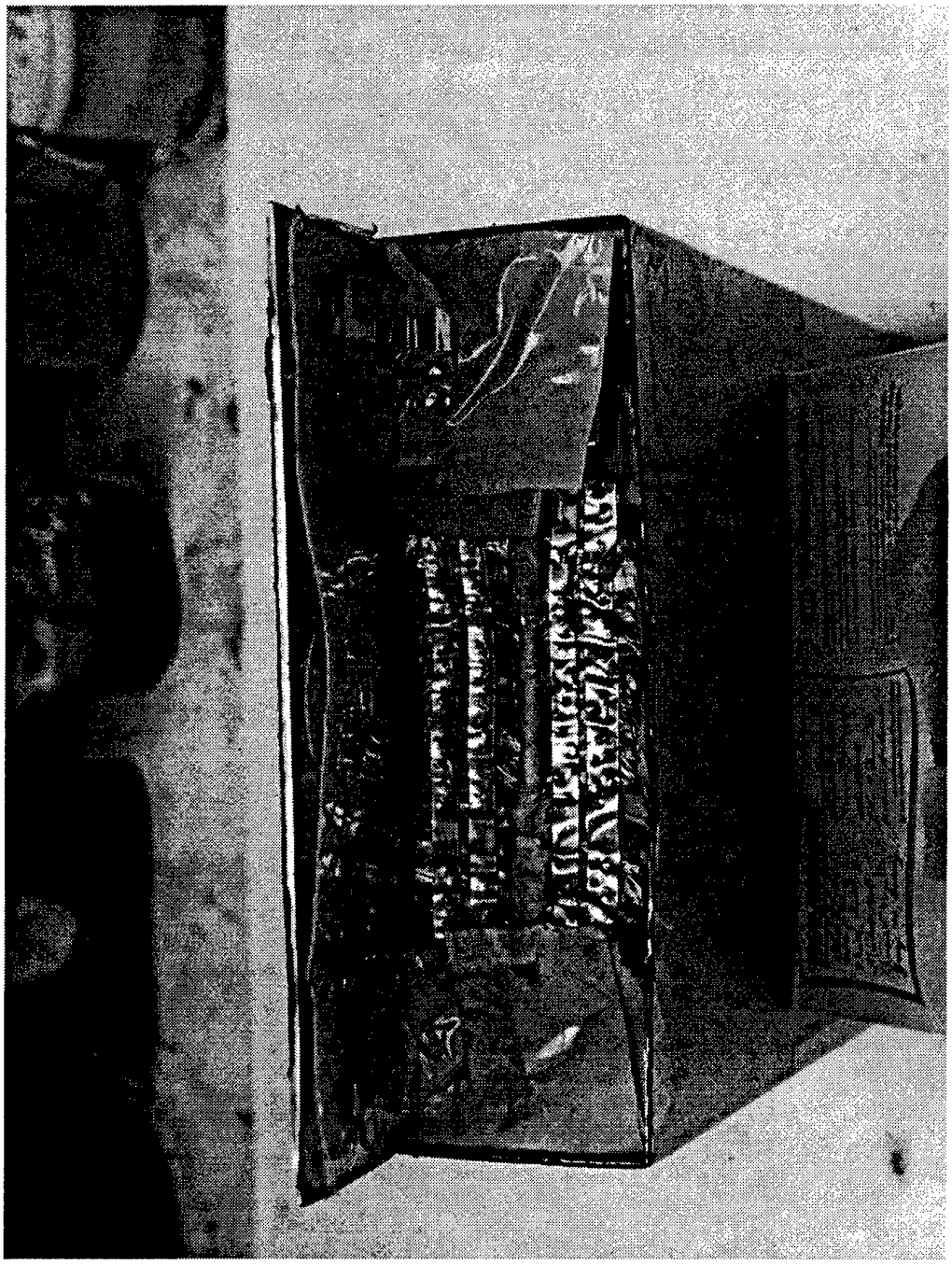

Figure 7.30 Photograph of Cell Navy T231 After Opening

Figure 7.31 Photograph of Cell Navy T231 Showing Positive Bussing

Table 7.1 Comparison of Performance at the Battery Level of the Metallic Lithium System and the Lithium Ion System

	Estimated Battery Metallic Lithium Reinforced Cell as Building Block	**Estimated Battery LiON® Full Plates**
Energy Density: (Wh/l)	200 -220	250 - 280
Specific Energy: (Wh/kg)	120 - 130	120
Cycles:	60 @ 80% nitial capacity	100 @ 95% initial capacity 500 @ 75% initial capacity

Table 7.2 Comparison Between $LiNiO_2$ and $LiCoO_2$ Electrochemistries

DIMENSIONS 44.4 mm x 147.3 mm x 184.1 mm
Volume 1206 cc.

ELECTROCHEMISTRIES COMPARATION

	LiNiO2	**LiCoO2**
Pos. plate porosity	30.3	30.5
Pos. plate thickness	0.0095	0.0105
No. of pos. plates	74	70
Pos. active mat'l. gms.	859.4	952
Neg. plate porosity	40.3	40.3
Neg. plate thickness	0.0079	0.0079
Carbon gms.	375.6	355.6
Separator 2400 K-869	Polypropylene Polyethylene	Polypropylene Polyethylene
Electrolyte gms.	471.7	475.3
Theorical Ah	**120.66**	**111.38**
Pos. surface cm2.	31491	29789
Cell weight gms.	3106	3176

Table 7.2 (Continued)

	LiNiO2	**LiCoO2**
Expected performances at + 23 C.		
ADV (avge. disch. volts)	3.5	3.85
WH	422.3	428.81
Wh/L	350.16	355.54
Wh/Kg	135.98	134.98
Wh/Lbs.	**61.811**	**61.358**

Cycling rates	Hrs	Amps	Hrs	Amps
Charge	5.89	20.47	7.19	15.49
Discharge	3.2	37.79	3.1	35.75
Number of cycles.	500		500	

Note: Performances at 0 C +,- 2 C would be reduce by about 5 %

Table 7.3 Design Characteristics of $LiNiO_2$ and $LiCoO_2$

	$LiNiO_2$	$LiCoO_2$
Density	4.78 gm/cc	5.16 gm/cc
Utilization	140 Ah/Kg	130 Ah/kg
Charging Rate	0.52 mA/cm^2	1.2 mA/cm^2
Average Discharge Voltage	3.5V	3.85V

Table 7.4 Comparison of Performance of the Narrow Plate Versus the Full Plate Design

CELL LEVEL

	Narrow Plates	Full Plates
Average Discharge Voltage (V):	3.5	3.5
Energy (Wh):	328	421
Energy Density (Wh/l):	272	349
Specific Energy (Wh/kg):	125	135
(Wh/lbs):	57	61.6

Cycling	Hours	Amp	Hours	Amp
Charge	6	15.5	6	19.9
Discharge	6 or less	28.6	6 or less	36.7

Number of Cycles: 100 Cycles with 95% of initial capacity
500 Cycles with 75% of inititial capacity

NOTE: Performances at 0 °C ± 2 reduced by about 5%.

Table 7.5 Proposed Twin Pack Design

Dimensions in mm.	44.4 x 147.3 x 184.1
Volume in cm3.	1206

Twin pack

Electrodes	Positive	Negative
Materials	LiNiO2	Lonza/Graphite
Plate dimensions in mm.	0.18 X 68 X 162	0.23 X 71 X 165
Loading in mgs/cm2.	44	24
Porosity %	21	40
Total number of plates	180	181
Total active material weight in gms.	840	520
Total plate surface, both sides in cm2.	38400	43500
Separator, Celgard : E-120	27 microns PP/PE /PP	
Electrolyte in gms.	500	
SS. Hardware weight in gms.	670	
Cell weight in gms.	3100	
Cycling capacity in Ah.	120	

Table 7.5 (Continued)

Expected performances at + 23 C.

Ah	120
Avge Discharge Voltag	3.58
WH	436
Wh/L	362
Wh/Kg	139
Wh/Lbs.	63

Cycling rates

	Hrs	Current
Charge	5	30 amps to 4.1 V. Trickle to 0.5 A.
Discharge	4	30 amps to 2.8 V.

Number of cycles. 500

Note: Performances at 0 C +,- 2 C would be reduce by about 10 %.

Table 7.6 Proposed Slitted Plate Design

Dimensions in mm.	44.4 x 147.3 x 184	
Volume in cm3.	1206	
	Slitted	
Electrodes	Positive	Negative
Materials	LiNiO2	Lonza/Graphite
Plate dimensions in mm.	0.25 x 39 x 141	0.24 X 42 X 144
Loading in mgs/cm2.	52	25
Porosity %	30	40
Total number of plates	340	341
Total active material weight in gms.	920	530
Total plate surface, both sides in cm2.	37400	41200
Separator, Celgard : E-120	27 microns PP/PE /PP	
Electrolyte in gms.	520	
SS. Hardware weight in gms.	580	
Cell weight in gms.	3200	
Cycling capacity in Ah.	128	

Table 7.6 (Continued)

Slitted

Expected performances at + 23 C.

Ah	128
Avge Discharge Voltag	3.58
WH	458
Wh/L	382
Wh/Kg	148
Wh/Lbs.	67

Cycling rates

	Hrs	Current
Charge	5	30 amps to 4.1 V. Trickle to 0.5 A.
Discharge	4	30 amps to 2.8 V.

Number of cycles. 500

Note: Performances at 0 C +,- 2 C would be reduce by about 10 %.

Table 7.7 Proposed Slitted Plate Design Using $LiCoO_2$ as the Cathode

( ) Intented design.

Dimensions in mm.	44.4 x 147.3 x 184.1
Volume in cm3.	1206

SLITTED PLATES	NAVY T 231			
Electrodes	Positive		Negative	
Materials	LiCoO2		Lonza/Graphite	
Plate dimensions in inches	1.55 x 6.750		1.66 x 6.875	
Thickness	(0.0086)	0.009	(0.0078)	0.0085
Loading in mgs/cm2.	(45)	41.8	(21)	22.2
Porosity %	(41)	48.1	(40)	42.7
Total number of plates	(309)	280	(311)	277
Total active material weight in gms.	(883)	733	(470)	453
Total plate surface, both sides in cm2.	(39148)	35094	(42000)	40930
Separator, Celgard : E-120	27 microns PP/PE /PP			
Electrolyte in gms.	(630)	612		
SS. Hardware weight in gms.	(585)	684		
Cell weight in gms.	(3098)	3060		
Cycling capacity in Ah.	(115)	**85**		

Distribution of the plates in the cell with three stacks.

Stack	Number and average weight in gms. of positives plates.		Number and average weight in gms. of negatives plates.	
# 1	85	4.2	86	2.57
# 2	101	3.1	102	2.54
# 3	91	3.1	92	2.53

Chapter 8

Electronics for the Navy SEAL Delivery Vehicle

In order for a lithium rechargeable battery to operate in a safe and efficient manner, its voltage range and limits during the charge and discharge must be controlled accurately. Because the SEAL Delivery Vehicle Battery will consist of 8 modules of 16 volts and 600 Ah, each module will be charged individually and connected in series for the discharge of the full battery.

Each of the eight electronics controls will handle one module. The module is made up of a group of four cells connected in parallel and four of each such group connected in series.

System Description

The battery module electronics will be mounted on a printed circuit board that will extend over the tops of the cells, with holes placed such that the cells can be bolted into the proper physical location and connected into the circuitry (Figure 8.1). The board will be reinforced so that the cells can be removed from their carrier by lifting the board and cell assembly. Cells can then be unbolted and replaced if necessary.

The electronics will control the individual cell voltage on charge and assure that each cell does not draw excessive current. Should a cell heat excessively, the electronics will disconnect it from charge. Likewise, on discharge, cell voltages will be monitored and individual cells disconnected should their voltage fall below the discharge cutoff. A module supervisor circuit will be provided that will monitor and control battery charging. This system will receive cell performance data from the cell controllers, evaluate charge performance and provide the appropriate control information to the battery charge power supply. Additionally, it will operate the parallel string bypass circuitry that is necessary to provide optimum charging to each of four parallel strings of cells in the battery. The module supervisor will also provide system diagnostics in the form of a serial data stream that can be monitored on a hand held terminal or personal computer.

System Design

The electronics system is composed of the following modules, or subsystems:

- Cell Controller (one for each cell - 16 total)
- Bypass Controller (four per module)
- Module Supervisor (one for each module)
- Charge Power Supply (one per module in charge)
- Mechanical (physical accommodation)

Figure 8.2 shows an overview of the module electronics in block diagram form. The following sections describe the principles of operation of each of the subsystems.

Cell Controller

The cell controllers are microcontroller-based systems that monitor the voltage, current and temperature of the individual cells (Figure 8.3). They disconnect the cell from charge, or discharge if the cell voltages rise or fall past their full charge voltage or minimum cutoff voltage respectively. Charge cutoff is implemented by a low conduction loss transistor switch (MOSFET or IGBT). When the charge voltage limit is reached, the microcontroller opens the charge control switch and cell charging stops. Likewise, when the discharge voltage limit is reached, the discharge control switch is opened and cell discharge stops. The proper conduction modes are reset when cell voltage returns to the correct operational range. Voltage cutoffs are compensated by cell temperature, which is also measured by the microcontroller so that optimum performance is maintained and safe cell operation assured.

The cell controller also measures cell current, both charge and discharge. This allows the microcontroller to remove the cell from charge or discharge if current limits are exceeded. Because control is implemented digitally, parameters such as temperature and cell voltage can be incorporated into the cutoff decision algorithm. Cell operating parameters are provided to the module supervisor so that bypass control can be implemented for the charge current control, or the entire module disconnected for discharge current and voltage control.

The cutoff devices are important parts of the system. They need to be sized to handle cell currents, both charge and discharge as well as providing as low a conduction loss as possible. Because of the series nature of the module connections, conduction losses from individual cells are cumulative and quickly become a significant consideration in system design. An important portion of the proposed effort will concern component selection and system design of the cell cutoff devices.

Charge control is made easier by the parallel connection of four cells and their controllers. When cells are connected in series, the more degraded cells in the string tend to elevate the string voltage, reducing the string charge current that causes incomplete charging of the less degraded cells, reducing the overall charge acceptance of the battery. The proposed arrangement clamps the charge voltage of the four cells, eliminating excessive charge voltage of the four-cell pack.

Bypass Controller

The function of the bypass controller is to allow the full charge current from the charger to flow through the series string of four cell packs (which are connected in parallel) even if one or more of the packs are receiving lower levels of charge current. As in the series string example above, the bypass controller prevents a single four-cell pack from reducing the charge received by the other packs in the module. The bypass controller operates by allowing a certain amount of charge current to shunt around the four-cell pack, therefore reducing the amount of current received by the pack. The module supervisor, based on information collected from the cell

controllers, determines the bypass setting. The bypass controller only operates during charge mode and is inactive during discharge and storage.

Module Supervisor

The module supervisor has several functions:

- Collect cell performance information from the cell controllers
- Manage operation of the bypass controller during charge
- Coordinate the cutoff operation of the cell controllers during charge and discharge
- Provide module performance diagnostics to an external user terminal or personal computer.
- Control the operation of the Charge Power Supply.

The Supervisor is another micro-controller-based system which communicates with each cell controller (16 per module) to collect cell status information. Supervisor-to-cell controller communication will be performed over a simple serial data link, where each controller will be periodically polled to obtain its current status. A current set of cell status parameters such as voltage, current, temperature, charge cutoff status and discharge cutoff status is maintained. The data will be processed in order to determine the necessary operating parameters of the module.

The module supervisor will control bypass controller operation because the supervisor has the cell data necessary to perform this function. Bypass current will be controlled such that the parallel-connected cells are not exposed to excessive charge current. This mode is necessary if one parallel cell pack requires less charge current, as at the end of a charge cycle. The current supplied from the charge power supply will be reduced. During charge and discharge, if one cell in a parallel pack disconnects, the other cells in the pack will experience higher current levels. If these levels become excessive, or if there is an unacceptable rise in temperature, the module supervisor can direct all the cell controllers in the pack to open, effectively shutting off the battery. Even though this function is also supported in each cell controller, operation by the Supervisor assures a safety backup.

The Supervisor also provides system diagnostics to an external user terminal or personal computer. This feature provides insight into the operation of the module during charge and test or operational discharges, allowing the detection and diagnosis of a performance problem that would otherwise be difficult to detect. Data, such as state of charge, load and charge sharing between cells and parallel packs, cell heating and cycle history, could be available both during charge and after the various modules are assembled into a complete battery. The data system will be designed to support not only the user terminal during charge, but also to interact with other module supervisors in a complete battery to provide status and diagnostic information to the user vehicle.

Charge Power Supply

The Charge Power Supply will be a commercial power supply designed for use in battery chargers and will be capable of supplying the required 60-amp module charge current. The unit will accept control inputs for both output voltage and output current limit. It will also provide a current measurement output. Instrumentation connections will be made directly to the module supervisor circuitry and the power connections will be made to the charger connections on the module electronics board.

Mechanical Design

As mentioned previously, the cells will bolt directly into the module electronics board allowing easy cell replacement and easy maintenance as well as a low profile bussing. The board will be reinforced with bus bars to carry the charge and discharge currents, and at the same time add stiffness to the board. Insulated metal rails will be attached to the long edges of the boards and will have grab points for module extraction. They could serve as a heat sink for the power semiconductors used in the module electronics. The conducting surfaces of the board and the electronics components would be protected from moisture and salt water by a diversity of conforming coatings and waterproofing material.

Prototype Board

For the single cell, a smaller prototype board was designed and built. It was the same size as the top of the cell and bolted directly into the cell terminals (Figure 8.4). This small board, which was built with off-the-shelf electronic components, will monitor the cell voltage, current, and temperature. It also protects the cell from over-discharge to 3.0 volts ($LiCoO_2$), external short-circuit over 25 amps, and temperature over 75°C. The microprocessor, with the integration of a digital potentiometer can modify the discharge voltage limits according to the temperature input and provide temperature compensation. This provides a cell that has a better balanced discharge capacity between 0°C and 60°C.

The board disconnect or MOSFET can handle a load up to 25 amps and has a low voltage drop of 40 millivolts. Because the electronics requires 5 volts for a single cell application, a DC converter has been added that supplies 5 volts from a 1.2-volt to 9-volt input. Also, a watchdog timer was added to force the MOSFET to switch to the open position in any case of electronics malfunction. This insures the safety of the cell.

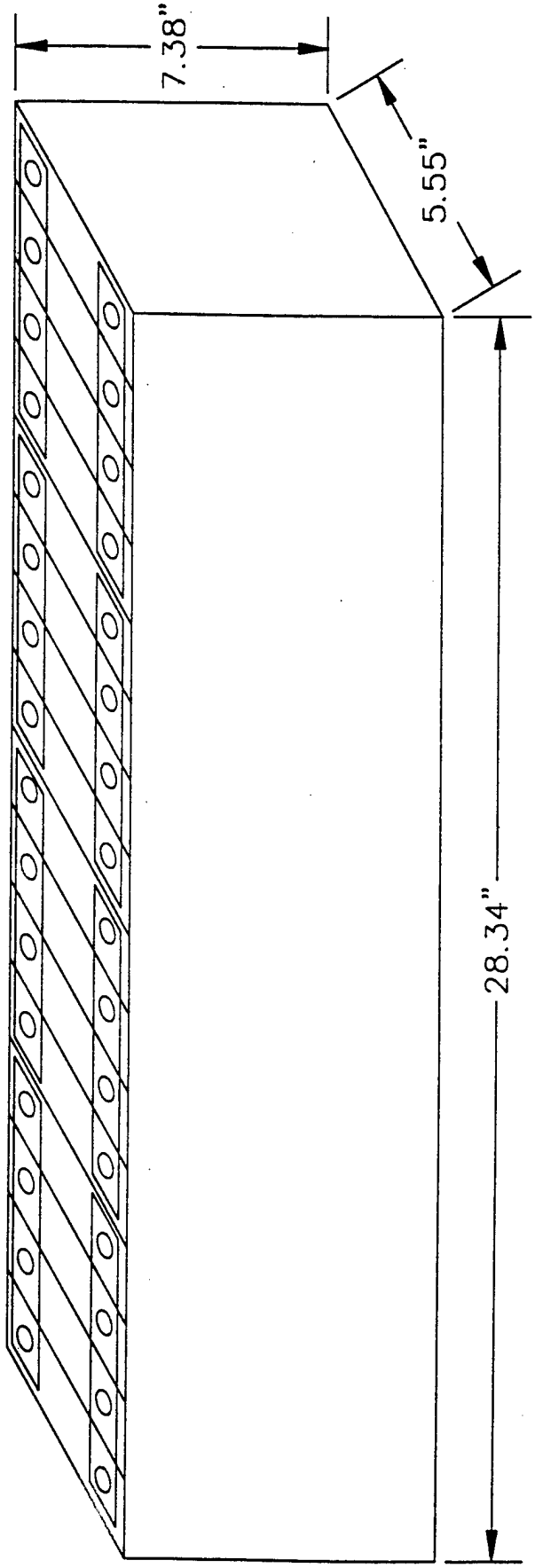

Figure 8.1 Module Electronics for the SEAL Delivery Vehicle Battery

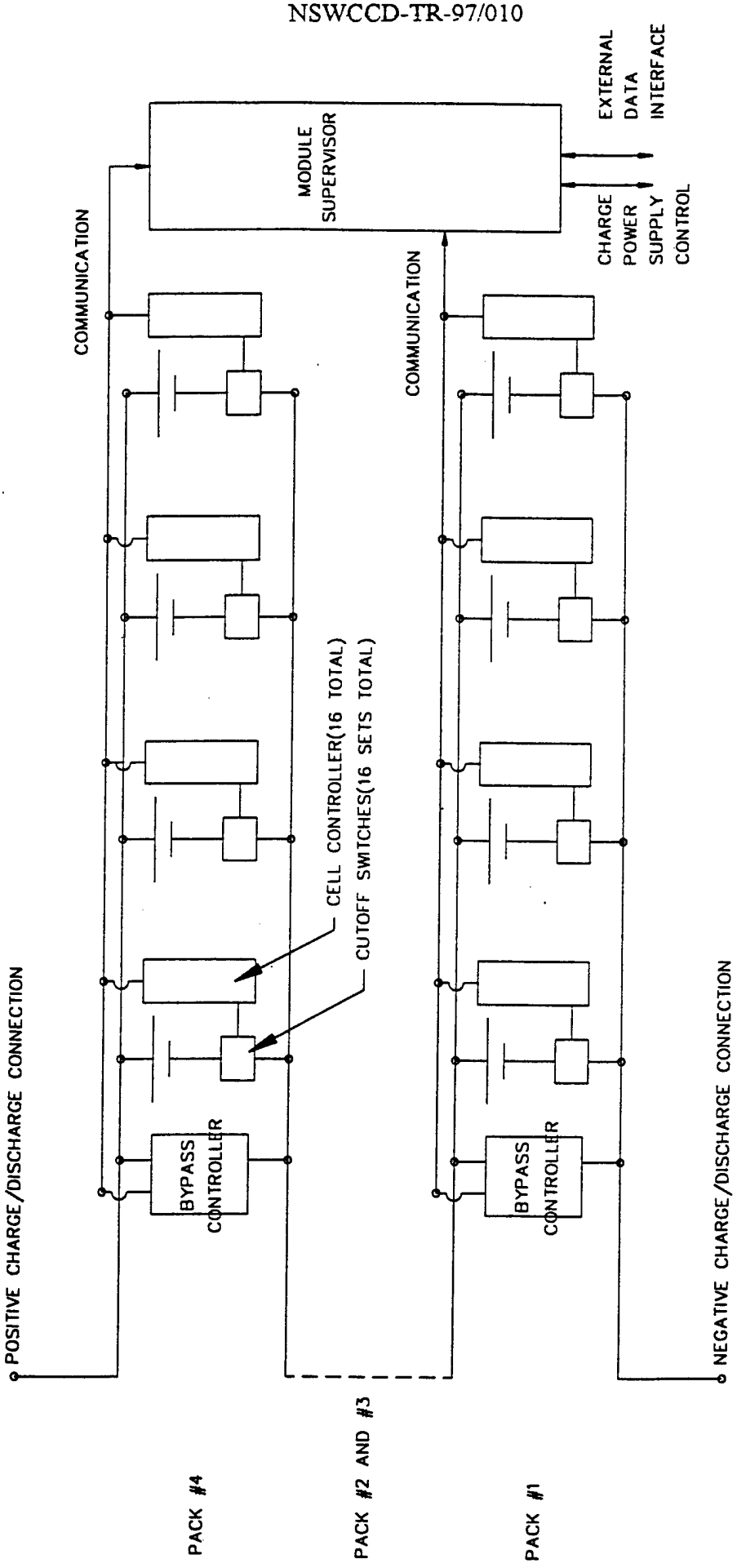

Figure 8.2 Block Diagram of the Module Electronics

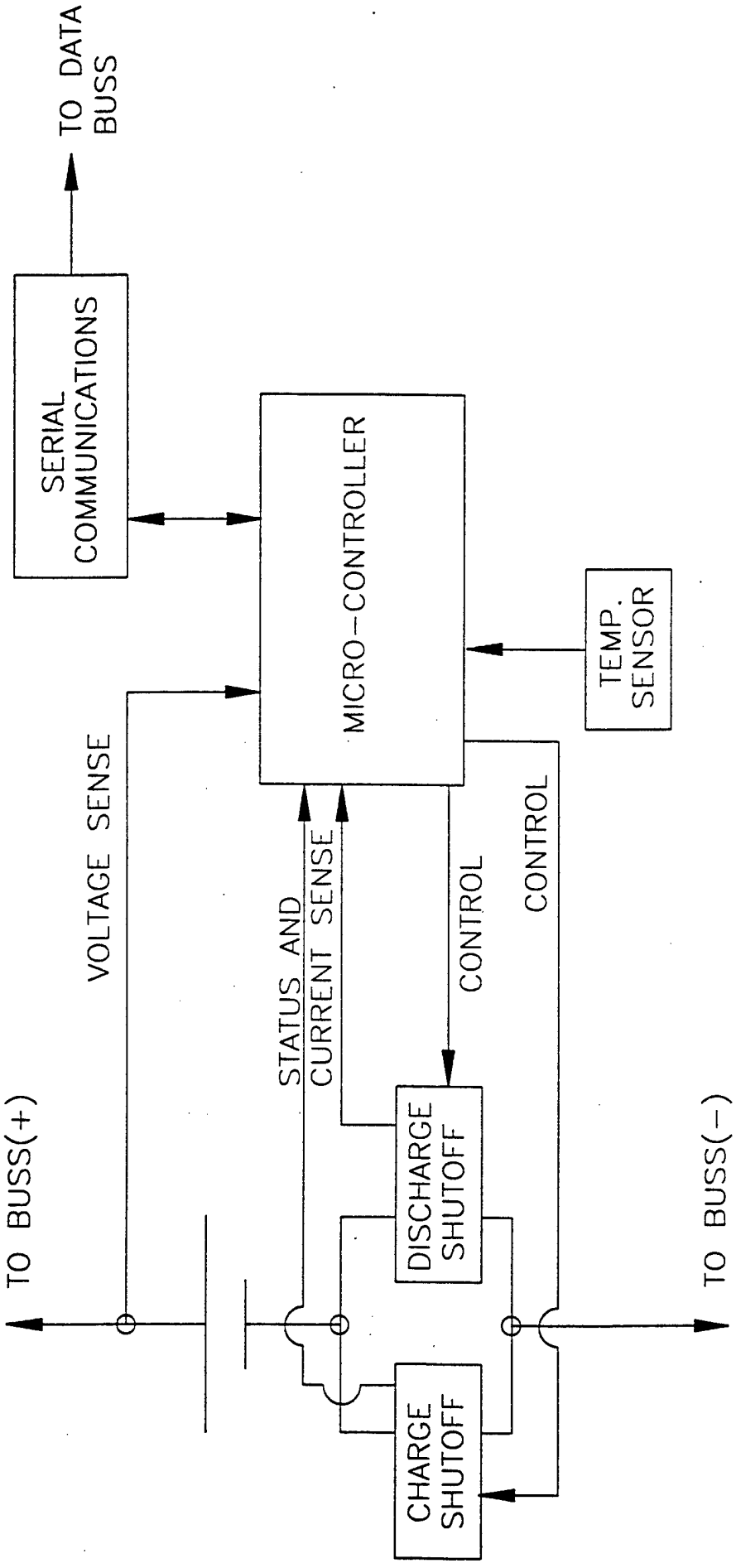

Figure 8.3 Cell Controller Concept

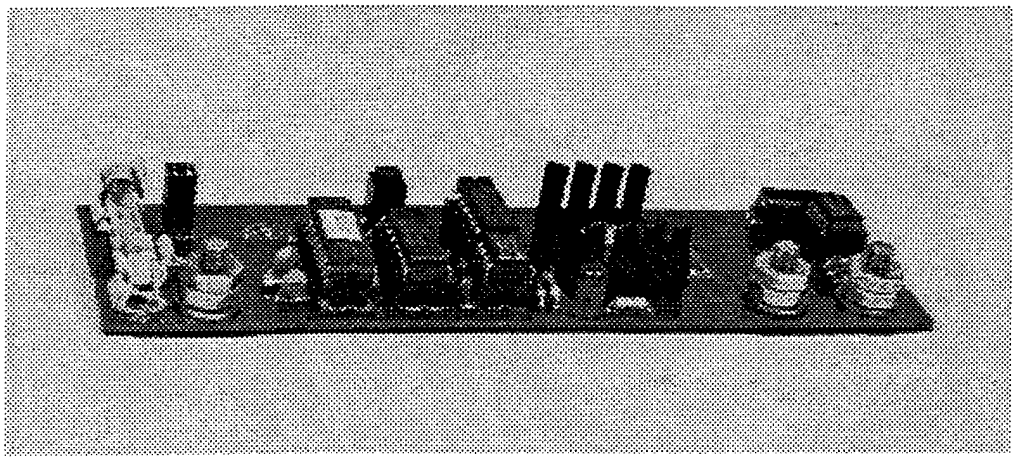

"Smart Battery" Control:

Electronic Charge/Discharge/Safety Circuitry

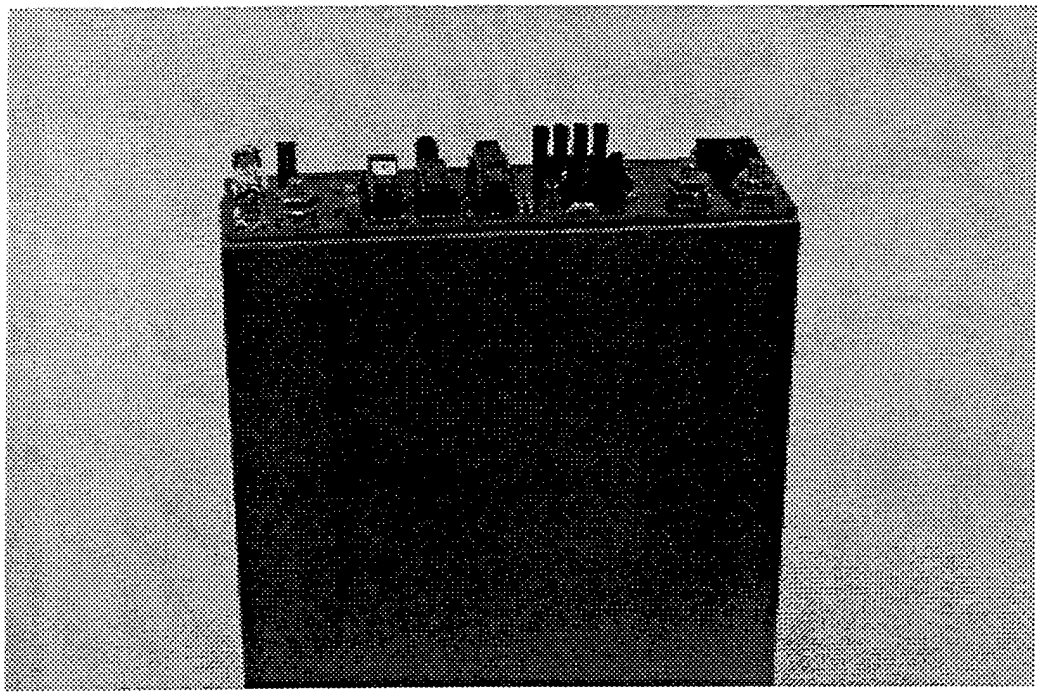

"Smart Battery" Control Position on the Cell

Figure 8.4 Photographs of the Prototype Electronic Boards

Chapter 9

Conclusions and Recommendations

The object of this procurement was to design a rechargeable Li/$LiCoO_2$ cell with a minimum capacity of 100 Ah. The cell would deliver at least 100 Wh/lb every cycle for at least 50 cycles. The lithium metallic cell delivered more than 140 Ah at 23°C and 130 Ah at -2°C; however, its specific energy was only 81 Wh/lb. The cells had these capacities for 38 cycles at 23°C and 18 cycles at -2°C.

During charging, the physical expansion of the lithium electrode occurred unimpeded by the planar faces or by the rivets. There was more deflection at the cold temperature (-2°C) than at 23°C. The design of the cell hardware must account for this deflection of the cell stack within a fixed volume, as happens in a cylindrical design. Based on the experience gained from the lithium ion design, this could be accomplished by increasing the thickness of the end plate (Figure 4.2) to 0.125 inches, changing the design of each end-plate rivet to one similar to the can center rivet (Figure 7.14), and by using a pop rivet. With these changes, the thickness of the can could be reduced from 0.035 to 0.015 inches. However, design changes that would strengthen the container would not solve the fundamental problem that lithium in rechargeable cells of over 100 Ah would always have a potential for a fault mode.

Safety tests (Chapter 6) under abusive electrical conditions were performed on small 4/5 A-size cylindrical cells that were 0.62 inches in diameter, and which had an overall length of 1.75 inches. The electrodes, electrolyte, and separators were the same as that used in the large Navy prismatic cell. The separator was one ply of polypropylene (Celgard 2400 on the negative and one ply of polyethylene (Celgard K-869) on the positive. There was clear evidence that the polyethylene had acted as a "shut down" separator in the cells that were cycled at room temperature. The cell that was cycled at the low temperature showed lithium build-up through the separator because of an increase in the anode thickness. Under this condition, the "shut down" mechanism did not work because the clogged separator was not able to stop the ionic conduction when it reached its melting temperature.

There were limitations in the lithium ion design because the electrode coating process produced plates that were only 4.5 inches wide and therefore could not produce the electrodes (Figure 7.3) that would be required for a full plate design. Attempts to add a strip (Figure 7.4) led to other problems. The electrode coating process produced plates with coating thickness variation across the plates in both directions. Because of this thickness variation and the tolerance build-up, it was not possible to maintain an even pressure on the stack of the Twin Pack design. During charging, the low-pressure side expanded more causing the tabs to break.

The Slitted Plate design offered the best approach because it avoided the stack pressure on the large planar surfaces by assembling the plates in the transverse direction. It eliminated the peeling of the edges of the electrodes caused by cutting the electrodes with steel rule dies. The two internal dividers eliminated the deflection of the planar surfaces of the can which led to better control of the stack pressure during temperature cycling. This permitted the filling of the cell with electrolyte at a higher pressure without requiring a fixture (Figure 4.4) and would assure that the electrode plates were impregnated with electrolyte.

With improvements in the electrode coating process, it is now possible to make plates by a process of intermittent coating so that the plates would have areas without active material that could be used to form the tabs. The surface of the tab would be suitable for resistance welding to the bussing tabs.

With the latest improvements in the manufacturing of thin foil electrodes, Saft can fabricate a lithium ion cell with $LiNiO_2$ as the positive material and graphite as the negative material with a capacity of 115 Ah and a specific energy of 66 Wh/lb (Table 9.1).

Table 9.1 Summary of Lithium Ion Designs that Fit the Process and Manufacturing Capabilities

Dimensions of positive electrode in inches
Dimensions of negative electrode in inches.

Design	Thickness	Width	Length	Porosity	Loading mgm/cm2	No of plates	Capacity Ah	Energy density Wh/Lbs.
Narrow plates	0.0117	4.25	6.125	40	58	61	83	53
LiNiO2 / Carbon	0.0085	4.5	6.5	40.8	24	62		
Full plates	0.008	5.5	6.25	30	44	83	120	64
LiNiO2 / Carbon	0.0082	5.68	6.5	40	20	84		
Full plates	0.0125	5.5	6.25	35.7	68	64	118	66
LiCoO2 / Carbon	0.009	5.68	6.5	39	26	65		
Twin plates	0.007	2.69	6.38	30	45	180	118	62
LiNiO2 / Carbon	0.0089	2.81	6.5	40	22	182		
Twin plates	0.0087	2.69	6.38	40	45	176	113	60
LiCoO2 / Carbon	0.0077	2.81	6.5	38	20	178		
Slitted plates	0.0095	1.55	5.5	34	53	312	120	63
Desing I	0.01	1.66	5.62	47	23	313		
LiNiO2 / Carbon								
Slitted plates	0.0098	1.55	6.25	35	53	243	115	66
Desing II 3 Stacks	0.01	1.66	6.75	36	24	246		
LiNiO2 / Carbon								
Slitted plates	0.0089	1.55	6.75	41	45	280	115	60
Desing II 3 Stacks	0.0078	1.66	6.87	40	21	283		
LiCoO2 / Carbon								

References

1. C. J. Kelly and D. L. Chua, "Large Capacity Li/Li_xCoO_2 Batteries for Underwater Propulsion," Battery Exploratory Development Workshop, Myrtle Beach, SC, June 16-29, 1995, sponsored by the Office of Naval Research, Arlington VA, coordinated by the High Energy Battery Project, Naval Surface Warfare Center, White Oak, MD.*

* Now located at Carderock, MD.

DISTRIBUTION

DOD - CONUS

Copies

ATTN ONR 321 (D JOHNSON) 1
ONR 322 (T GOLDSBERRY) 1
ONR 322 (K DIAL) 1
ONR 322 (R VARLEY) 1
ONR 322 (S LITTLEFIELD) 1
ONR 331 (R DEMARCO) 1
ONR 333 (C LLOYD) 1
ONR 333 (S LEKOUDIS) 1
ONR 333 (J FEIN) 1
ONR 333 (D STEIGER) 1
OFFICE OF NAVAL RESEARCH BT 1
800 N QUINCY STREET
ARLINGTON VA 22217-5660

ATTN PMS393 1
PMS395 (T STANFORD) 1
PMS325J (R CUMMINS) 1
PMS403 (V FIEBIG) 1
PMS403B (H GONZALES) 1
PMS403C (M ALPERI) 1
92D (C YOUNG) 1
92RC (C SIEL) 1
COMMANDER
NAVAL SEA SYSTEMS COMMAND
2531 JEFFERSON DAVIS HWY
ARLINGTON VA 22242-5160

ATTN CODE 634 (P MOSS-BOSSIER) 1
COMMANDER
NAVAL COMMAND CONTROL AND
OCEAN SURVEILLANCE CENTER
SAN DIEGO CA 92512-5000

ATTN D RADZKEWYCZ 1
COMMANDER
PHILLIPS LABORATORY
KIRTLAND AFB NM 87117-6008

ATTN PMA 264C (R SPIOTTA) 1
PMA 264 (R DAVIS) 1
PMA 264E (T TAMPA) 1
COMMANDER
PROGRAM EXECUTIVE OFFICE
AIR ASW ASSAULT AND SPECIAL
MISSION PROGRAMS
47123 BUSE ROAD UNIT# IPT BLDG
SUITE 148
PATUXENT RIVER MD 20670-1547

Copies

ATTN CODE E232 3
CODE E35 1
CODE N742 (GIDEP) 1
COMMANDER
NAVAL SURFACE WARFARE CENTER
DAHLGREN DIVISION
17320 DAHLGREN ROAD
DAHLGREN VA 22448-5100

ATTN L DUBOIS 1
R ROSENFELD 1
R NOWAK 1
DARPA/DSO
3701 NORTH FAIRFAX DRIVE
ARLINGTON VA 22203-1714

ATTN CODE 6091 (B SECREST) 1
CODE 609 (J GUCINSKI) 1
CODE 6091 (H LEWIS) 1
CODE 609A (D MAINS) 1
COMMANDER
NAVAL SURFACE WARFARE CENTER
CRANE DIVISION
300 HIGHWAY 361
CRANE IN 47522-5083

ATTN CODE 8231 (G GABRIEL) 1
CODE 8231 (C EGAN) 1
CODE 8291 (D GOODRICH) 1
CODE 8292 (P DUNN) 1
COMMANDER
NAVAL UNDERWATER WARFARE
CENTER
CODE 8231 BLDG 1302
NEWPORT RI 02841

ATTN LIBRARY 1
NAVAL TECHNICAL INTELLIGENCE
CENTER
4301 SUITLAND ROAD
WASHINGTON DC 20390

ATTN CODE 2310 (E RICHARDS) 1
CODE 2330 (G COOPER) 1
COMMANDER
NAVAL SURFACE WARFARE CENTER
DAHLGREN DIVISION
COASTAL SYSTEMS STATION
6703 WEST HIGHWAY 98
PANAMA CITY FL 32407-7001

DISTRIBUTION (CONT.)

	Copies
ATTN CODE 714 (K E ROGERS)	1
COMMANDER	
NCCOSC RDTE DIV 714	
49590 LASSING RD RM A456	
SAN DIEGO CA 92152-6161	
ATTN CODE 8520 (M CERVI)	1
CODE 824 (J WOERNER)	1
COMMANDER	
NAVAL SURFACE WARFARE CENTER	
CARDEROCK DIVISION	
ANNAPOLIS LABORATORY	
3A LEGGETT CIRCLE	
ANNAPOLIS MD 21401	
ATTN R MARSH	2
COMMANDER	
US AIR FORCE	
WL/POOB BATTERY BRANCH	
1950 FIFTH STREET BLDG 18	
WRIGHT-PATTERSON AFB OH 45433-7251	
ATTN R HAMLEN	1
S SLANE	1
M BRUNDAGE	1
G AU	1
T ATWATER	1
COMMANDER	
US ARMY CECOM RDEC	
AMSEL-RD-C2-PS-B	
FORT MONMOUTH NJ 07703	
ATTN A GOLDBERG	1
S GILMAN	1
F KRIEGER	1
COMMANDER	
US ARMY RESEARCH LABORATORY	
AMSRL-SE-DC	
2800 POWDER MILL ROAD	
ADELPHI MD 20783-1197	
DEFENSE TECHNICAL	
INFORMATION CENTER	
8725 JOHN J KINGMAN DR	
SUITE 0944	
FT BELVOIR VA 22060-6218	2
NON-DOD	
ATTN OTS (T X MAHY)	1
US GOVERNMENT	
130 DUVALL LANE APT T-1	
GAITHERSBURG MD 20877	

	Copies
ATTN EE-321 (R SUTULA)	1
EE-321 (P B DAVIS)	1
DEPARTMENT OF ENERGY	
1000 INDEPENDENCE AVENUE	
WASHINGTON DC 20585	
ATTN T MURPHY	1
G HUNT	1
IDAHO NATIONAL ENGINEERING AND	
ENVIRONMENTAL LABORATORY	
LOCKHEED MARTIN IDAHO TECH CO	
PO BOX 1625	
IDAHO FALLS ID 83415-3830	
ATTN SPACE POWER APPLICATIONS-	
BRANCH (CODE 711)	2
NASA GODDARD SPACE FLIGHT	
CENTER	
GREENBELT ROAD	
GREENBELT MD 20771	
ATTN CRS-ENR (A ABELL)	1
CRS-SPR (F SISSINE)	1
LIBRARY OF CONGRESS	
WASHINGTON DC 20540	
ATTN R GUIDOTTI	1
G NAGASUBRAMANIAN	1
K GROTHAUA	1
D INGERSOLL	1
D DOUGHTY	1
R JUNGST	1
SANDIA NATIONAL LABORATORIES	
PO BOX 5800 MAILSTOP 0613	
ALBUQUERQUE NM 87185-0613	
ATTN P NARENDRA	1
C KELLY	1
D ROLLER	1
ALLIANT TECHSYSTEMS INC	
104 ROCK ROAD	
HORSHAM PA 19044	
ATTN LIBRARY	1
R HIGGINS	1
D SPENCER	1
EAGLE-PICHER INDUSTRIES INC	
PO BOX 47	
JOPLIN MO 64802	
ATTN LIBRARY	1
POWER CONVERSION INC	
495 BOULEVARD	
ELMWOOD PARK NJ 07407	

DISTRIBUTION (CONT.)

	Copies
ATTN C SCHLAIKJER BATTERY ENGINEERING INC 100 ENERGY DRIVE CANTON MA 02021	1
ATTN R REA J PASSANITI T MESSING RAYOVAC CORP PO BOX 44960 601 RAYOVAC DRIVE MADISON WI 53744-4960	1 1 1
ATTN F WALSH ECO 20 ASSEMBLY SQUARE DR SOMERVILLE MA 02145	1
ATTN T REDDY YARDNEY TECHNICAL PRODUCTS INC 82 MECHANIC STREET PAWCATUCK CT 06379	1
ATTN N PAPADAKIS NORTHRUP GRUMMAN 18901 EUCLID AVENUE CLEVELAND OH 44117	1
ATTN E TAKEUCHI WILSON GREATBATCH LTD 10000 WEHRLE DRIVE CLARENCE NY 14031	1
ATTN A MAKRIDES EIC LABORATORIES INC 111 DOWNEY STREET NORWOOD MA 02062	1
ATTN A HIMY J J MCMULLEN ASSOCIATES INC 2341 JEFFERSON DAVIS HWY ARLINGTON VA 22202	1
ATTN D CHUA H LIN MAXPOWER INC 220 STAHL RD HARLEYSVILLE PA 19438	1 1
ATTN W EBNER FMC CORP LITHIUM DIV HIGHWAY 161 BOX 795 BESSEMER CITY NC 28016	1
ATTN N ISAACS P SHAH MSA COMPANY 38 LOVETON CIRCLE SPARKS MD 21152	1 1
ATTN R STANIEWICZ J GESSLER N RAMAN A ROMERO SAFT AMERICA INC 109 BEAVER COURT COCKEYSVILLE MD 21030	1 1 1 1
ATTN C FLEISCHMANN A MESKIN G ZOSKI ADVANCED TECHNOLOGY & RESEARCH CORP. 15210 DINO DRIVE BURTONSVILLE MD 20866-1172	2 1 1
ATTN F DAMPIER LITHIUM ENERGY ASSOCIATES INC 225 CRESCENT STREET WALTHAM MA 02154	1
ATTN K ABRAHAM COVALENT ASSOCIATES INC 10 STATE STREET WOBURN MA 01801	1
ATTN G TORLONE I HILL CANADIAN DND POWER SOURCES LABORATORY 33 MANN AVENUE OTTAWA ONTARIO KIN 6N5 CANADA	1 1
ATTN A MANNING LITHIUM TECHNOLOGY CORP 5115 CAMPUS DRIVE PLYMOUTH MEETING PA 19462-1129	1
ATTN L MARCOUX BLUESTAR ADVANCED TECHNOLOGY CORP 1155 WEST 15TH STREET NORTH VANCOUVER BC CANADA V7P 1M9	1

DISTRIBUTION (CONT.)

	Copies
ATTN M THACKERAY G HENRIKSEN CHEMICAL TECHNOLOGY DIVISION ARGONNE NATIONAL LABORATORY 9700 SOUTH CASS AVENUE ARGONNE IL 60439	1 1
ATTN W SMYRL DEPT. OF CHEMICAL ENGINEERING & MATERIALS SCIENCE UNIVERSITY OF MINNESOTA 221 CHURCH STREET SE MINNEAPOLIS MN 55455	1
ATTN M KLEIN ELECTRO ENERGY INC SHELTER ROCK LANE DANSBURY CT 06810	1
ATTN G RAO NASA/GODDARD SPACE FLIGHT CENTER CODE 734, B-20, ROOM 166 GREENBELT MD 20771	1
ATTN P BURGHART ERGENICS INC 247 MARGERET KING AVENUE RINGWOOD NJ 07456	1
ATTN L DOMINEY OMG INC 2301 SCRANTON ROAD CLEVELAND OH 44114	1
ATTN E CUELLAR ULTRALIFE BATTERIES 1350 ROUTE 88 SOUTH	1
ATTN C CHANG CARNEGIE MELLON UNIVERSITY MATERIAL SCIENCE & ENGINEERING DEPT. 5000 FORBES AVE PITTSBURG PA 15213-3890	1
ATTN M SCHIMPT POWER CONNECTION INC 495 BOULEVARD ELMWOOD PARK NJ 07407	1
ATTN E WHITLOCK US ARMY 5925 QUATRELL AVE #202 ALEXANDRIA VA 22312	1
ATTN G BLOMGREN EVEREADY BATTERY CO TECHNOLOGY LABORATORY PO BOX 43035 WESTLAKE OH 44145	1
ATTN M SINK SAFT LITIUM AND MILITARY BATTERY DIVISION 313 CRESCENT STREET VALDESE NC 28690	1
ATTN R SURAMPUDI JET PROPULSION LABORATORY 4800 OAKGROVE DRIVE PASEDENA CA 91109	1
ATTN S ARGADE TECHNOCHEM COMPANY 203-A CREEK RIDGE ROAD GREENSBORO NC 27406-4419	1
ATTN D FOUCHARD POLYSTOR 6918 SIERRA COURT DUBLIN CA 94568	1

NSWC CARDEROCK DIVISION INTERNAL DISTRIBUTION

		Copies
011	(CORRADO)	1
0112	(DOUGLAS)	1
0112	(HALSALL)	1
0115	(CAPLAN)	1
0119	(MESSICK)	1
3442	(TECHNICAL INFORMATION CENTER)	1
60	(WACKER)	1
601	(MORTON)	1
603	(CAVALLARO)	1
604	(DESAVAGE)	1
65R	(BROWN)	2
68	(MUELLER)	1
681	(WELLER)	1
683	(BARNES)	1
683	(SMITH)	10
683	(FILES)	30